Natural Resources Canada Ressources naturelles Canada

GEOLOGICAL SURVEY OF CANADA
OPEN FILE 8406

2017 Korea-Canada-U.S.A. Beaufort Sea (offshore Yukon and Northwest Territories) research program: 2017 *Araon* expedition (ARA08C) cruise report

Y.K. Jin, M.M. Côté, C.K. Paull, and E.L. King (editors)

2018

Canada

GEOLOGICAL SURVEY OF CANADA
OPEN FILE 8406

2017 Korea-Canada-U.S.A. Beaufort Sea (offshore Yukon and Northwest Territories) research program: 2017 *Araon* expedition (ARA08C) cruise report

Y.K. Jin[1], M.M. Côté[2], C.K. Paull[3], and E.L. King[4] (editors)

[1] Division of Polar Earth-System Sciences, Korea Polar Research Institute, KIOST, 26 Songdomirae-ro, Yeonsu-gu, Incheon 21990, Korea
[2] Geological Survey of Canada, 9860 West Saanich Rd., Sidney, British Columbia V8L 4B2 Canada
[3] Monterey Bay Aquarium Research Institute, 7700 Sandholdt Road, Moss Landing, California 95039 U.S.A.
[4] Geological Survey of Canada, 1 Challenger Drive, Dartmouth, Nova Scotia B2Y 4A2 Canada

2018

Permanent link: https://doi.org/10.4095/308396

Recommended citation
Jin, Y.K., Côté, M.M., Paull, C.K., and King, E.L. (ed.), 2018. 2017 Korea-Canada-U.S.A. Beaufort Sea (offshore Yukon and Northwest Territories) research program: 2017 Araon expedition (ARA08C) cruise report; Geological Survey of Canada, Open File 8406, 206 p. https://doi.org/10.4095/308396

2017 Korea-Canada-U.S.A. Beaufort Sea (offshore Yukon and Northwest Territories) research program: 2017 Araon expedition (ARA08C) cruise report

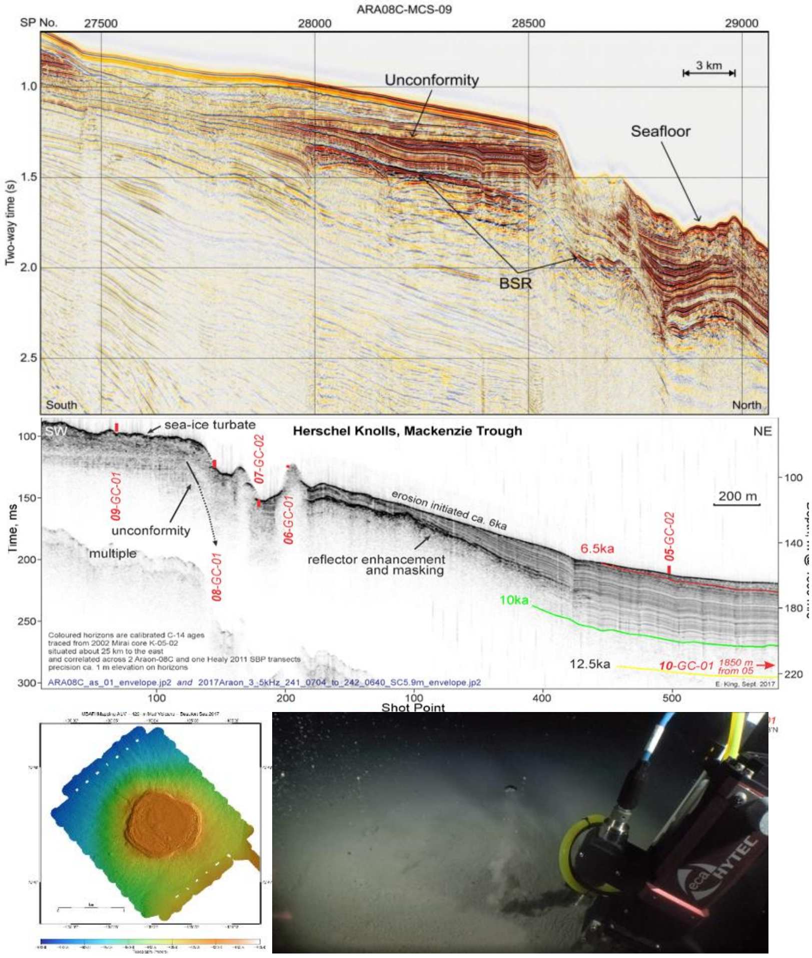

Barrow, USA-Beaufort Sea-Nome, USA
August 27 – September 16, 2017

Contact Information

Young Keun Jin

Division of Polar Earth-System Sciences

Korea Polar Research Institute, KIOST

26 Songdomirae-ro, Yeonsu-gu, Incheon 21990, Korea

Tel : +82 32-760-5403

Email : ykjin@kopri.re.kr

ARA08C cruise report

Contents

Summary 1
Y.K. Jin, M.M. Côté, C.K. Paull, and E.L. King

Chapter 1. Background 5
Y.K. Jin, M.M. Côté, C.K. Paull, and E.L. King

1.1. Context of Research Collaboration 5
1.2. Geologic Setting 5
1.3. Research Activity 6
1.4. Permits and Licensing... 6

Chapter 2. Multichannel Seismic Survey.. 9
S.-G. Kang, M.J. Duchesne, E.L. King, U. Jang, S. Kim, Y.J. Choi, and M.K. Lee

2.1. Introduction 9
  2.1.1. Mackenzie Margin geologic setting 9
  2.1.2. MCS survey goals 10
  2.1.3. Multichannel seismic program 10
2.2. Methods 11
  2.2.1. Multichannel seismic system on the Araon.. 11
  2.2.2. Acquisition parameter 12
2.3. Results 13
  2.3.1. Data acquisition 13
  2.3.2. Survey layout 15
  2.3.3. Data processing and analysis 15
2.4. Summary.. 19

Chapter 3. Multibeam Survey 20
H.J. Kim and J.H. Jung

3.1. Introduction 20
3.2. System Description and Data Acquisition.. 21
3.3. Results 22
  3.3.1. Detailed survey of Western edge of Mackenzie Trough 22
  3.2.2. Detailed survey of Yukon Shelf 22

Chapter 4. Sub-bottom Profiler Survey.. 215
E.L. King, H.J. Kim, S. Kim, and J.H. Jung

4.1. Introduction 25
4.2. System Description 26
4.3. Results 28
  4.3.1. Data coverage 28
  4.3.2. Highlights from SBP data 29
    4.3.2.1. Yukon Shelf 29
    4.3.2.2. Mackenzie Trough 30
    4.3.2.3. Outermost Mackenzie Trough 30
    4.3.2.4. Beaufort Shelf 31

Chapter 5. Seafloor Mapping Using Autonomous Underwater Vehicle 32
D.W. Caress, C.K. Paull, D. Conlin, and E. Trauschke

5.1. Introduction 32
5.2. MBARI Dorado Mapping AUV 32
  5.2.1. Overview of the mapping AUVs 32
  5.2.2. AUV launch and recovery on the Araon 34
  5.2.3. Mapping AUV Data Processing 34
5.3. High Resolution Seafloor Mapping Results 37
  5.3.1. Summary 37
  5.3.2. Mission 20170905m1 – West Mackenzie Trough margin 40
  5.3.3. Mission 20170908m1 – 420 m Mud Volcano 47
  5.3.4. Mission 20170910m1 – East Mackenzie intact margin with pingo-like features 53

Chapter 6. MiniROV Diving Program 60
C.K. Paull, L. Lundsten, D.W. Caress, D. Graves, and R. Gwiazda

6.1. Introduction 60
6.2. MiniROV System 60
  6.2.1. MiniROV operations off the Araon 61
  6.2.2. ROV data types 65
6.3. Summary of MiniROV dive sites 66
  6.3.1. Dive observations: western flank of Mackenzie Trough 67
  6.3.2. Dive observations: headwall of major slide scar 76
  6.3.3. Dive observations: 420 m mud volcano 85
  6.3.4. Dive observations: shelf edge pingo area 96
  6.3.5. Dive observations: top of conical mud volcano in 740 m 104
6.4. MiniROV Samples 109
6.5. Summary of MiniROV Dives 110

Chapter 7. Heat Flow Measurements 112
Y.-G. Kim

7.1. Introduction 112
7.2. Methods 112
7.3. Results 116
7.4. Summary 122

Chapter 8. Sediment Coring 124
R. Gwiazda, D.H. Lee, Y.M. Lee, J.-H. Kim, K.K. Kim, H. J. Koo, Y.K. Lee, and S.J. Lee

8.1. Introduction 124

8.2. Background 124
8.3. Methods 126
  8.3.1. Gravity coring 126
  8.3.2. Box coring 127
  8.3.3. Push coring 129
8.4. Results 130
  8.4.1. Pore water sampling 130
  8.4.2. Observations of split gravity cores 130
8.5. Summary 132

Chapter 9. Water Column Study 142
M. Kim, T.S. Rhee, and Y.S. Choi

9.1. Introduction 142
9.2. Methods 144
  9.2.1. CTD casting 144
  9.2.2. Ocean current measurement 144
  9.2.3. Seawater sampling 145
  9.2.4. CH_4, N_2O, and CO_2 analyses 145
  9.2.5. Dissolved inorganic carbon and total alkalinity 146
  9.2.6. Nutrients 146
  9.2.7. Underway pCO_2 measurement 146
9.3. Results 147

Chapter 10. Biological Study 150
T.-Y. Park and J.-H. Kihm

10.1. Introduction 150
10.2. Methods and Results 151
  10.2.1. Benthic invertebrates from box core 151
  10.2.2. A net trap equipped at gravity core 153
  10.2.3. Bycatch of MiniROV 154
10.3. Summary and Conclusion 156

Chapter 11. Atmospheric Observations 158
J. Park, Y. Kim, C.-K. Lim, L. Peng, and Y. Li

11.1. Introduction 158
11.2. Instruments 159
  11.2.1. Foremast 159
  11.2.2. Radarmast 160
  11.2.3. Radiosonde observations 160
  11.2.4. Physicochemical properties of aerosols 160
  11.2.5. Laboratory-scale chamber experiments 163
11.3. Preliminary Results 165
  11.3.1. Surface meteorological variables 165
  11.3.2. Radiosonde profile 168

Appendix 1. Research Permits 173

Appendix 2. Participants 187

Appendix 3. List of Stations and Line Survey 189
Appendix 4. Marine Mammal Observations Report 197
Appendix 5. Group Photos 205

ARA08C cruise report

Summary

Y.K. Jin, M.M. Côté, C.K. Paull, and E.L. King

Research experiments conducted and preliminary findings

The Expedition ARA08C was a highly multi-disciplinary international undertaking in the southern Beaufort Sea, carried out as a collaboration between the Korea Polar Research Institute (KOPRI), the Geological Survey of Canada (GSC), and the Monterey Bay Aquarium Research Institute (MBARI). These research activities took place over a period of 22 days (August 26 to September 16, 2017) on the KOPRI icebreaker RV Araon. This is the third expedition for the RV Araon in the Canadian Beaufort Sea, and builds upon research expeditions in 2013 and 2014.

During the expedition, multiple research activities were undertaken to investigate the geology, permafrost and gas hydrate conditions of the outer shelf and upper slope of the Beaufort Sea to assess the glacial history, paleoceanography, microbiology. The expedition also characterized the geochemistry and geothermal setting of the upper-ocean waters and undertook a variety of atmospheric science investigations. These activities address issues related to active geologic processes and fluid/gas flux, offshore geohazards, ocean variability and the broad consequences of global climate change. The research will contribute to the assessment of Arctic shelves as past and present atmospheric sources of methane and will quantify a range of geohazard/environmental processes associated with gas migration and release that have not been documented to date.

The expedition focused on two main research areas in the Canadian Beaufort Sea: the Mackenzie Trough and its western shelf and slope area (Yukon continental margin) from August 29 to September 7, and the Beaufort shelf and slope areas to the east of Mackenzie Trough from September 8 to September 12 (Figure S1).

During five days (from 31 August to 4 September), multichannel seismic (MCS) data on 12 lines were collected in the Mackenzie Trough and the Yukon Shelf using airgun array comprised of two Sercel Generator-Injector (G.I.) airguns. The total survey length was about 890 line-km with 35,496 shot gathers including test and transit lines (Figure S1). This MCS program was designed to address a wide variety of the outstanding conceptual issues in the study area including 1) a relatively unknown geologic architecture, 2) the state of shelf-based permafrost or permafrost degradation, and 3) slope-situated methane, including gas hydrates, and slope mass transport phenomena. These MCS data complement the existing industry wells and boreholes, deep seismic and 3-D seismic datasets, which together with the sub-bottom profile data (SBP), create a multi-resolution dataset well suited to the study goals (see Chapter 2 for details). During the MCS survey, 23 XCTD profilers were deployed on the survey lines (where water depths were greater than 200 m) for seismic oceanography research in Mackenzie Trough area. All MCS equipment operated in good conditions and without any operational issues.

Continuous multibeam (MB) and SBP data for total line-length of 2,537 and 2,154 km respectively were collected along all ship tracks (Figure S1) for detailed surface and subsurface imaging of sediment structures and permafrost, and to assist in core sites selection. These data significantly augment the existing SBP data on the Yukon Shelf.

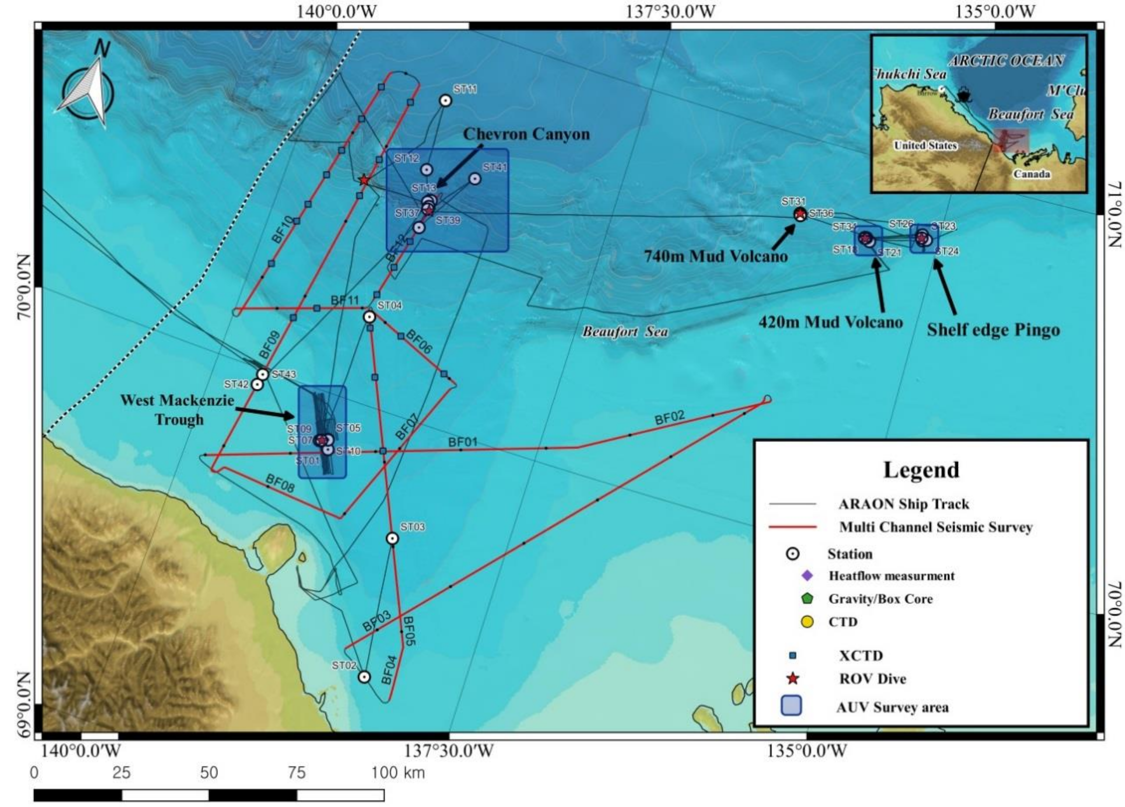

Figure S1. Overview map of the ship track, seismic lines, sampling stations, ROV dives and AUV survey areas for Expedition ARA08C.

The SBP and MB data were processed during the survey and viewed immediately. These datasets were used as a basis for choosing autonomous underwater vehicle (AUV) survey sites and remotely operated vehicle (ROV) dives. These datasets identified elongated troughs and ridges, and pingo-like features (PLFs) along the western shelf. Subsequent MB and SBP transects crossing the marked bank edge and into the Mackenzie Trough confirmed its continuity (see Chapters 3 and 4 for details).

The MBARI mapping AUV was used to acquire high-resolution seafloor mapping information. The AUV (0.53 m diameter and 6 m length) was equipped with a 400 kHz MB sonar, 110 and 410 kHz side-scan sonars, and a 1-6 kHz SBP, allowing for the acquisition of bathymetric data with about 1 m horizontal and 10 cm vertical resolution. Four AUV missions were conducted during the expedition. One AUV mission failed because the inertial navigation system (INS) was not receiving the Doppler velocity logger (DVL) estimates of velocity over bottom that are necessary for successful navigation. The other three missions were completed successfully and collected excellent MB, sidescan, and SBP data (see Figure S1 for the survey areas). During the expedition, the new and previously collected MBARI mapping AUV data provided high-resolution observations of seafloor morphology, character, and structure, as well as context for MiniROV-based inspections and sampling and ship-based coring (see Chapter 5 for details).

During Expedition ARA08C, detailed visual inspections of the seafloor and precise sampling were successfully conducted on 10 dives of MBARI's MiniROV. The MiniROV (1,500 meters inspection class) was capable of light duty work functions such as limited sampling, video transects, instrument deployment and recovery and was outfitted with the following suite of instruments: HD camera, scanning sonar, lasers, LED lights and CTD. The MiniROV dives were located in the following areas: the Western Flank of the Mackenzie Trough, Slide Scar area, 420 m mud volcano (MV), the Shelf Edge Pingo area, and 740 m MV. MiniROV video from the 740 m MV showed very active mud eruptions that produced circular highs (from <5 cm to >50 cm) on the obviously partly fluidized surface (see Chapter 6 for details).

To study the thermal conditions of fluid expulsion features and background areas, geothermal gradients and thermal conductivity were measured at 11 sites (14 measurements as some sites were revisit) and at 5 sites, respectively, at water depths ranging from 93 to 1750 m (see Chapter 7 for details). Thermal conductivity measurements were not undertaken at pingo-like features where ice-bearing seabottom with little sediment cover occurs and at mud volcanos where sediments are too soupy. Based on a plot of temperature-depth-tilt with time, unexpected results were obtained at sites in the 420 mud volcano area. Further detailed analyses are required to determine whether the results indicate an abnormal thermal/kinematic status of the seafloor or if instrument failure occurred.

A coring program was conducted to 1) evaluate the presence, effects on seafloor morphology, and geohazard impacts of possible freshwater inputs to sediments of the Beaufort Sea shelf and slope west of the Mackenzie Trough, 2) investigate the geographical extent of deposition of glacially transported materials along the axis and flanks of the Mackenzie Trough, and 3) evaluate the microbial diversity and activity as a function of the age of the vents deposits found in active mud volcanoes in the Beaufort Sea slope. A total of 10 box and 31 gravity cores were acquired with the sampling equipment on the Araon, and 29 push–cores were acquired using the MiniROV from a variety of environments within the Canadian Beaufort Sea (see Figure S1 for sampling stations). Most sediment analyses on the recovered cores will be performed post-expedition at various laboratories at KOPRI, MBARI, and other University-based collaborators in Korea. Of interest are small fragments of clear ice recovered at the top of a pingo-like feature west of the Mackenzie Trough and crystal/thin flakes of gas hydrate collected by gravity and box corers on the top of 420 m MV (see Chapter 8 for details).

Water column studies consisted of water sampling and Conductivity-Temperature-Depth (CTD) profiling at 13 stations, and continuous underway methane concentration measurement at the surface water. The objectives of these research activities were to 1) quantify the air-sea CH_4 flux from the survey area of the Beaufort Sea, 2) estimate the amount of the CH_4 released from the sediment floor, and 3) evaluate temporal and spatial variability of the dissolved CH_4 content in the Beaufort Sea through comparisons with the observations collected in 2013 and 2014. Most samples taken will be analyzed for DIC/TA, nutrients, DOC, and POC post-expedition at KOPRI. Measurements of the pH of seawater, and underway datasets of pCO_2, CH_4, and N_2O, will be processed at KOPRI to produce accurate data sets. Further details on the water sampling measurements are presented in Chapter 9.

KOPRI has been working on interpreting the Cambrian animal fossils from Sirius Passet, northern Greenland, since 2016, to understand the origin of animals during the event called the Cambrian explosion, which began at ca. 541 Ma. During this expedition, present-day diverse marine invertebrates were collected by the box coring and MiniROV sampling to investigate their detailed morphology and to compare them with the Cambrian fossils from Greenland. This study will help provide a better understanding on the morphological origin of animals during the Cambrian explosion (see Chapter 10 for details).

Atmospheric observations were undertaken during the expedition. The observations included basic meteorological parameters (e.g., air temperature, humidity, pressure and wind), radiative fluxes (e.g., net shortwave and longwave radiations), physicochemical properties of aerosols (e.g., total particle concentration, particle size distribution, black carbon, morphology, elemental composition, condensation cloud nuclei (CCN) concentration, etc.), and a laboratory-scale bubble bursting chamber study. An all-sky camera, a MPL (micro-pulse LiDAR) and radiosonde sounding system were used to observe cloud properties and generate atmospheric vertical profile (see Chapter 11 for details). Table S1 provides a summary of the datasets obtained during the expedition.

Table S1. Summary of the datasets obtained in expedition ARA08C.

Items	Lines/Stations
Sub-bottom profiler	2,154 km
Multibeam bathymetry	2,537 km
Multichannel seismic	890 km
XCTD	23
CTD	13
Heat flow	19
Box core	10
Gravity core	31
AUV missions	4 (3)
MiniROV dives	10

Acknowledgments

The ARA08C marine research program was part of a long-term research collaboration between Korea, Canada and the United States of America, which began in 2009. Lead organizations in the collaboration are the Korea Polar Research Institute, Natural Resources Canada and the Department of Fisheries and Oceans Canada, and the Monterey Bay Aquarium Research Institute. We thank the Steering Committee members of this collaboration for their vision and perseverance to bring this research program from concept to reality.

The research expedition was conducted within the Inuvialuit Settlement Region (ISR). We thank the members of the communities in the ISR for their support and helpful comments to the planning team during consultation meetings. The professionalism of the Captain and crew of Araon contributed significantly to the high productivity of this marine program, and is graciously acknowledged. Coordination of operations between the deck and the bridge were facilitated with the effectual translating by Somang Chung.

Funding for the research program was provided by the Ministry of Oceans and Fisheries (MOF), Korea. Natural Resources Canada conducted their studies as part of Public Safety Geoscience Program with support from the Panel for Energy Research and Development (PERD) and the Polar Continental Shelf Program (PCSP). Personnel and equipment support for the MBARI participation was provided by the David and Lucile Packard Foundation and operations logistics for the AUV and ROV components of the research were strongly supported by Imperial Oil Resources Ventures Limited.

Scott Dallimore is acknowledged for his role guiding the research collaboration since its inception in 2009 and for acting as a critical reviewer of this contribution.

ARA08C cruise report

Chapter 1. Background

Y.K. Jin, M.M. Côté, C. Paull, and E.L. King

1.1. Context of Research Collaboration

The Korea Polar Institute (KOPRI) is engaged in long-term collaborative studies in the Arctic Ocean with the Geological Survey of Canada/Natural Resources Canada (GSC), the Monterey Bay Aquarium Research Institute (MBARI) and Fisheries and Oceans Canada (DFO). The ongoing focus of research activities on the KOPRI icebreaker RV Araon is to investigate degrading permafrost and gas hydrates in the outer shelf and upper slope, glacial history, paleoceanography, microbiology, monitoring of the upper-ocean waters and atmospheric science. These activities address issues related to active geologic processes and fluid/gas flux, offshore geohazards, ocean variability and the broad consequences of global climate change. Our goal is to identify and describe changes in the Arctic marine environment, and subsequently to understand why changes are occurring and whether they will continue into the future.

The core program for the KOPRI activities is enabled through independent bilateral memoranda of understanding (MOU) between the participating organizations. As such, the research program compliments ongoing research priorities and regional studies that have been conducted by NRCan and DFO over the past several decades primarily using Canadian Coast Guard icebreakers Sir Wilfred Laurier and Amundsen.

1.2. Geologic Setting

The shelf of the Canadian Beaufort Sea is underlain by thick terrestrial permafrost which has been inundated by relatively warm seawater as a consequence of post-glacial sea level rise. As described by Taylor et al. (2013) the permafrost body beneath the shelf extends far offshore pinching out at the shelf–slope break at approximately 100 m water depth. Gas hydrates, a solid form of natural gas wherein water molecules are arranged in a cage-like structure with methane (or occasionally other gases) are also found in this setting. Gas hydrates are unstable at atmospheric pressure and temperature, decomposing spontaneously into gas and water. Gas hydrates exist beneath the Beaufort Sea in two locales: conventionally in deep water (slope and basin) where pressure of more than 30 atmospheres provides stability, and as permafrost gas hydrate in shallow water over the continental shelf where low formation temperatures can maintain their stability at somewhat shallower depths. Geothermal modeling by Taylor et al. (2013) suggests that gas hydrates do not occur between the outer edge of subsea permafrost (~110 m water depth) and approximately 300 m water depth.

Warming and possible thawing of the permafrost and dissociation of permafrost gas hydrate as a consequence of the sea level rise may weaken subsurface sediments and lead to subsidence, reduction of sediment strength and release of free gas. Field studies, including those from CCGS Sir Wilfrid Laurier in 2003, 2010 and 2012, 2013, 2016 have documented the escape of methane from the seabed of the outer shelf and slope. Gas venting has been observed from some conical mounds on the shelf which are referred to as pingo-like features (Paull et al., 2007). Gas venting has also been observed from an area of large landslides at top of the continental slope near 100 m depth and from the upper slope associated with large conical features that appear similar to mud volcanoes described in other settings around the world. We propose that degrading permafrost and gas hydrates liberate gas and pore water that reduce the strength of subsurface sediments, leading to possible seabed instability.

1.3. Research Activity

The RV Araon's 2017 science program sought to investigate the relationship between subsea permafrost, gas hydrates and seabed terrain features at various depths in the upper slope and outer shelf. A primary objective of the 2017 field work was to fill in gaps in the geophysical data (primarily seismic data) in specific areas of scientific interest. Our research will also assist interpretations of geologic processes in the Canadian Beaufort Sea and the understanding of the geologic and glacial history of this area.

The principal activities were:

- Multichannel seismic surveys to document the geology, permafrost and gas hydrate setting of the upper slope and outer shelf
- Collection of sediment core samples with gravity coring and box-coring equipment
- Deployment of drop probes for geothermal heat flux
- Deployment of water sampling and profiling equipment (CDT) to measure the physical properties of the ocean
- High-resolution seafloor mapping surveys using an Autonomous Underwater Vehicle (AUV)
- Ground-truthing of seafloor features using a small Remotely Operated Vehicle (ROV)
- Underway multibeam sonar for high resolution mapping of selected seabed features
- Underway surveys using ship-mounted 3.5-kHz CHIRP sonar for seismic visualization of shallow (10's of meters) sediments
- Underway measurements of water chemistry
- Underway measurements of atmospheric chemistry
- Deployment of light balloons with radiosonde to study the atmospheric conditions to maximum altitudes of up to 25 km.

1.4. Permits and Licensing

The scientific research activities on the RV Araon were reviewed by a number of agencies who are responsible for administering marine research activities in the Canadian Beaufort Sea. The permits and licenses obtained for the 2017 research activities were based on submissions made for a similar program undertaken in 2013 and amended in 2014. The following key permits pertain to the 2017 program:

Inuvialuit Environmental Impact Screening Committee (EISC) – Submission 10/12-02

The Inuvialuit Environmental Impact Screening Committee reviews all research activities in the Inuvialuit Settlement Region. The 2017 program was approved as an amendment of the 2013 submission which was entitled Canada-Korea-USA Beaufort Sea Geoscience Research Program. In addition to the program commitments made in the Project Description, the Screening Panel recommended several environmental terms and conditions which have been incorporated into the 2013, 2014 and 2017 field programs.

Items that have changed from our 2013 Project Description are listed below. Approval of the Amendment Request was granted by the EISC on June 15, 2017. A copy of this approval is in Section 1.6.

- The addition of Autonomous Underwater Vehicle (AUV) surveys;
- The use of a smaller airgun volume for multichannel seismic program;
- A shorter duration multichannel seismic program with only 4-5 days of surveying;
- An adjustment to our Program Area to undertake regional studies along the Yukon Shelf and in the Mackenzie Trough area, a region in which much less is known compared to our main study area in the central Shelf;
- The Korean Polar Research Institute (KOPRI) will once again be taking on the lead role ("Role of the Developer") for 2017. NRCan will have 3 scientists onboard;
- We have secured permission from the Canadian Border Services Agency to mobilize the Marine Mammal Observers from Herschel Island to the Araon for their work.

Marine Scientific Research Permit – IGR-176

The activity of foreign research vessels in Canadian waters is administered by the Department of Foreign Affairs, Trade and Development Canada (DFAIT). DFAIT approved the 2017 RV Araon research activities on 18 of August, 2017 under permit number IGR-176. Their letter of authority is in Section 1.6.

Northwest Territories Scientific Research License – Scientific Research License # 16158

The Government of the Northwest Territories coordinates all scientific investigations in Northwest Territories through their Scientific Research License program. A scientific research license for the "Canada-Korea-USA Beaufort Sea Geoscience Research Program: 2017 Activities" was issued on 16 August, 2017. A principle obligation under this license is to publish the results of the research. This publication helps fulfill this commitment. A copy of this license is in Section 1.6.

Yukon Scientists and Explorer License – Scientific Research License # 17-70S&E

The Government of Yukon's Cultural Heritage Branch coordinates all scientific investigations in Yukon Territory through their Yukon Scientists and Explorers Act License. A scientific research license for the "Canada-Korea-USA Beaufort Sea Geoscience Research Program: Geophysical Surveying, Geological Sampling and Oceanographic Measurements Relating to Subsea Permafrost Thawing and Gas Hydrate" was issued on 1 August, 2017. A principle obligation under this license is to publish the results of the research. This publication helps fulfill this commitment. A copy of this license is in Section 1.6.

Yukon Parks Land Use Permit – Permit 17-LU-HU-10

The Government of Yukon’s Parks Branch coordinates all activities in Yukon Territorial Parks through their Yukon Parks Land Use Permit system. A Park Permit to access Herschel Island Territorial Park to transfer the Marine Mammal Observers to and from the vessel was issued on 27 August, 2017. A copy of this permit is in Section 1.6.

References

Paull, C.K, Ussler, W., Dallimore, S.D., Blasco, S.M., Lorenson, T.D., Melling, H., Medioli, B.E., Nixon F.M., and McLaughlin, F.A. 2007. Origin of pingo-like features on the Beaufort Sea Shelf and their possible relationship to decomposing methane gas hydrates. Geophysical Research Letters, 34: 1-5.

Taylor, A.E., Dallimore, S.D., Hill, P.R., Issler, D.R., Blasco, S., and Wright, F. 2013. Numerical model of the geothermal regime on the Beaufort Shelf, arctic Canada since the Last Interglacial. Journal of Geophysical Research: Earth Surface, 118: 2365-2379.

Chapter 2. Multichannel Seismic Survey

S.-G. Kang, M.J. Duchesne, E.L. King, U. Jang, S. Kim, Y.J. Choi, and M.K. Lee

2.1. Introduction

2.1.1. Mackenzie Margin geologic setting

As summarized in Grantz et al. (2011), the Canada Basin development initiated with early Cretaceous rifting followed by upper Cretaceous flooding and shales derived largely from the south and into the Mackenzie Basin. This was followed by further tectonism and input of unconformity and sequence-bounded mixed clastics from the Mackenzie River and Amundsen Gulf in early to mid-Tertiary (beginning Eocene) followed by east-west compression, folding and thrusting to develop the Beaufort Foldbelt in the Mackenzie Valley region. Oligocene pull-apart created a deep basin beneath the Beaufort Shelf and local broad folding. A late Miocene unconformity is overlain by a thick, prograding sequence of Plio-Pleistocene muds including deltaic bodies, shelf-edge facies and abundant mass failure. The stratigraphic units defined by Dixon et al. (1994) and Graves et al. (2010) include the Kugmallit Formation associated with the most recent pull-apart, the thick Mackenzie Bay (over the Miocene unconformity), followed by the equally thick Akpak Formation, and a Pliocene shelf-top wedge with thick and multiple-failed slope equivalents termed the Iperk Formation. These stratigraphic units have been cut, up to 300 m, in the Mackenzie Trough by glaciations (Batchelor et al., 2013) which have largely filled the Mackenzie Trough. The new multichannel seismic (MCS) data image much of this stratigraphy, including the Cretaceous rocks of the Beaufort Foldbelt.

Recent fieldwork across the continental slope imaged this unique Arctic geological setting with interconnected permafrost and shallow fluid plumbing systems. This unique setting presents challenges for understanding deep and shallow hydrologic systems to which high-resolution and unique approaches to seismic imaging can contribute.

Compared to the Mackenzie Basin, little is known about the geological architecture or the permafrost state on the Yukon Shelf. No studies comparable to the adjacent Alaskan Shelf permafrost extent have been conducted, primarily due to lack of survey and well data. Bottom simulating reflectors (BSRs) have been identified (Riedel et al., 2017) and data of higher resolution and broader spatial coverage will improve the understanding of this area.

Likewise, the Mackenzie Trough permafrost occurrence and distribution, and the relatively deep preserved glacial stratigraphy and paleo-trough geometry have not been studied with high-resolution seismic. The relationship to glacial erosion and deposits, permafrost or paleo-permafrost and related fluid and gas extent and potential shallow (to seabed) migration paths remains a significant knowledge gap.

The Beaufort Shelf presents challenges in identifying deeply buried permafrost and its role in shallow gas occurrences is of interest. MCS processing techniques are under development by KOPRI and GSC and should complement ocean-bottom seismometer (OBS)-derived imaging (Riedel et al., 2015).

2.1.2. Multichannel seismic survey goals

The multichannel seismic (MCS) program was designed to address a wide variety of the outstanding conceptual issues related to the geology of the Canadian margin of the Beaufort Sea (see 1, 2). Specifically, the goals of this expedition included gaining new insights on the following:

- The geologic architecture of the Yukon Shelf and the distribution of ice-bonded permafrost;
- Potential evidence of glaciation of the Yukon Shelf and Mackenzie Trough;
- Controls of subsurface geology on seabed processes including gas and fluid migration from depth, slope mass failure and transport phenomena and gas hydrate occurrence;
- Linking of 2017 MCS data with studies conducted by the RV Araon in 2014 to assess geology and permafrost from the central Beaufort Shelf, across the Mackenzie Trough to the Yukon Shelf;
- Provide a rich MCS data set suitable for research geophysics applications including new geophysical processing techniques to quantify subsurface conditions and assessment of the oceanographic conditions using seismic oceanography techniques.

One approach of the ARA08C survey was to replicate portions of industry seismic lines (ION/GXT) which were recently (summer 2017) made available to the GSC. The high-resolution KOPRI MCS system fills a resolution gap by better imaging the upper 1 to 2 seconds, covering the depth range where most of the geo-phenomena noted above occur. These data complement the deep seismic, which together with the sub-bottom profile (SBP) data, create a multi-resolution dataset well suited to the study goals. Given a 5-day program, the survey layout optimized ties with existing MCS data from previous Araon surveys, existing hydrocarbon industry wells and boreholes, existing 3-D datasets and improved geometry to characterize the shallow glacial and permafrost/fluid phenomena.

2.1.3. Multichannel seismic program

The MCS survey was conducted on the Mackenzie Trough in the Canadian Beaufort Sea, from 31 August to 4 September 2017. During the five-day survey, MCS data were collected on 12 lines with a total survey length of ~890 line-km and 35,496 shots. The resultant MCS data will contribute to the understanding of subglacial histories, seismic sequence stratigraphy and estimate the spatial distribution of the gas hydrate bearing zone and subsea permafrost interval using a full waveform inversion method. During the MCS survey, 23 XCTDs were deployed on the survey lines (over 200 m water depth area) for seismic oceanography research in Mackenzie Trough area. XCTD data will be use to understand the physical properties of the water column and to tie with seismic oceanography sections, which will be constructed using a frequency domain reverse time migration algorithm from the MCS data.

Seismic data acquisition followed the guidelines for operation as defined in the seismic permit documents provided through the Fisheries and Oceans Canada (DFO) and the Inuvialuit Environmental Impact Screening Committee (EISC). A safety zone of 1 km radius around the vessel was defined, based on the maximum airgun array volume of 420 in^3. Prior to any airgun operations, the marine mammal observers (MMOs) were on watch for at least one hour to observe that no marine mammals were within the safety zone.

2.2. Methods

2.2.1. Multichannel seismic system on the Araon

The MCS system on Araon consisted of an airgun array, a streamer, two compressors, and survey control systems (Figure 2.1). The airgun array was comprised of two Sercel Generator-Injector (G.I.) airguns (each 210 in^3 volume) and a float system that maintains the source at a depth of ~6 m in the water. The airguns released compressed air simultaneously and generated an acoustic wave that was used as the source wave of the MCS survey. The total volume of the source was 420 in^3. The shot interval was 25 m, approximately every 7 seconds, for a 30-fold coverage.

The streamer had ten solid type sections that record reflected acoustic wave and other signals such as direct wave, refracted wave and background noise using hydrophones mounted in the streamer. The streamer was operated at ±6 m below the surface of the water. The group interval and channel number of the streamer were 12.5 m and 120 channels, respectively. Total length of the streamer was 1.75 km, including the tail buoy, fluid section and lead-in cable. Six cable levelers (birds) were attached on the streamer every 300 m to insure that the streamer was maintained at a constant depth in the water column. The recording length and sampling rate were 8.0 seconds and 1 millisecond, respectively. The recording file format was SEG-D. Shot and receiver intervals specified above resulted in fold-coverage of 30.

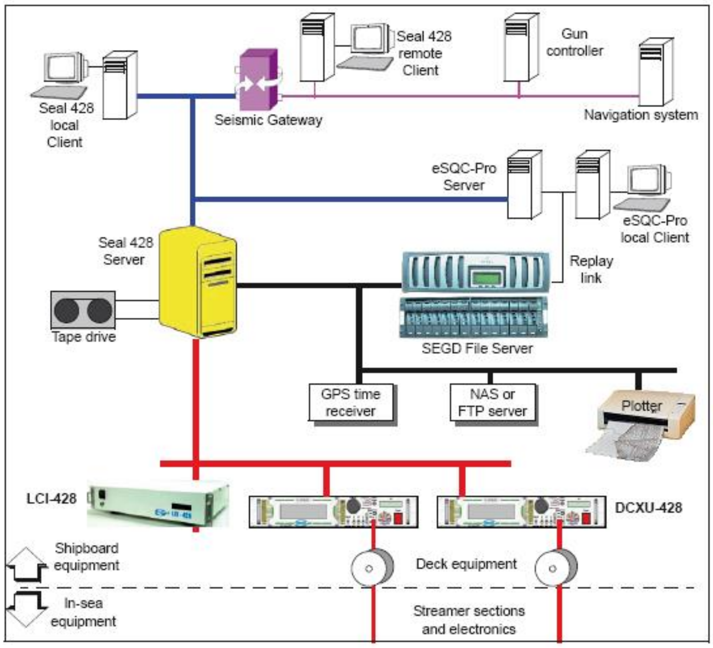

Figure 2.1. Schematic diagram of the multichannel seismic system on the Araon.

The survey control system in the Main Dry Lab on the Araon housed the navigation control system, airgun controller, bird controller, recording system, quality control system and navigation editing system (Figure 2.1). The navigation system, NaviPac from EIVA, provided navigation information and positioning calculations during the survey and controlled the event type, shot interval, event start/stop with the airgun controller and recording system. The airgun controller, Bigshot from RTS (Real Time Systems), received the event signal from NaviPac and triggered the airguns from which the acoustic waves were generated. Bigshot displayed the shot-timing and wave shape for quality control (QC) purposes. The bird controller defined the streamer depth and displayed the location and heading of the birds. The recording system, Baby Seal from Sercel, recorded the seismic data and sent it to a large data storage system. The QC system, e-SQC pro from Sercel, displayed real-time data such as shot gathers and near trace sections. The navigation editing system, NaviEdit from EIVA, transformed the NaviPac survey file to a standard navigation file such as UKOOA P1/90 or other formats. Figure 2.2 shows a selection of photos from the MCS program.

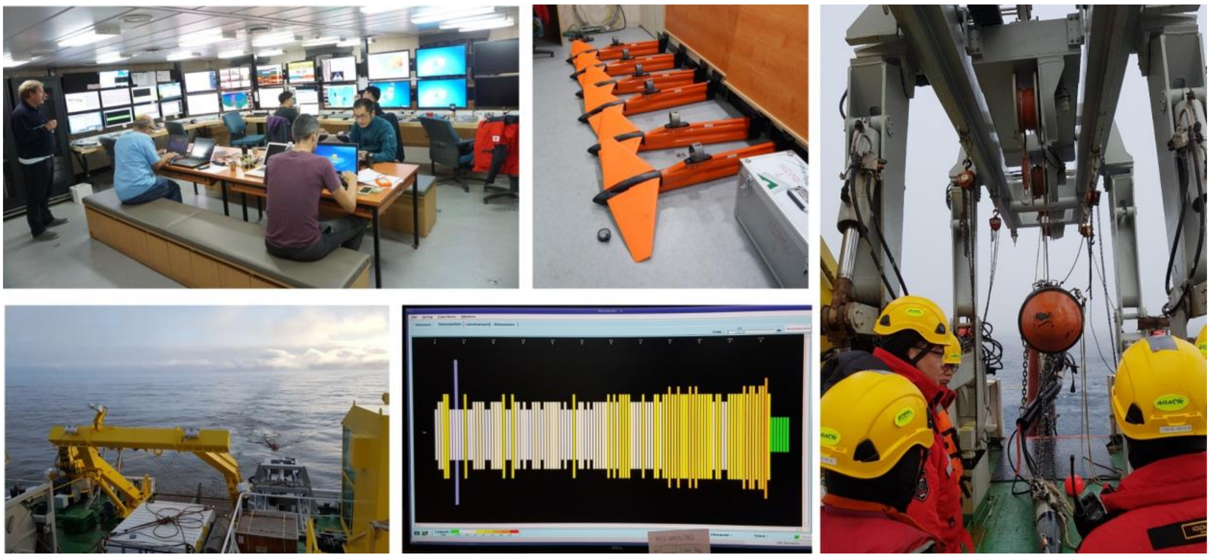

Figure 2.2. Selection of photos taken during the MCS program. From top left: MCS survey control room in the Main Dry Lab of Araon; Birds used to control the depth of the streamer; Airgun system being deployed; Airgun system in active survey; Bigshot display to monitor noise distribution on the streamer for quality control purposes.

2.2.2. Acquisition parameters

Table 2.1 shows the acquisition parameters of the multichannel seismic survey used during ARA08C. Figure 2.3 shows the towing offsets used during the seismic survey.

Table 2.1. Seismic acquisition parameters.

Shot Interval	25.0 m
Channel Number	120 ch
Group Interval	12.5 m
Source Depth	6 m
Streamer Depth	6 m
Fold of Coverage	30 folds
Work Pressure	140 ~ 150 bar
Recording Length	8.0 sec
Sample Rate	1 ms
Tape Format	SEG-D

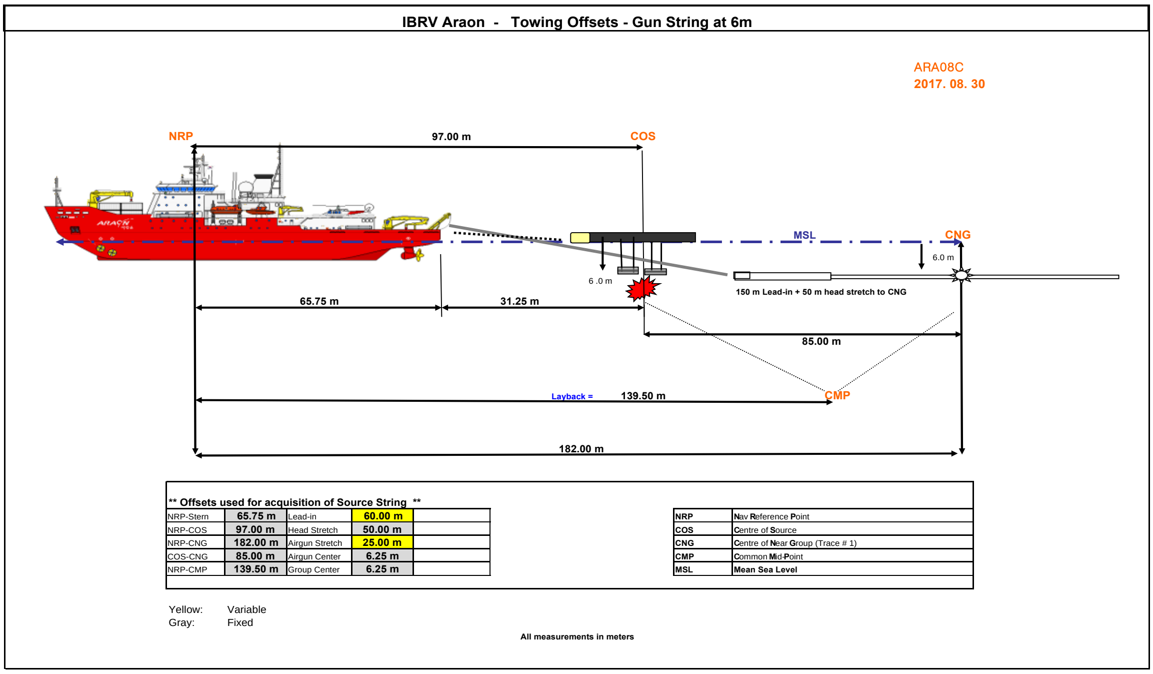

** Offsets used for acquisition of Source String **

NRP-Stern	65.75 m	Lead-in	60.00 m	
NRP-COS	97.00 m	Head Stretch	50.00 m	
NRP-CNG	182.00 m	Airgun Stretch	25.00 m	
COS-CNG	85.00 m	Airgun Center	6.25 m	
NRP-CMP	139.50 m	Group Center	6.25 m	

NRP	**N**av **R**eference **P**oint
COS	**C**entre of **S**ource
CNG	**C**entre of **N**ear **G**roup (Trace # 1)
CMP	**C**ommon **M**id-**P**oint
MSL	**Mean Sea Level**

Yellow:	Variable
Gray:	Fixed

All measurements in meters

Figure 2.3. Field acquisition parameters and layouts.

2.3. Results

2.3.1. Data acquisition

From offshore of Herschel Island, the airgun array and streamer were deployed over a 6-hour period. A ramp-up procedure took place to ensure that no marine mammals were within the defined safety radius. After the ramp-up, the MMOs indicated that the vessel was clear to begin the MCS survey. After the first day, the weather conditions for the MCS became ideal with calm winds and flat seas. This resulted in very clear shot-gathers and near offset sections and over-all excellent data quality. The track chart of the seismic survey lines of ARA08C is presented in Figure 2.4, while the seismic acquisition field log is presented in Table 2.2.

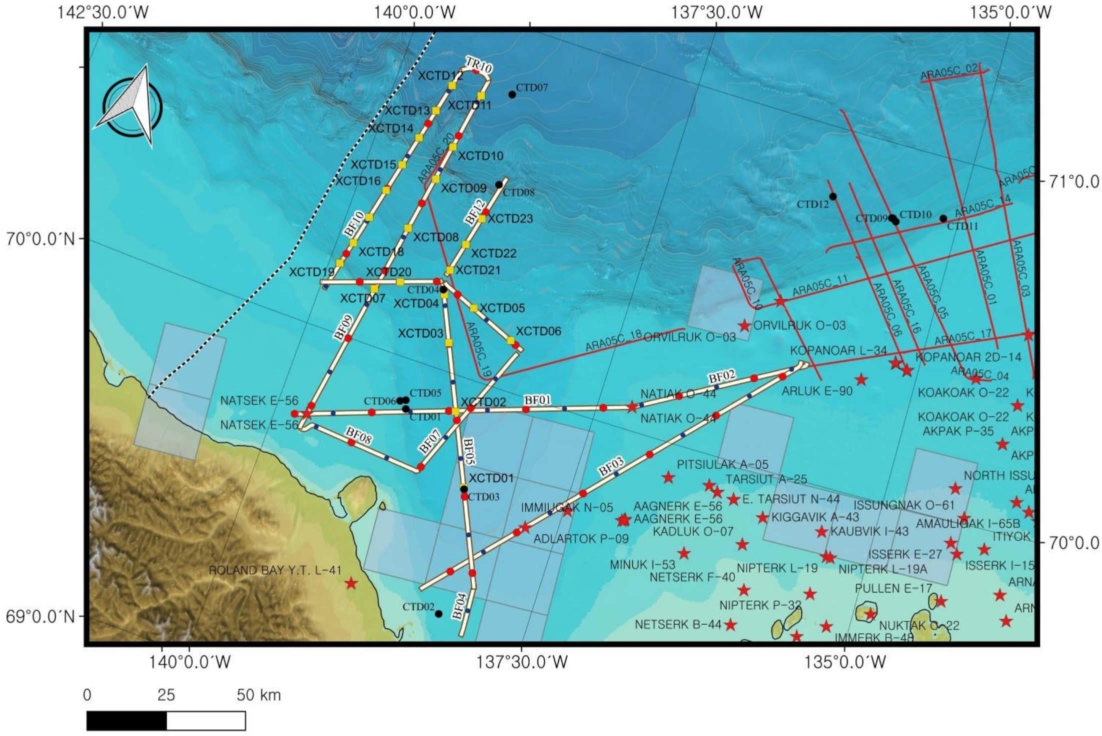

Figure 2.4. Track chart of the seismic survey of ARA08C (white solid lines: MCS track chart; yellow circle: XCTD stations; red circles: Shot number grid point in 1000th shotpoints; red stars: well sites).

Table 2.2. Seismic acquisition field log.

Line Name	Start of Line					End of Line					First Good Shot Point	Last Good Shot Point	Length (km)
	Shot Point	Date	Time	Latitude	Longitude	Shot point	Date	Time	Latitude	Longitude			
BF01	1998	2017.08.31	07:50	69°43.9492'N	139°52.2262'W	6373	2017.08.31	20:08	70°03.9800'N	137°12.8722'W	2021	6373	106.90
BF02	6374	2017.08.31	20:08	70°03.9716'N	137°12.9813'W	8705	2017.09.01	03:05	70°19.5895'N	135°55.3687'W	6374	8651	57.13
BF03	8707	2017.09.01	03:25	70°19.3148'N	135°58.2346'W	14428	2017.09.01	20:15	69°23.6800'N	138°23.7659'W	8775	14413	139.96
BF04	15182	2017.09.01	22:48	69°18.2646'N	137°58.9085'W	15819	2017.09.02	00:41	69°26.7426'N	138°00.5723'W	15240	15801	15.52
BF05	15820	2017.09.02	00:42	69°26.7854'N	138°00.6151'W	19796	2017.09.02	12:20	70°14.0947'N	139°02.4036'W	15820	19786	97.03
BF06	19797	2017.09.02	12:41	70°14.0573'N	139°00.4899'W	21089	2017.09.02	16:30	70°07.5377'N	138°14.6725'W	19813	21084	31.56
BF07	21090	2017.09.02	16:53	70°06.1594'N	138°16.6670'W	23071	2017.09.02	22:54	69°42.3256'N	138°44.3987'W	21105	23054	48.36
BF08	23072	2017.09.02	22:54	69°42.2804'N	138°44.5509'W	24690	2017.09.03	03:53	69°42.9769'N	139°45.6140'W	23148	24542	40.78
BF09	24691	2017.09.03	03:54	69°42.9953'N	139°45.6079’W	29820	2017.09.03	19:03	70°49.5177'N	139°14.8411'W	24771	29794	125.31
BF10	30160	2017.09.03	20:13	70°49.6779'N	139°29.2177'W	33515	2017.09.04	06:15	70°06.6840'N	139°57.5006'W	30228	33514	82.09
BF11	33516	2017.09.04	06:47	70°07.4476'N	139°59.5814'W	35051	2017.09.04	11:13	70°14.2267'N	139°03.9393'W	33594	35045	37.50
BF12	35052	2017.09.04	11:35	70°15.8733'N	139°02.0927'W	36496	2017.09.04	15:58	70°34.3468'N	138°49.3588'W	35110	36496	35.29

2.3.2. Survey layout

BF01 and BF02 crossed from the middle of the Yukon shelf, across the Mackenzie Trough and tie with the Araon 2014 surveys to the east. This transect had a strong permafrost imaging goal, building on velocity derivations from the eastern area in an attempt to visualize the changing permafrost regime. It will also provide an excellent profile of the glacial setting. These lines passed through the Natsek and Natiak wells to provide lithological and permafrost control. BF03 also extended from the central shelf across the Mackenzie Trough to the Yukon Shelf. The transect passed through or near three industry exploration well sites, some of which have encountered significant shallow overpressures. It should also reach beyond the western paleo-ice stream erosional flank. BF04 provided a tie with a 73 m long geotechnical borehole through thick Mackenzie River mud, and into the glacial section. It joined BF05, which followed the Mackenzie Trough axis along the thickest and best-preserved glacial sequences as identified from published isopachs (Batchelor et al., 2013), and as such will provide the optimal geometry for characterizing the sequences and their geometry.

BF06 provided a partial transect across Mackenzie Trough potentially imaging the glacial sediments in the Trough and permafrost characteristics. It was also anticipated to intersect large shelf-break mass failures and the glaciation limits. BF07 replicated the outer part of an industry seismic line, recently made available to the GSC, to achieve the multi-resolution goal. BF08 provided a further transect to contrast the Mackenzie Trough with the Yukon Shelf for permafrost and glacial erosion and stratigraphy information.

BF09 extended across the relatively unknown Yukon Shelf in a dip line from the Natsek E-56 exploration well to the deep water offshore of the Mackenzie Trough. The line layout addresses Yukon shelf Cenozoic and glacial geology, intersects locations of published marine BSRs and potentially assesses glacial stratigraphy and features.

BF10 is located in the westernmost Yukon Shelf and Slope, placed to address similar unknowns as BF09. BF11, provided a transect from the Yukon shelf to deep water and ties to BF06 to complete an outer Mackenzie Trough strikeline. It crossed the shelf-break glacial deposits and structural anomalies, and could potentially image permafrost phenomena. BF06 and BF11 both tie with BF12 which was designed to duplicate part of the industry (ION-GXT) line. The upper part provides a basis to assess thick glacial sequences interpreted by Batchelor et al. (2013) with higher resolution. Deep water BSRs and potential deep-water seabed efflux phenomena are also expected.

2.3.3. Data processing and analysis

The seismic data were processed onboard the Araon to generate a brute-stack with in-house signal processing algorithms and software, and the seismic data processing software VISTA 10.0 from GEDCO (Geophysical Exploration and Development Company). Raw data (SEG-D format) loading, band-pass filtering and recording delay correction were conducted using an in-house preprocessing algorithm. Geometry setting, velocity analysis, normal moveout (NMO) correction, and common mid-point (CMP) stacking were performed using GEDCO VISTA 10.0 software. Line BF01~03 contained swell noise in the data, but the plan is to remove it using swell noise attenuation modules. In the shot gathers, which were acquired on continental shelf (shallow water depth around 40-60 m) the direct wave and refraction wave were overlapped. Figure 2.5 presents a 3-D visualization of the seismic stacked sections collected during the cruise using OpenDetect Software.

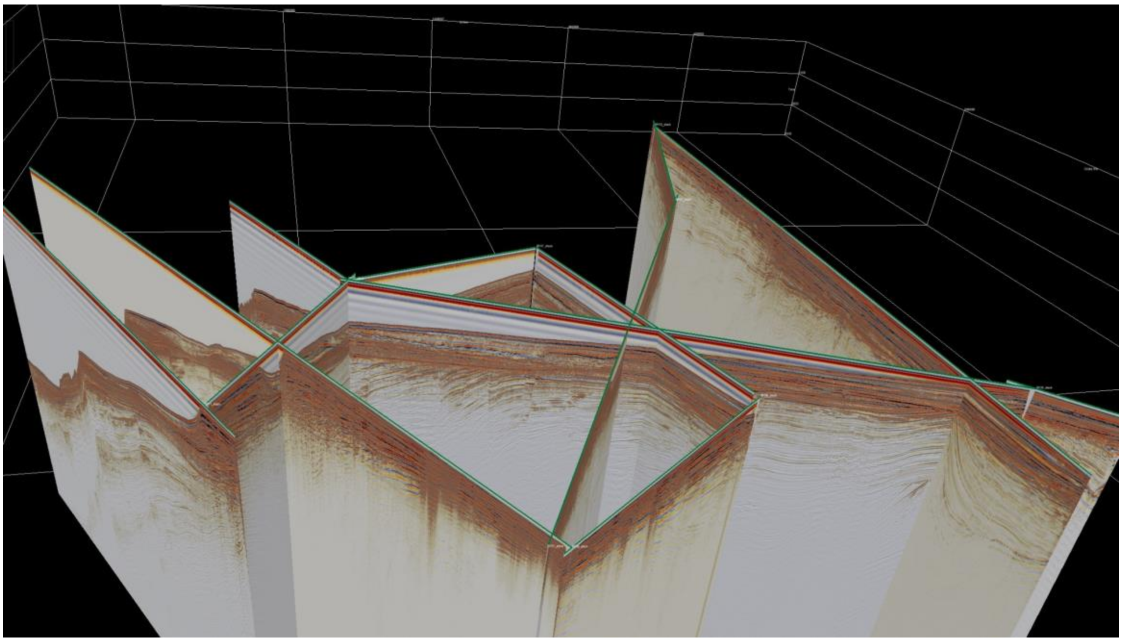

Figure 2.5. 3-D visualization of the seismic stacked sections collected during the cruise using OpenDetect Software.

Four seismic stacking images are presented below with basic interpretations based on initial processing. Advanced processing techniques will be conducted which will allow for a more developed interpretation of the seismic images.

Line BF03 (Figure 2.6) traversed the Beaufort Shelf and Mackenzie Trough. Deepest in the section are low to medium amplitude reflections attributed to the Beaufort Foldbelt, consisting of Cretaceous and Tertiary strata (Graves et al., 2010). The Beaufort Foldbelt has been affected by several phases of deformation in response to sediment loading and compressional events induced by northeastern motion of the Yukon-Alaska Cordillera that occurred between the Eocene to Miocene (Lane and Dietrich, 1995). These deformation phases are recorded by faults located along anticlines and in strata gently draping the Beaufort Foldbelt. Some anticline faults on line BF03 are imaged between 2.0 and 0.5s in weak to medium amplitude reflections. Some bright spots are observed at the top of anticlines and faults. In such contexts, bright spots have been classically interpreted as hydrocarbon accumulations (Hilterman, 2001). In the southwestern portion of the line, the top of the foldbelt (most likely part of the Iperk Formation of Pliocene age) is characterized by an erosional unconformity corresponding to a high amplitude reflection with reversed polarity. Just above the Iperk Formation sits another erosional unconformity characterized by truncated flat lying reflections that is tied to the Mackenzie Trough, containing younger sediments (Pleistocene-Holocene). On the Beaufort Shelf (left), primary reflections are obscured by high amplitude multiples attributed to shallow water depths and a hard surface immediately below the seafloor.

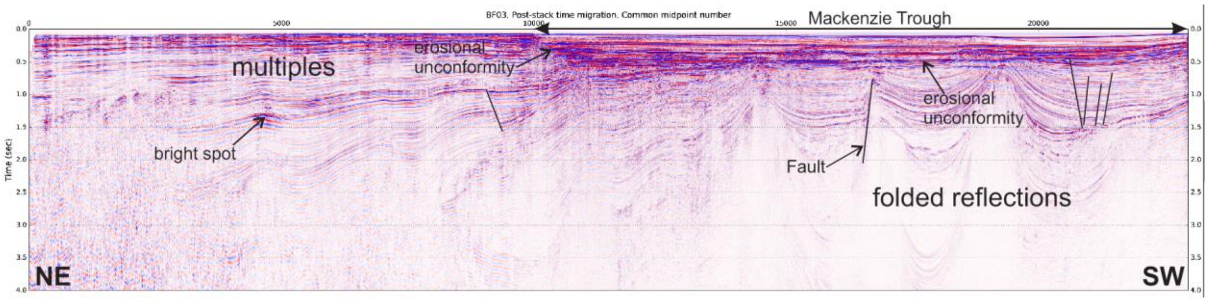

Figure 2.6. Line ARA08C-BF03 stacked section with preliminary interpretations.

Line BF05 (Figure 2.7) was located along the Mackenzie Trough, parallel to its long axis. Weak amplitude folded reflections of the Beaufort Foldbelt are imaged below 2.0s (Graves et al., 2010). Several faults of different scales are resolved from ~2.65 and ~0.5s. Three highly faulted zones are imaged respectively from south to north, between CMP 0 to 1775, CMP 2200 and 4000, and between CMP 9500 and 10100. These zones display closely spaced faults having a small throw compared to larger faults imaged throughout the section. Some bright spots and blanked zones are observed above the faults suggesting that these structures may act as conduits for upward fluid flow. The same high amplitude reversed polarity reflection imaged on line BF03, corresponds to an erosional unconformity cutting the upper Iperk Formation (Pliocene), visible across this entire section between 1.0 and 0.4s. Above it, sediments of assumed Pliocene to Quaternary age present a contrasting depositional style, laterally passing from low to medium amplitude gently seaward-dipping reflections between CMP 0 and ~4000, to mostly high amplitude chaotic reflections from CMP ~4500 to ~9000, and further along the line becoming low amplitude wavy reflections lying above a wedge consisting in high amplitude chaotic reflections. In contrast to line BF03, this transect orientation images a uniform time-thickness of the Pliocene/Pleistocene succession above another regional unconformity.

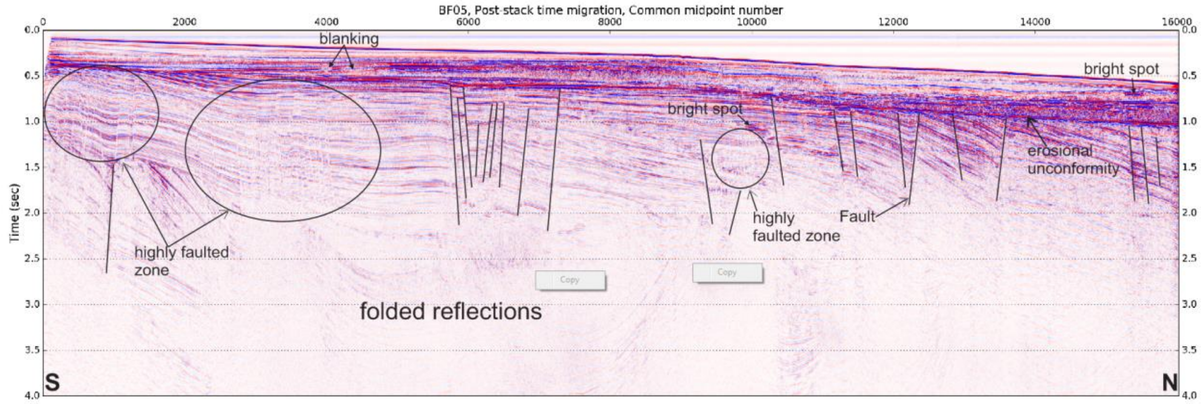

Figure 2.7. Line ARA08C-BF05 stacked section with preliminary interpretations.

Line BF09 (Figure 2.8) lies west of the Mackenzie Trough. On the shelf, deep imaging was compromised by multiples of strong amplitude and most likely a highly attenuating seafloor and/or near-surface geological features. On the slope, deeper imaging was achieved. However, as opposed to lines BF03 and BF05, no folded reflections are resolved at late arrival times. Some multiples also obscure the imaging of primaries on the slope on a time-distance window extending from CMP ~800 at 1.2s to CMP ~18000 at 4.0s. Nevertheless, the shallow part of the slope presents features of interest. A bright spot is revealed above a small fault located at CMP ~13000 and ~1.2s. Downslope, at CMP ~13500 and at an equivalent two-way travel time as the bright spot, a high amplitude reversed polarity reflection cross-cutting other seismic events is imaged. This marker is tied on the SSW to a fault located ~0.1s beneath, before fading after the shelf break at CMP ~1600 and 2.0s. This seismic event presents characteristics of a BSR that are traditionally interpreted as the base of the gas hydrate stability field (Shipley et al., 1979). Between the western flank of the Mackenzie Trough and the shelf break, an erosional unconformity is identified. This feature truncates high amplitude, gently dipping parallel reflections. As opposed to the erosional unconformity documented at similar two-way travel times on the previous two sections, this seismic event exhibits a strong amplitude but does not have a reversed polarity. The erosional unconformity is overlain by draping weak amplitude reflections having a time-thickness that varies from 0.2 to 0.5s. NNE from the shelf break to the last CMP. This section is dominated by high amplitude chaotic reflection packages forming the seafloor and the shallow subsurface that are resting on a succession of high amplitude parallel reflections.

Line BF12 (Figure 2.9) parallels line BF09, extending from the middle of Mackenzie Trough through the continental slope. Deeper reflections consist of gently seaward-dipping events of weak amplitude that are intersected by faults; one on the SSW side is particularly deeply rooted at ~2.7s. Bright spots are associated with both faults. Faults and bright spots apparently terminate at the same seismic stratigraphic level. As imaged on several of the previous lines, a highly reflective wedge extends from the shelf break to CMP~2200 between 1.2s and 1.5s.

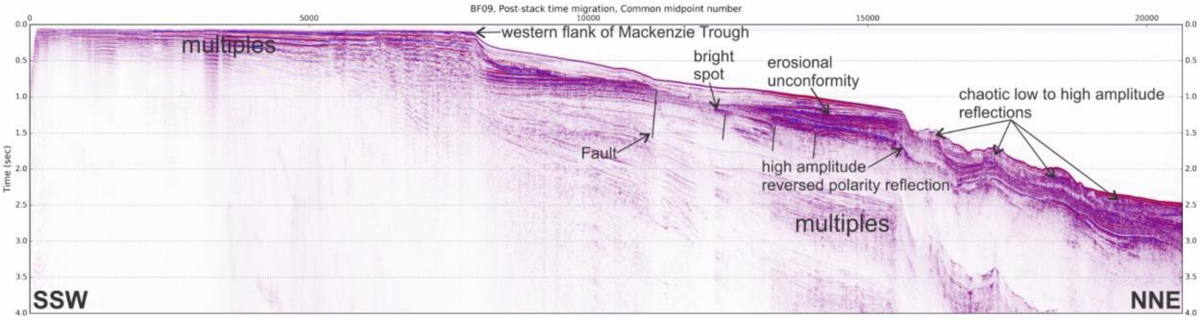

Figure 2.8. Line ARA08C-BF09 stacked section with preliminary interpretations.

The wedge is bounded at its top by a high amplitude reversed polarity reflection that truncates it as well as the gently dipping reflections imaged beneath also described above. This marker is overlain by a chaotic reflection package that has amplitudes ranging from low to high. From the SSW to CMP ~1000 the chaotic package is intersected by a flat lying high amplitude reflection. The time-thickness of this package decreases seaward from ~0.5s to ~0.1s. It is draped by weak reflections that are difficult to resolve that gradually increase in amplitude towards the shelf break, forming the near-surface. Between the shelf break and the upper continental slope, the subsurface from 2.2s to 1.25s is formed by series high amplitude chaotic reflections most likely representing mass-transport deposits.

For more accurate and detailed seismic sequence interpretation, post-cruise seismic data processing sequences are required. These will begin with de-bubble, deconvolution, additional advanced filtering, NMO muting, multiple attenuation, detailed velocity analysis and migration.

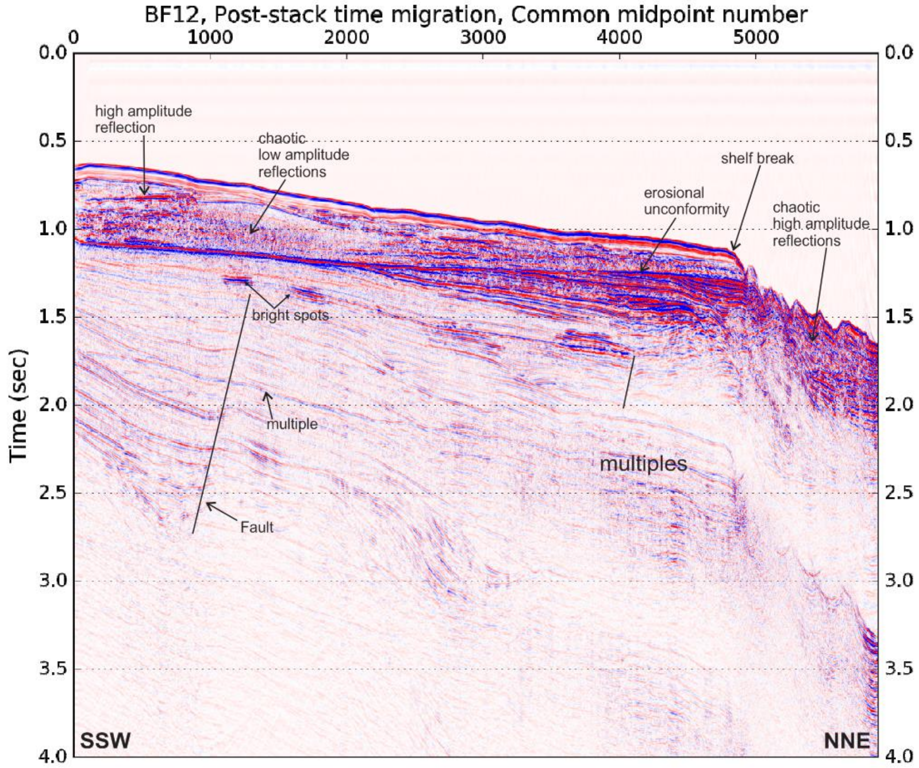

Figure 2.9. ARA08C-BF12 stacked section with preliminary interpretations.

2.4. Summary

During the ARA08C cruise, multichannel seismic data were acquired on the Mackenzie Trough and Yukon margin in the westernmost part of the Canadian Beaufort Sea. Twelve seismic lines covering 890 line-km and 35,496 shot gathers were collected from 31 August to 4 September 2017. During the survey, all seismic equipment operated continuously with no technical issues or maintenance needed on the airguns or streamer during acquisition. This resulted in high signal-to-noise and high quality seismic data.

References

Batchelor, C.L., Dowdeswell, J.A., and Pietras, J.T. 2013. Seismic stratigraphy, sedimentary architecture and palaeo-glaciology of the Mackenzie Trough: evidence for two Quaternary ice advances and limited fan development on the western Canadian Beaufort Sea margin. *Quaternary Science Reviews*, 65: 73-87.

Dixon, J., Morrell, G.R., Dietrich, J R., Taylor, G.C., Procter, R.M., Conn, R.F., Dallaire, S.M., and Christie, J.A. 1994. *Petroleum resources of the Mackenzie Delta and Beaufort Sea*. Geological Survey of Canada, Bulletin 474.

Grantz, A., Hart, P.E., and Childers, V.A. 2011. Geology and tectonic development of the Amerasia and Canada Basins, Arctic Ocean. *Arctic Petroleum Geology: Geological Society of London Memoirs 35*, 771-799.

Graves, J., Chen, Z., Dietrich, J R., and Dixon, J. 2010. *Seismic interpretation and structural analysis of the Beaufort - Mackenzie Basin*. Geological Survey of Canada, Open File 6217.

Hilterman, F.J. 2001. *Seismic amplitude interpretation: short course notes*. Distinguished Instructor Series no 4. Society of Exploration Geophysicists, Tulsa, Oklahoma.

Lane, L. S. and Dietrich, J. R. 1995. Tertiary Structural Evolution of the Beaufort Sea - Mackenzie Delta Region, Arctic Canada. *Bulletin of Canadian Petroleum Geology*, 43: 293-314.

Riedel, M., Brent, T.A., Taylor, G., Taylor, A.E., Hong, J.-K., Jin, Y.-K., and Dallimore, S.R. 2017. Evidence for gas hydrate occurrences in the Canadian Arctic Beaufort Sea within permafrost-associated shelf and deep-water marine environments. *Marine and Petroleum Geology*, 81: 66-78.

Riedel, M., Ulmi, M., Conway, K.W., Standen, G., Rosenberger, A., Hong, J.-K., Jin, Y.-K., Kim, H.S., and Dallimore, S.R. 2015. *Ocean Bottom Seismometer Experiment on the Beaufort shelf and slope region conducted during Expedition ARA04C on the IBRV Araon*. Geological Survey of Canada, Open File 7621.

Shipley, T.H., Houston, M.H., Buffler, R.T., Shaub, F. J., McMillen, K.J., Ladd, J.W., and Worzel, J.L. 1979. Seismic reflection evidence for the widespread occurrence of possible gas-hydrate horizons on continental slopes and rises. *American Association of Petroleum Geologists Bulletin*, 63: 2004-2213.

Chapter 3. Multibeam Survey

H.J. Kim and J.H. Jung

3.1. Introduction

Swath (or multibeam) bathymetry surveys were conducted utilizing a hull-mounted EM122 multibeam echo sounder. Data acquisition began when the vessel entered Canadian waters. The survey continued for the duration of the science program and was terminated as the vessel left Canadian waters on September 12 (Figure 3.1). This includes continuous swath and SBP collection during the multichannel seismic acquisition.und velocity profiles were updated frequently using the profiles obtained from XCTD casts. The bathymetry data were processed onboard using CARIS HIPS&SIPS 9.0 version and Fledermaus, a specialized bathymetry processing software. The results were plotted using Generic Mapping Tool (GMT) and QGIS software.

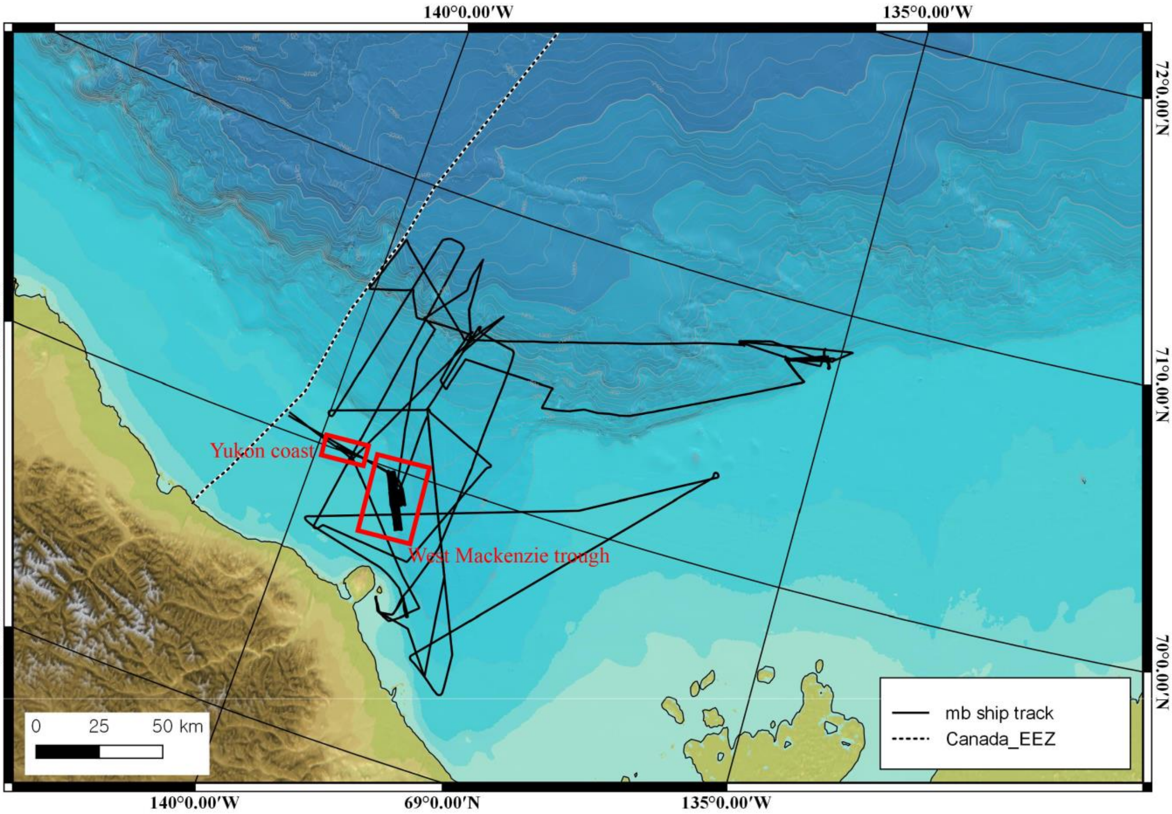

Figure 3.1. Location map of the survey area in ARA08C. Areas where detailed surveys were conducted are shown with red boxes.

The main purposes of the multibeam surveys are to aid in the regional bathymetric mapping of the study area, reveal unknown seabed features not previously mapped, and to confirm specific seafloor morphological features of target areas recognized in earlier studies. Simultaneous sub-bottom profiler data were collected, also contributing toward understanding the seabed features. Processed seafloor bathymetric images were also utilized to determine sites of geological sampling and heat flow measurement. Some of the processed data will potentially contribute to the international bathymetry data sets (i.e., International Bathymetric Chart of the Arctic Ocean (IBCAO), and General Bathymetric Chart of the Ocean (GEBCO)). Copies of all bathymetric data will be transferred to the Canadian Hydrographic Service for inclusion in their databases.

During the survey, recording errors occurred on occasion, mainly due to a malfunction of the supporting navigation system (Seapath system). When a navigation error occurred, the software could not calculate water depth correctly. In most cases the navigation error recovered automatically after several minutes, but sometimes the problem required rebooting of the system, resulting in data gaps of approximately one hour.

3.2. System Description and Data Acquisition

The multibeam system consists of hull-mounted transmit and receive transducer arrays, a transceiver unit, and an operator station (Figure 3.2). The EM122 multibeam system has a wide beam angle (-65 ~ +65 degrees) and a water depth range of 20 to 11,000 m. The technical specifications of the EM122 system are listed in Table 3.1.

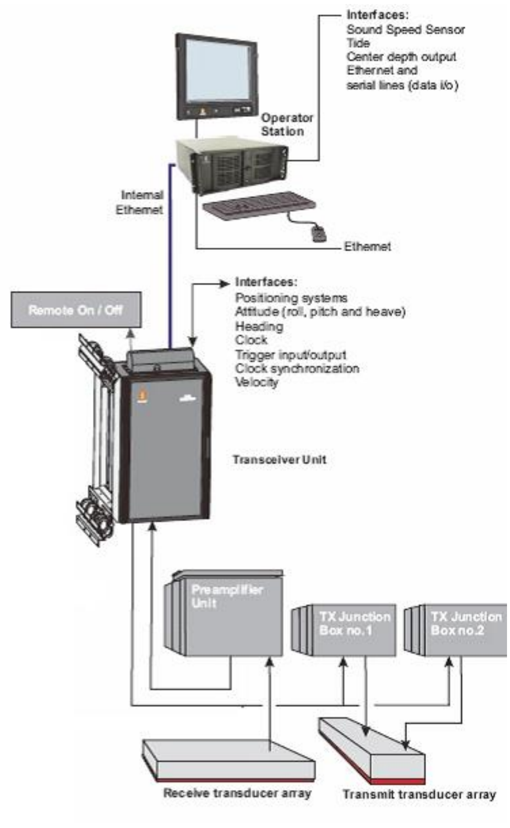

Figure 3.2. System diagram of the EM122 multibeam system.

Table 3.1. Technical specifications of the EM122 multibeam system.

Operating frequency		12 kHz
Depth range		20 – 11,000 m
Swath width		6 × Depth, to approx 30 km
Pulse forms		CW and FM chirp
No. of beams		288
Swath profiles per ping		1 or 2
Motion compensation	Yaw	± 10 degrees
	Pitch	± 10 degrees
	Roll	± 15 degrees
Sounding pattern		Equi-distant on bottom/equiangular
Depth resolution of soundings		1 cm
High resolution mode		High Density processing
Sidelobe suppression		-25 dB
Modular design, beamwidth		0.5 to 4 degrees

3.3. Results

3.3.1. Detailed survey of Western edge of Mackenzie Trough

The Western Mackenzie Trough has very limited seafloor-mapping information. We conducted a targeted multibeam survey in this area with survey lines of ~20 km in length trending in a northwest-southeast direction. Water depths of the survey area ranged from ~70 m to ~180 m. We identified two primary targets, a narrow trough aligned sub-parallel to the survey lines and several possible Pingo-Like Features (PLF) with heights of ~10 m and widths of ~20 m (Figure 3.3). The multibeam data collected during this survey formed the base data for the subsequent Autonomous Underwater Vehicle (AUV) survey (see Chapter 5).

3.3.2. Detailed survey of Yukon Shelf

We conducted a second multibeam bathymetric survey of a target area off the Yukon coast where the only multibeam seafloor mapping information was collected on the incoming transit toward Herschel Island from the Yukon border (Figure 3.4). This transit crossed a seabed feature of potential significance to understanding the glacial imprint on this shelf area. The survey was conducted in an ESE-WNW orientation, parallel to the incoming survey line. Eight additional parallel lines progressing southward were surveyed at about 100 m spacing. Each covered a slightly expanded length to accomplish coverage of the target feature. The goal of this survey was to image a greater extent of a curvi-linear feature that may be an esker deposit or a moraine trending in an east-west direction. Water depths in this survey area range from ~40 m to ~ 60 m. The feature rises 4 to 5m above the seafloor, as indicated by the orange colour in Figure 3.4. The seabed in the survey area also registered multiple ice scours of varying width and orientation, some cross-cutting the raised feature.

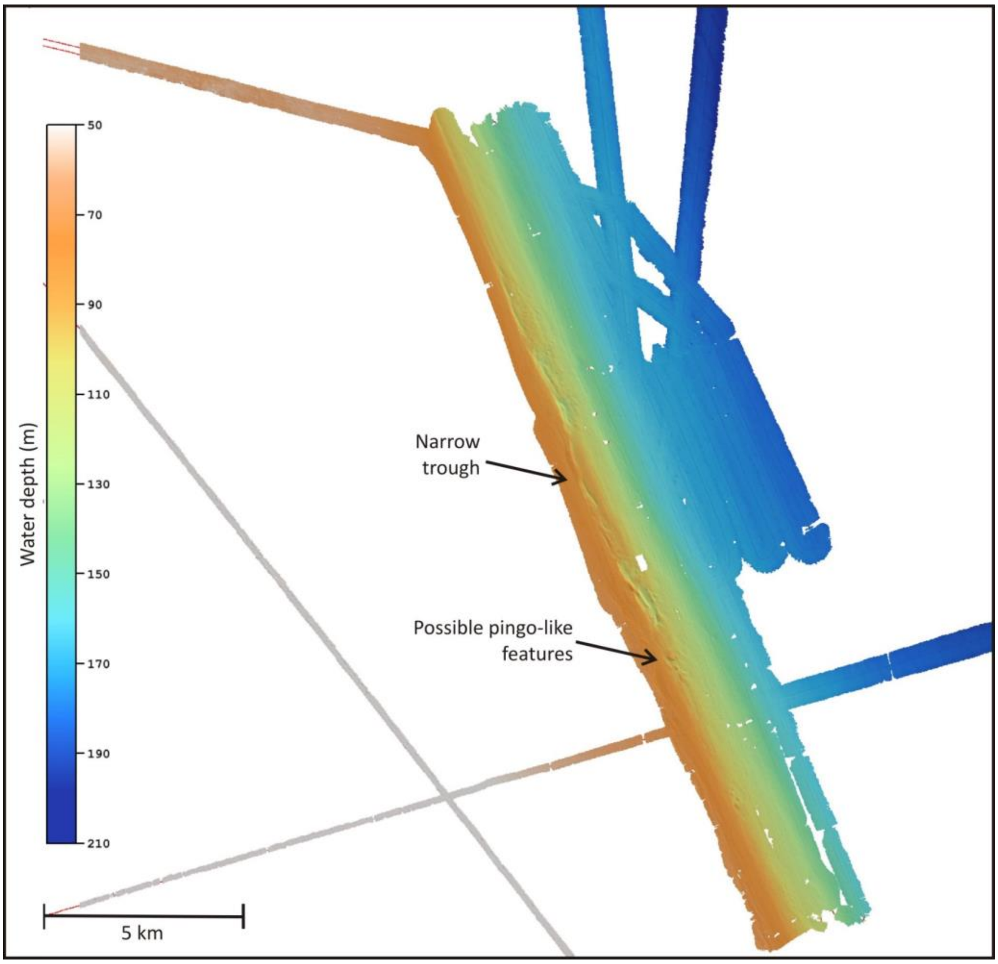

Figure 3.3. Bathymetry of Western Mackenzie Trough survey. Location of survey shown in Figure 3.1.

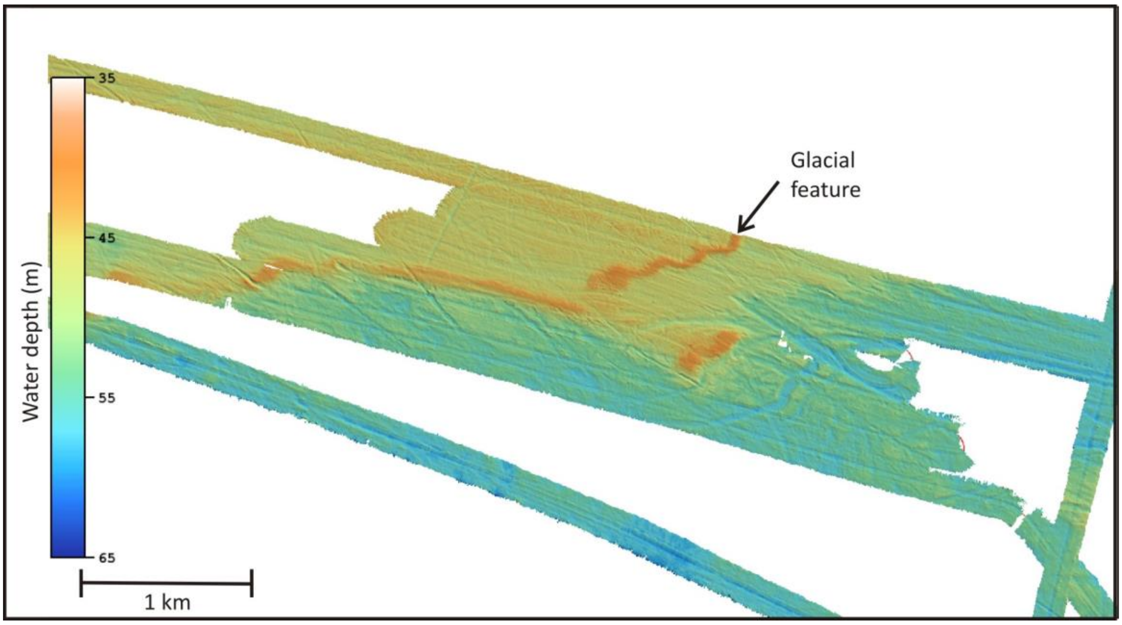

Figure 3.4. Bathymetry of Yukon Coast targeted survey area with the glacial feature shown in orange. Location of survey shown in Figure 3.1.

Chapter 4. Sub-bottom Profiler Survey

E.L. King, H.J. Kim, S. Kim, and J.H. Jung

4.1. Introduction

Subsurface images obtained from sub-bottom profiler (SBP) can reveal detailed sediment structure to shallow depths (10s of metres) below the seabed. Conventional SBP equipment transmits 3.5 kHz acoustic signals and receives reflections. The resolution of SBP is typically higher other seismic reflection methods such as Sparker, Boomer, and airgun seismic instruments. Theoretically, SBP has vertical resolution of up to 10 cm, depending on the sediment P-wave velocity structure. In most cases, vertical resolution is ~0.5 m or better.

In the survey area of the Canadian Beaufort Sea, many subsurface structures are closely related to the geologic evolution of glaciation, permafrost, gas expulsion, submarine landslides and slumps. Sub-bottom images will provide additional insight on these features. Sub-bottom images are also utilized to define the optimum site for sediment coring, CPT and heat flow measurements (Figure 4.1).

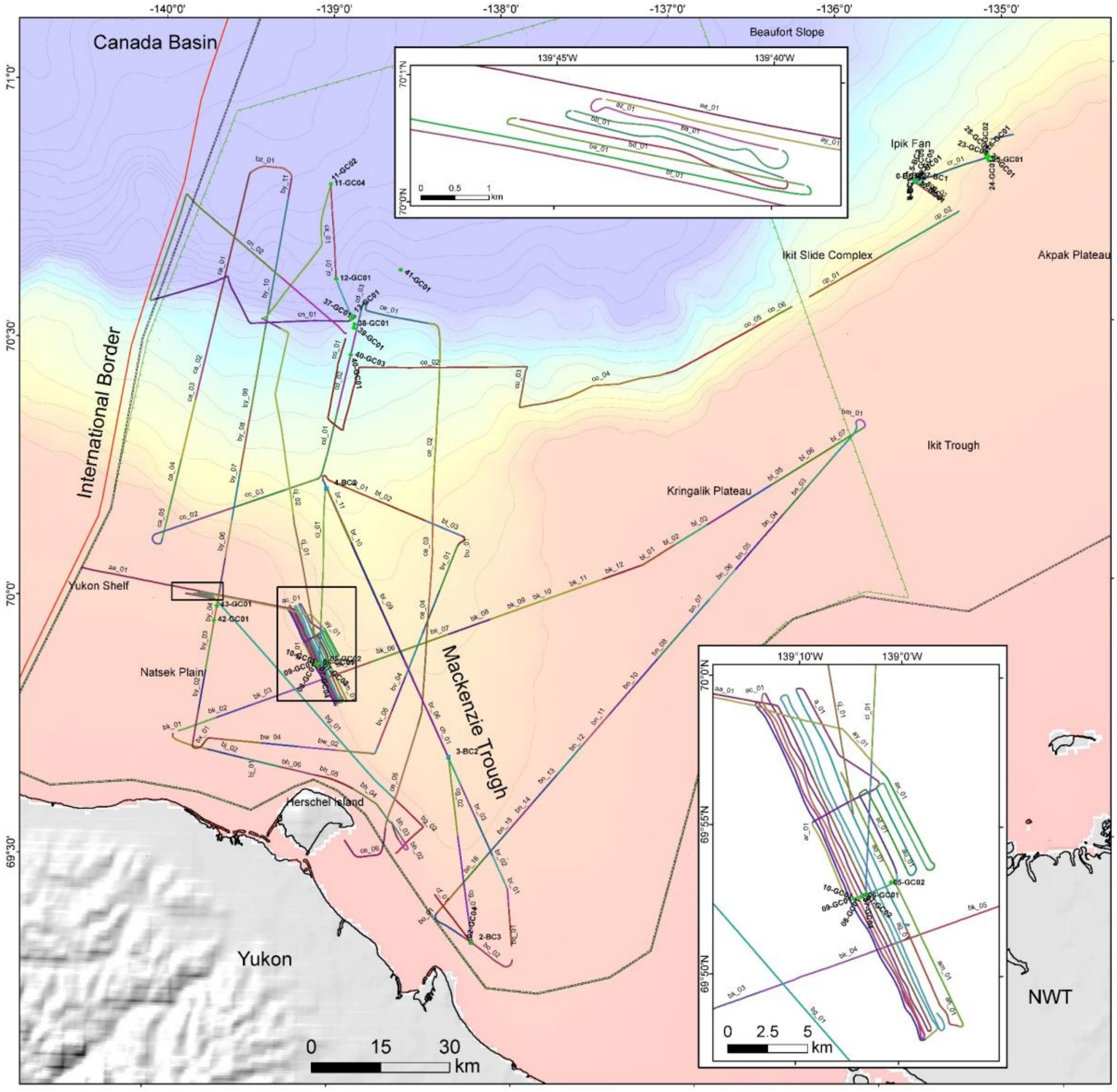

Figure 4.1. Tracklines of Kongsberg 120 SBP data collected during the ARA08C expedition. Stations are also shown.

4.2. System Description

The SBP120 sub-bottom profiler installed on the ARAON is an optional extension to the EM122 multibeam echo sounder. Figure 4.2 shows the SBP system diagram.

The receiving transducer hydrophone array used by the EM122 multibeam system is a broadband system; by adding a separate low frequency transmitting transducer and electronic cabinets and operator stations, the EM122 can be extended to include the sub-bottom profiling capability, as provided by the SBP120. System beam width is 12 degrees with 24 transducers, equivalent to a footprint of 20 m in 100 m water depth (or 20% of water depth).

The frequency range of the SBP120 is 2.5 to 7.0 kHz. The SBP120 beam is electronically stabilized for roll and pitch. It can also be steered to take into account bottom slope. The ping rate is synchronized to that of the multibeam echo sounder transmitter if both are running simultaneously.

The data produced by SBP120 are logged in the Kongsberg proprietary Topas .raw format and can be converted to SEG-Y format that allows post-processing by standard seismic processing software packages. The SBP120 settings used during ARA08C are summarized in Table 4.1. The system was operated simultaneous with the MCS survey, and on all transects related to transiting to other shipboard operations (e.g. AUV, ROV, sampling) while in Canadian waters.

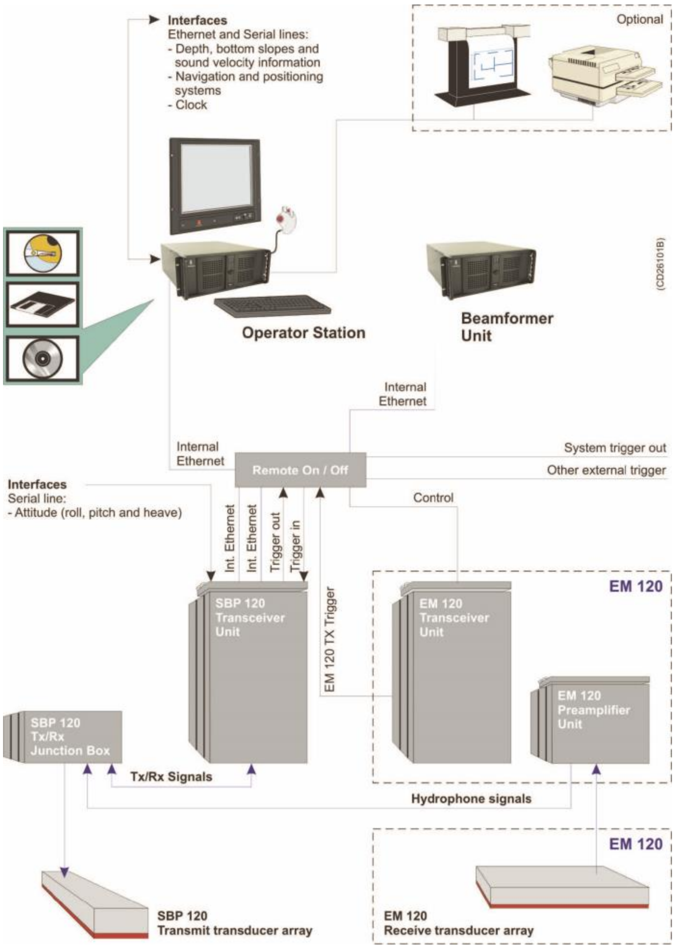

Figure 4.2. System diagram of SBP120 sub-bottom profiler system.

The SBP SEG-Y formats were converted to JP2000 format for convenient viewing and preliminary onboard interpretation. This is a freeware wavelet-based high-fidelity process developed and distributed by the Geological Survey of Canada (Courtney, 2013) whereby the screen presentation is dynamically drawn from the trace waveforms (i.e. not a fixed image) to a full zoom, pan and aspect ratio (vertical versus horizontal scale) adjustable screen presentation. The JP2000 seismic viewer has embedded filtered navigation and provides a flexible user-generated point (marker) and polyline (i.e. interpreted horizon picks with x,y,z coordinates) interpretation scheme with flexible GIS shapefile export capability. Images are approximately 10% of the SEG-Y file size yet maintain at least 95% of the trace waveform fidelity. Individual (relatively short-transit) SEG-Y files derived from the .raw files were concatenated (with ship-speed-corrected navigation) into much longer-transit seismic profiles with a start and end Julien Day and UTC time stamp in the filenames such that the entire cruise dataset comprises 41 files.

Table 4.1. Setting information of SBP120 during cruise ARA08C.

Used Settings	Value	Unit
Runtime Parameter		
Trasmit mode	Normal	
Synchronization	Fixed ping rate	ms
Acquisition delay	Manual & automatic mode	ms
Acquisition window	400	ms
Pulse form	Linear chirp up	
Sweep low frequency	2500	Hz
Sweep high frequency	6500	Hz
Pulse shape	80	%
Pulse length	30	ms
Source power	0	dB
Beam widths Tx	Normal	
Beam widths Rx	Normal	
Number of Rx beams	1	
Beam spacing	3	1 deg
Calculate delay from depth	X	
Delay hysteresis	30	%
Bottom screen position	50	%
Automatic slope corrections	On	
Gain	15 & 20 & 30	dB
Bottom tracker		
Window start	Manual & automatic mode	ms
Window length	20	ms
Threshold	80	%
Time Variable Gain		
TVG control	Manual	

4.3. Results

4.3.1. Data coverage

The sub-bottom profiler collected 2,174 km of continuous profiler data (Figure 4.1). These add significantly to the amount of exisiting SBP data collected on the Yukon Shelf, mostly under the ArcticNet programme and by the USCGS Healy. Failure of the system on September 10, due to hardware issues, prevented any further profiling for the cruise duration.

Preliminary viewing and interpretation of the data were conducted onboard using both the freeware Open Detect and GSC JP2Viewer software, largely to provide the setting and context for other operations, including details of AUV dive-sites and identifying gravity core targets. Figure 4.3 shows a typical SBP profile and its utility in establishing basic stratigraphic and geomorphic setting in selecting sediment core sites.

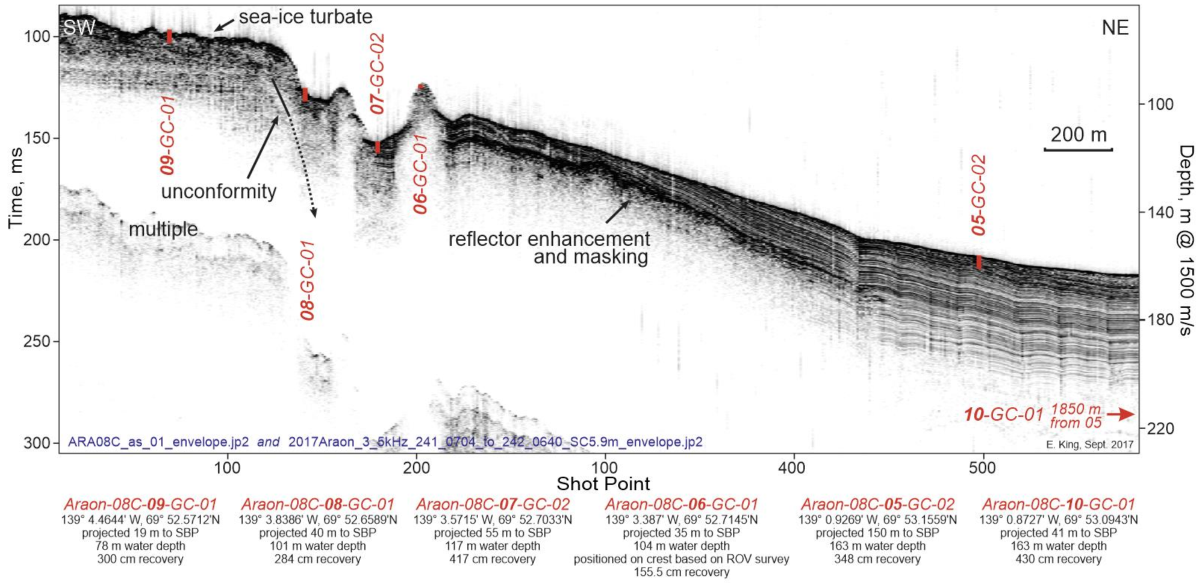

Figure 4.3. An ARA08C SBP example from the western flank of the Mackenzie Trough with a series of coresites.

4.3.2. Highlights from SBP data

The ARA08C expedition has contributed significantly to an increase in the SBP coverage collected and available for interpretation, both for the Mackenzie Trough and moreso for the Yukon Shelf. The SBP and MCS datasets complement each other with some overlapping penetration range. Horizons visible even in the brute stack MCS have equivalents in the SBP.

Two target areas for detailed SBP and MB surveys were chosen; the first one was located on the western flank of the Mackenzie Trough and the second one was across a sinuous seabed ridge identified from the MB data during the transit eastward from Alaska (see Figure 4.1 inserts for locations). The ARA08C SBP and MB data were processed and viewed immediately onboard and were used as a basis for planning ROV and AUV surveys. These datasets identified elongated troughs and ridges and Pingo-Like Features (PLFs) as shown in Figure 4.3 and discussed in Chapter 3. Subsequent SBP and MB transects crossing the marked bank edge and into the Mackenzie Trough confirmed its continuity.

4.3.2.1. Yukon Shelf

The widely spaced regional network of survey lines targeted the nearly entirely unknown morphology, stratigraphy and permafrost condition of the Yukon Shelf. Some elements of the geology are readily correlated in a broad sense, such as a basal, nearly impenetrable (to SBP) surface, both buried and exposed at the seabed, locally matching a stratigraphic horizon. A very slightly dipping stratified unit overlies this but is largely eroded, manifest as an angular unconformity with a broadly sculpted topography. Pervasive iceberg or sea-ice (or both) scour reaching several metres below the seabed, characterizes all but the basal unit. Features such as broad, tabular banks with superimposed topographic features, typically with 10 m relief, are not well delimited from the sparse survey network on initial inspection. Neither is the geometry of the even finer-scale seabed features immediately recognized except where one or occasionally two adjacent MB passes were collected. These have 3-5 m relief, ridges and/or mounds.

At the shelf break, both large slide headwalls and erosional seabed are now recognized as ubiquitous, with the increase survey coverage.

4.3.2.2. Mackenzie Trough

The Mackenzie Trough is generally covered with 40 to 80 m of glacimarine and post-glacial well stratified muds (Figure 4.4). Several axial and cross lines were collected which, together with the ArcticNet coverage, are deemed sufficient to correlate facies and features related both to the late glacial, the deglacial, the post-glacial and several diagenetic processes within the Trough. This will contribute greatly toward glacial deposit mapping and a broad stratigraphic and chronologic context for a range in rather unique anomalous acoustic facies. These are associated with glacial and iceberg processes, late glacial and postglacial environmental evolution, subsequent structural disturbances, erosion events, mass failures and suspected fluid and locally gas efflux.

4.3.2.3. Outermost Mackenzie Trough

The shelf break is commonly marked by headwalls of mass failures but this is not ubiquitous. A near continuous blanket of stratified sediment is confirmed from earlier, but sparse survey coverage. This continues out to more than 1700 m water depth where groundtruth was collected in a short core. Occasional mass failure deposits were also targeted with cores for which the SBP will provide sufficient continuity to trace a rough chronology via key horizons.

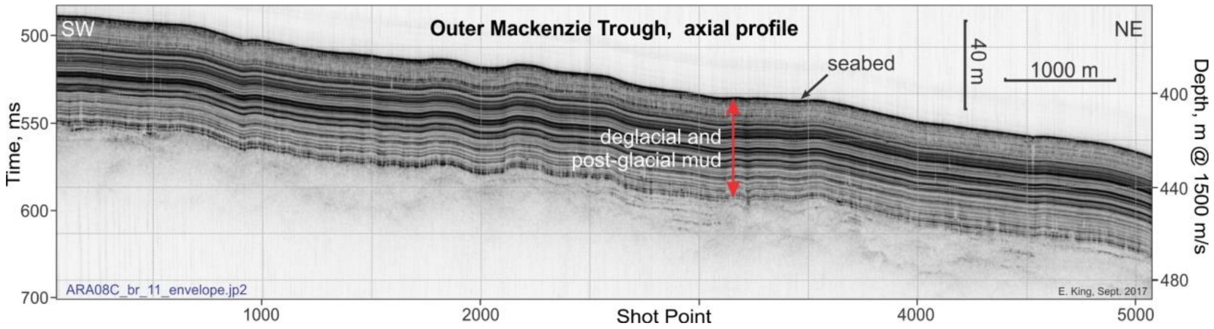

Figure 4.4. SBP from the axial line in outer Mackenzie Trough.

4.3.2.4. Beaufort Shelf

The shallow shelf of the Beaufort registered a rather transparent and continuous acoustic unit with chaotic reflections in the upper 5 to 10 m, all with an ice-scoured seabed. An unconformity below this is marked with structurally or depositionally more complex facies and the unconformable surface registers both high and low amplitudes (Figure 4.5).

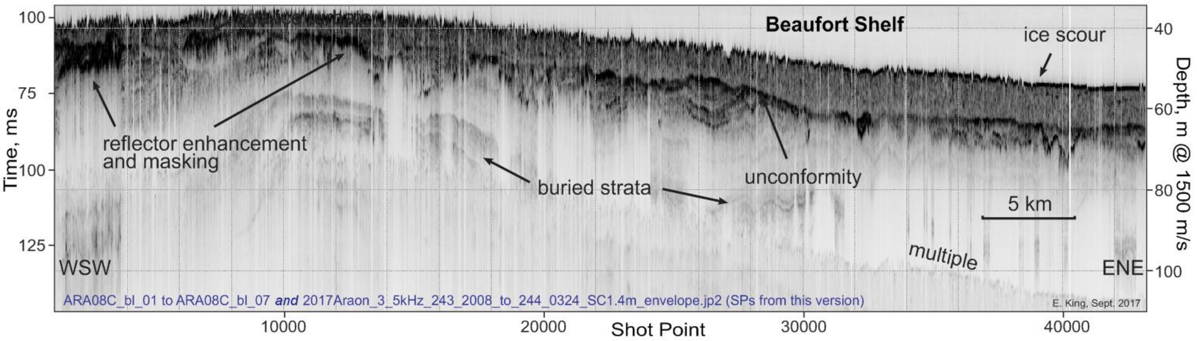

Figure 4.5. SBP across the mid Beaufort Shelf registering a uniform surficial mud and complex geometry and stratigraphy below an unconformity.

References

Courtney, R.C. 2013. Canada GEESE 2: Visualization of Integrated Marine Geoscience Data for Canadian and Proximal Waters. *Geoscience Canada*, S.l.: 141-148.

Chapter 5. Seafloor Mapping Using Autonomous Underwater Vehicle

D.W. Caress, C.K. Paull, D. Conlin, and E. Trauschke

5.1. Introduction

Due to the importance of the seafloor as an interface and as the locus of many globally important geological, geochemical, and biological processes, seafloor mapping through acoustic remote sensing of topography, bottom character, and subsurface structure is one of the fundamental activities in Oceanography. In order to achieve high-resolution seafloor mapping, the sonars must be operated close to the seafloor. The most efficient means currently available are autonomous robots called autonomous underwater vehicles (AUVs) equipped with both high frequency mapping sonars and high precision navigation systems. On this expedition, one of the Dorado class AUVs designed, built, and operated by MBARI was used to obtain 1-m-scale bathymetry and backscatter seafloor maps along with CHIRP sub-bottom profiles.

During this expedition, the new and previously collected MBARI Mapping AUV data have provided basic observations of seafloor morphology, character, and structure along with providing context for ROV-based inspection and sampling and ship-based coring.

5.2. MBARI Dorado Mapping AUV

5.2.1. Overview of the Mapping AUVs

The MBARI mapping AUVs (Caress et al., 2008) are 0.53 m diameter, Dorado class autonomous underwater vehicles equipped with 400 kHz multibeam sonar, 110 and 410 kHz sidescan sonars, and a 1-6 kHz sub-bottom profiler (Figure 5.1). All components of the vehicles are rated to 6,000 m depth. Using precise navigation and attitude data from a laser-ring-gyro-based inertial navigation system (INS) integrated with a Doppler velocity log (DVL) sonar, MBARI Mapping AUVs can image the deep-ocean seafloor and shallow subsurface structure with much greater resolution than is possible with sonars operated from surface vessels. Typical survey operations use a vehicle speed of 1.5 m per second (3 knots) and an altitude of 50 m to achieve about 1 m horizontal and 10 cm vertical resolution. Mission durations are up to 20 hours, allowing survey tracklines as long as 100 km. Battery recharge and data download between missions requires about 5 hours. The MBARI Dorado AUVs are maintained and operated by the AUV Group within the Division of Marine Operations. Since 2006, some 255 successful surveys have been conducted using the Mapping AUVs, including the three achieved during this expedition. MBARI Mapping AUVs have been operated on several non-MBARI vessels, include *R/V Thomas Thompson*, *R/V Atlantis*, *CCGS Sir Wilfrid Laurier*, *Ocean Researcher 1*, *Ocean Researcher 5*, and now the icebreaker *Araon*.

Although the vehicle fielded during ARA08C has been in operation for over a decade, many key systems have been upgraded or replaced as the available mapping and navigation technology have improved. The systems integrated with the Mapping AUV on this expedition include:

- Multibeam sonar: Reson 7125-AUV 400 kHz
- Sidescan sonar: Edgetech FSAU 110 kHz CHIRP sidescan
- Sub-bottom sonar: Edgetech FSAU 1-6 kHz sub-bottom profiler
- CTD: SeaBird Electronics SBE49 Fastcat CTD
- Doppler Velocity Log (DVL): 300 kHz Teledyne-RDI Workhorse Navigator DVL
- Inertial Navigation System (INS): Kearfott SeaDevil w/300 kHz DVL
- Pressure Sensor: Paroscientific 8CB4000 4000-m rated Intelligent Depth Sensor
- Ultra Short Baseline tracking beacon: Sonardyne AvTrak 6G
- Acoustic Modem: Teledyne-Benthos 3G LF Acoustic Modem, directional transducer
- Batteries: Two MBARI-design 5 kWhr battery spheres using lithium ion battery packs from Inspired Energy

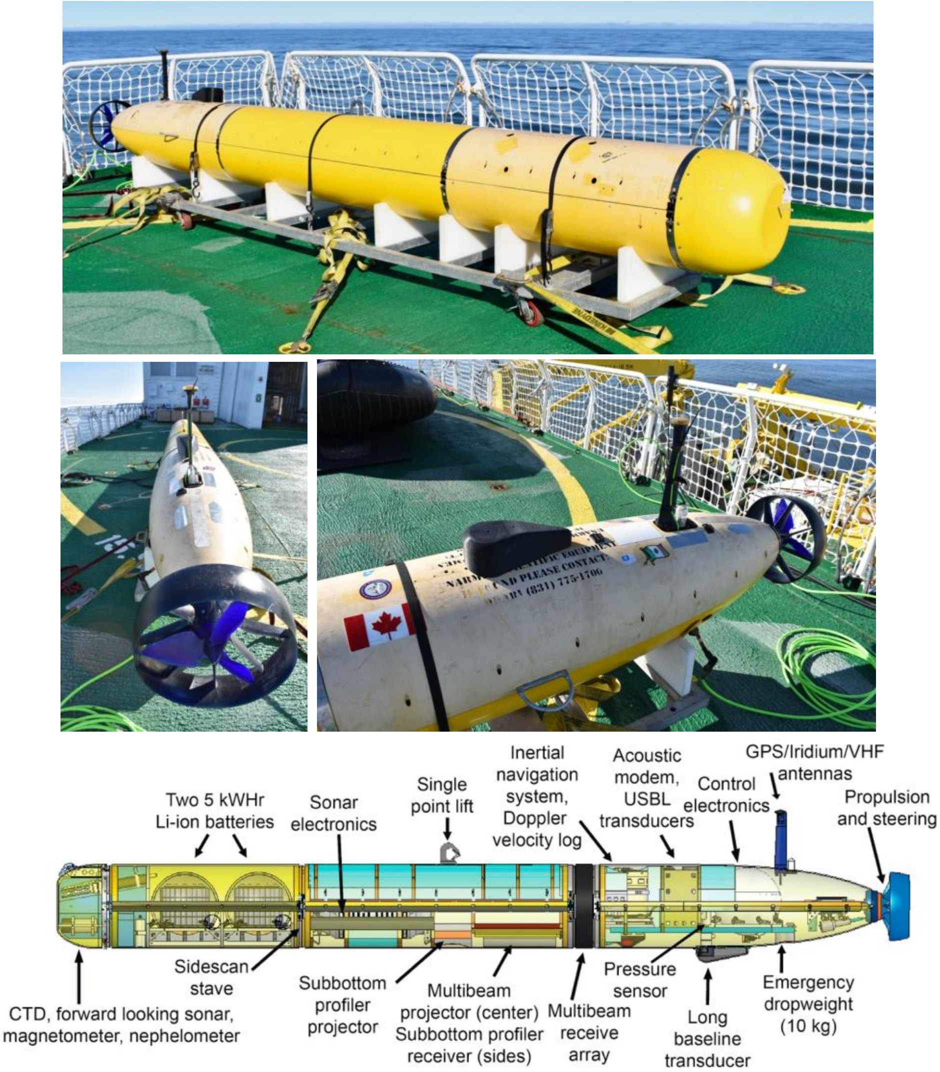

Figure 5.1. (Top) MBARI Mapping AUV secured on the Araon helideck during ARA08C. The AUV was charged, maintained, and launched from the helideck. (Middle) Views of the AUV tail showing the single articulating propeller and the propeller duct, which is the sole control surface on this torpedo shaped robot. (Bottom) CAD drawing showing system level layout of the AUV internals.

5.2.2. AUV launch and recovery on the Araon

The approach used for launch and recovery of large AUVs such as Dorado vary between ships according to the available deck space, crane configuration, and crew comfort level for small boat operations. Following a detailed review of previous MBARI AUV launch and recovery scenarios, the MBARI AUV team and the Araon crew jointly chose to locate the AUV on the heliport between operations, to launch and recover the AUV over the starboard side using the large starboard crane located on the fantail, and to use the ship's small boat to capture and side-tow the AUV to the Araon where it could be hooked into the crane. The pictures shown in Figure 5.2 illuminate the key aspects of the small boat based recovery. Four launch and recovery operations were conducted without incident.

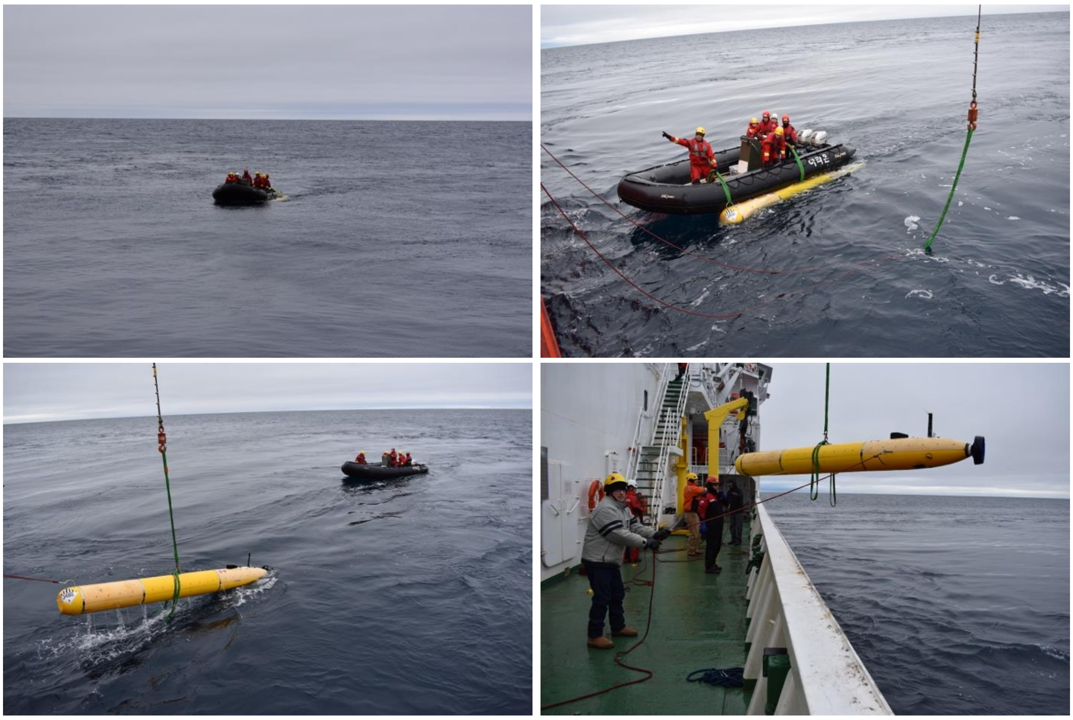

Figure 5.2. Recovery of the AUV on Araon using the ship's small boat. The boat crew side-towed the AUV up to the ship and then clipped the crane lifting strap into the AUV's lifting bale, also attaching two tag lines to the AUV nose. The boat then stood clear as the AUV was lifted onto the lower deck. At that point the tag lines were reset to safely conduct an immediate lift up to the AUV cradle on the helideck.

5.2.3. Mapping AUV data processing

The Mapping AUV multibeam, sidescan, and sub-bottom profiler data have been processed using the open source software package MB-System (Caress and Chayes, 1995; Caress et al., 2017). The workflow largely proceeded as follows:

- Data download from AUV (approximately one hour), typically 150 GB raw data.
  - Multibeam data are logged in the Reson s7k format, with file suffixes *.s7k.
  - Sidescan and sub-bottom profiler data are logged together in files in the Edgetech jstar format, with file suffixes *.jsf.
  - AUV INS navigation and attitude data, CTD data, and other AUV data streams are logged in MBARI Dorado MVC log files, with file suffixes *.log. These files are in a

format particular to MBARI, but all data can be extracted using the MB-System program mbauvloglist.

- Multibeam data
  - Preprocessing using program mbpreprocess
    : Apply platform offsets and time latencies
    : Recalculate bathymetry using improved sound speed values
    : Apply autofiltering of soundings based on sonar data metrics
  - Interactive editing of soundings using program mbeditviz
  - Navigation adjustment using program mbnavadjust, which identifies overlapping and crossing swathes, picks relative navigation offsets required for bathymetric features to match in overlapping data, and solves for an optimal navigation model.
  - Calculate empirical multibeam backscatter correction function using program mbbackangle. MBbackangle uses the multibeam bathymetry to determine bottom grazing angles for each backscatter value, allowing the calculation of an average backscatter versus grazing angle model.
  - Apply all edits and corrections, merge the adjusted navigation, and produce a set of processed swath files using the program mbprocess. The processed multibeam data are in the same data format as the original logged data, which is the Reson s7k format. Since s7k files are supported by MB-System as format 88, the processed files all have the suffixe *p.mb88 according to MB-System file naming conventions.

- Edgetech Sidescan and Sub-bottom data
  - Sidescan data are in the form of match filtered envelope time series, not yet associated with position on the seafloor
  - Sub-bottom data are in the form of the raw match filtered, complex correlate time series
  - Preprocessing using program mbpreprocess
    : Merge optimal navigation model from multibeam processing
    : Apply platform offsets
    : Output still in Edgetech jstar format, though with MB-System file suffix *.mb132

- Sidescan data
  - Extract sidescan using program mbsslayout
    : Lays out raw time series sidescan onto a 1-m bathymetry model derived from the multibeam data
    : Organizes sidescan data into sequential lines organized according to the waypoints of the AUV mission
    : Output is sidescan in the form of pixels on the seafloor, stored in MB-System generic format 71, with file suffixes *.mb71
    : Calculate empirical sidescan backscatter correction function using program mbbackangle. MBbackangle uses a bathymetric model from the multibeam data to determine bottom grazing angles for each sidescan sample, allowing the calculation of an average backscatter versus grazing angle model.
    : Apply the backscatter correction using program mbprocess. The processed sidescan files have the suffixe *p.mb71.
    : Apply a spatial smoothing filter to the sidescan using program mbfilter.

- Sub-bottom profiler data
  - Extract sub-bottom using program mbextractsegy.
    : Calculate envelope times series
    : Output SEGY format files (SIOSEIS variant with deep water delay field in trace header). Figures 5.3 and 5.4 show examples of the AUV data visualization and editing capabilities.

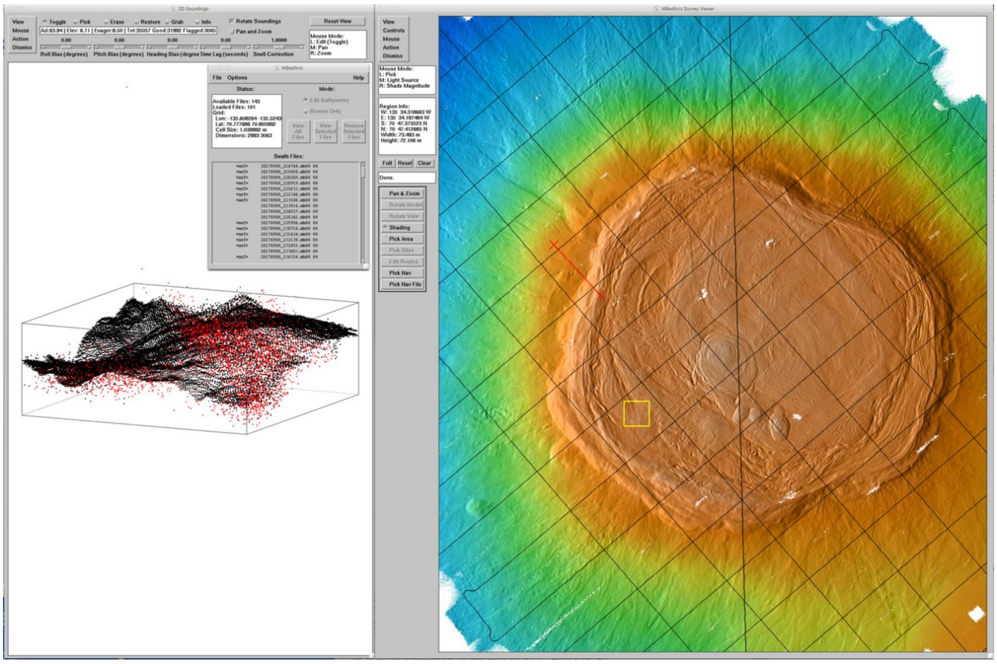

Figure 5.3. MB-System program MBeditviz used to edit the Mapping AUV multibeam bathymetry from mission 20170908m1.

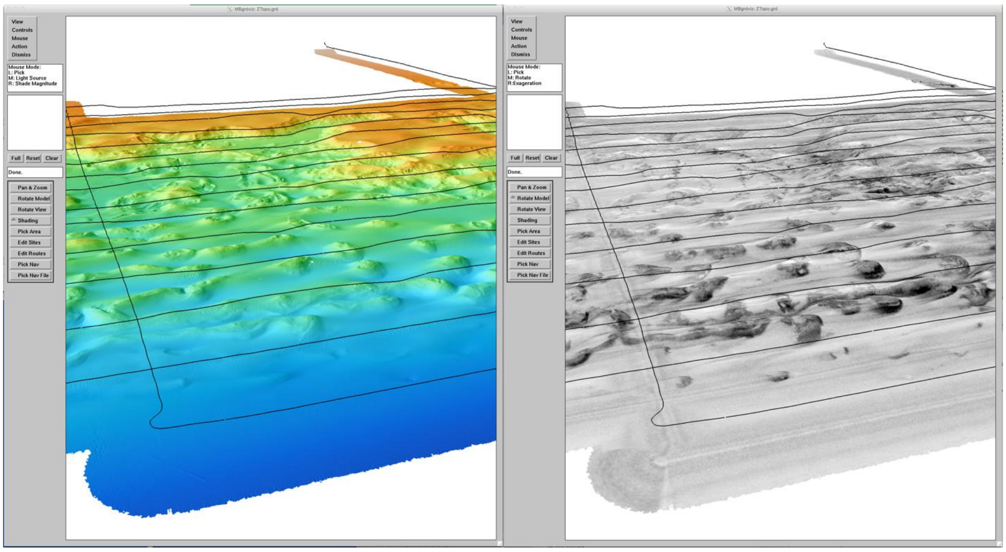

Figure 5.4. MB-System program MBgrdviz used to visualize Mapping AUV multibeam data from mission 20170910m1, showing both color illuminated bathymetry and bathymetry draped with multibeam backscatter (high amplitudes dark).

5.3. High Resolution Seafloor Mapping Results

5.3.1. Summary

Four AUV missions were conducted during the second phase of the expedition, after the completion of the multichannel seismic reflection profiling. One AUV mission failed because the INS was not receiving the DVL estimates of velocity over bottom that are necessary for successful navigation. The other three missions were completely successful and collected excellent multibeam, sidescan, and sub-bottom data. Figure 5.5 shows previous and current missions. Table 5.1 summarizes the AUV deployments during ARA08C and Figures 5.6 to 5.29 show various aspects, including bathymetry, slope, backscatter and sub-bottom profiles.

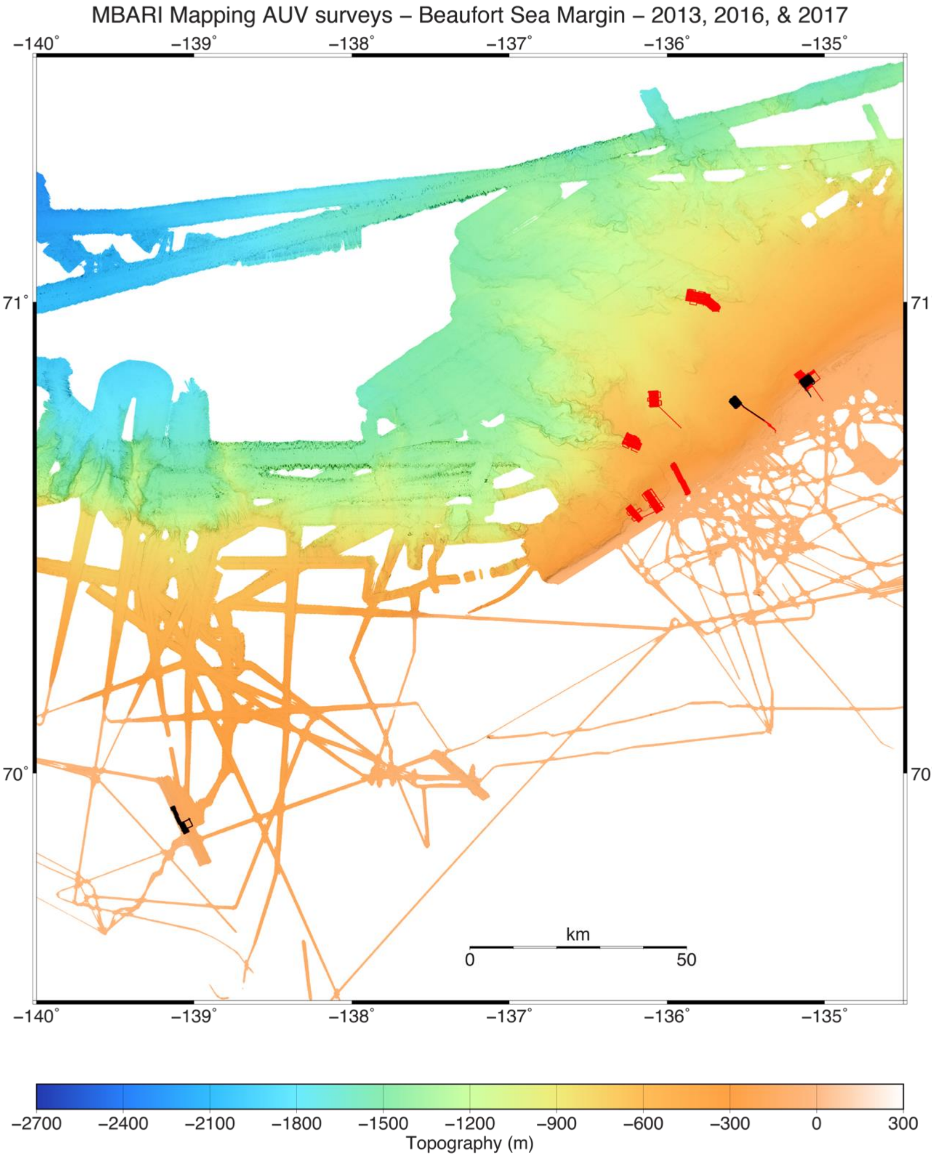

Figure 5.5. Locations of MBARI Mapping AUV surveys on the Canadian Beaufort Sea margin shown overlain on regional ship-based multibeam survey data, including EM122 data collected by the Araon during ARA08C. The red tracklines show Mapping AUV surveys conducted from the CCGS Sir Wilfrid Laurier from expeditions during 2013 and 2016. The black tracklines show the surveys conducted from Araon during this expedition.

Table 5.1. MBARI Mapping AUV deployments during ARA08C.

Mission ID	**20170905m1**	**20170908m1**	**20170909m1**	**20170910m1**
Mission Name	WesternFlankMackenzie_S__m1_v4	MudVolcano420m_M1V8	ShelfedgePingo_alongstrike_M1_V5	ShelfedgePingo_alongstrike_M1_V10
Success / Failure	Success	Success	Failure	Success
Launch Longitude	-139.055351	-135.314064	-135.086333	-135.086383
Launch Latitude	69.87478	70.727946	70.80603	70.802401
Launch Depth	107 m	103 m	99 m	97 m
Launch Time	2017-09-05-23:00 UTC	2017-09-08-21:14 UTC	2017-09-09-22:15 UTC	2017-09-11-04:10 UTC
Recovery Time	2017-09-06-15:25 UTC	2017-09-09-16:04 UTC	2017-09-10-16:05 UTC	2017-09-11-17:20 UTC
AUV Data Recorded	14.58 hours	17.31 hours	0 hours	11.07 hours

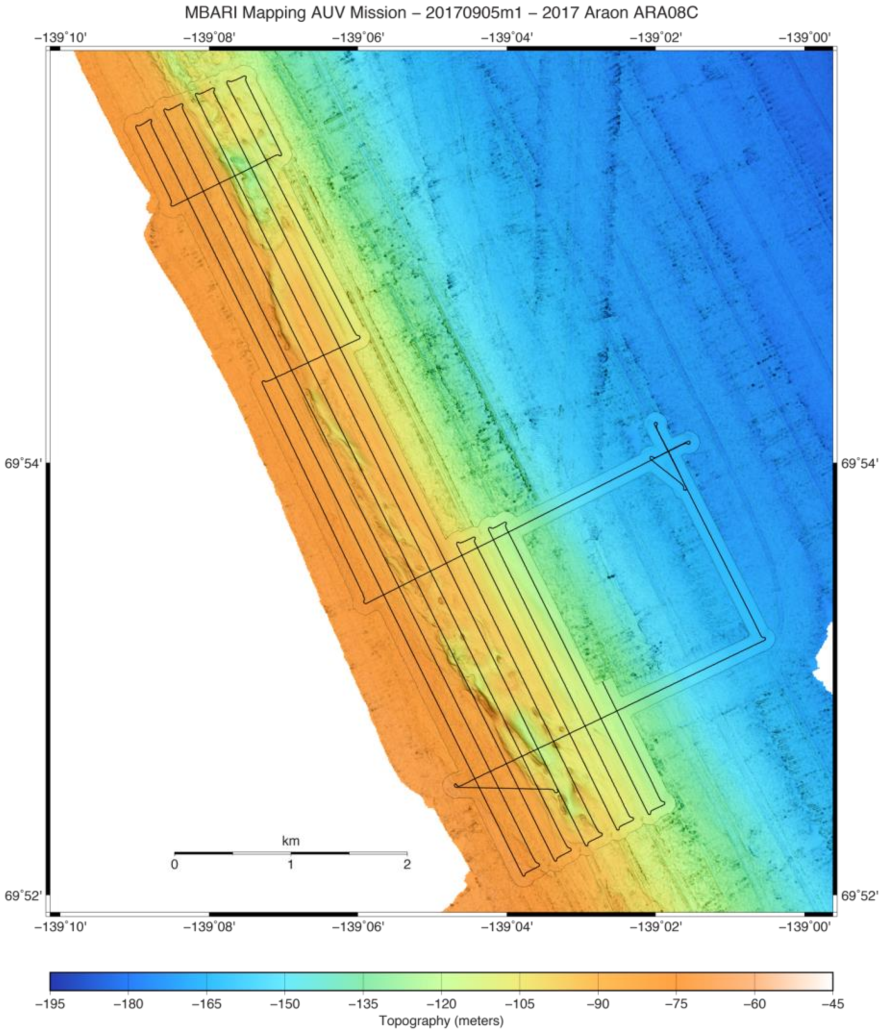

Figure 5.6. Location of Mapping AUV Mission 20170905m1 in the West Mackenzie Trough margin area. AUV tracks are shown overlain on Mapping AUV multibeam bathymetry, which is in turn overlain on the available hull mounted multibeam bathymetry (mostly collected from the Araon on this expedition).

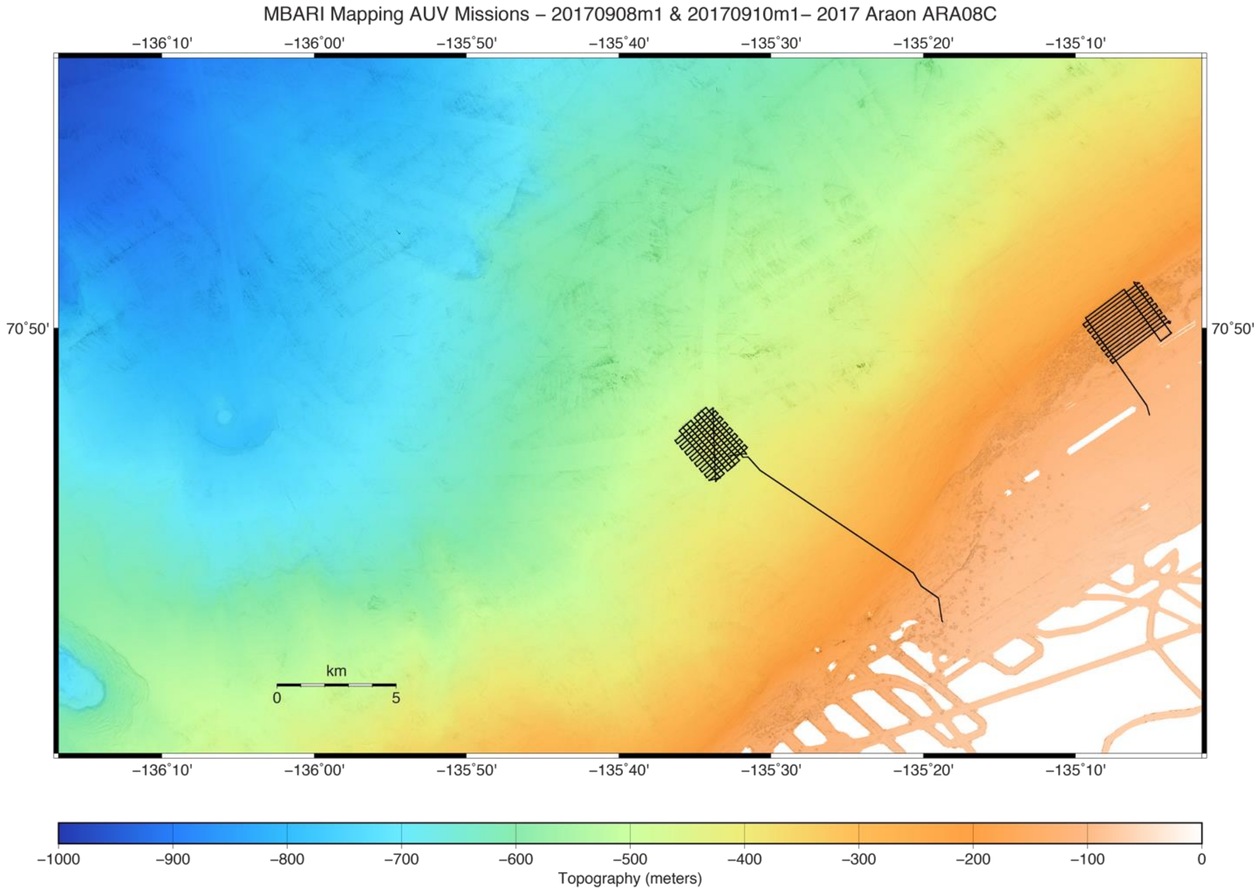

Figure 5.7. Location of Mapping AUV missions 20170908m1 and 20170910m1 in the West Mackenzie Trough margin area. AUV tracks are shown overlain on the available hull mounted multibeam bathymetry, most of which were collected by CCGS Amundsen between 2009 and 2014.

5.3.2 Mission 20170905m1 – West Mackenzie Trough Margin

The multibeam data collected during mission 20170905m1 are summarized in Table 5.2. The sidescan and sub-bottom data correspond to the same time and spatial domain, but are organized in 38 sequential line files delineated by the waypoints in the AUV mission.

Table 5.2. Multibeam data statistics from Mapping AUV Survey 20170905m1.

MBARI Mapping AUV Mission 20170905m1 Multibeam Data Totals:
Number of Records: 163980
Bathymetry Data (512 beams):
Number of Beams: 83957760
Number of Good Beams: 59969871 71.43%
Number of Zero Beams: 19092498 22.74%
Number of Flagged Beams: 4895391 5.83%
Amplitude Data (512 beams):
Number of Beams: 83957760
Number of Good Beams: 59969871 71.43%
Number of Zero Beams: 19092498 22.74%
Number of Flagged Beams: 4895391 5.83%
Sidescan Data (2048 pixels):
Number of Pixels: 335831040
Number of Good Pixels: 70827770 21.09%
Number of Zero Pixels: 0 0.00%
Number of Flagged Pixels:265003270 78.91%
Navigation Totals:
Total Time: 14.5762 hours
Total Track Length: 69.3595 km
Average Speed: 4.7584 km/hr (2.5721 knots)
Start of Data:
Time: 09 05 2017 23:34:32.818000 JD248 (2017-09-05T23:34:32.818000)
Lon: -139.055482828 Lat: 69.874840423 Depth: 105.3970 meters
Speed: 4.3486 km/hr (2.3506 knots) Heading: 121.6962 degrees
Sonar Depth: 48.8161 m Sonar Altitude: 56.6515 m
End of Data:
Time: 09 06 2017 14:09:07.100999 JD249 (2017-09-06T14:09:07.100999)
Lon: -139.045287856 Lat: 69.883156948 Depth: 124.5433 meters
Speed: 5.0330 km/hr (2.7205 knots) Heading: 334.1714 degrees
Sonar Depth: 74.7729 m Sonar Altitude: 50.8809 m
Limits:
Minimum Longitude: -139.152542569 Maximum Longitude: -139.006496396
Minimum Latitude: 69.867272379 Maximum Latitude: 69.930603095
Minimum Sonar Depth: 17.4319 Maximum Sonar Depth: 120.2442
Minimum Altitude: 45.9100 Maximum Altitude: 75.3900
Minimum Depth: 65.3962 Maximum Depth: 168.7925
Minimum Amplitude: -20.5608 Maximum Amplitude: 76.4755
Minimum Sidescan: 0.0000 Maximum Sidescan: 15961.9727

Included below are representative maps of the multibeam bathymetry, multibeam backscatter, and mosaicked sidescan imagery from this mission. Also included is an example of a sub-bottom profiler section plot.

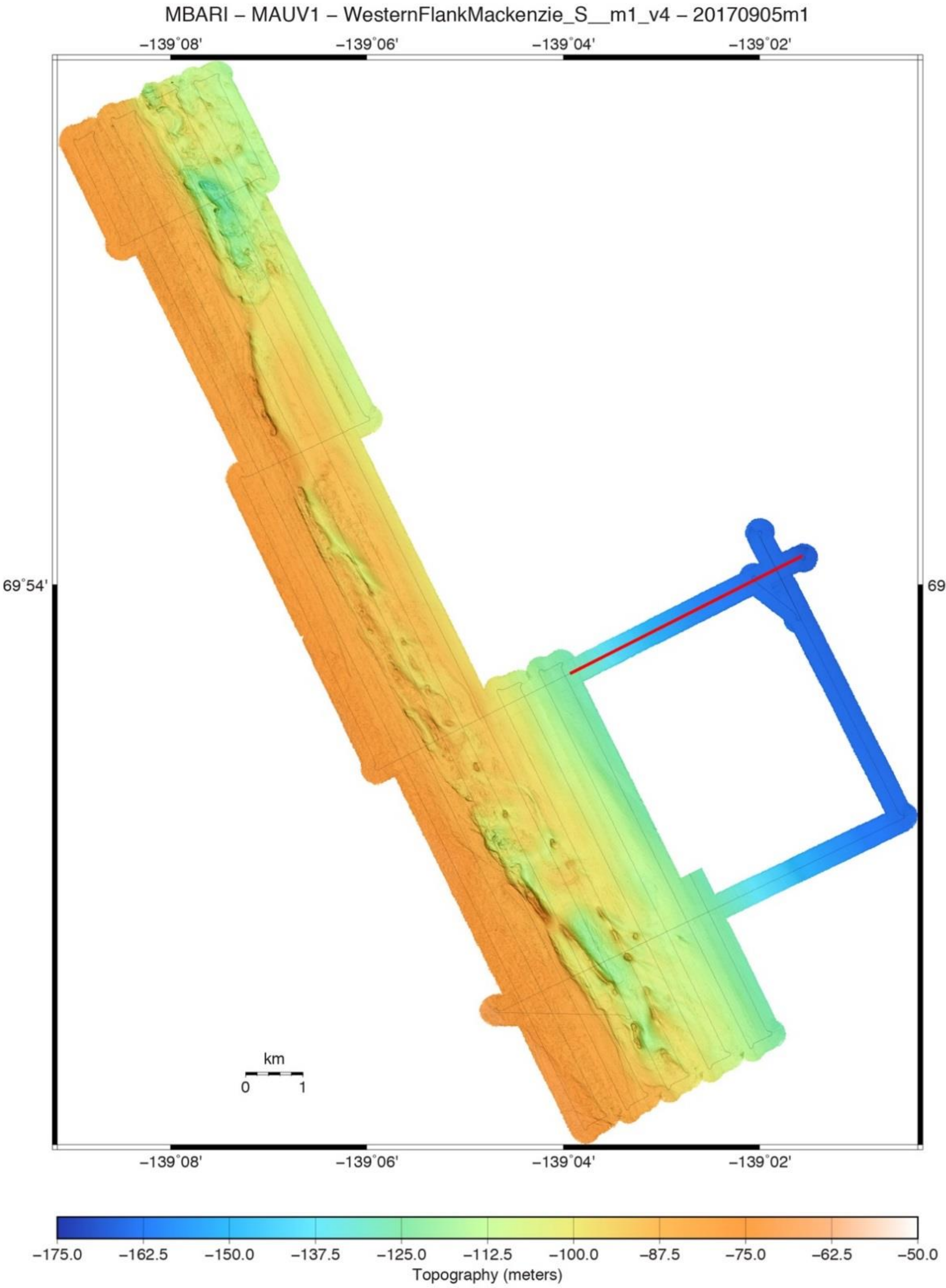

Figure 5.8. Mapping AUV 1-m resolution multibeam bathymetry from mission 20170905m1 displayed with slope magnitude shading overlain by the AUV tracklines. Three MiniROV dives and several cores were sited in this area. The red line indicates the location of the sub-bottom profiler section shown in Figure 5.13.

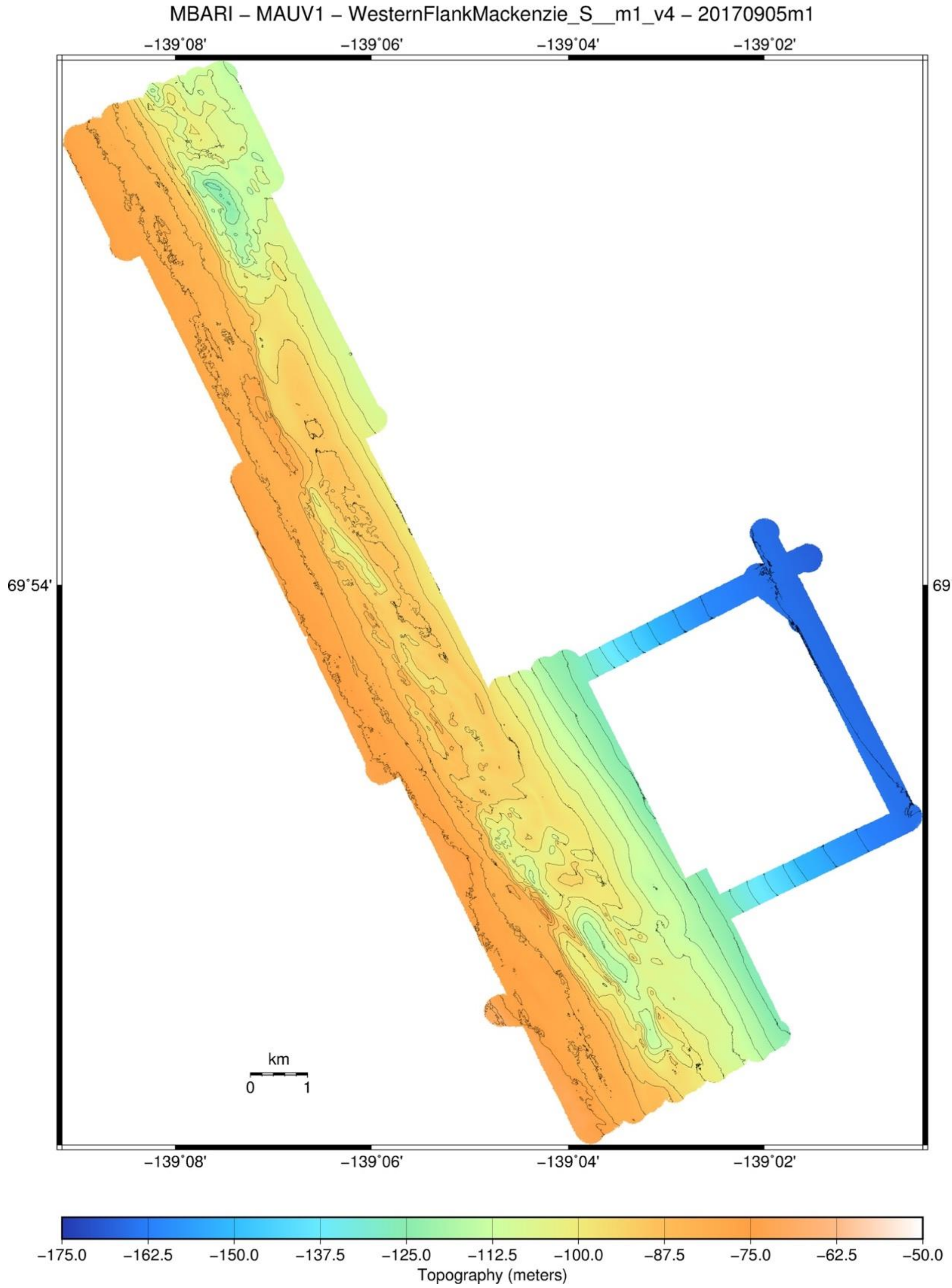

Figure 5.9. Mapping AUV 1-m resolution multibeam bathymetry from mission 20170905m1 displayed with 10-m contours. Three MiniROV dives and several cores were sited in this area.

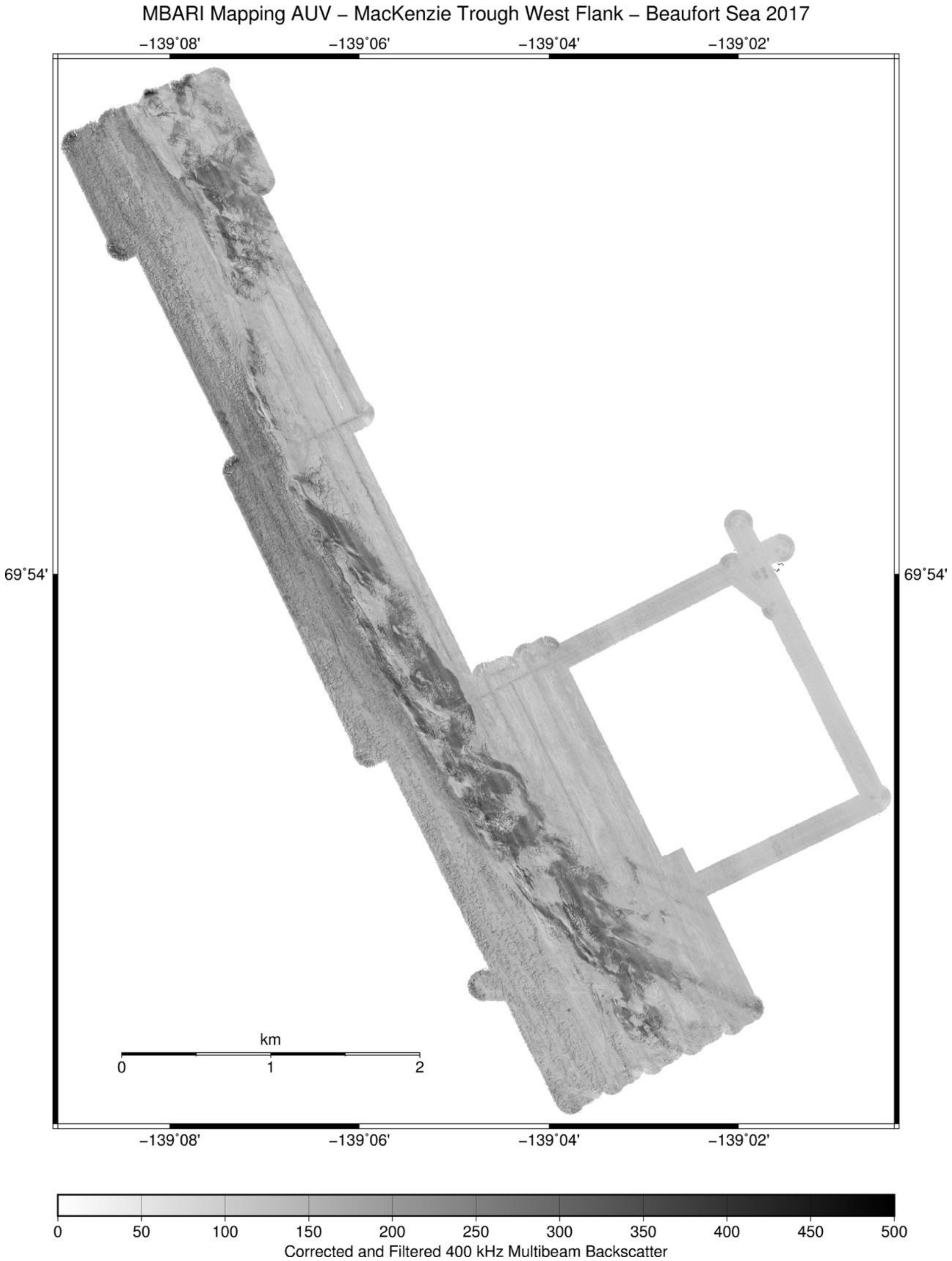

Figure 5.10. Mapping AUV 1-m resolution multibeam backscatter from mission 20170905m1. Three MiniROV dives and several cores were sited in this area. The backscatter has been corrected using an empirical amplitude-vs-grazing angle model and had a Gaussian smoothing filter applied. High amplitudes are shown dark.

Figure 5.11. Mapping AUV 1-m resolution CHIRP 110 kHz sidescan from mission 20170905m1. Three MiniROV dives and several cores were sited in this area. This mosaic has been constructed from east-northeastward-looking data only. The sidescan has been corrected using an empirical amplitude-vs-grazing angle model and had a Gaussian smoothing filter applied. High amplitudes are shown dark.

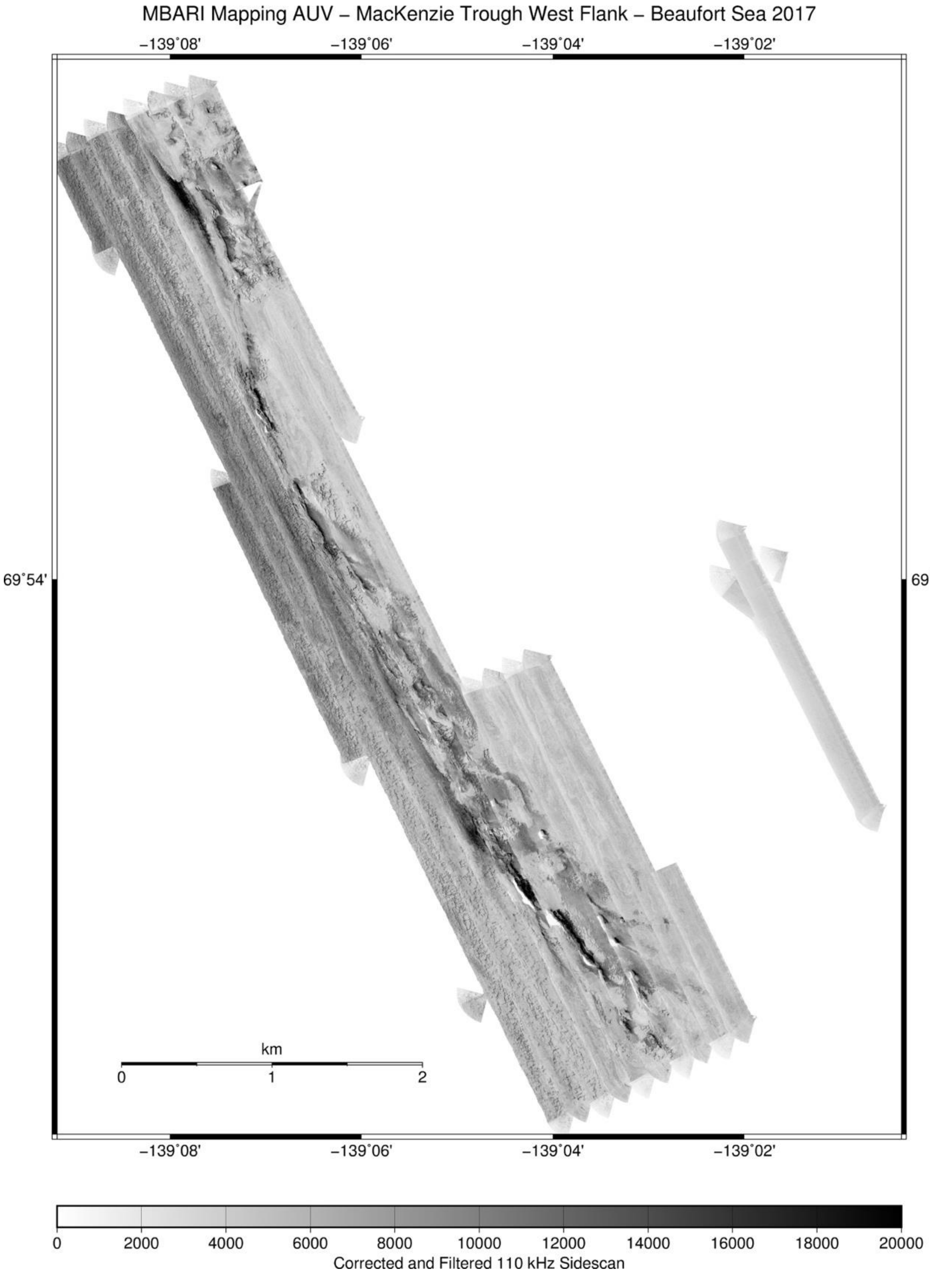

Figure 5.12. Mapping AUV 1-m resolution CHIRP 110 kHz sidescan from mission 20170905m1. Three MiniROV dives and several cores were sited in this area. This mosaic has been constructed from west-southwestward-looking data only. The sidescan has been corrected using an empirical amplitude-vs-grazing angle model and had a Gaussian smoothing filter applied. High amplitudes are shown dark.

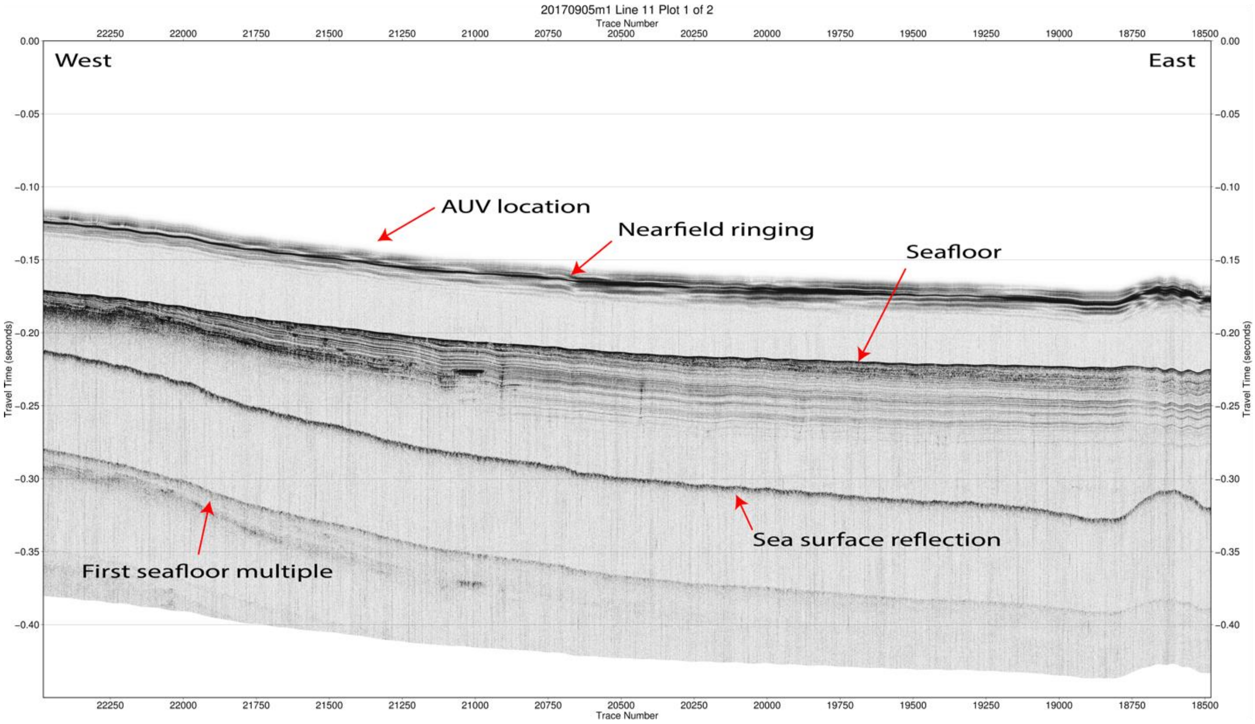

Figure 5.13. Mapping AUV CHIRP 1-6 kHz sub-bottom profiler data from mission 20170905m1. The section is shown "hung" from the AUV's location in the water column, generally about 50-m above the seafloor. The location of this profile is shown be a red line on Figure 5.8. Arrows indicates locations of sub-seafloor and multiple reflections. Surface reflections are seen in the AUV collected CHIRP profiles when the vehicle is operated in <150 m water depths.

5.3.3. Mission 20170908m1 – 420 m mud volcano

The multibeam data collected during mission 20170908m1 are summarized in Table 5.3. The sidescan and sub-bottom data correspond to the same time and spatial domain, but are organized in 79 sequential line files delineated by the waypoints in the AUV mission.

Table 5.3. Multibeam data statistics from Mapping AUV Survey 20170908m1.

MBARI Mapping AUV Mission 20170908m1 Multibeam Data Totals:
Number of Records: 194750
Bathymetry Data (512 beams):
Number of Beams: 99712000
Number of Good Beams: 62686359 62.87%
Number of Zero Beams: 30984964 31.07%
Number of Flagged Beams: 6040677 6.06%
Amplitude Data (512 beams):
Number of Beams: 99712000
Number of Good Beams: 62686359 62.87%
Number of Zero Beams: 30984964 31.07%
Number of Flagged Beams: 6040677 6.06%
Sidescan Data (2048 pixels):
Number of Pixels: 398848000
Number of Good Pixels: 71920946 18.03%
Number of Zero Pixels: 0 0.00%
Number of Flagged Pixels:326927054 81.97%
Navigation Totals:
Total Time: 17.3105 hours
Total Track Length: 85.0623 km
Average Speed: 4.9139 km/hr (2.6562 knots)
Start of Data:
Time: 09 08 2017 21:47:44.752998 JD251 (2017-09-08T21:47:44.752998)
Lon: -135.313401959 Lat: 70.727861025 Depth: 102.0037 meters
Speed: 4.7156 km/hr (2.5490 knots) Heading: 57.8871 degrees
Sonar Depth: 52.8383 m Sonar Altitude: 49.1654 m
End of Data:
Time: 09 09 2017 15:06:22.582000 JD252 (2017-09-09T15:06:22.582000)
Lon: -135.545877106 Lat: 70.793572930 Depth: 431.7865 meters
Speed: 4.2009 km/hr (2.2708 knots) Heading: 310.9851 degrees
Sonar Depth: 397.3683 m Sonar Altitude: 35.6421 m
Limits:
Minimum Longitude: -135.608263567 Maximum Longitude: -135.310842323
Minimum Latitude: 70.727253980 Maximum Latitude: 70.805991908
Minimum Sonar Depth: 35.5905 Maximum Sonar Depth: 423.0259
Minimum Altitude: 18.6731 Maximum Altitude: 72.7583
Minimum Depth: 82.9516 Maximum Depth: 475.8319
Minimum Amplitude: -19.7927 Maximum Amplitude: 72.4181
Minimum Sidescan: 0.0000 Maximum Sidescan: 4012.8599

Included below are representative maps of the multibeam bathymetry, multibeam backscatter, and mosaicked sidescan imagery from this mission. Also included is an example of a sub-bottom profiler section plot.

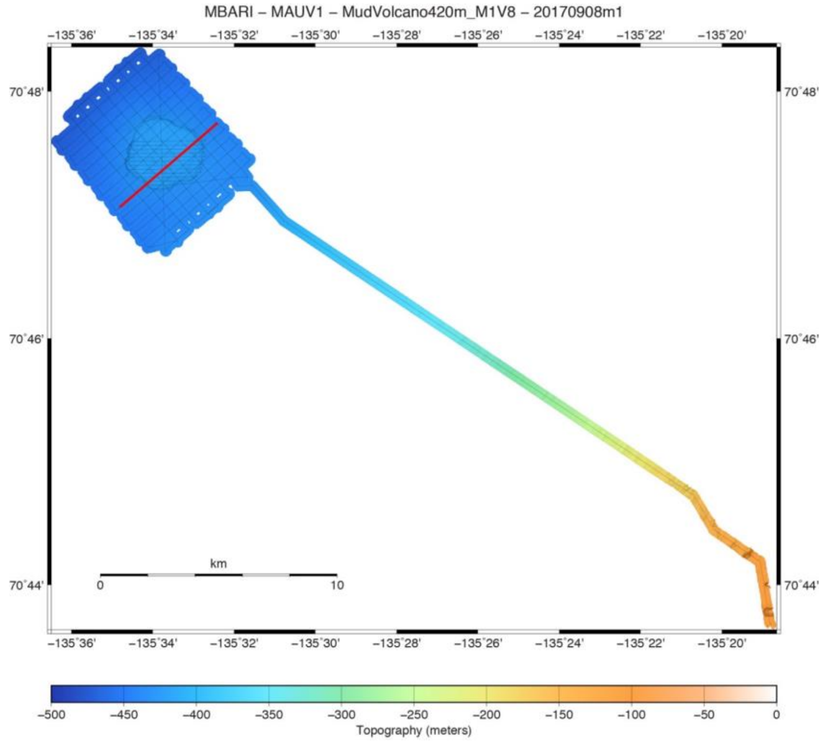

Figure 5.14. Mapping AUV 1-m resolution multibeam bathymetry from mission 20170908m1 displayed with slope magnitude shading overlain by the AUV tracklines. The red line indicates the location of the sub-bottom profiler section shown in Figure 5.21.

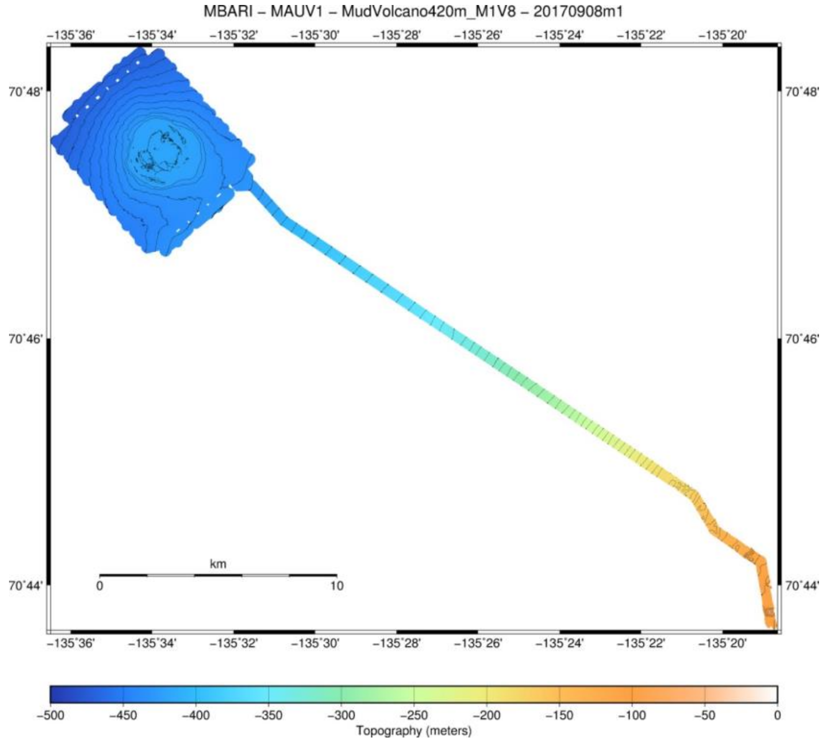

Figure 5.15. Mapping AUV 1-m resolution multibeam bathymetry from mission 20170908m1 displayed with 10-m contours.

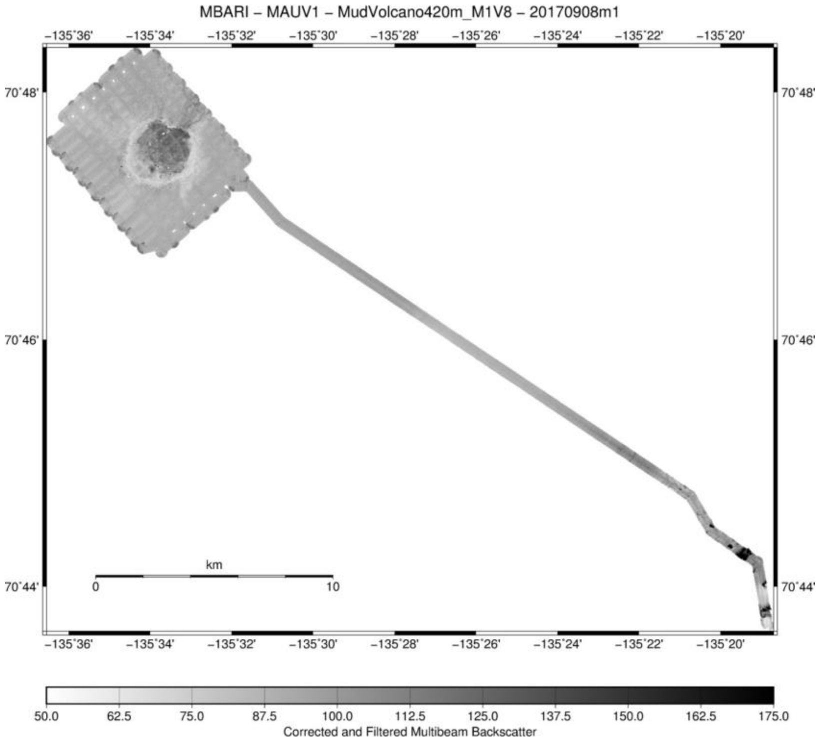

Figure 5.16. Mapping AUV 1-m resolution multibeam backscatter from mission 20170908m1. The backscatter has been corrected using an empirical amplitude-vs-grazing angle model and had a Gaussian smoothing filter applied. High amplitudes are shown dark.

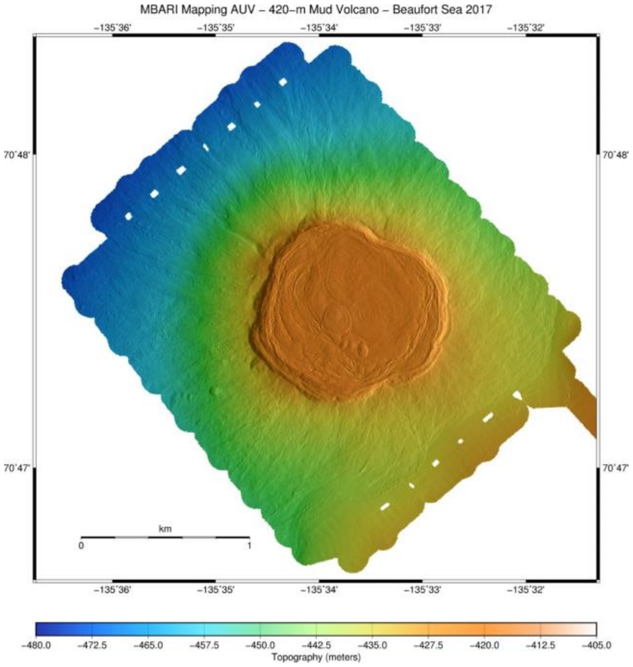

Figure 5.17. Mapping AUV 1-m resolution multibeam bathymetry from mission 20170908m1 displayed illuminated from the east. This map shows the 420-m mud volcano that was also a focus of two MiniROV dives and several gravity and box cores.

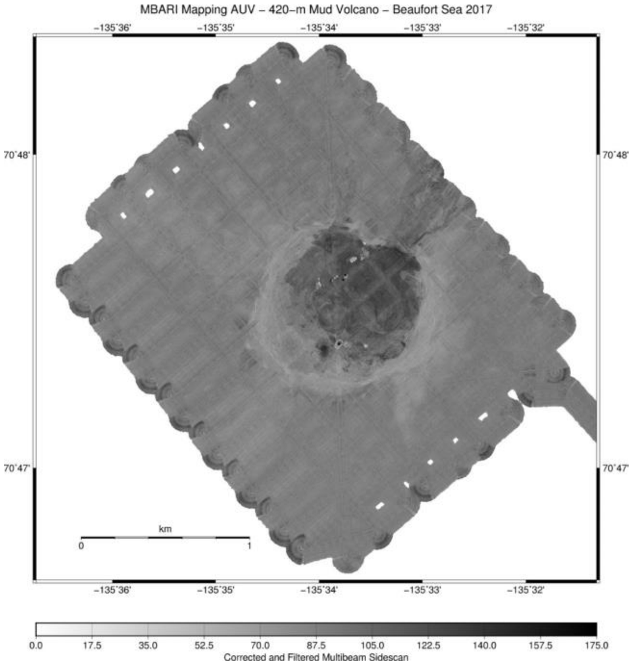

Figure 5.18. Mapping AUV 1-m resolution multibeam backscatter from mission 20170908m1. This map shows the 420-m mud volcano that was also a focus of two MiniROV dives and several gravity and box cores. The backscatter has been corrected using an empirical amplitude-vs-grazing angle model and had a Gaussian smoothing filter applied. High amplitudes are shown dark.

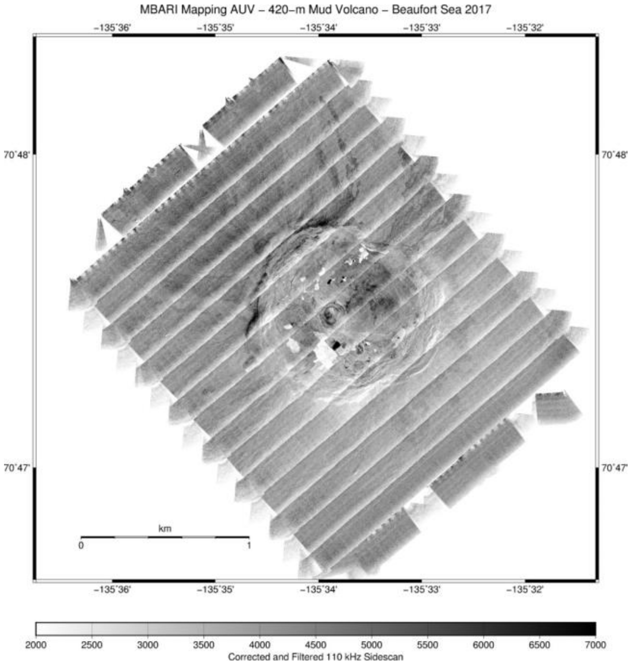

Figure 5.19. Mapping AUV 1-m resolution CHRIP 110 kHz sidescan from mission 20170908m1. This map shows the 420-m mud volcano that was also a focus of two MiniROV dives and several gravity and box cores. This mosaic has been constructed from southeastward-looking data only. The sidescan has been corrected using an empirical amplitude-vs-grazing angle model and had a Gaussian smoothing filter applied. High amplitudes are shown dark.

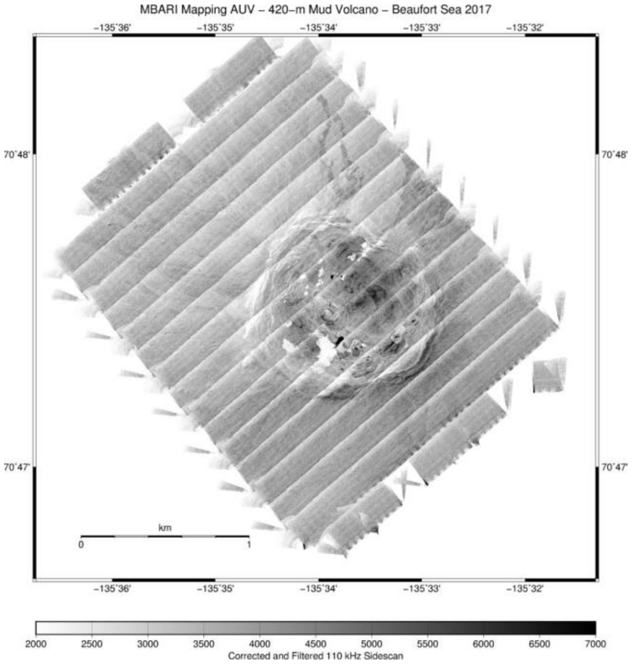

Figure 5.20. Mapping AUV 1-m resolution CHIRP 110 kHz sidescan from mission 20170908m1. This map shows the 420-m mud volcano that was also a focus of two MiniROV dives and several gravity and box cores. This mosaic has been constructed from northwestward-looking data only. The sidescan has been corrected using an empirical amplitude-vs-grazing angle model and had a Gaussian smoothing filter applied. High amplitudes are shown dark.

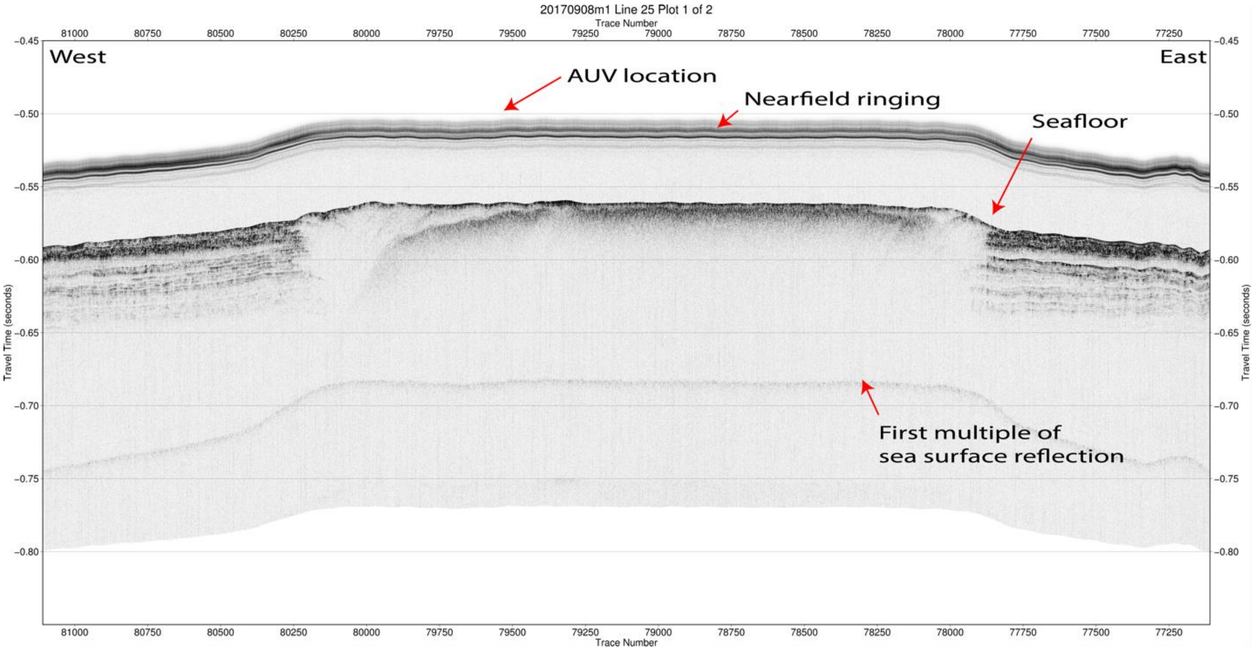

Figure 5.21. Mapping AUV CHIRP 1-6 kHz sub-bottom profiler data from mission 20170905m1. The section is shown "hung" from the AUV's location in the water column, generally about 50-m above the seafloor. The location of this profile is shown be a red line on Figure 5.14. Arrows indicates locations of sub-seafloor and multiple reflections. Surface reflections are seen in the AUV collected CHIRP profiles when the vehicle is operated in <150 m water depths; at 420 m depth the first multiple of the sea surface reflection is visible.

5.3.4. Mission 20170910m1 – East Mackenzie intact margin with pingo-like features

The multibeam data collected during mission 20170910m1 are summarized in Table 5.4. The sidescan and sub-bottom data correspond to the same time and spatial domain, but are organized in 52 sequential line files delineated by the waypoints in the AUV mission.

Table 5.4. Multibeam data statistics from Mapping AUV Survey 20170910m1.

MBARI Mapping AUV Mission 20170910m1 Multibeam Data Totals:
Number of Records: 124525
Bathymetry Data (512 beams):
Number of Beams: 63756800
Number of Good Beams: 42752659 67.06%
Number of Zero Beams: 18465689 28.96%
Number of Flagged Beams: 2538452 3.98%
Amplitude Data (512 beams):
Number of Beams: 63756800
Number of Good Beams: 42752659 67.06%
Number of Zero Beams: 18465689 28.96%
Number of Flagged Beams: 2538452 3.98%
Sidescan Data (2048 pixels):
Number of Pixels: 255027200
Number of Good Pixels: 46357339 18.18%
Number of Zero Pixels: 0 0.00%
Number of Flagged Pixels:208669861 81.82%
Navigation Totals:
Total Time: 11.0687 hours
Total Track Length: 54.9347 km
Average Speed: 4.9630 km/hr (2.6827 knots)
Start of Data:
Time: 09 11 2017 05:41:12.253999 JD254 (2017-09-11T05:41:12.253999)
Lon: -135.086439467 Lat: 70.802400265 Depth: 116.9862 meters
Speed: 3.2727 km/hr (1.7690 knots) Heading: 343.7403 degrees
Sonar Depth: 44.1062 m Sonar Altitude: 72.8800 m
End of Data:
Time: 09 11 2017 16:45:19.739999 JD254 (2017-09-11T16:45:19.739999)
Lon: -135.066348580 Lat: 70.835666719 Depth: 127.5370 meters
Speed: 3.7454 km/hr (2.0245 knots) Heading: 17.4766 degrees
Sonar Depth: 76.6721 m Sonar Altitude: 53.6862 m
Limits:
Minimum Longitude: -135.161924388 Maximum Longitude: -135.059948633
Minimum Latitude: 70.801855341 Maximum Latitude: 70.851008354
Minimum Sonar Depth: 44.1062 Maximum Sonar Depth: 157.7006
Minimum Altitude: 33.4990 Maximum Altitude: 75.7400
Minimum Depth: 89.6860 Maximum Depth: 250.9833
Minimum Amplitude: -20.1772 Maximum Amplitude: 75.6544
Minimum Sidescan: 0.9766 Maximum Sidescan: 1236.3475

.

Included below are representative maps of the multibeam bathymetry, multibeam backscatter, and mosaicked sidescan imagery from this mission. Also included is an example of a sub-bottom profiler section plot.

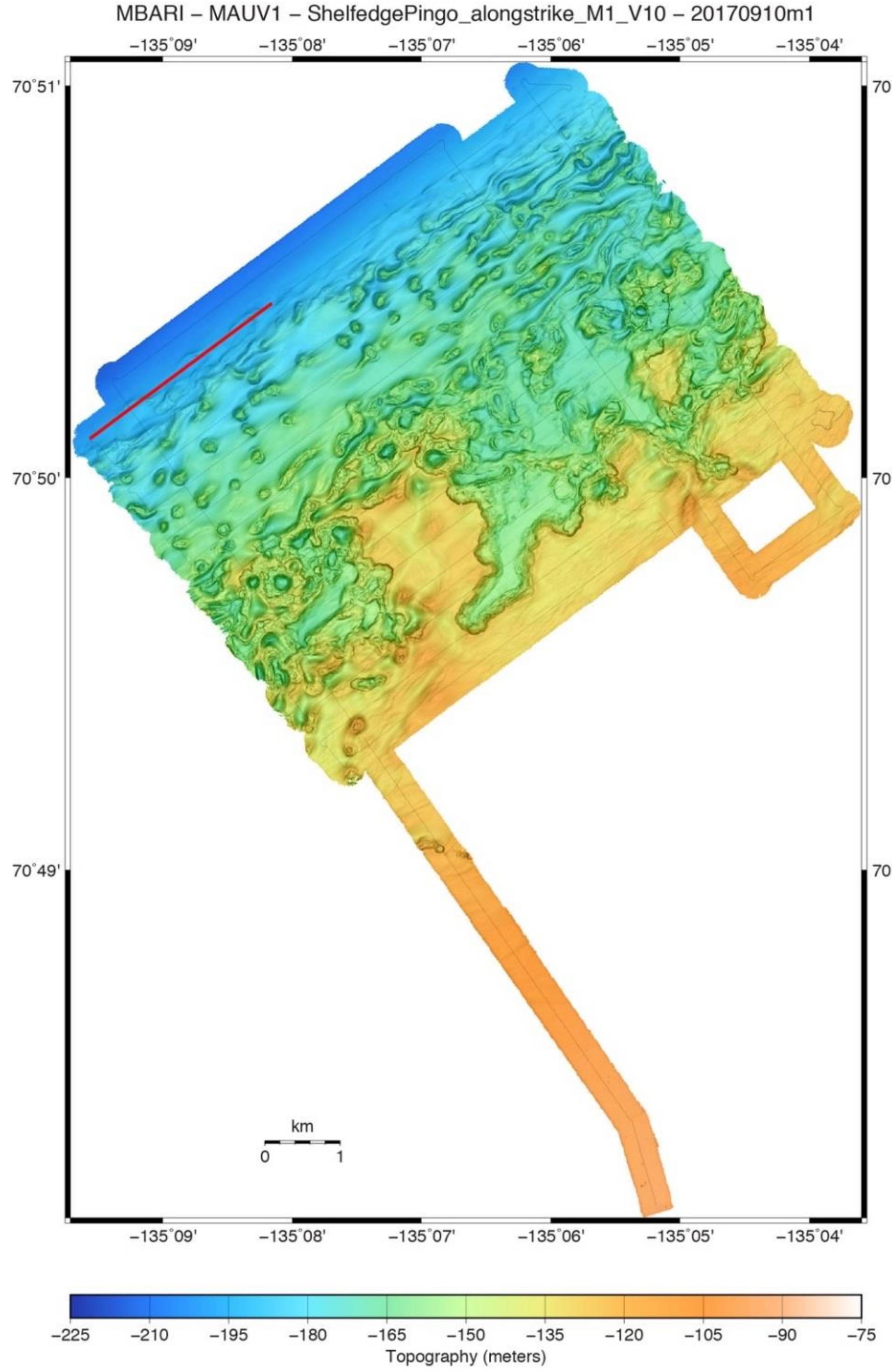

Figure 5.22. Mapping AUV 1-m resolution multibeam bathymetry from mission 20170910m1 displayed with slope magnitude shading overlain by the AUV tracklines. The red line indicates the location of the sub-bottom profiler section shown in Figure 5.29.

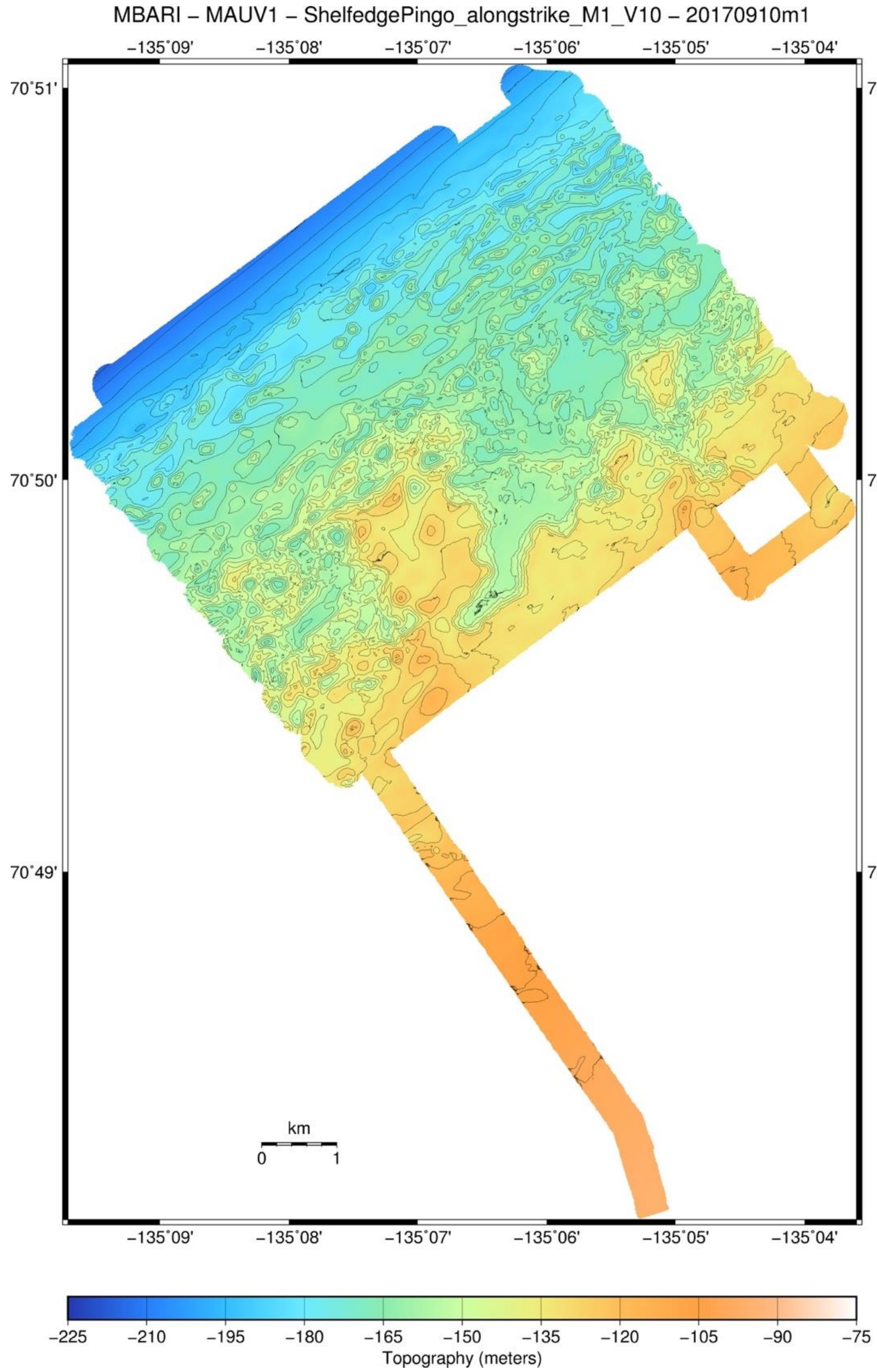

Figure 5.23. Mapping AUV 1-m resolution multibeam bathymetry from mission 20170910m1 displayed with 10-m contours.

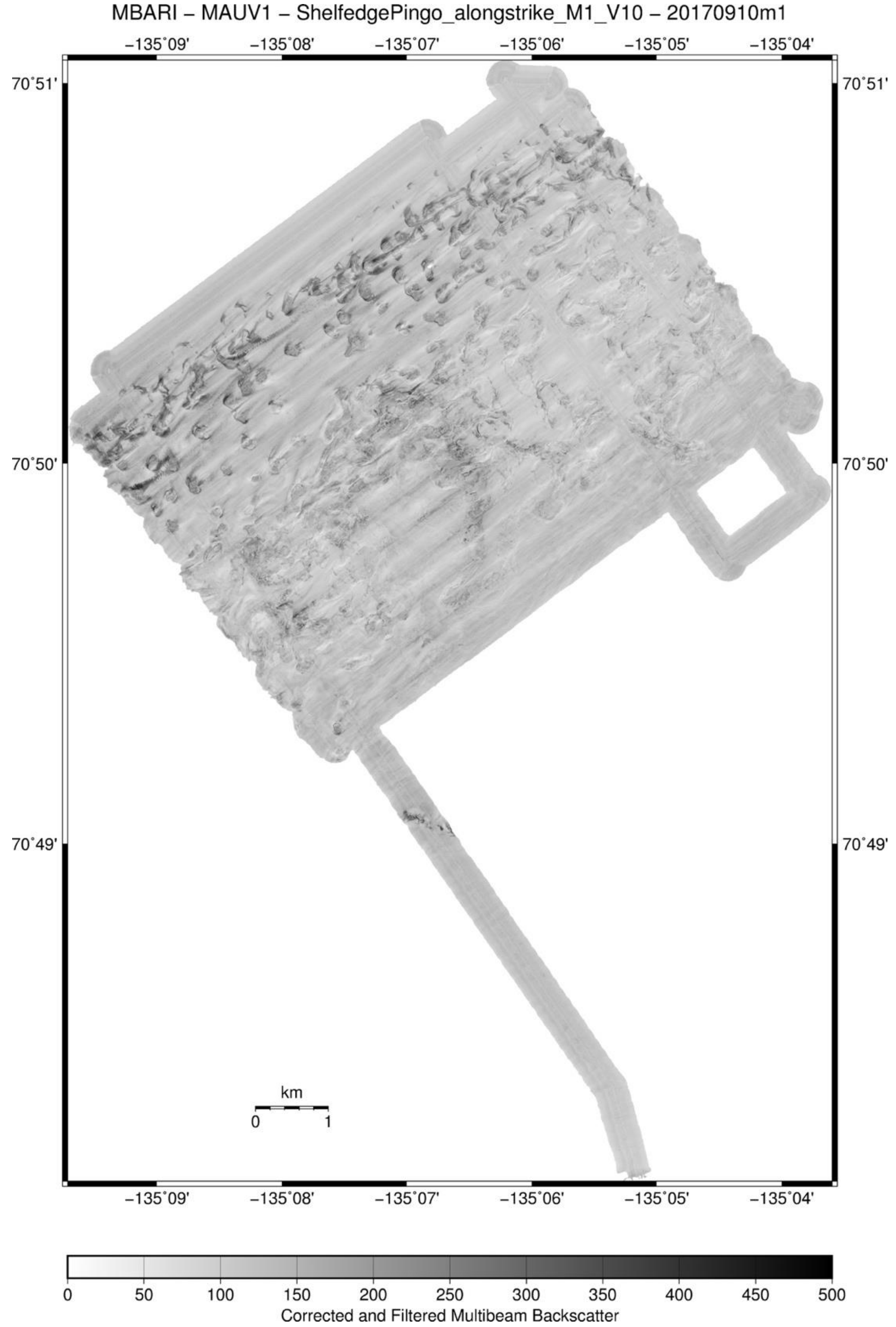

Figure 5.24. Mapping AUV 1-m resolution multibeam backscatter from mission 20170910m1. The backscatter has been corrected using an empirical amplitude-vs-grazing angle model and had a Gaussian smoothing filter applied. High amplitudes are shown dark.

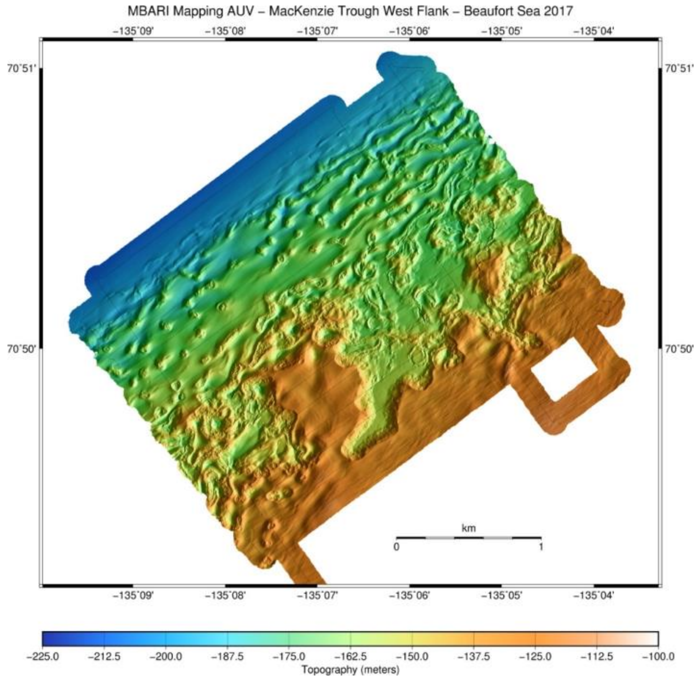

Figure 5.25. Mapping AUV 1-m resolution multibeam bathymetry from mission 20170910m1 displayed illuminated from the east. Two MiniROV dives and several cores were sited in this area.

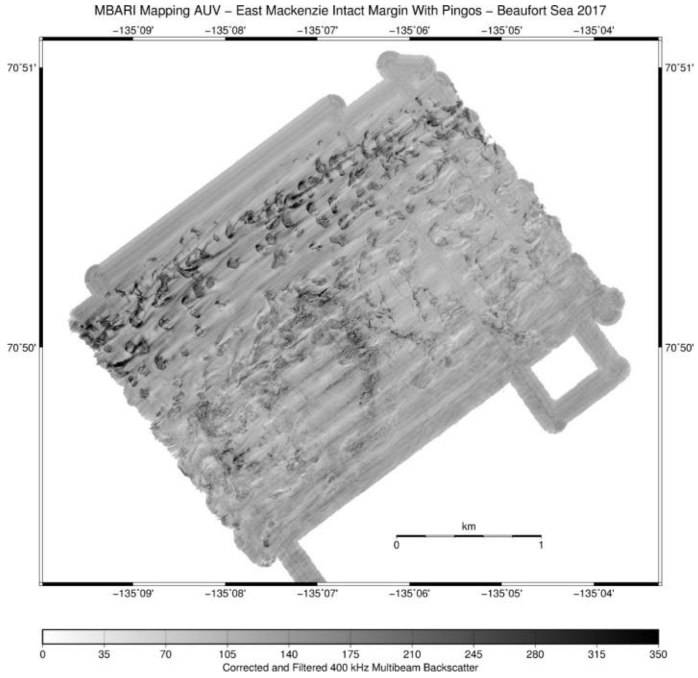

Figure 5.26. Mapping AUV 1-m resolution multibeam backscatter from mission 20170910m1. Two MiniROV dives and several cores were sited in this area. The backscatter has been corrected using an empirical amplitude-vs-grazing angle model and had a Gaussian smoothing filter applied. High amplitudes are shown dark.

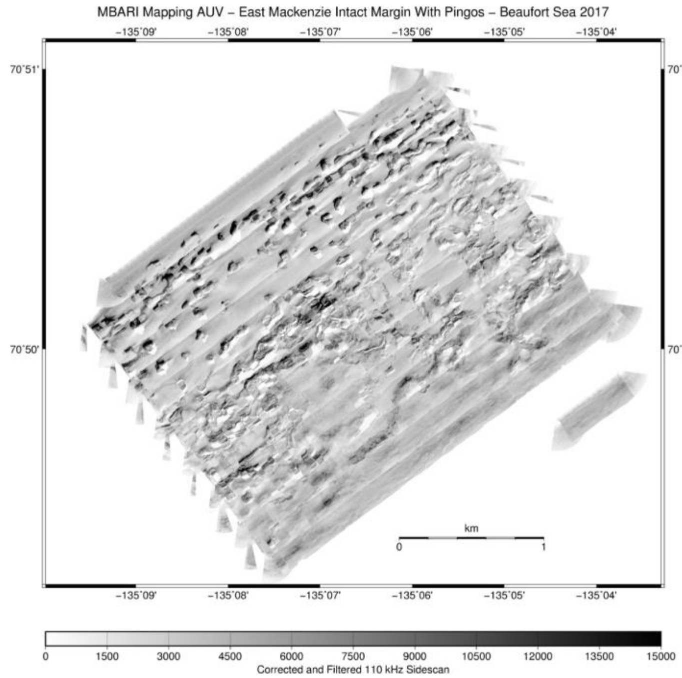

Figure 5.27. Mapping AUV 1-m resolution CHIRP 110 kHz sidescan from mission 20170910m1. Two MiniROV dives and several cores were sited in this area. This mosaic has been constructed from east-northeastward-looking data only. The sidescan has been corrected using an empirical amplitude-vs-grazing angle model and had a Gaussian smoothing filter applied. High amplitudes are shown dark.

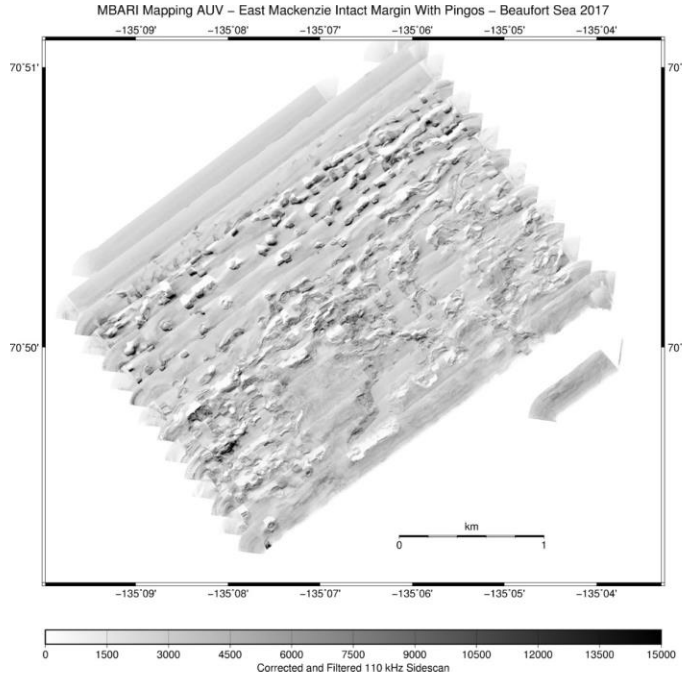

Figure 5.28. Mapping AUV 1-m resolution CHIRP 110 kHz sidescan from mission 20170910m1. Two MiniROV dives and several cores were sited in this area. This mosaic has been constructed from west-southwestward-looking data only. The sidescan has been corrected using an empirical amplitude-vs-grazing angle model and had a Gaussian smoothing filter applied. High amplitudes are shown dark.

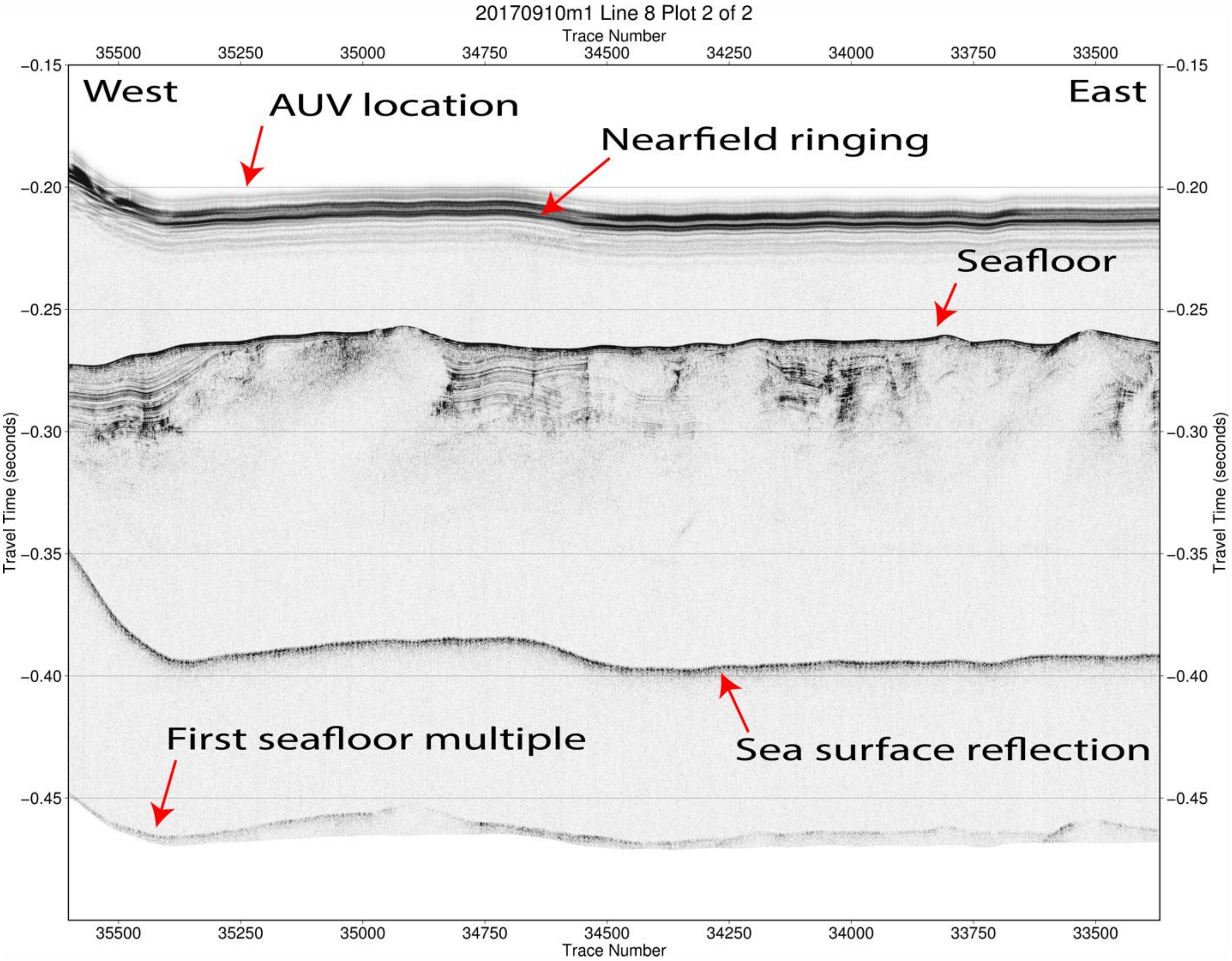

Figure 5.29. Mapping AUV CHIRP 1-6 kHz sub-bottom profiler data from mission 20170910m1. The section is shown "hung" from the AUV's location in the water column, generally about 50-m above the seafloor. The location of this profile is shown be a red line on Figure 5.22. Arrows indicates locations of sub-seafloor and multiple reflections. Surface reflections are seen in the AUV collected CHIRP profiles when the vehicle is operated in <150 m water depths.

References

Caress, D.W. and D.N. Chayes, D.N. 1996. Improved processing of Hydrosweep DS Multibeam Data on the R/V Maurice Ewing. *Marine Geophysical Researches*, **18**, 631-650. http://dx.doi.org/10.1007/BF00313878

Caress, D.W.,Thomas, J., Kirkwood, W.J., McEwen, R. Henthorn, R., Clague, E.A., Paull, C.K., Paduan, J., and Maier, K.L. 2008. High-Resolution Multibeam, Sidescan, and Subbottom Surveys Using the MBARI AUV D. Allan B. *Marine Habitat Mapping Technology for Alaska*, J.R. Reynolds and H.G. Greene (eds.) Alaska Sea Grant College Program, University of Alaska Fairbanks. http://dx.doi.org/10.4027/mhmta.2008.04

Caress, D.W., Chayes, D.N., and Ferreira. C. 2017. MB-System Seafloor Mapping Software: Processing and Display of Swath Sonar Data. Open source software available from http://www.mbari.org/data/mbsystem.

Chapter 6. MiniROV Diving Program

C.K. Paull, L. Lundsten, D.W. Caress, D. Graves, and R. Gwiazda

6.1. Introduction

During the ARA08C research expedition detailed visual inspection of the seafloor and sampling was conducted on 10 dives of MBARI's MiniROV. The MiniROV dives were all located in areas where either AUV surveys had been conducted in previous years, AUV surveys were planned for this cruise, or along multichannel seismic lines to provided ground truth calibration. These observations provide a basic understanding of seafloor conditions.

6.2. MiniROV System

MBARI's MiniROV is a portable, low cost, 1,500 meter inspection class system providing a compact fly away ROV capable of operating with a small dedicated crew (1-2 people) on ships of opportunity around the world. The MiniROV was specifically designed and built at MBARI for this purpose. The vehicle is capable of light duty work functions such as limited sampling, video transects, instrument deployment and recovery (with a 120 pound instrument payload) and is outfitted with the following suite of core instruments: HD camera, scanning sonar, lasers, LED lights and CTD. In addition, the vehicle has bolt on tool skids for mission specific payload and sampling requirements. Table 6.1 provides detailed specifications of the MiniROV and the instrumentation onboard.

Table 6.1. MiniROV Specifications & Instrumentation

Depth rating = 1500 meters
Vehicle type = Electric
Dimensions = ~ 48"L x 35"W x 24"H
Weight in air = ~ 800 pounds
Science payload = 120 pounds
Power Requirements = 3 phase 208VAC (5kW)
Thrusters = (6x) ~.75hp electric DC brushless

Auxiliary instrument power & available voltages

- ~1kW
- 240, 48, 24, 12, and 5 VDC

Auxiliary Video & Data

- (2) spare single mode fibers
- RS-232 serial ports
- (2) spare video channels

Core Instrumentation

- Insite Mini Zeus HDTV video camera
- Insite IT1000 low light B&W camera

- Imagenex 881-A scanning sonar
- CTDO
- (6) Main LED lights (5,000 lumens each)
- 5 function ECA manipulator arm
- ROWE 1.2 MHz DVL
- Camera/light tilt platform
- PNI 3-axis digital compass

ROV Auto Functions
- Auto Depth
- Auto Heading
- Observation mode (MBARI mode)
- Advanced Navigation mode (Dynamic station keeping)

Umbilical = 1,700 meter .625” OD

Umbilical Winch
    Aluminum construction
    Variable speed Electric drive motor
    Power requirements = 220VAC (4Kw)
    Dimensions = ~ 60”x 60”x60”

6.2.1. MiniROV operations off the Araon

MiniROV control room is a 10’ by 10’ container that is also outfitted as a workshop. The control room was positioned on the aft deck of the Araon in Incheon, Korea for the Araon’s transit north and first leg of the 2017 expedition.

There was also a 20’ shipping container, which held the tether winch, a diesel generator, and four ROPACs containing assorted equipment necessary for its operation. The contents of this container were unloaded from the 20’ shipping container in Inchon and positioned out of the weather in various places on the Araon. These components were used to mobilize the ROV during the transit from Barrow to the operating area in Canadian waters.

The MiniROV was launched off the Araon’s starboard rail, forward of the main crane. The ROV was lifted using a whip from the crane and connected to the top of the ROV using a latch, which will not release under a load. However, when the ROV is floating in the water the load is released, the latch can be released using a pull string. Seven floats were attached at an even spacing along the first 50 m of the tether. A strain release on the tether served as the attachment site for a 60 kg clump weight. This weight kept the tether down. The MiniROV had a 50 m swimming range from the clump weight in which it can operate without the ship moving. The clump weight also had a Ultra-short Base Line (USBL) acoustic tracking beacon on it. The positions of both the MiniROV and clump weight were tracked using the Araon’s hull-mounted Ranger 1 system. Figures 6.1 to 6.6 show the ROV configuration and deck operations.

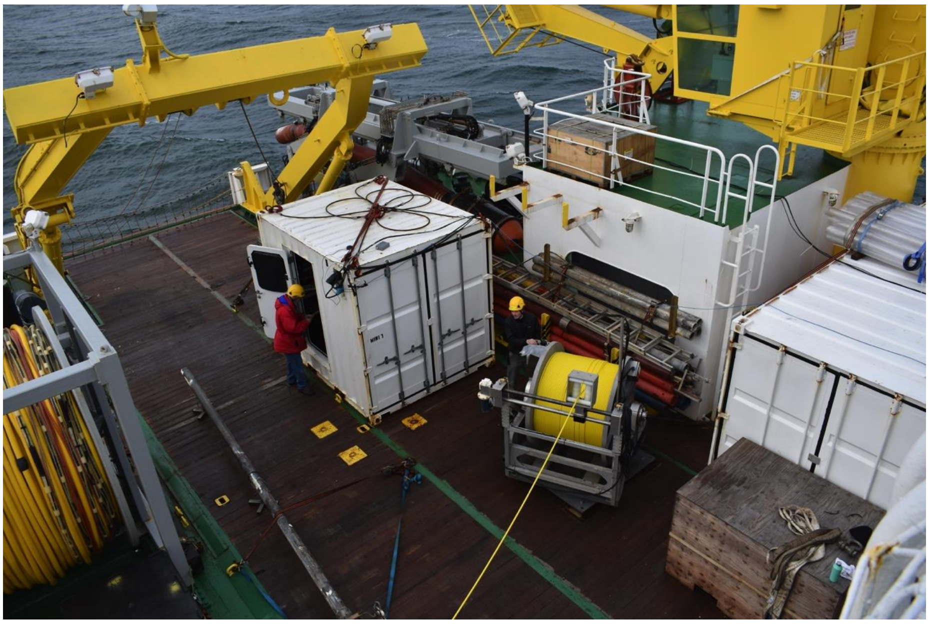

Figure 6.1. Location of ROV control room and winch on the aft deck of the Araon.

Figure 6.2 Image of screens within the ROV control room and Chief Pilot flying the ROV while the co-pilot is operating the mechanical arm. Note the multiple screens showing the main color digital video image, small subsidiary cameras, USBL tracking displays, and part of scanning sonar display.

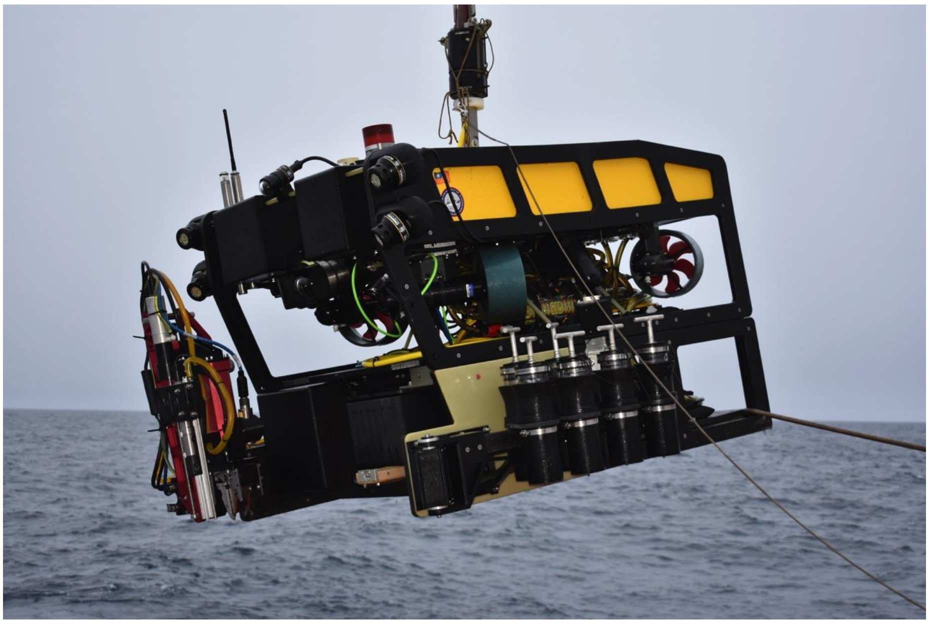

Figure 6.3 Photo showing MiniROV during deployment. Note the swing arm holding the push core tubes and mechanical arm.

Figure 6.4 Image showing the MiniROV being deployed. The tether is routed through a turning block suspended below the crane.

Figure 6.5 Photograph showing the clump weight being attached to the ROV tether. The clump weight also has a USBL beacon attached to it.

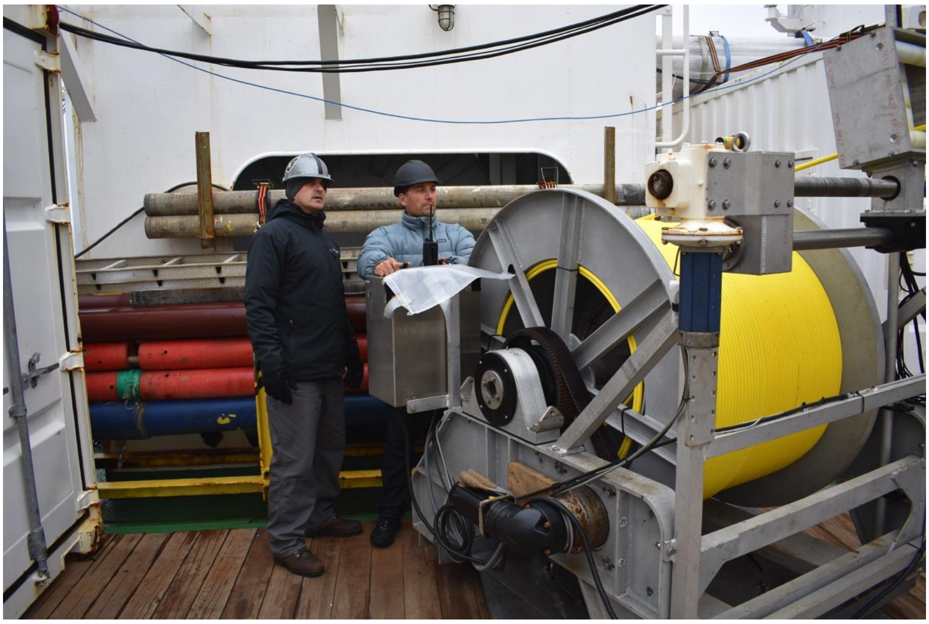

Figure 6.6 Photograph showing MiniROV winch and tether. Winch was operated manually using control box. Instructions were communicated via hand-held radio from the control room.

The 10 MiniROV dives all went smoothly. No significant issues were encountered. A translator was in or near the ROV control room during diving operations, which assisted with the communications to the bridge. Requested movements of the Araon were sent by hand-held radio to the bridge usually as distance to move (usually in 100 m increments), length of move, and speed to move (usually 0.2 knots). The bridge entered the information directly into dynamic positioning system.

6.2.2 ROV data types

Video images were recorded continuously during all dives. The video recordings usually have two red dots near the center of the image. These dots are from parallel laser beams, which were 13.6525 cm apart and projected from the ROV. These dots provide a scale bar independent of camera zoom or range.

The mechanical manipulator arm on the MiniROV enabled sampling during the ARA08C cruise. The arm allowed solid objects such as rocks and biological samples to be picked up off the seafloor. Samples were dropped into a drawer that was mechanically extended from the front of the MiniROV. After sampling the drawer was retracted, enclosing the samples, and preventing them from being lost during the dive and recovery.

The MiniROV was also equipped to take up to seven push cores on each dive. The core tubes are carried in quivers mounted onto its swing arm. The swing arm is stowed against the port side of the ROV during normal operations, but mechanically swung out into the field of view of the ROV's main cameras and in reach of the ROV's mechanical arm when push cores were to be collected. The push core tubes are 20 cm long and 8 cm in diameter. The contents of the push cores were extruded in the laboratory after each dive, so that the tubes could be reused on subsequent dives. As tubes are reused, to provide a unique identification of a particular sample requires both the dive number and core tube number (i.e., M100 PsC-1).

For this cruise the MiniROV carried a temperature probe, which was mounted on its manipulator mechanical arm so the arm can be positioned over the area of interest. When actuated, the probe will advance up to 30 cm into the sediment. This probe has a temperature range of -3.00 to + 24.00°C, with an accuracy of 0.24 °C.

The ROV also carried two conductivity, temperature, depth sensors (CTDs), one built into the vehicle and the other attached to the temperature probe on the swing arm.

6.3. Summary of MiniROV Dive Sites

The 10 MiniROV dives, were focused to support studies in five operating areas: (1) Dives M100, M102, and M103 were along the western flank of the Mackenzie Trough. This is an area that was surveyed with the Araon's 12 kHz multibeam system before the Araon reached Herschel Island at the beginning of this expedition. (2) Dives M103 and M109 were located on steep slopes near the major slide scar that was crossed in ~800-900 m water depths on seismic lines BF09 and BF12 of the ARA08C MCS program. (3) Dives M104 and M105 were on top of the 420 m mud volcano, which corresponds with the area resurveyed by the mapping AUV on this expedition. (4) Dives M106 and M107 were within the Shelf Edge Pingo area, which was also within the area resurveyed with the mapping AUV on this expedition. (5) Dive M108 was on the crest of the 740 m mud volcano.

The main activities that occurred during each dive along with the selected video images are outlined in the next section by operating area (Figure 6.7) rather than in chronological order.

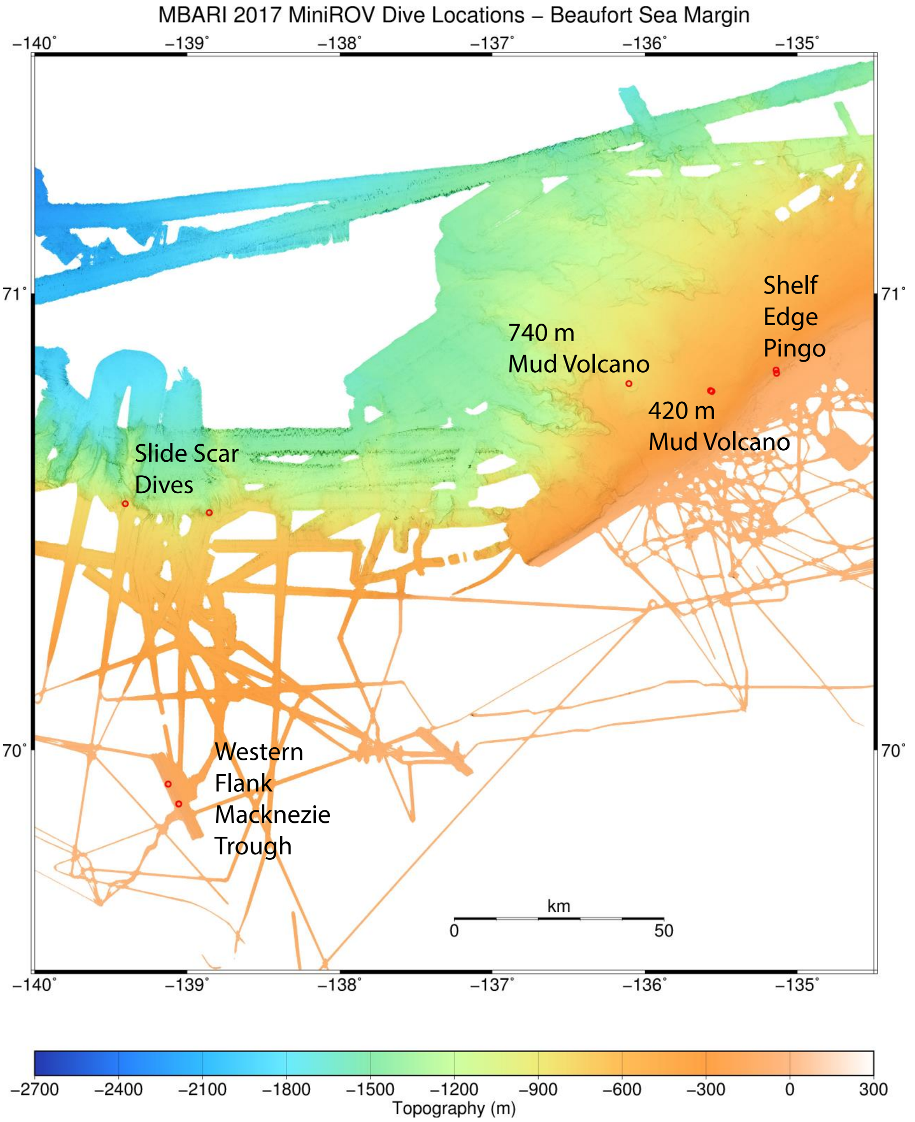

Figure 6.7 Location of MiniROV dives conducted during ARA08C indicated with small red circles. Basemap shows existing multibeam bathymetry.

6.3.1. Dive observations: western flank of Mackenzie Trough

The locations of the three MiniROV dives, M100, M101, and M103, on the western flank of the Mackenzie Trough are shown in Figures 6.8 and 6.9.

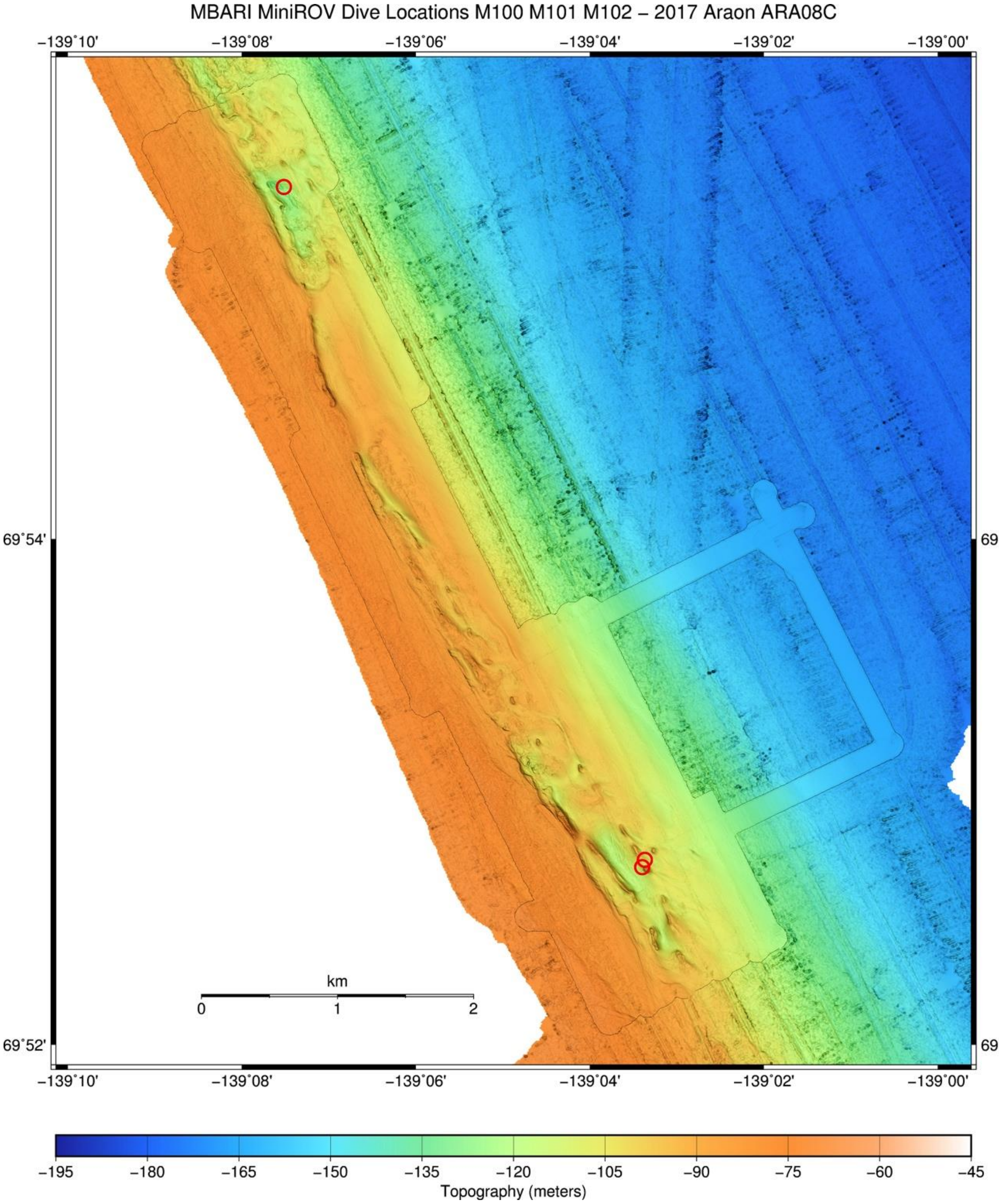

Figure 6.8. Map showing location (small red circles) of three MiniROV dives (M100, M101, and M103). Basemap includes the survey conducted using the Araon's 12 kHz hull-mounted multibeam system with the 2017 AUV data superimposed.

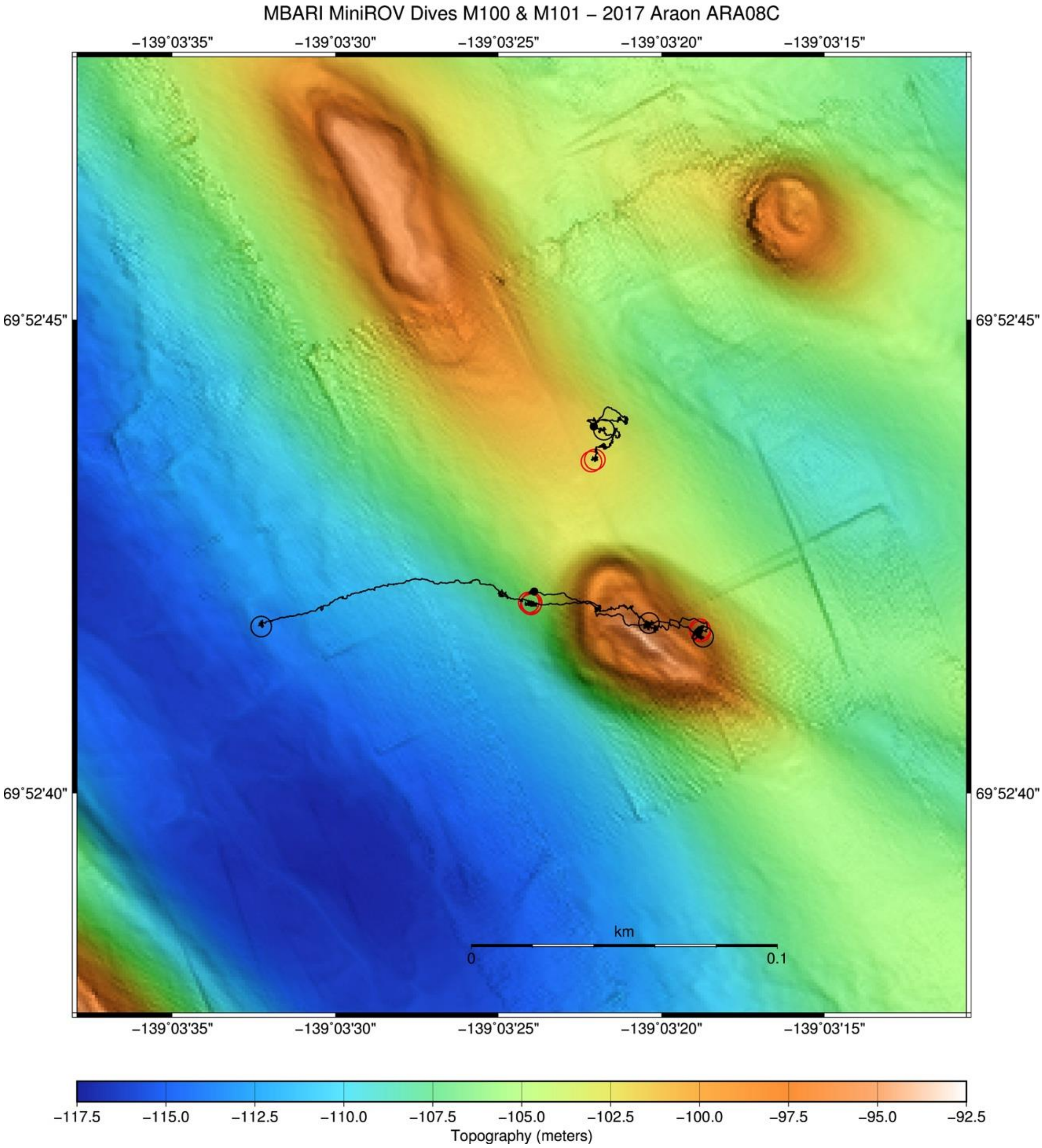

Figure 6.9. Map showing location of MiniROV dives M100 and M101 in more detail. Dive M100 was on the ridge between PLF features and only covered a small area. Dive M102 was on a PLF and then circled back to the east, covering more than 100 m on this transect. The background bathymetry is the 1-m grid resolution AUV data.

MiniROV Dive 100 (M100) Narrative (September 5, 2017, Tuesday)

09:45 L – Launched for M100. At 28 m water depth the temperature was -0.02°C.

16:54 Z –101 m - On bottom. Bottom temperature -1.28°C. Bottom covered with scattered rubble, crawling with small brittle stars and scallops. Numerous pebbles and cobbles covered with a dusting of sediment. Rough texture.

M100 Sequential image 1 – Rough textured bottom with scattered rubble and various organisms.

17:00 Z to 17:41 Z – 101.7 m - Collected 12 of the exposed rocks, which were both rounded and angular. Many of the rocks initially had crinoids attached.

17:49 L – 101.6 m - Took two push cores (M100 PsC-1 and M100 PsC-2) close together.

M100 Sequential image 2 – MiniROV arm taking push core.

17:56 Z – 101.6 m - Off bottom M100. During entire dive the Araon used dynamic positioning to maintain position.

MiniROV Dive 101 (M101) Narrative (September 5, 2017, Tuesday)

12:48 L (M101), Back to same launch site as M100.

20:07 Z – 106.9 m - On bottom and encountered similar rough texture as previous dive. Initially traveled east to a target identified with the scanning sonar, which was presumably the PLF feature.

20:13 Z – 104.3 m - Noted that there were at first both more rocks (cobbles) and even a few ~30 cm sized boulder exposed on the lower flank of the PLF.

M101 Sequential image 1 – Lower flank of PLF with cobbles.

20:16 Z – 98.2 m - The number of rocks decreased as the surface appeared to be composed of firm cohesive mud and the local topography was more complicated, as the crest of the mound was scarred by ~ 30 cm deep, ~1 m wide, and >3 m long grooves. The interior of the grooves were distinguished by their smooth surfaces. In other places the bottom was composed of a jumbled mess of orientations and small depressions, offset by cracks or joints. Looked like a mélange of cohesive extruded clay.

20:22 Z – 97.1 m - See several ~4 cm wide burrows with antennas sticking out from them. Also see a 7-8 cm long elongated cobble within the firm clay. This cobble was pulled it out of the formation (Rx-1). Note that this was not surface float.

(M10100002-new.png)

20:38 Z – 94.3 m - The crest of the mound was ovoid with side slopes estimated to be ~20° on the NE and SE sides, less along the ridge crest. The sonar allowed the very top to be located at 94.2 m. At the top there was a distinctive groove (whale mark?) seen repetitively in other ROV dives in this area.

Push cores M101 PsC-7 and M101 PsC-6 were taken near each other within this groove. These were short cores (~5 cm), as the bottom was firm and of a uniform grey colored lithology. Also sampled another isolated rock that was exposed on the side of the groove on the crest, which was crossed with distinctive white lines (Rx-2). Turned out these were quartz veins. Noted that the top of this feature as being at 69° 52.6944´N 139° 03.3138´W (USBL position) and subsequently used this coordinate to direct coring operations that night.

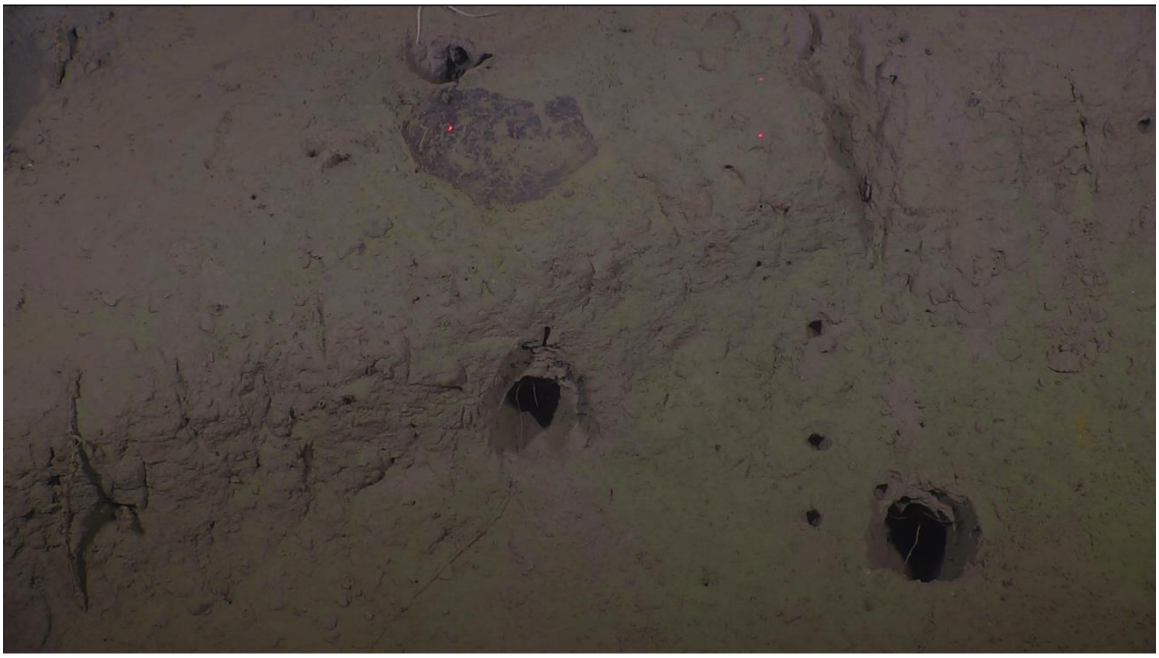

M101 Sequential image 2 - Burrows with antennas sticking out, note red lasers points are 13.6525 cm apart.

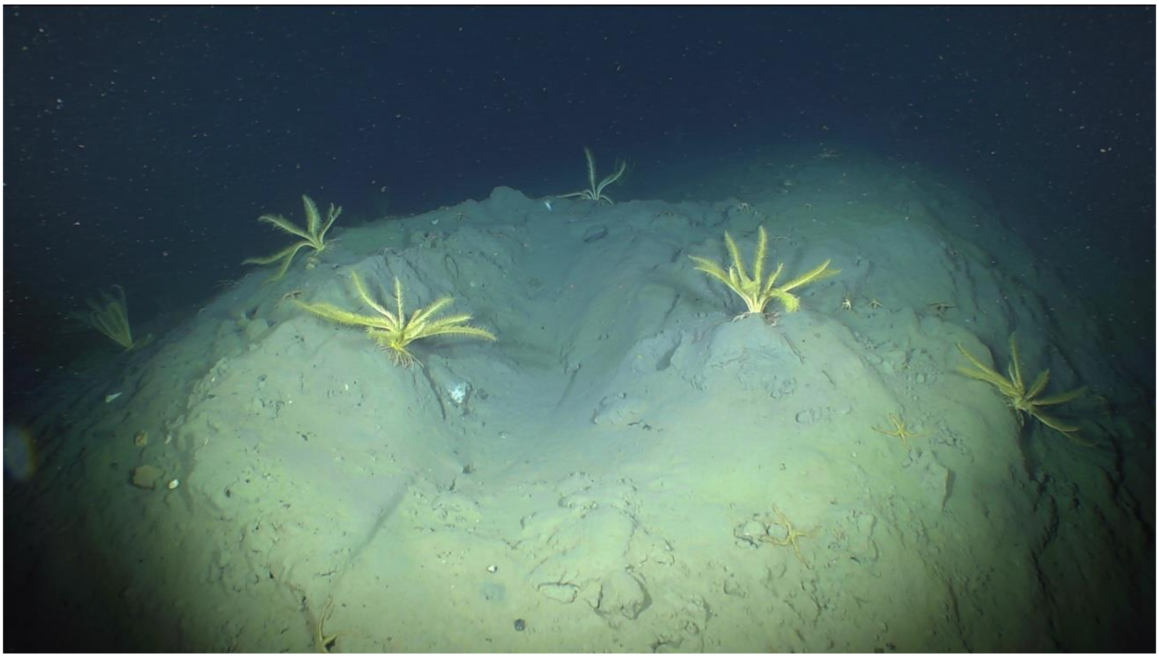

M101 Sequential image 3 – Distinctive groove on top of mound.

20:45 Z – 93.1 m - Started ROV moving along a course of 245°. Again noted irregular bottom topography going down side of mound, with surface dip changes over just lengths of 1-2 m in the smooth clay surface. At 103 m again numerous cobbles seen on the surface near base of mound and scattered rocks persisted as the ROV proceeded slowly along the transect on somewhat flatter seafloor.

21:05 Z – 107.3 m - See a ‘pear-shaped’ patch of white mat which that was ~1 m or less across. The main pear-shaped feature was covered with white mat and stood up ~5 cm in relief from the surrounding seafloor.

(M10100003-new.png)

M101 Sequential image 4 – Pear-shaped white mat on seafloor.

Requested Araon hold position. MiniROV landed at edge of this white mat to enable sampling. USBL position noted as being 69° 52.69978´N 139° 03.39967´W. Within the patch there were smaller roughly circular 1-2 cm deep depressions which were ~5-10 cm in diameter. The centers of these depressions were jet-black in color and appeared to be riddled with small holes or burrows. Push core M101 PsC-8 was taken in center of one of the depressions. On insertion, puff of black sediment squired up ~20 cm into overlying water column. Cores were short (<8 cm) as bottom firm. After removal core tube was observed to contain white mat on top (~1 cm), followed by ~ 1 cm black sediment, over steel grey color apparently uniform and cohesive sediment.

(M10100005-new.png)

Push core M101 PsC-9 was taken in an area initially observed to have the most distinct mat cover, at edge of pear-shaped feature, without a depression. However, the dusting of jet-black sediment had settled on this spot.

21:20 Z – See some gas bubbles coming out from core site, both during and after the coring. A third push core (M101 PsC-3) was taken in one another small depression with the white mat rim and jet-black center.

21:36 Z – 108.5 m - Until this point the Araon remained at same dynamic positioning point, with the ROV moving within the 50 m range allowed by its floating tether connecting to the clump weight. The ROV had stretched out to the NE to reach the top of the PLF and had moved to the other side to reach the pear-shaped depression. But now requested the Araon move of 100 m at 0.2 knots on a course of 245°, so ROV could conduct a transect. The ROV passed over rubble bottom with extensive exposed cobbles on the bottom. The bottom apparently was getting slightly deeper along this transect.

M101 Sequential image 5 – MiniROV arm taking push core.

21:51 Z – 112.9 m - Came to a change in bottom texture, where cobble cover seemed to go away. As the remaining goal was to collect cobbles, turned and circled back perhaps 5 m to collect cobbles. Rock samples Rx-3 to Rx-11 were collected from one relatively small area. A couple of attempts to pick up cobbles showed that along with the hard rocks, there were a few chunks on the seafloor which crushed while during sampling, showing that there were mud clasts interspersed with these cobbles.

(M10100006-new.png)

M101 Sequential image 6 – MiniROV arm collecting cobble samples.

22:05 Z – ROV left bottom.

22:23 Z (15:23 L) – At surface, coming on deck.

MiniROV Dive 102 (M102, Figure 6.10) Narrative (September 5, 2017, Tuesday)

18:50 L - ROV launched.

01:55 Z (9/6/2017 Z) – 122.1 m - ROV on bottom. Landed in area of rough rubble covered bottom.

Immediately started to sample cobbles. Picked up M102 Rx-1 to Rx-12. These were ultimately combined into one sample bag.

2:15 Z - Headed off at 245°, crossing similar rough bottom. Did see one boulder estimated to be 23 cm across based on laser beams. Scanning sonar noted to show diffuse area of rough bottom.

02:27 Z – 121.5 m - See a hole in bottom, with upturned material on its side. Grey color suggests hole is fresh. Origin unknown, but speculated it might be site of recent box core. The Laurier worked in this area earlier this summer.

02:39 Z – 123.4 m - Transect and dive ended.

20:00 L - ROV on deck and secured.

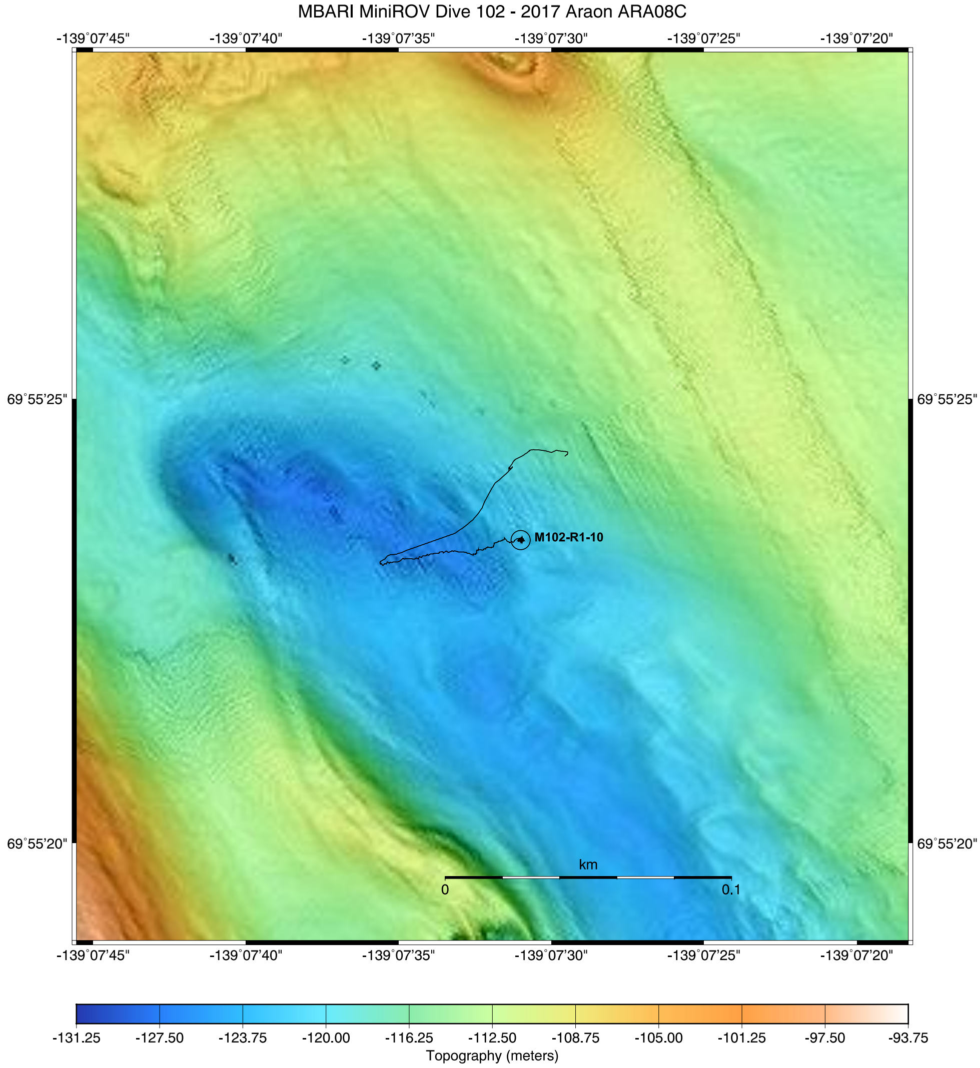

Figure 6.10. Detailed map showing location of Dive M102 on AUV bathymetry.

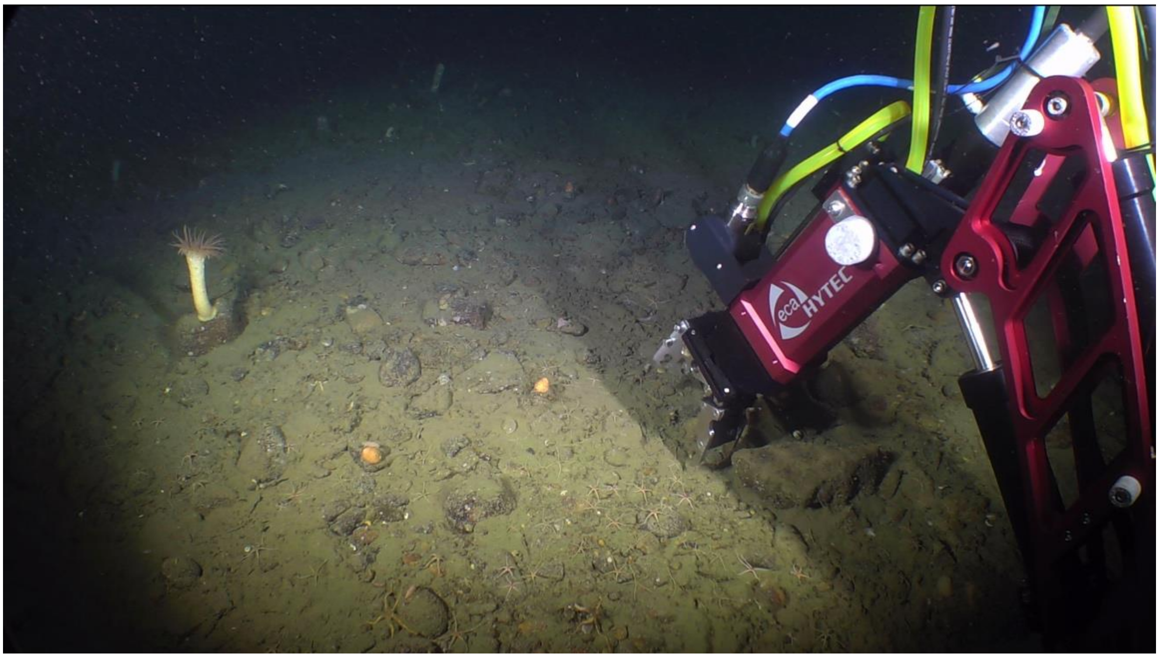

M102 Sequential image 1 – MiniROV arm collecting cobble samples.

M102 Sequential image 2 – Upturned material on seafloor.

6.3.2. Dive observations: headwall of major slide scar

ARA08C seismic lines BF09 and BF12 crossed a major slide scar in ~800-900 m water depths. The goal of dives M103 (Figures 6.11 and 6.12) and M109 (Figure 6.11) was to provide ground truth observations about the material exposed by the slide.

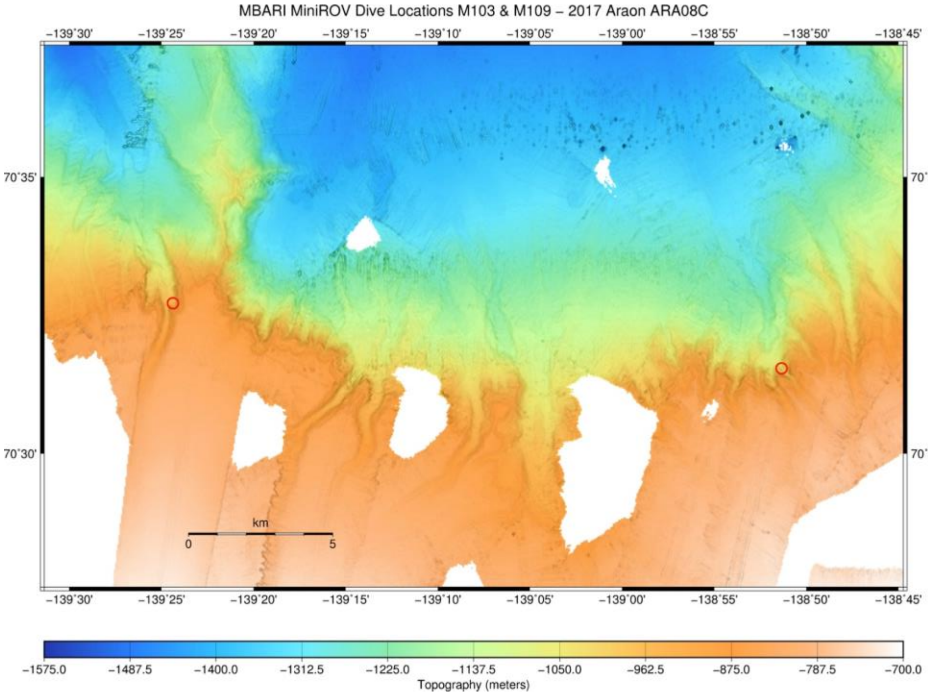

Figure 6.11. Location of ROV dives M103 and M109 (red circles). Dive M103 was located on the eastern side and M109 to the western side of this map. Bathymetry is surface ship multibeam data.

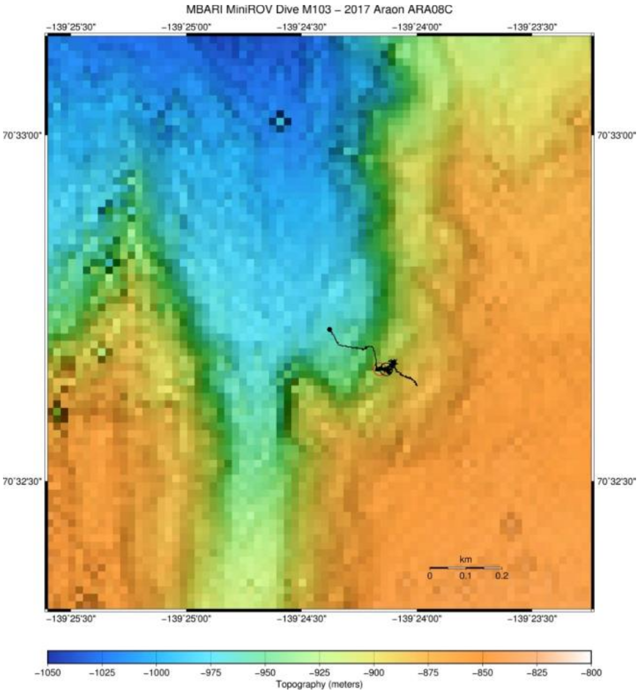

Figure 6.12. Map showing location of dive M103 with respect to bathymetry in more detail.

MiniROV Dive 103 (M103) Narrative (September 6, 2017, Wednesday)

12:35 L - At ROV launch site.

19:45 Z - Clump weight in water and headed down.

20:56 Z – 971.5 m - ROV on bottom. Bottom covered with 'fluffy" sediment, drape easily stirred up by ROV wash. Seafloor surface cut up of with extensive tracks and trails (i.e., bioturbation). Not much mega fauna. Generally bland sonar, but can see up slope side to SE.

20:59 Z - Requested Araon move 50 m to SE (135°) to start our upslope transect.

21:09 Z – 954 m - Note increase in megafauna and the first occurrence of same scattered cobbles, as slope based on visual observation and increased signal in scanning sonar.

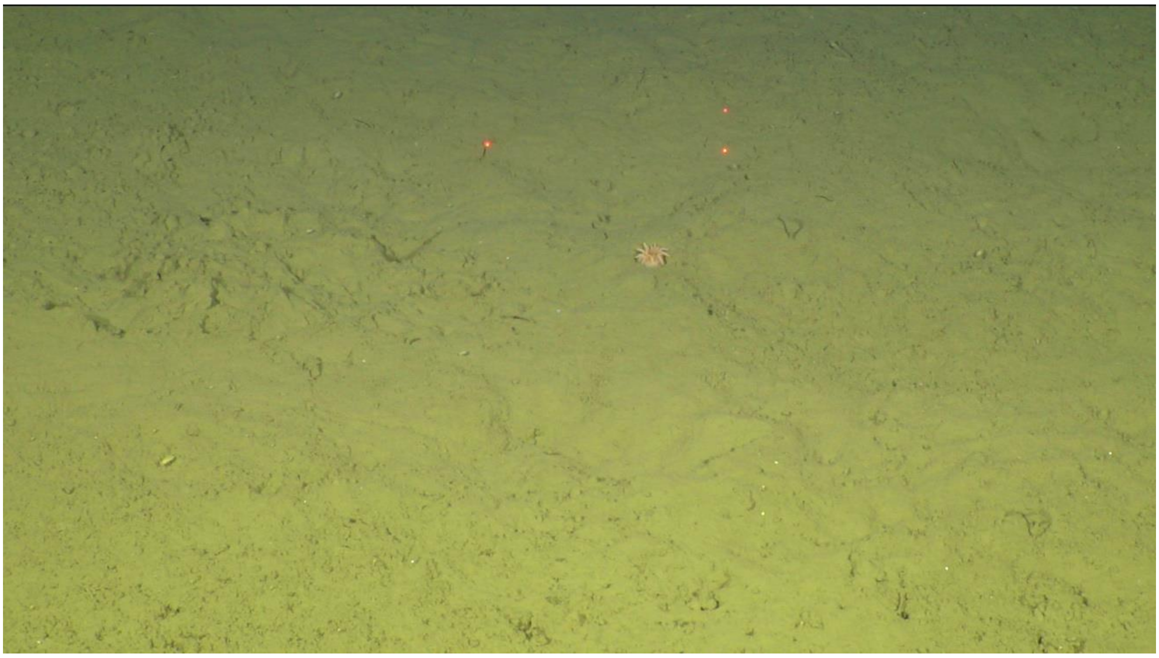

M103 Sequential image 1 – "Fluffy" sediment drape on the seafloor.

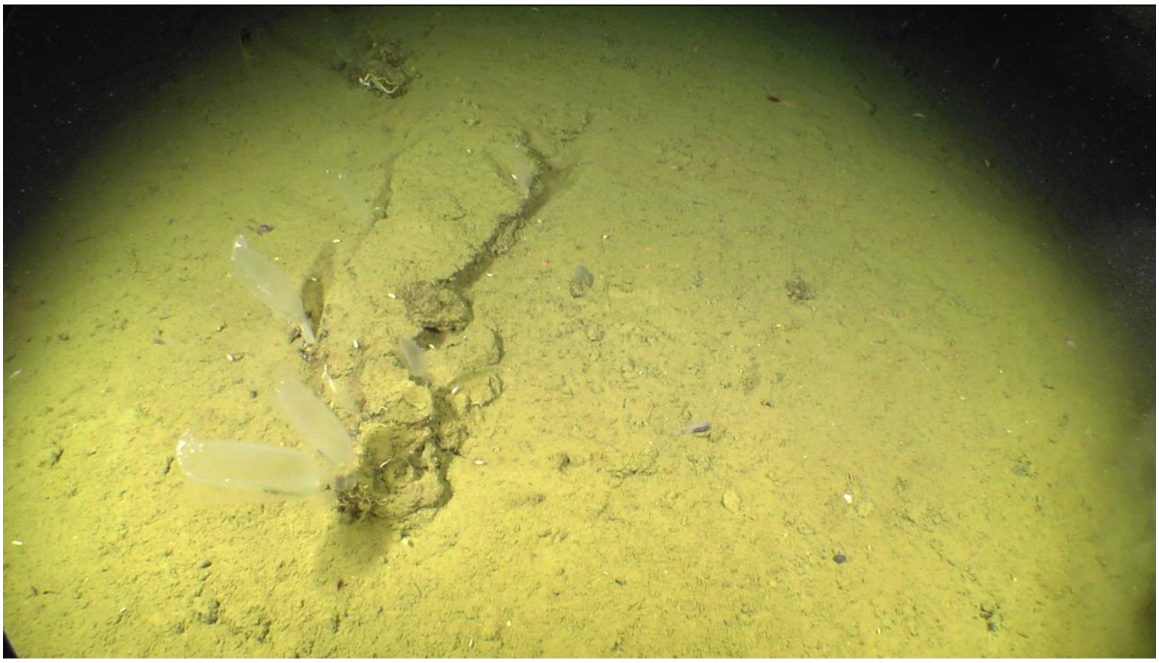

M103 Sequential image 2 – Megafauna on seafloor.

21:14 Z – 941.9 m - The edge of exposed dipping bed <5 cm high outcrops. Within this outcrop is a cobble that is entombed in the formation. Scattered rocks are also seen on the surrounding seafloor.

947 m - Numerous exposed rocks.

21:16 Z – 944 m - see one boulder 22 to 24 cm across.

21:17 Z - Lateral over to south near base of slope trying to get into a gully. 926 m – No rocks were seen in the gully. T=0.189°C.

21:21 Z – 924 m - Returned to the edge of gulley. See a few scattered cobbles on the flank of gulley and even a boulder.

(M10300003-new)

21:38 Z – 920 m - See dipping bed exposed on gulley sidewall.

Used ROV arm to scrap sidewall. Determined there was a few cm of soft sediment veneer over much firmer surface. Took horizontal push core (M103 PsC-12 in 923.5 m. Worked hard to penetrate ~6 cm into side wall of scarp. Later learned that the base of core was very stiff plastic sediment fine sediment.

21:42 Z to 21:32 Z - Moved around in the 919 to 912 m depth range searching back and forth along the contours to collect rocks Rx-1 to Rx-8. These were ultimately placed in one bag. Could not find any more cobbles and gave up searching.

22:32 Z - 912 m - Continued up slope on course of 135°. Had Araon move several times in 50 m then 100 m increments. Continued along this transect up to 889 m. Relatively barren of megafauna. Shallower than 919 m depth there were no rocks or indications of strata in subcrop were seen. Bottom was completely sediment covered.

22:46 Z – 886 m - End of dive. Did not see a single feature identified as being a ‘whale mark’ during entire dive.

M103 Sequential image 3 – Cobble on seafloor.

M103 Sequential image 4 – Sediment covered seafloor.

MiniROV Dive (M109, Figure 6.13) Narrative (September 12, 2016, Tuesday)

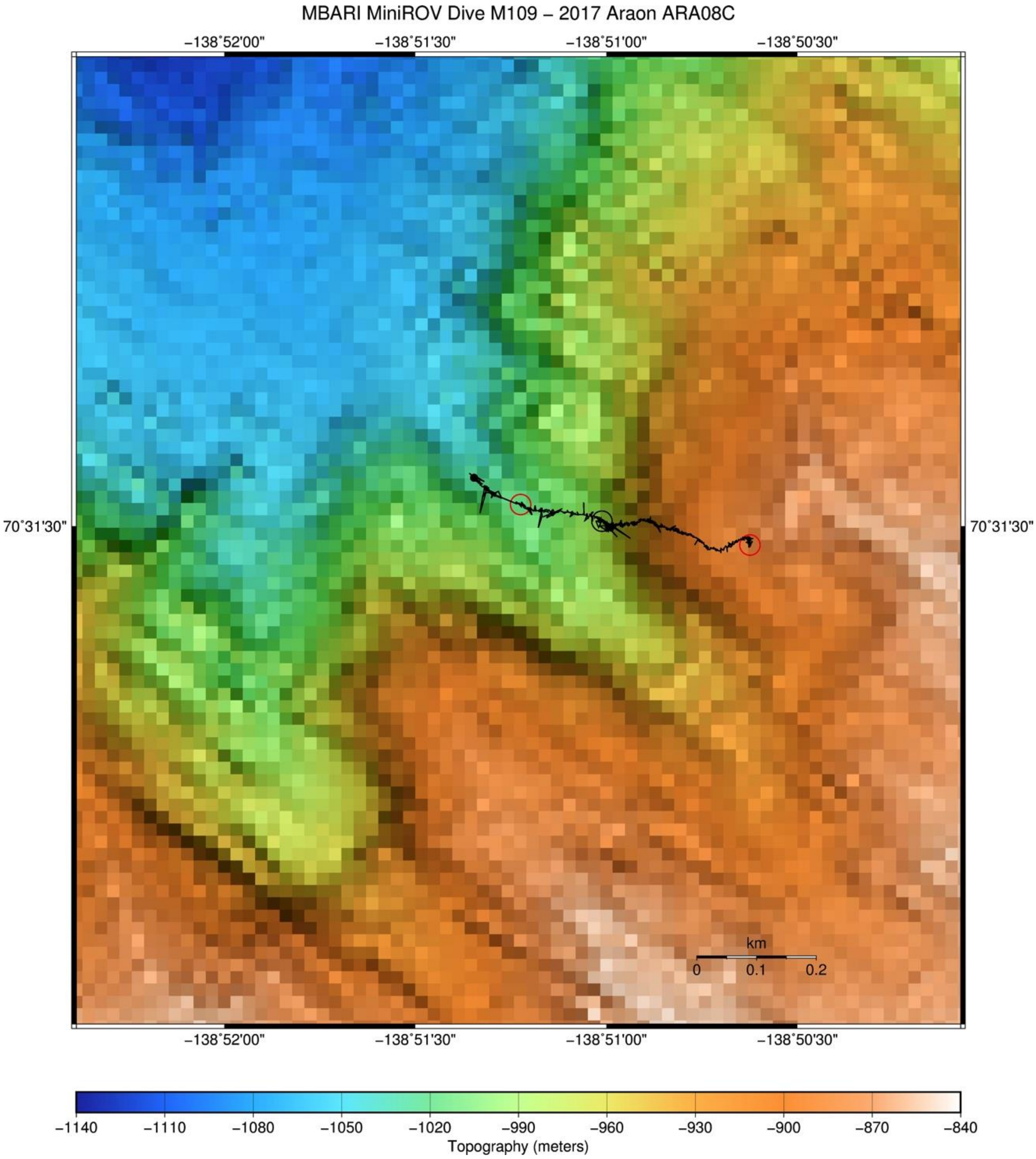

Figure 6.13. Dive track for M109 with respect to the bathymetry.

08:20 L - Launched for M109.

08:30 L - ROV going down.

16:41 Z - ROV approaching bottom in 1035 m. Bland bottom with a few anemones and brittle stars. No sonar targets. Turned on sonar recording on (file # win881al09-sep-2017-664208).

16:44 Z – 1037.6 m - Landed to sample.

16:48 Z – 1035.6 m - Took M109 PsC-13 with ½ penetration, but had to core as on slope. Tan color sediment throughout the core.

16:42 Z – 1035.1 m - Zooming into sediment surface around an anemone and one small brittle star shows extensive millimeter scale disruption by bioturbation and fecal material. Impression is this is a massive sediment drape over a smooth bottom.

(M10900001-new.png)

M109 Sequential image 1 – Anemone on seafloor.

Between 16:57 Z – 1031 m and 17:57 Z – 980 m there was a steady climb as transited along sediment draped seafloor seeing in total one old gouge mark, two skates, two >3 cm open burrows, one very small (1 cm deep x 20 cm long) surficial sediment failure, and a few >2 m long bioturbation tracks.

M109 Sequential image 2 – Skate on seafloor.

17:27 Z – 979.8 m - The first rock was seen. At this time the sonar also showed an increase in seafloor steepness.

17:32 Z – 973 m - Lots of rocks.

17:34 Z – 969.0 m - See edges of exposed bed with apparently dips of ~20° down slope to the west. Bed contains gravel.

M109 Sequential image 3 – Edges of exposed bed.

17:48 Z – 967.4 m - Tried to sample bed by breaking off corner of overhang. However, matrix crumbled easily and was not successful. The pebbles and cobbles are entombed within the exposed strata.

M109 Sequential image 4 – MiniROV arm attempting to collect seabed sample.

17:54 Z to 18:18 Z - Sample cobbles (RX-1 to RX-12) between 967.2 m and 966.4 m.

18:28 Z – 966.4 - Sampled a sponge which was attached to a rock.

18:25 Z – 965 m - Started moving up slope again.

18:29 Z – 957.9 m - See a ~ >30 cm long boulder sticking out of the formation. On top of boulder is a fish which appears to be brooding eggs. Serpulid worm tubes encrusts overhang under boulder.

M109 Sequential image 5 – Fish on boulder with eggs.

20:34 Z – 942.1 m - Still seeing sides of exposed beds with in place gravel exposed.

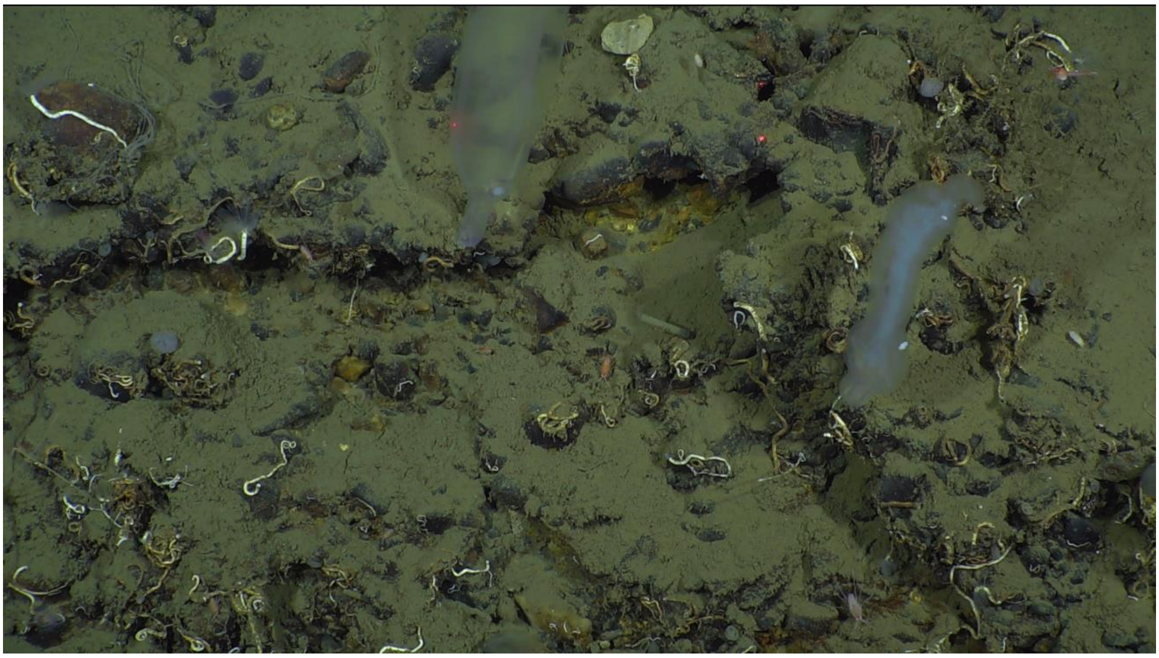

M109 Sequential image 6 – Serpulid worm tubes.

18:46 Z – 915.9 m - See dipping beds exposed on side of steep slope. These beds are thinner and composed of generally finer grained material than those seen further down slope. However, there are still a few cobbles on the surface.

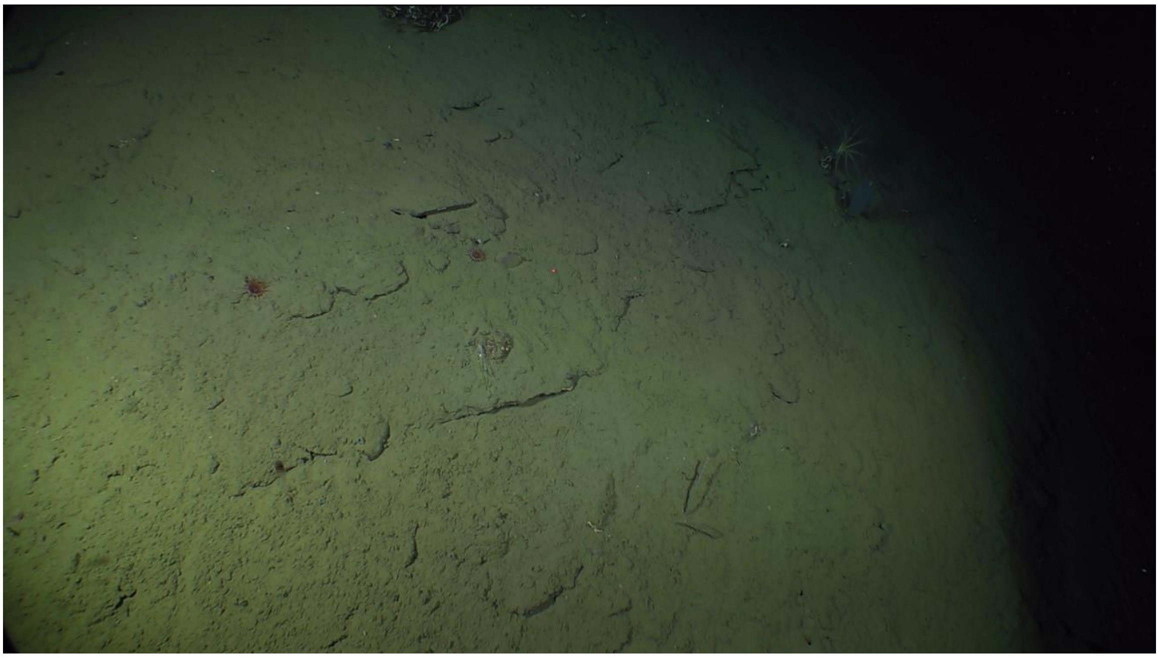

M109 Sequential image 7 – Dipping beds.

18:49 Z – 909 m - On bland sediment covered bottom. No more rocks were seen during the dive. Seems that the entire bottom from here on was sediment covered.

19:01 Z – 883 m - See sloping edge off to SE. However, looks entirely sediment covered.

19:12 Z – 874.9 m - Landed to take sediment core (M109 PsC- 12).

19:16 Z - End of dive.

13:00 L - ROV on deck.

6.3.3. Dive observations: 420 m mud volcano (Figure 6.14)

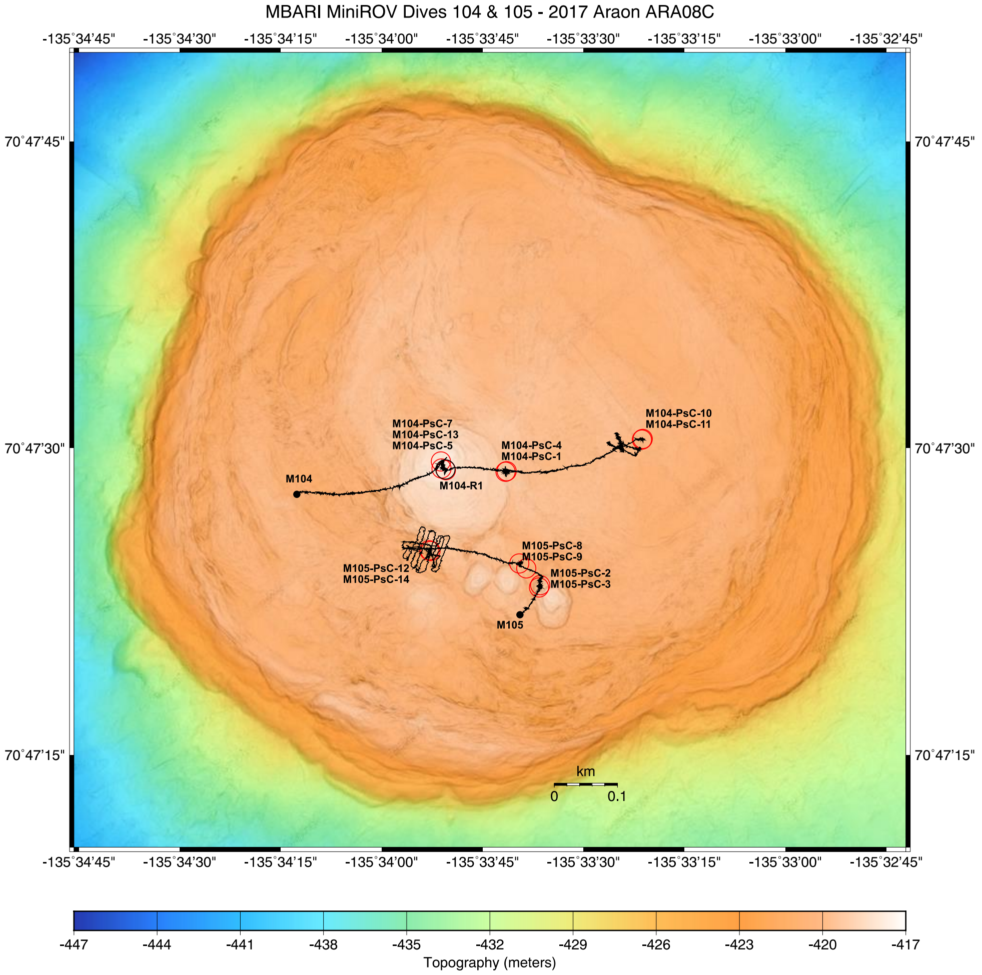

Figure 6.14. Dive tracks for the two dives (M104 and M105) conducted on top of 420 m mud volcano are shown along with location of samples. This is projected onto AUV bathymetry collected in 2017.

ROV dive M104 was planned as a ~450 m long W-E transect on the top of the 420 m mud volcano starting at 135° 34.047174′W, 70° 47.484414′N and a depth of 419.5 m. The transect was laid out to cross one of the most prominent features seen in the 2016 AUV survey, which consists of an ~160 m diameter circular feature that is 1 to 2 m higher than most of the crest of this mud volcano. The eastern end of this transect was anchored by where an OSMO Sampler was deployed at 135° 33.880200′W, 70° 47.415600′N ~420.0 m) in 2016, which was to be recovered at end of this dive.

The variation in depth on top of the 420 m mud volcano is restricted to 5 m, and in a general sense the top of this mud volcano is nearly level. However, in detail the ROV video shows considerable local morphologic changes, which occur at the <1 m scale and even finer textural patterns. These changes pass by quickly and make it impossible to record in detail, thus this description is generalized.

The most prominent texture is associated with ridges which that crossed through the ROV's field of view and based on the bathymetry and previous observations can be traced laterally for >10's of meters. Some of these ridges separate otherwise generally flat sections of the seafloor, but are higher on one side than the other. Sometimes these ridges form boundaries between other textures, but in other cases the ridges seem to cut across the similar textures on both sides of the ridge. Several types of texture were noted with the smaller scale being made up of patches of mats and hummocky mounds.

Sometimes these hummocky areas are organized into symmetrical ridges, other places mounds of which just a few cm of relief.

MiniROV Dive (M104) Narrative (September 8, 2017, Friday)

08:59 L - In water MiniROV Dive M105

16:30 Z – 421.5 m - Landed on hummocky bottom with scattered white areas which are here after assumed to be bacterial mats.

M104 Sequential image 1 – Hummocky bottom with bacterial mats.

16:34 Z – 421.2 m - ROV proceeded along a course of 080°. See some scattered patches of tubeworm patches varied from being <10 cm to >2 m across. Tubeworms occur preferentially in topographic lows and mats preferentially occur on the crests of the ridges.

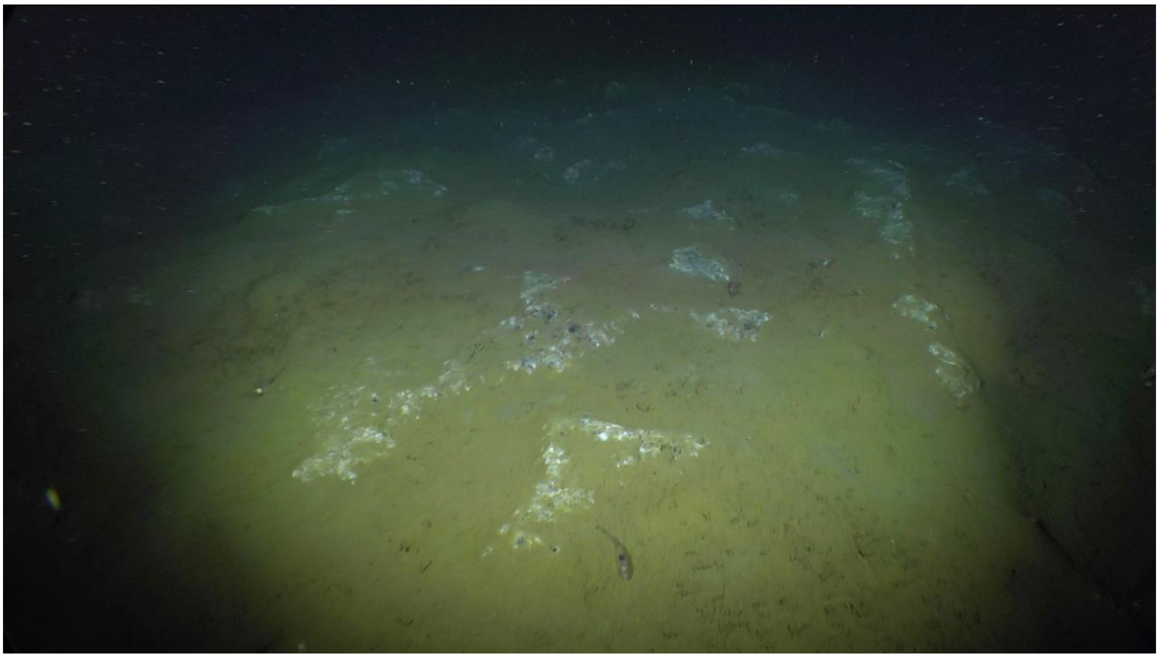

M104 Sequential image 2 – Bacterial mats on seafloor.

At 16:45 Z – 420 m - Crossed a group of ~50 cm high mounds and parallel ridges which were oriented roughly perpendicular to the transect NNW-SSE and bottom depth decreased to 419 m. Crossing these ridges corresponded with passing onto the central circular high. The bottom was noted to have a smoother sediment surface, which was generally light tan in color, and lacking worm patches. In a few places small black spots showed through the light tan cover.

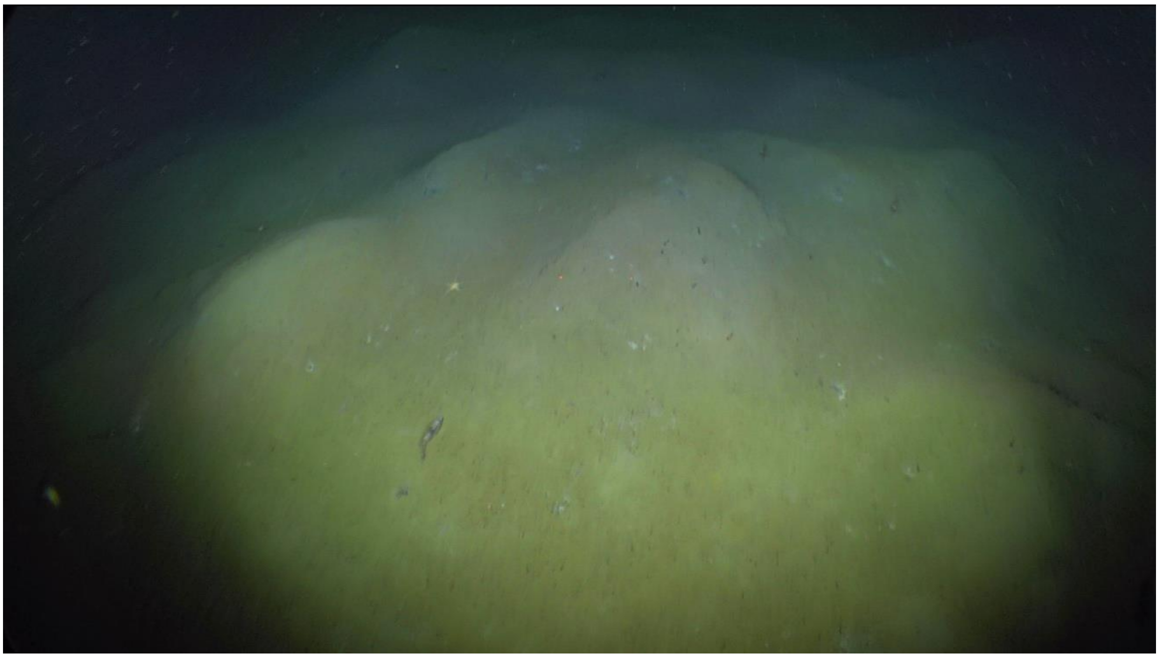

M104 Sequential image 3 – Area of light tan, smoother sediment surface.

16:50 Z – 419.3 m - Saw multiple small mounds and/or ridges 20-30 cm wide, usually estimated to be 5-10 cm high. Initially the ridges were preferentially oriented roughly NNW-SSE.

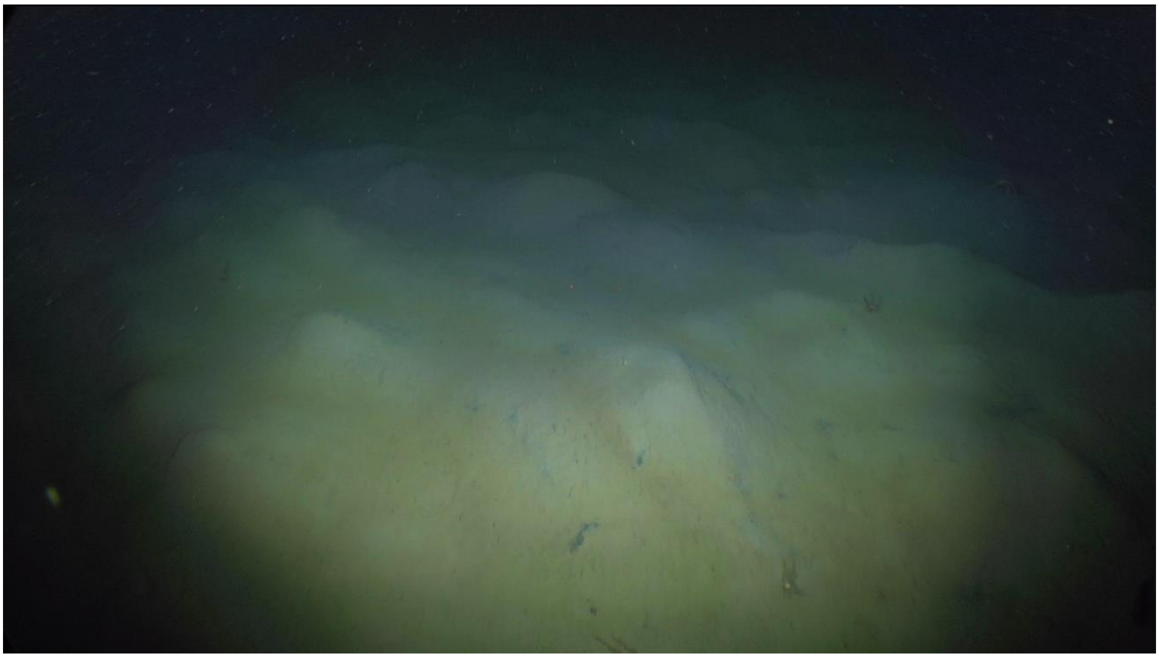

M104 Sequential image 4 – Example of small mounds/ridges.

17:01 Z - Stopping ROV Transect to sample. Took M104 PsC-7 and M104 PsC-13 in 419.9 m. Zooming in showed a few worms on the surface with slight depressions with black centers.

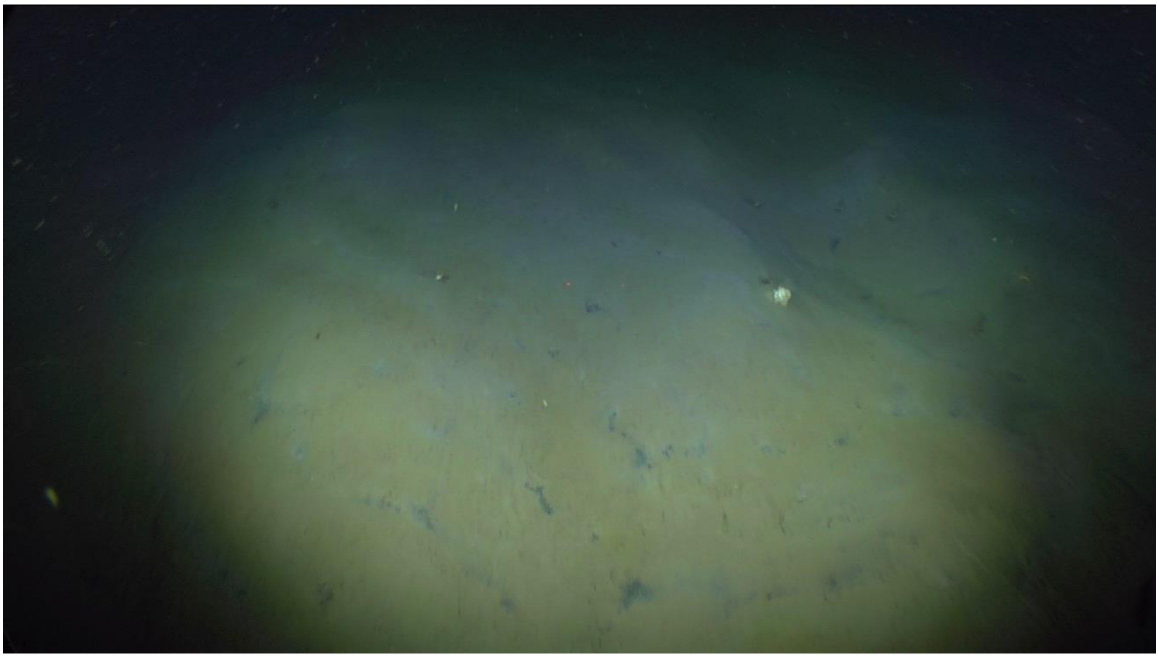

M104 Sequential image 5 – Worms on seafloor.

17:15 Z - Stopped to sample rock on surface. Rx-1 at 420 m. Rock sank into sediment during the sampling process, which suggests it was sitting on soft sediment. On recovery, the lithology was a grey mudstone, at least similar in composition to the muds cored on top of this mud volcano. As this lithology is different than most other rocks sampled in this area, it suggest that this clast might have been carried up from below.

17:19 Z – 420 m - Got underway on a course of 080°. Noted that mats, black depressions and worms were seen and at an increased frequency.

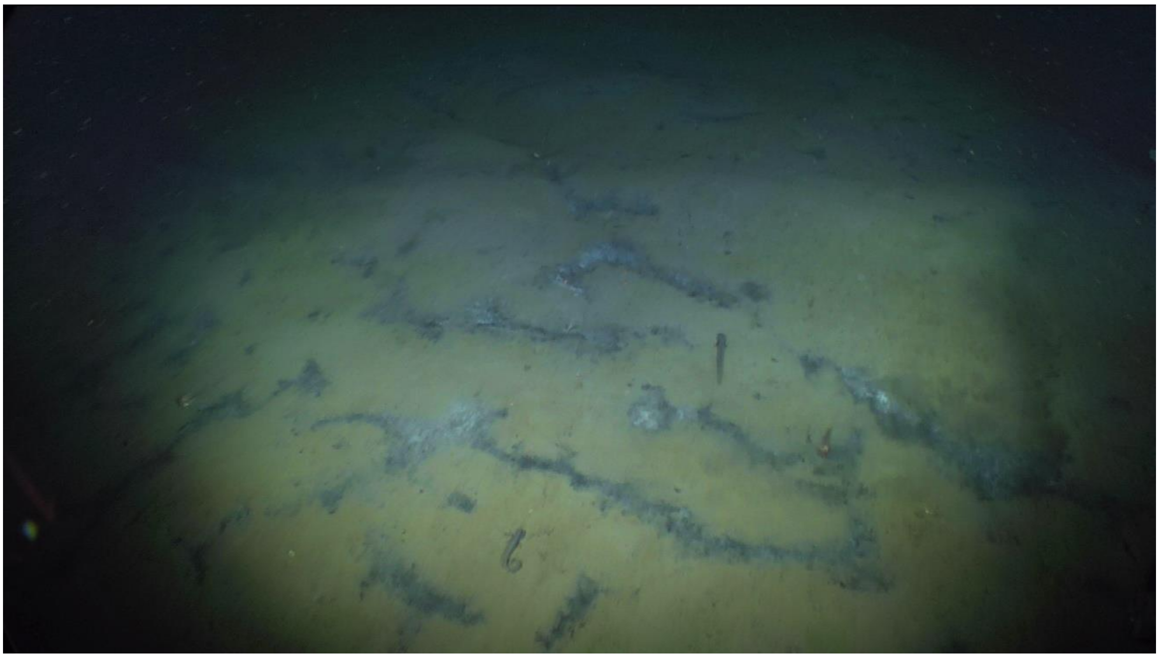

M104 Sequential image 6 - Example of mats and black depressions.

17:27 Z – A series of ridges oriented NW-SE were encountered. This corresponded with passing the edge of the distinctive 160 m wide circular feature in the AUV map. After this, the frequency and density of the worm patches increased.

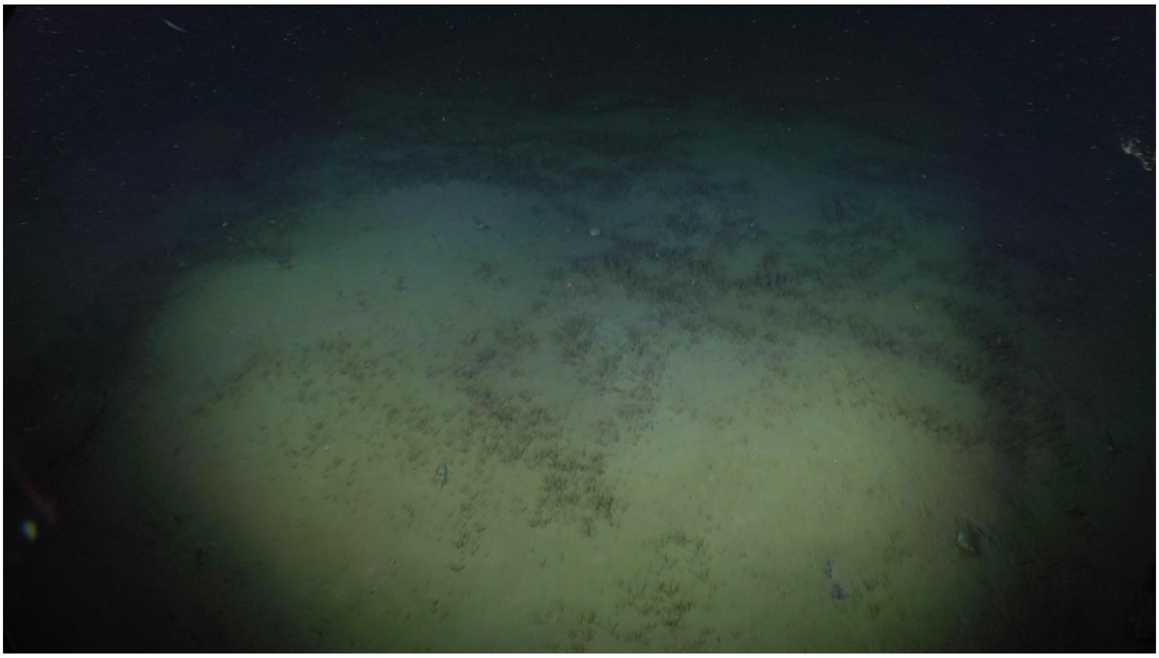

M104 Sequential image 7 – Examples of ridges.

17:32 Z – 421.6 m - Area of dense tube worms developed in an area with hummocky bottom with muffled texture (comparatively older looking).

17:31 Z – 421.1 m - Zoomed in image of tubeworms. Sampled from this area. M104 PsC-5 was seen to have worms coming out of its bottom. M104 PsC-4 was noted to have ~2 cm tan top, overlying 3 cm black sediment, than grey to base of core. Also used arm to grab worms and pull them out of the sediment and place them into the drawer.

M104 Sequential image 8 - Zoomed in image of tubeworms.

18:01 Z - Underway at 085°. Continued to see dense beds of tubeworms, particularly in the lower areas. Density of tubeworm beds increasing. This is in an area, which previous surveys have shown to be of intermediate reflectivity.

18:15 Z - Note that the orientation of the ridges changed to NE-SW, suggesting the fabric was from a different, and probably earlier, eruption. However, there was smoother sediment in the troughs. Between 18:17 Z and 18:19 Z one area with distinctively less worms and black patches was crossed, but after this returned to a similar high density or both. At 18:26 Z reached area where OSMO Sampler was expected.

18:26 Z to 18:58 Z - Conducted roughly star shaped searched pattern consisting of 5 radial lines crossing purported position going out to 30 to 40 m from site. Expected that the sonar would detect OSMO Sampler within ~25 m range. Thus, covered surrounding area out to >40 m with full coverage. Under pressure of time, the search was ended.

18:26 Z - Landed to collect three push cores in 421.7 m water depth. Core M104 PsC-1 was in small worm patch. M104 PsC-10 had worms coming out the bottom. Third core was M104 PsC-11. After retraction, cores were seen to have ~2 cm tan sediments on top, overlaying ~2 cm black sediment, then grey to bottom.

M104 Sequential image 9 – MiniROV arm taking push core.

19:12 Z - Off bottom.

MiniROV Dive 105 (M105) Narrative (September 8, 2017, Friday)

15:30 L - At site for M105 (135°33.587634´W, 70°47.377752´N Depth: 418.478 m). This was the second dive on top of 420 m mud volcano. Target was an area of strong backscatter in 2017 AUV data. Intend to move to WNW to recover an OSMO Sampler at the end of the dive.

16:00 L - ROV in water for M105.

23:43 Z – 419.6 m - ROV on bottom in area of white nearly smooth seafloor. While there were numerous shrimp, there were no (attached) sessile organisms. This type of bottom texture is interpreted to indicate a young flow.

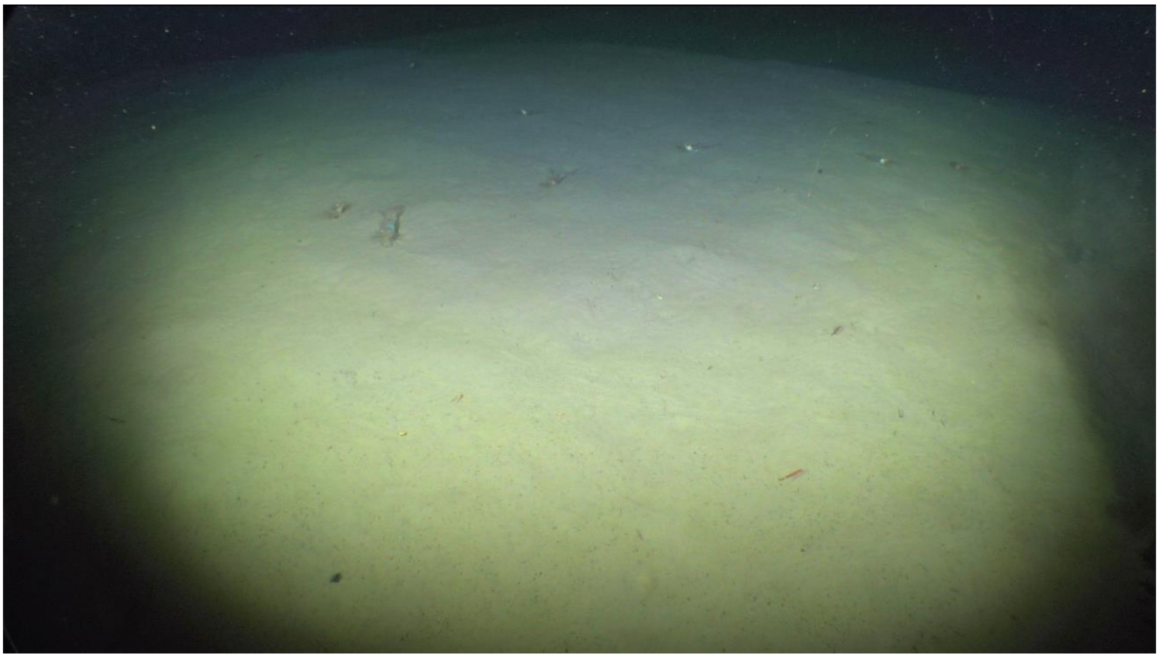

M105 Sequential image 1 – White, nearly uniform seafloor.

USBL tracking shows ROV landed 37 m to SW of target, but thus initially moved to target.

23:50 Z – 420.9 m - Crossed contact between bland white seafloor and seafloor characterized by the numerous tubes worm. At this contact estimated that the white flow was ~10 cm thick.

23:51 Z – 421.8 m - Crossed back onto the fresh flow. Can clearly see the white flow (to left below) is high and apparently blanketed and area with tubeworms (to the right below).

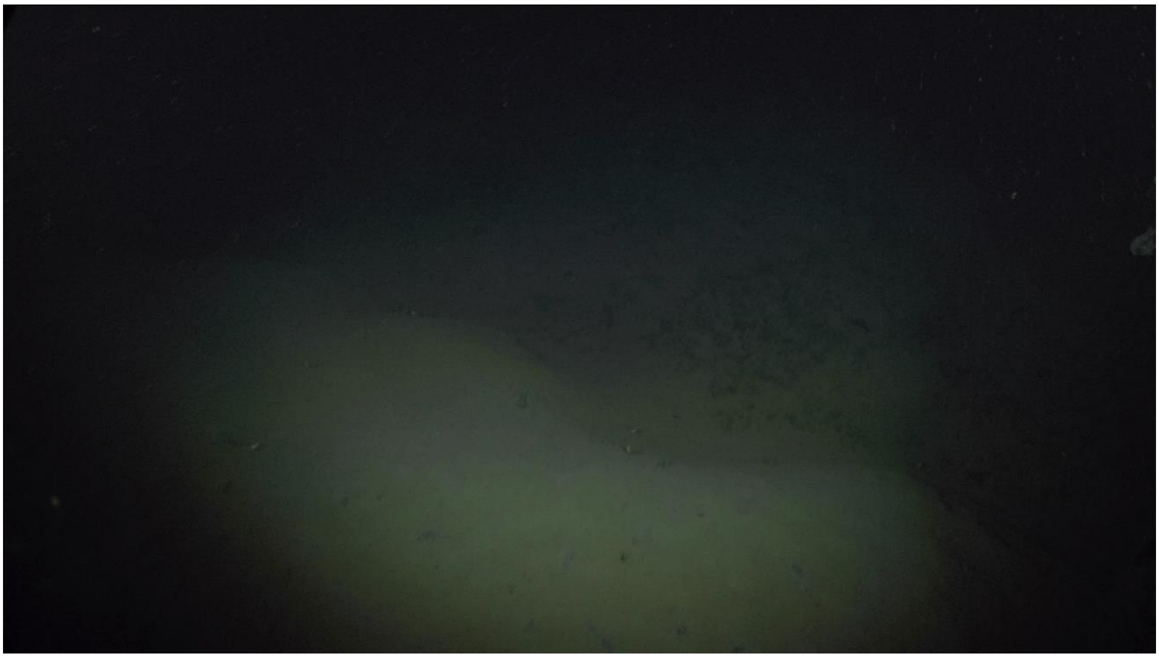

M105 Sequential image 2 – Contact between white seafloor and seafloor characterized by tubeworms.

M105 Sequential image 3 – Contrasting area of high flow and area with tubeworms.

23:56 Z – 421.8 m - Landed to sample in 421.8 m. Took M105 PsC-2 and M105 PsC-3. Both cores show that the surface is slightly tanner, but rest of core is white and uniform in color. Noted temperature is 0.373°C.

00:04 Z (September 9, 2017) – 421.8 m - During sampling, noted that the swing arm sank into the sediment, indicating the surface was soft.

M105 Sequential image 4 – MiniROV arm taking push core.

00:09 Z - Started moving ship on course of 290° to proceed along planned transect. Shortly after getting underway, again crossed a distinctive contact between white flow and the extensively tubeworm covered bottom. Where the fresh white mud flows thinned out laterally, could see worms that were progressively more buried at the edge. Presumably others were completely buried by the >10 cm thick flow, as the tubeworms typically only extend a few cm above the seafloor.

00:14 Z – 421.8 m - Crossed contact three times between 00:11 Z and 00:22 Z.

00:22 – 422 m - Stopped to sample. Took M105 PsC-8 and M105 PsC-9 in area with generally smooth bottom, but where the surface color was light tan and occasional patches of black sediment showed in the interior of small depressions, which may have been produced by grazing organisms. Did not see tubeworms at this site. Impression is that this site was a little older and more evolved that than the first cores of the dive.

00:37 Z – 422 m - Underway again on course of 280° traveling over similar white or light tan colored smooth seafloor.

00:41 Z – 421.8 m - Passed onto area characterized by tubeworm cover which persisted until 00:51 Z.

00:49 Z – 421.3 m - Encountered curious depression that is ~25 cm across and ~5 cm deep. Speculate that a fish excavated it.

00:51 Z - Crossed areas with smooth tan surface with common black spots surrounded by white mats lacking worm, which faded into area with tubeworms. 00:55 Z conscious of being 40 m from OSMO Sampler site, but no sonar targets

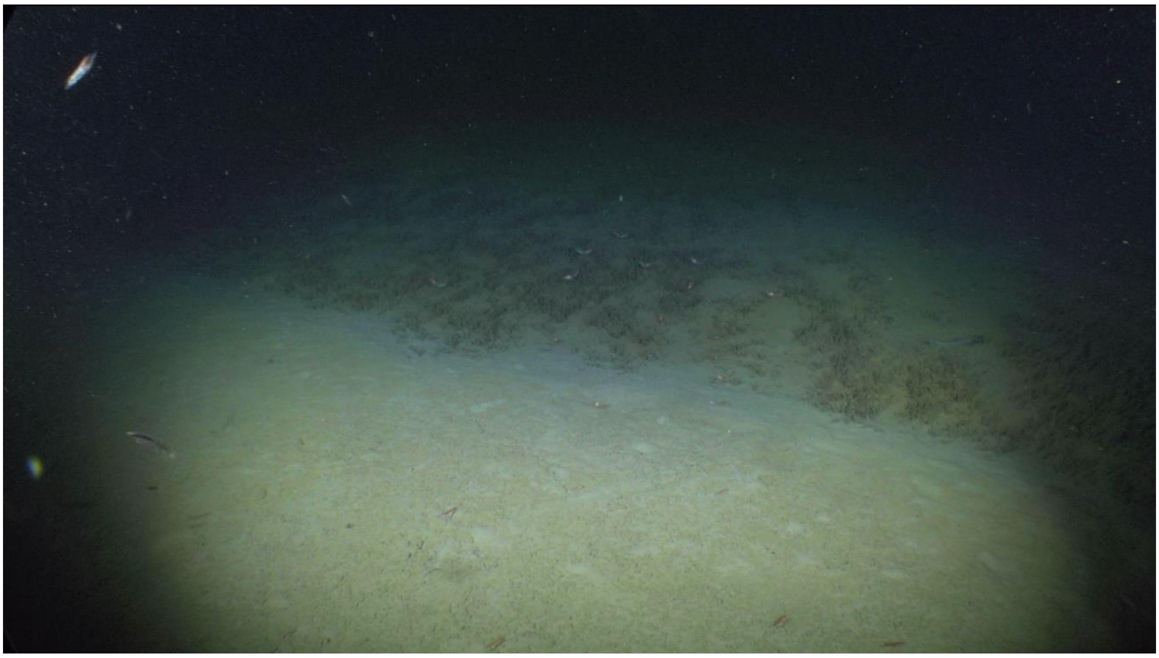

M105 Sequential image 5 – Example of area with sharp contrasting seafloor.

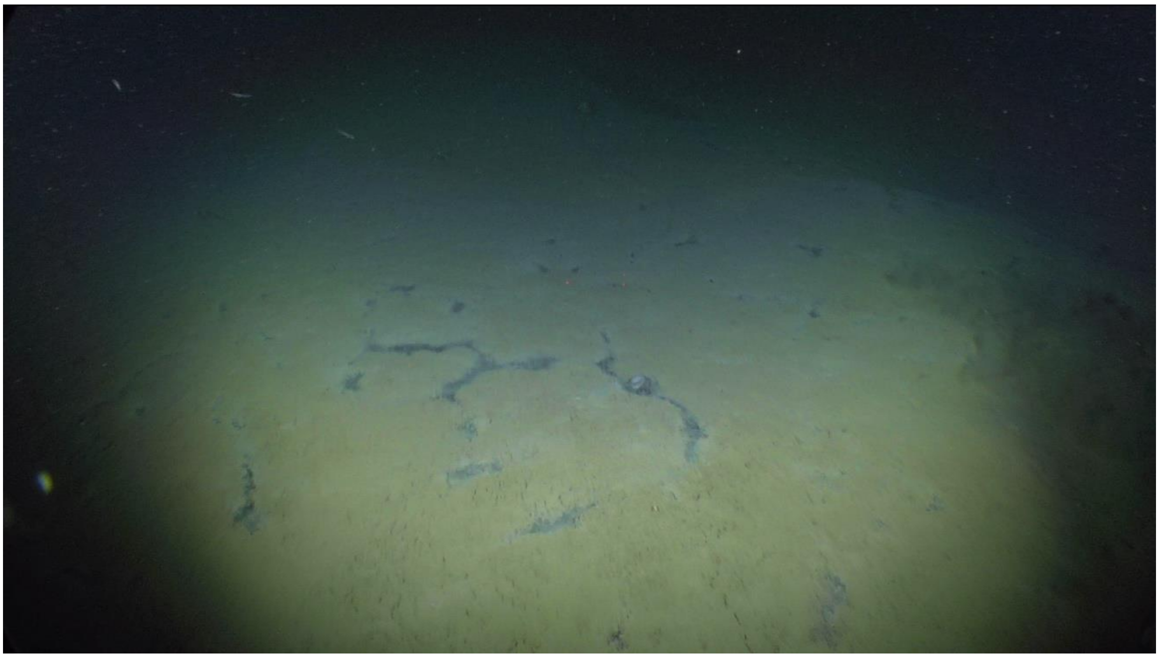

M105 Sequential image 6 – Area of light tan coloured seafloor with patches of black sediment.

01:00 Z - Near OSMO Sampler site. Crossed reported position without finding instrument. From 01:00 Z until 2:03 Z searched for the OSMO Sampler by conducting three WNW – ESE lines and nine NNE-SSW lines in area that were ~60 m long, but did not find OSMO Sampler. No appropriate sized or hard sonar targets were seen which covering a range of ~50 m from reported position. As time to pull approached, landed for final sample collection.

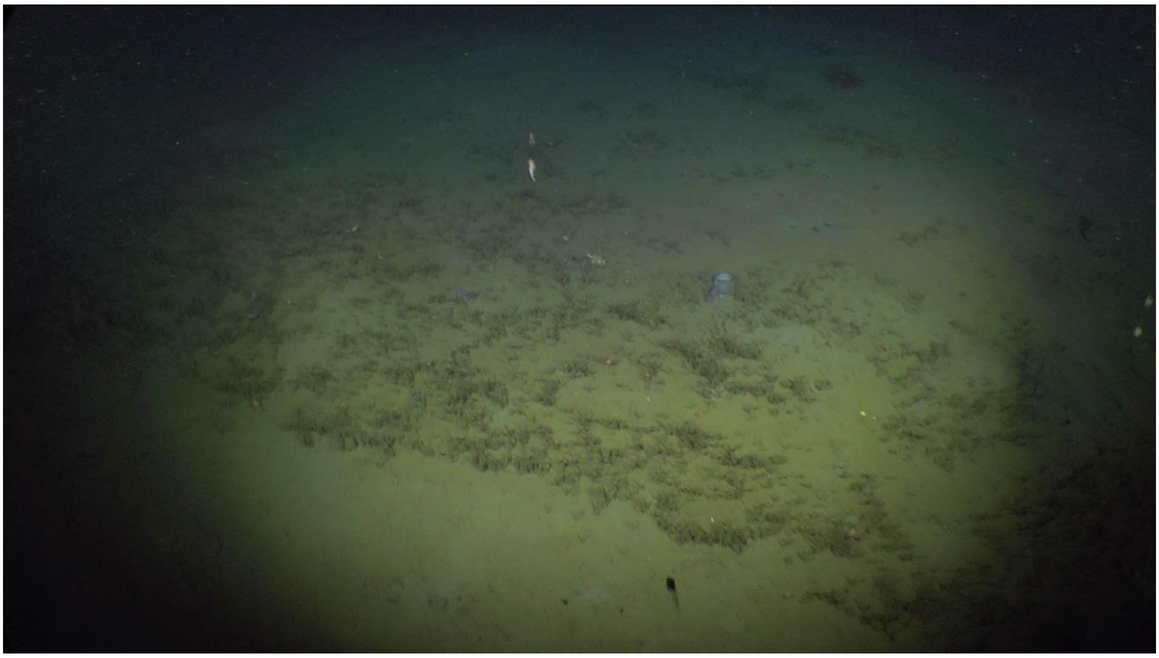

M105 Sequential image 7 – Area characterized by tube worms.

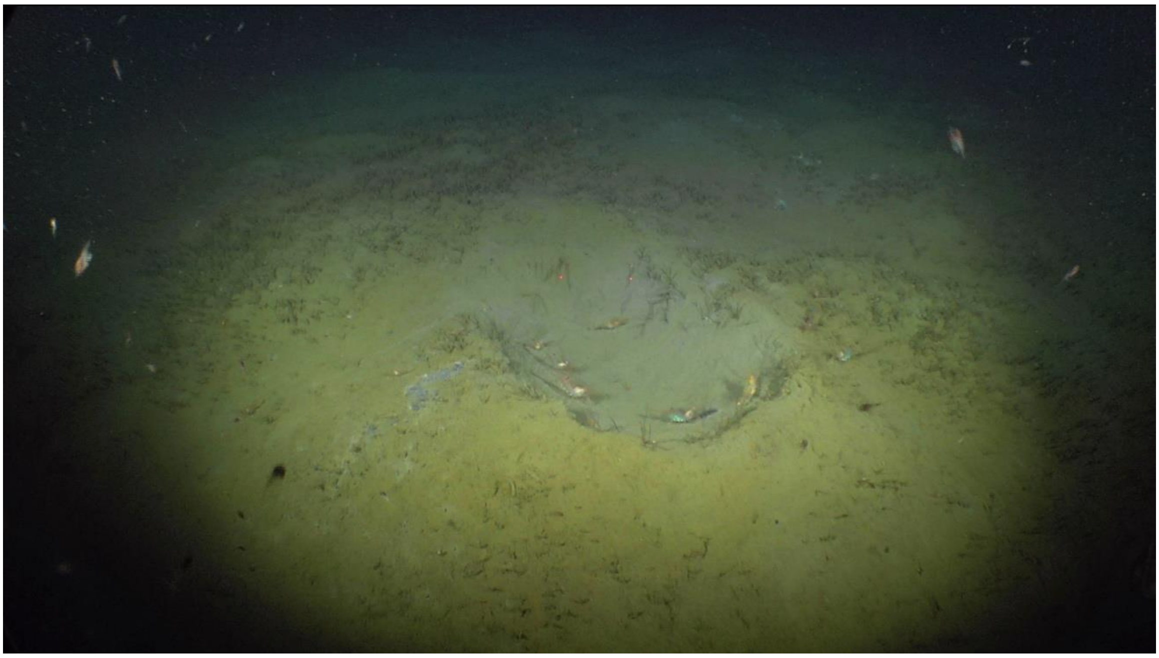

M105 Sequential image 7 – Seafloor depression ~ 25 cm by ~5 cm.

02:03 Z – 421.2 m - Took M105 PsC-12 and M105 PsC-14 in small worm patch. Saw a few cm of tan sediment over black sediment and worms that stuck out of the bottom. Took third core (M105 PsC-14 ~10 cm away), where there were no worms. However, did not encounter the black sediment in this core.

2:15 Z - End of dive, off bottom.

19:45 L - ROV on deck.

6.3.4. Dive observations: shelf edge pingo area

Although ROV dives on previous Laurier cruises have occurred in this area, the dives have not successfully inspected either the depression or the tops of PLF. Thus, the goal of dives M106 and M107 were to utilize the dynamic positioning of the Araon to inspect these specific areas (Figure 6.15).

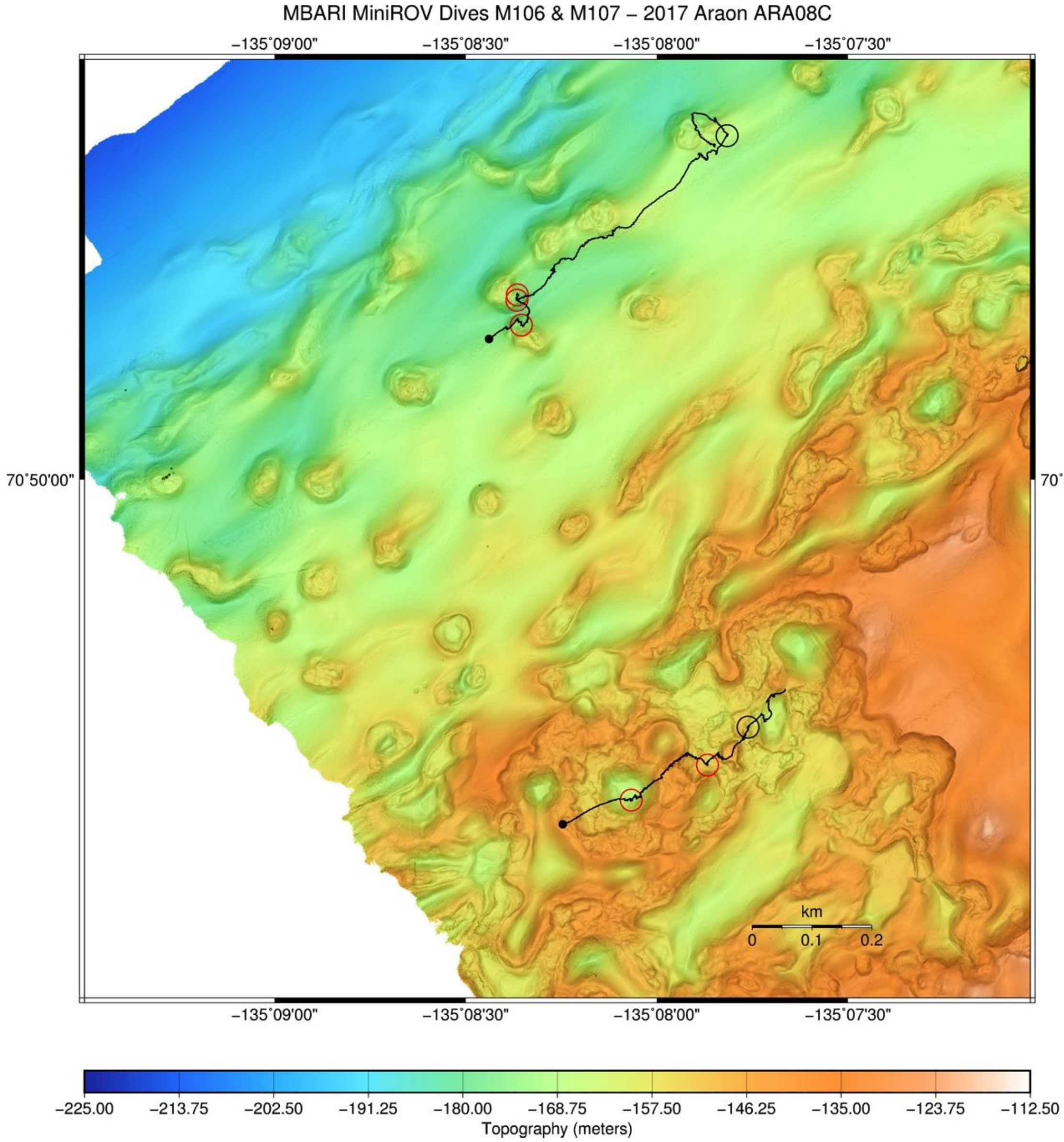

Figure 6.15. Dive tracks for ROV dives M106 and M107 plotted on 2017 AUV bathymetry. Dive M106 is the southern track. Suspect slight offset in bathymetry as Dive M107 crossed the crests of the PLF.

MiniROV Dive 106 (M106) Narrative (September 9, 2017, Saturday)

10:30 L - Arrived at Shelf Edge Pingo area and set up for M106 (135° 08.067624´W, 70° 49.731708´N, Depth 165.7 m). The launch site for this dive was located over a 20 m deep 150 m diameter topographic depression. Planned to transect ~450 m on bearing of 52°. Should cross another similar depression after 355 m at 135° 07.596873´W 70° 49.850376´N, Depth 167.47 m at end of transect.

10:40 L - Clump weight in water.

18:00 Z – 146.4 m - ROV landed on ‘doughnut’ shaped topographic high that rims depression. Thus, were ~125 m WSW from the center of depression. Seafloor surface was smooth, with no rocks exposed. However, seafloor was covered with a dense fauna consisting of numerous small brittle stars, scattered soft corals, and occasional basket stars. Used arm to probe for slightly buried rocks which suggested a veneer of sediment over a firmer buried surface that might be ~8 cm sub-bottom.

M106 Sequential image 1 – Large basket star on seafloor.

18:11 Z - Underway at 055°. Turned on sonar recording at 50 m range (file – win881al09-sep-2017-181347).

18:17 Z – 152.2 m - Locally the bottom slopes are several degrees, but change laterally to produce an undulating topography. USBL shows ROV still on ‘doughnut’ rim. Still see no clear rocks.

18:20 Z – 159 m - USBL track shows ROV entering side of depression.

18:22 Z – 161.1 m - Faced sidewall. Bottom is smooth with no significant texture beyond the dense cover of small brittle stars. Sonar shows only steep slope with no indications of outcropping strata. Bottom of depression is extremely bland. Only notable change was one area in 166.3 m where there was a patch of what appeared to be small (fish?) bones with larger starfish and a few basket stars. Appeared to be a dead fish fall.

M106 Sequential image 2 - Patch of seafloor with what appeared to be small bones with larger starfish and basket stars.

18:30 Z – 166.2 m - See angular flat rock on top of sediment and sampled it (M106 Rx-1). Sonar showed we were in the center of the depression. Also took push core (M106 PsC-3) which was a full penetration core, however sediments were sticky and bottom of core remained in the hole.

18:40 Z – 165.8 m - Weak gouge or ‘whale mark’.

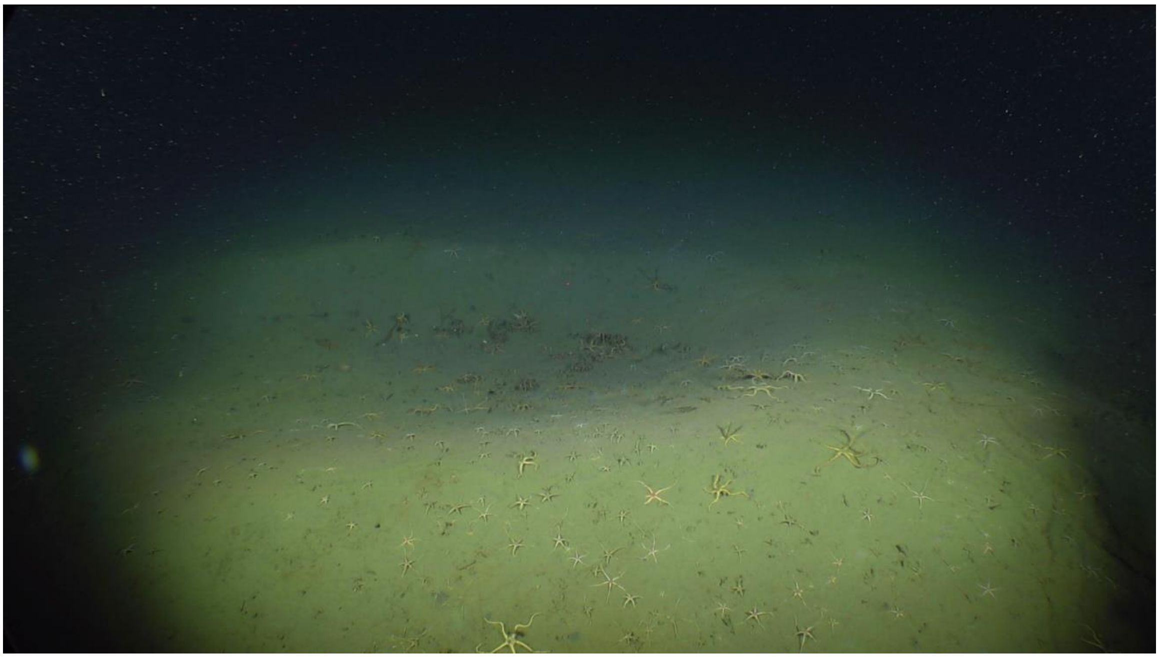

M106 Sequential image 3 – Weak gouge in seafloor.

18:42 Z – 165.2 m - Another gouge, this time estimated to be more ~1 m wide. On inspection saw several sea spiders in the gouge.

18:50 Z – 158.6 m - See cm-sized pebble.

18:51 Z – 155.3 m - Going almost straight up very steep slope. See another cm-sized pebble.

18:53 Z – 152.1 m - Still going up, note less brittle stars.

18:54 Z – 150 m - Increase in number of soft corals and decrease in brittle stars.

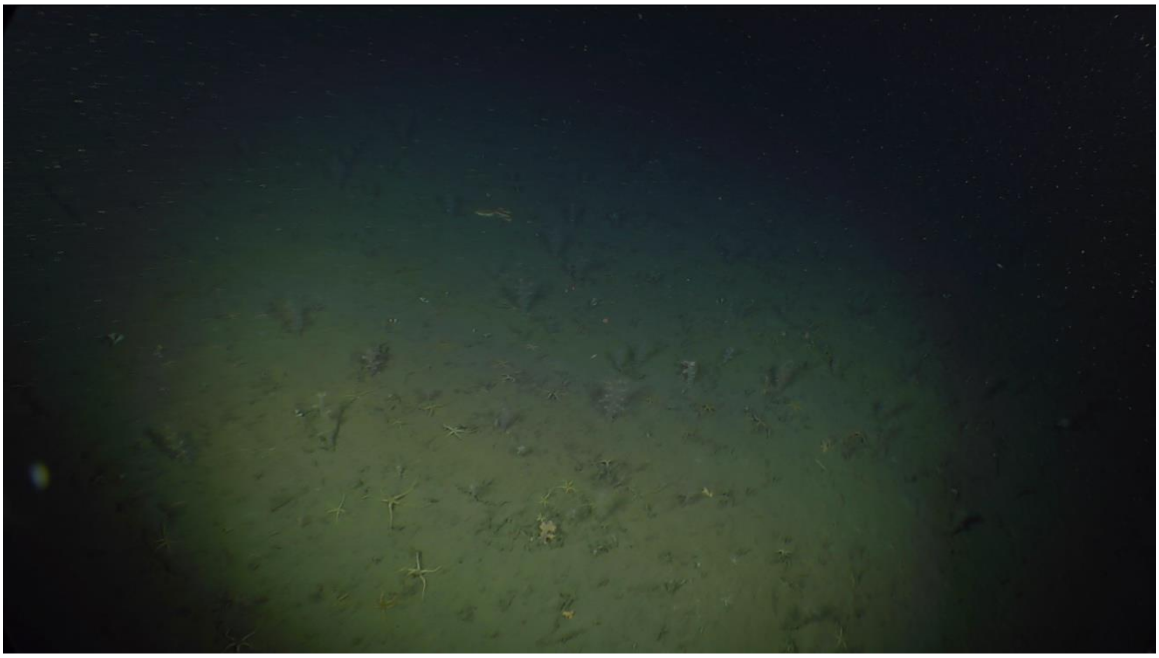

M106 Sequential image 4 – Area with soft corals.

18:57 – 147.7 m - See three small cobbles. Note that soft corals are common on the surrounding doughnut but not in the depression.

19:00 Z – 150 m - Sampled two sponges (M106 A1 and M106 A2) on flank of ridge dipping to NW.

19:24 Z – 148.1 m - Gouge-like depression which is 1 m long and ~40 cm across. Flanks of such depressions commonly have small ridges that are a few cm higher than the surrounding seafloor. Characteristically the cross sections are nearly semi-circular and the floor of the depression is smooth.

19:30 Z – 147.7 m - Sampled isolated flat rock (M106 Rx-1).

19:33 Z – 147.6 m - Sampled basket star (M106 A3).

19:36 – 147.6 m - See more gouges (whale marks?) and discuss whether they are fractures. Features seem to be preferentially occurring near or at the tops of slopes. In at least one case, there are at least three features that are in a line, with the down slope end being terminated at what is obviously the headwall of a younger side scar were the seafloor is locally steep. Note that in places two fractures were parallel.

19:48 Z – 154.6 m - Passing over area of very irregular bottom, with various slopes. No rocks exposed.

19:52 Z – 153.5 m - Landed on flat area with a relatively smooth bottom to sample. The core was taken in part to test the firmness of the seafloor. Took M106 PsC-5 penetrated ¾ into firm bottom.

20:02 Z – 155 m - Encountered three ~30 cm long x ~10 cm high clumps of darker grey colored fine sediment standing in relief from the surrounding sediments which were in a line separated by ~1 m. Each clump was broken along open fractures and formed sharp angles. Apparently, these were fresh. Took sample from third clump (M106 Rx-3 in 155 m). This turned out to be a mud clast with a plastic consistency. It was placed into a separate bag, but included with the other rocks from this dive.

M106 Sequential image 5 – Clump of darker grey, fine sediment standing in relief from the surrounding sediments.

As the ROV continued further down the slope, it became apparent that the clumps were part of a slide mass that continued further down slope.

20:16 Z – 152.9 m - See a grove running up slope. The side of this groove exposed lineations that appear to be bedding surfaces, which suggest steeply dipping strata. Such high dips suggest deformation.

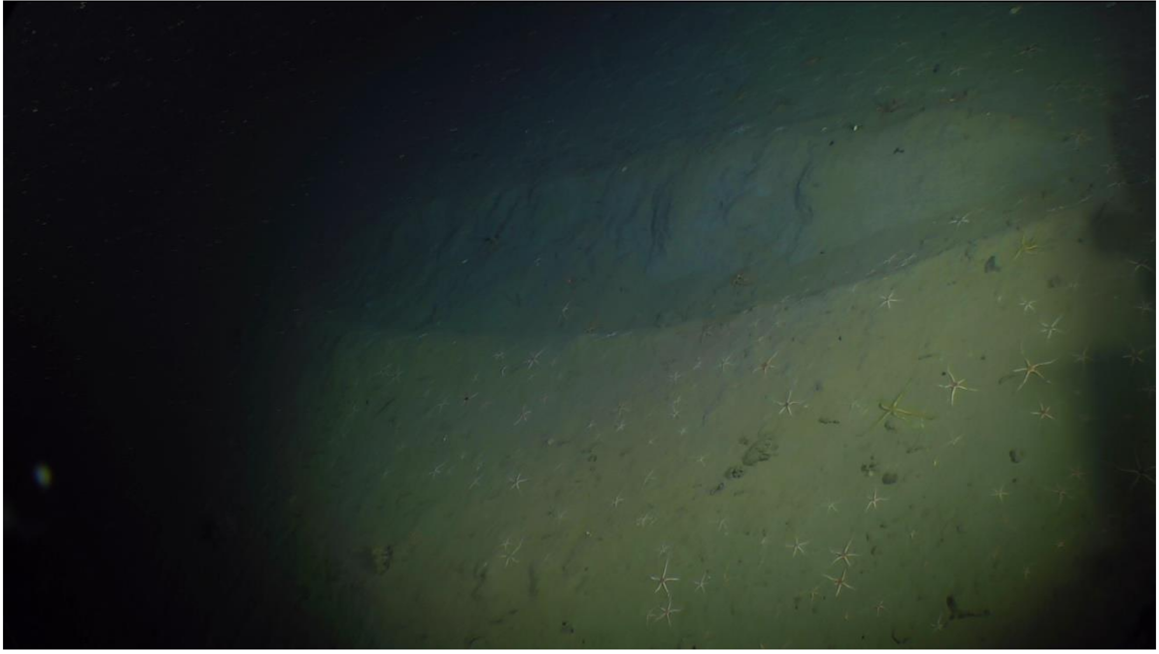

M106 Sequential image 6 – Groove running upslope.

20:20 Z –152.1 m - Sample coble (M106 Rx-4).

20:23 Z – 152.1 m - See another groove on side of ridge.

20:25 Z – 152.9 m - Lots of soft corals and sampled one (M106 A-4).

20:34 Z – 153 m - Sample five cobbles (M106 Rx-5 to M106 Rx-9).

20:55 Z – 159.1 m - On top of small ridge. Several more grooves on the NW flank of the ridge.

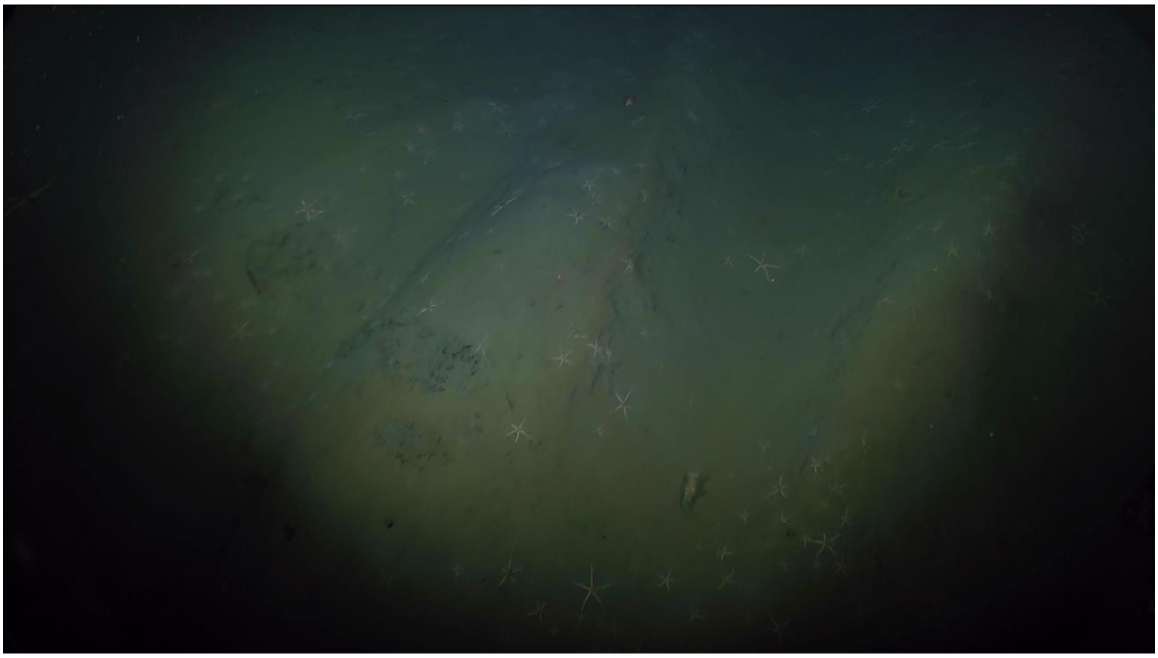

M106 Sequential image 7 – More grooves on flank of the ridge.

21:05 Z – 149 m - Stopped to sample two more rocks (M106 Rx-10 and M106 Rx-11). All the rocks from this dive were mixed into one sample bag.

21:12 Z – 149 m to 21:16 Z - See numerous pebbles and cobbles exposed on the surface. This dive ended while still on the doughnut of the second depression.

21:19 Z – 146 m - End of dive.

14:50 L – ROV on deck.

MiniROV Dive 107 (M107) Narrative (September 9, 2017, Saturday)

16:01 L (23:01 Z) - Launch for M107, the second ROV dive in Shelf Edge Pingo area (135° 08.363817′W, 70° 50.159774′N, depth 164 m). This dive is located to cross four PLF with different structures on their crests. The goal is to inspect their flanks and crests. Transect is oriented at 52°. NE end is at 135° 07.866885′W, 70° 50.291887′N, depth 166.6 m.

23:38 Z – 176.9 m - Landed on flat bottom ~30 m to the west of the mound based on the sonar. Bottom colonized with soft corals and small brittle stars. Did not see rocks exposed. Sonar recording started (last digits 234413).

23:47 Z – 178 m - Contact with PLF is abrupt in terms of both slope change and surface exposure. Numerous cobbles are seen on the flank of the PLF. Slope changed from flat to ~25° in less than 1 m coincident with sudden occurrence of cobbles. Went back to base and traveled ~10 m along the basal contact and persisted to see abrupt contact.

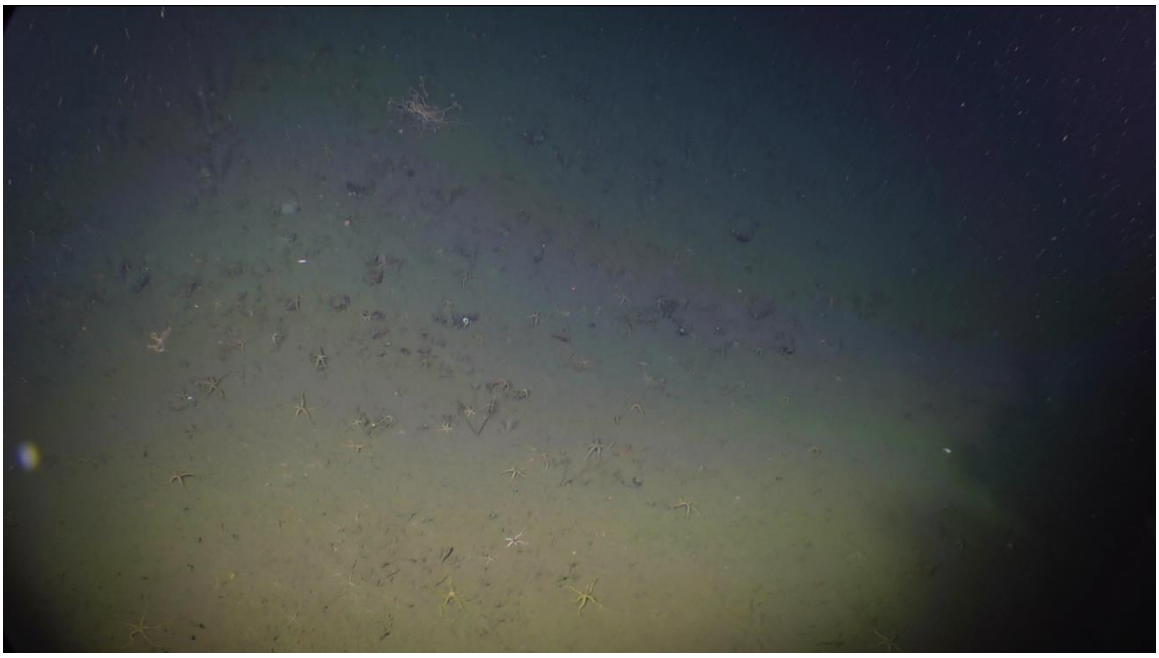

M107 Sequential image 1 – Numerous cobbles on the flank of the PLF.

23:52 Z – 178.6 m - Took push core (M107 PsC-1) on flat seafloor surface ~ 3 m from the base of the PLF. Firm sediment and ~1/2 penetration. On withdrawal, saw ~4 cm tan over grey sediment.

23:55 Z to 00:04 Z (September 10th GMT) - Proceeded up the side slope of the PLF. Above 175 m, the number of cobbles decreased progressively to the rim of the PLF in 164 m.

00:07 – 164 m - ROV cross over the ~1 m deep depression and reached the rim on the other side at the same depth.

00:07 Z – Took push core M107 PsC-11 on the rim. ~5 cm penetration and bottom of core stuck in hole.

00:13 Z – 165.1 m - Returned to floor of the depression and landed to take PsC-10. On withdrawal, saw ~4 cm tan over grey sediment.

00:21 Z – Underway to 050° down side of PLF to intervening ridge. Noted temperature =-0.02°C. This is warmer than measured in this area on previous years.

00:31 Z – 172.8 m - On bottom on ridge between PLFs.

00:34Z – 171.6 m - Lots of gravel going up flank of 2nd PLF.

00:34Z – 168.2 m - At edge of crater on top of PLF.

00:36 Z - Going down into crater on top of the PLF. The floor of the crater and its rim appear to be underlain by cohesive mudstones. Only a few rocks were seen on the seafloor within the crater. Some fractured blocks of uniform lighter grey color mudstone, which stand ~20 cm higher than the surrounding tan colored seafloor. These blocks appear to be of the same material as the craters rim and thus have been scraped off the craters rim.

00:44 Z - Rim of crater in ~162.9 m water depth.

00:54 Z – 165.6 m - Passing over ridge between 2nd and 3rd PLF. Bottom is covered with gravel. See some gravel up to 163.9 m on flank of 3rd PLF.

00:57 Z - See cross cutting groves on the rim of 3rd PLF.

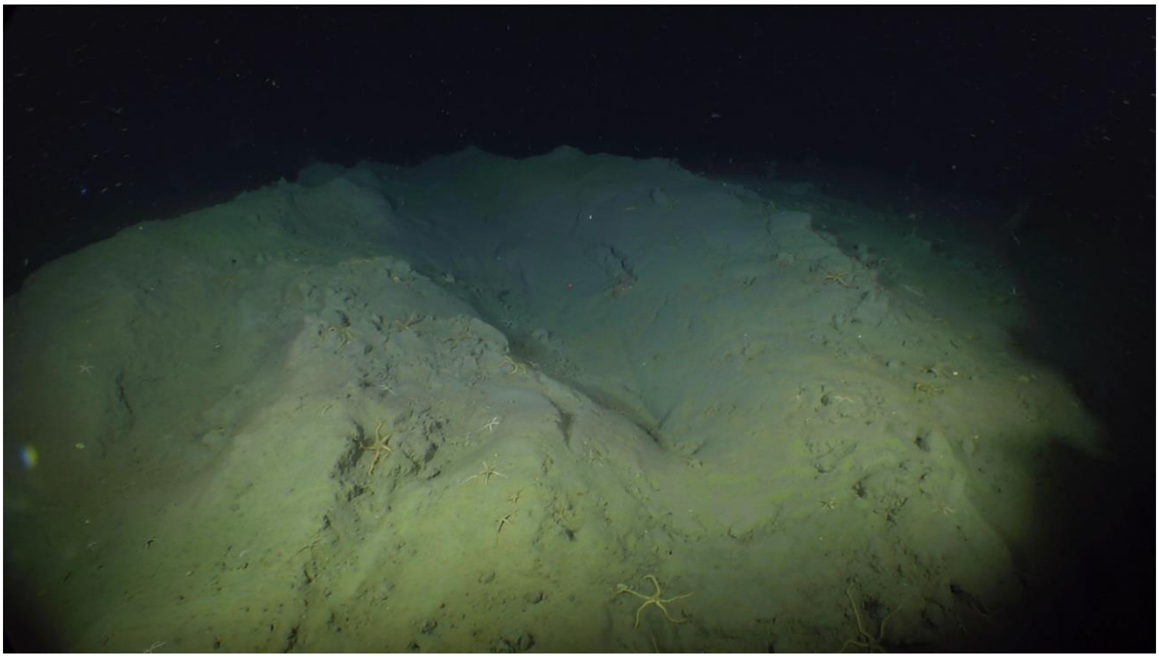

M107 Sequential image 2 – Groove on PLF.

1:09 Z – 161.4 m - At top of 3rd PLF and crater is again associated with smooth surface indicative of cohesive mudstone.

01:12 Z – 164.9 m - ROV underway fast with ship going at 0.3 knots to fourth PLF.

01:19 Z - Finished fast trip and slowed down ~40 m from base of 4th PLF.

01:20 Z – 168.8 m - Crossed over two more grooves.

01:24 Z – 164.8 m - Near base of the PLF. Again see numerous cobbles and gravel facies exposed on the lower flank of the PLF. Sampled 13 cobbles (M107 Rx-1 to M107 R-13) between 164.1 and 164.7 m depths.

01:51 Z – 164.7 m - After sampling rocks on PLF flank went NW perpendicular to the trend of the PLF and away from the PLF onto the surrounding sediment. At 167 m there were lots of rocks exposed, by 170 m water depths there were few, and by 173 m water depths were no more rocks.

02:00 Z – 181.7 m - On flats away from PLF – No rocks, smooth seafloor. Then turned first to the west than back to 160° to go back to PLF. As the slope increased at the base of the PLF (this time at 176 m) there were again lots of exposed rocks. However, as the ROV went further up the side the numbers of rocks decreased with depth. Sampled 2 soft coral at 167.2 m.

02:18 Z - End of dive M107.

19:50 L - ROV on deck.

6.3.5. Dive observations: top of conical mud volcano in 740 m water depth (Figure 6.16)

The top of this mud volcano was observed to be erupting during the 2016 ROV dive. The goal was to determine if it was still active.

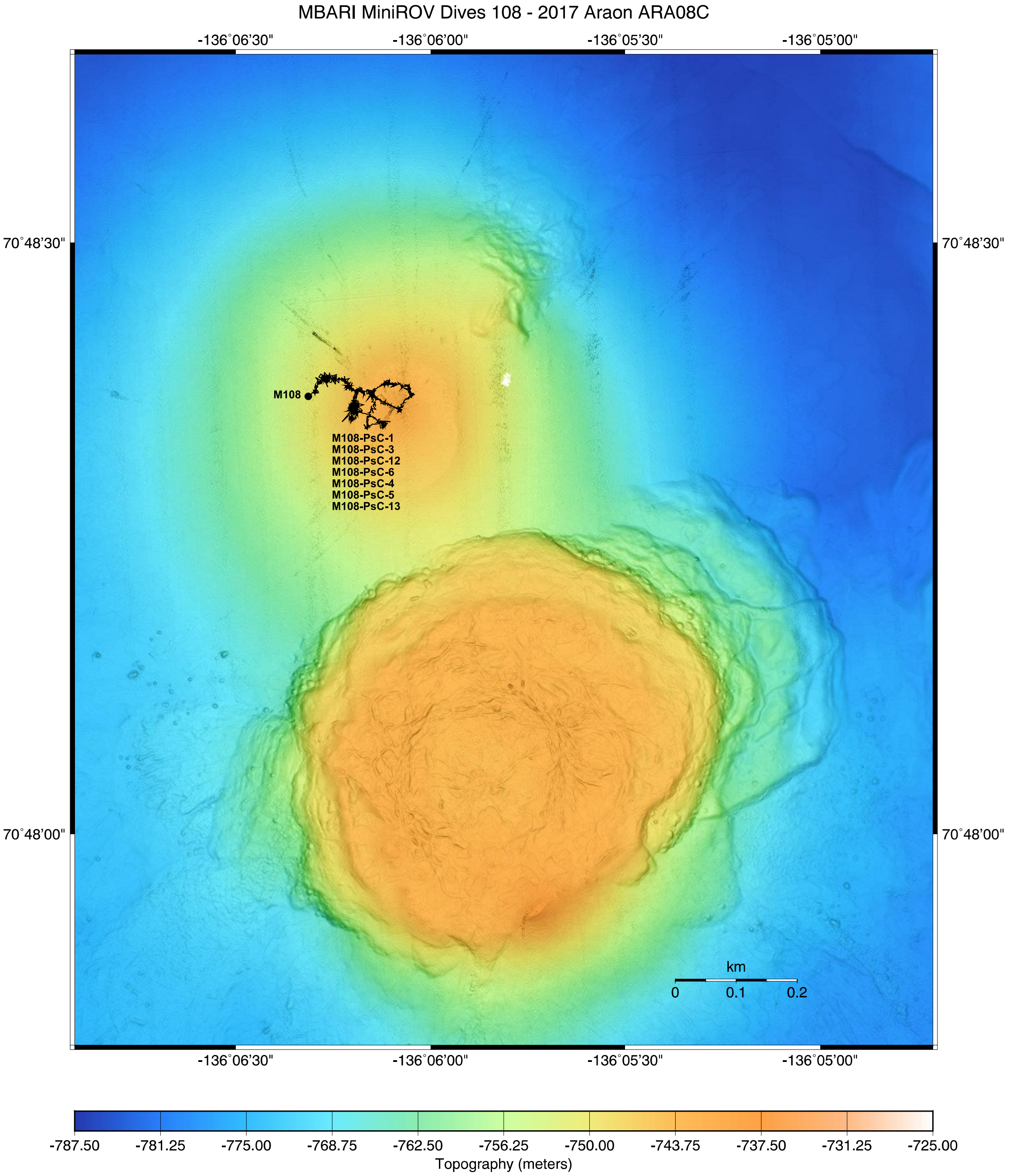

Figure 6.16. Map showing track of ROV dive M108 with respect to the bathymetry of the 740 m mud volcano.

MiniROV Dive 108 (M108) Narrative (September 10, 2017, Sunday)

11:22 L – 18:22 Z - At site (136° 06.085716´W 70° 48.360690´N, depth 741 m) for dive M108. Position picked based on 2016 AUV data to be the top of cone shaped mud volcano. However, there were known issues with the absolute position of this grid.

19:27 Z – 749 m - On white bland bottom with no sonar targets on flank of mud volcano to WNW of its top.

19:32 Z – 749.4 m - Landed and took push cores M108 PsC-1 and M108 PsC-3. Full cores. Bottom very soft as ROV swing arm sank into the muddy bottom.

19:45 Z – 748 m - Landed to look at fine scale topography. Lots of tracks and trails. See few echinoderms, but area devoid of sessile organisms.

19:51 Z – 748 m - Underway at 115°.

19:52 Z – 747 m - Saw a few small patches of white mat with suggestion of black sediment underneath.

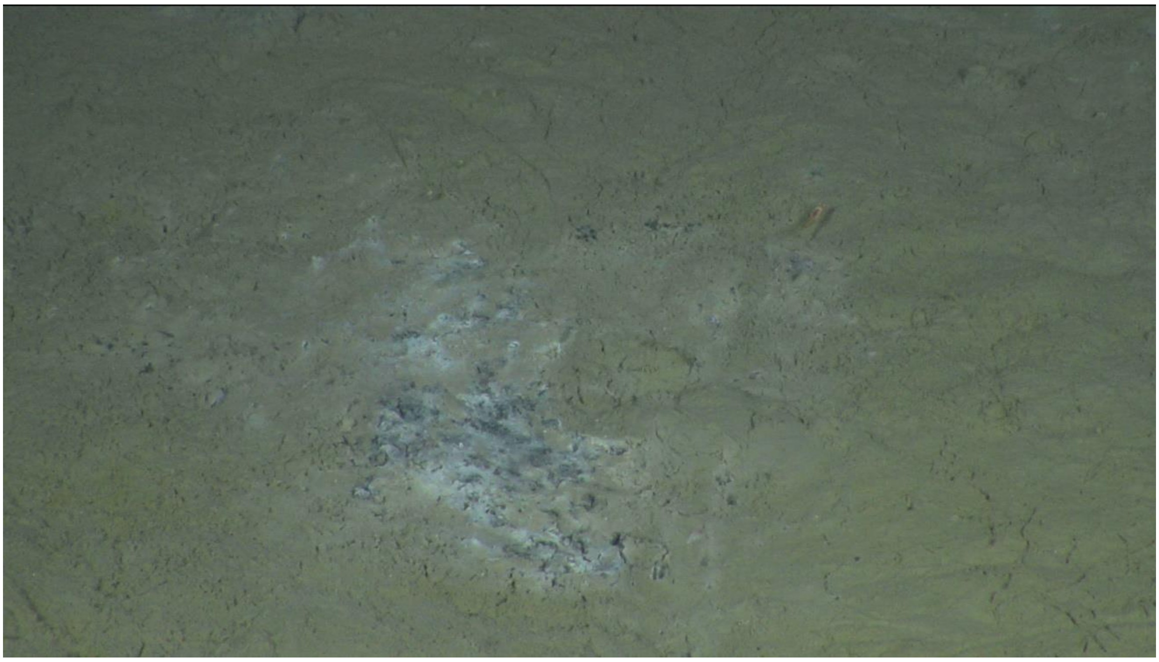

M108 Sequential image 1 – Small patches of white mat on bottom.

19:54 Z – 747.8 m - Stopped to do background measurement for thermal probe.

19:56:26 Z – 747.2 m - Inserted probe into sediment ~15 cm. Probe temperature rose to Tp=0.28°C.

7:58 Z - Retracted probe and temperature quickly fell back to 0.24°C.

19:59 Z – 747.2 m - Underway. See a ~1 m long strip of mat. However, this was atypical of nearly the rest of the dive.

From 08:00 Z until 08:54 Z - Ran search pattern to try to locate top of cone. This was by going along a course while it was getting shallower, but when it got deeper, we changed course usually by 90° and repeated the process. The bottom was uniform white. We encountered a skate.

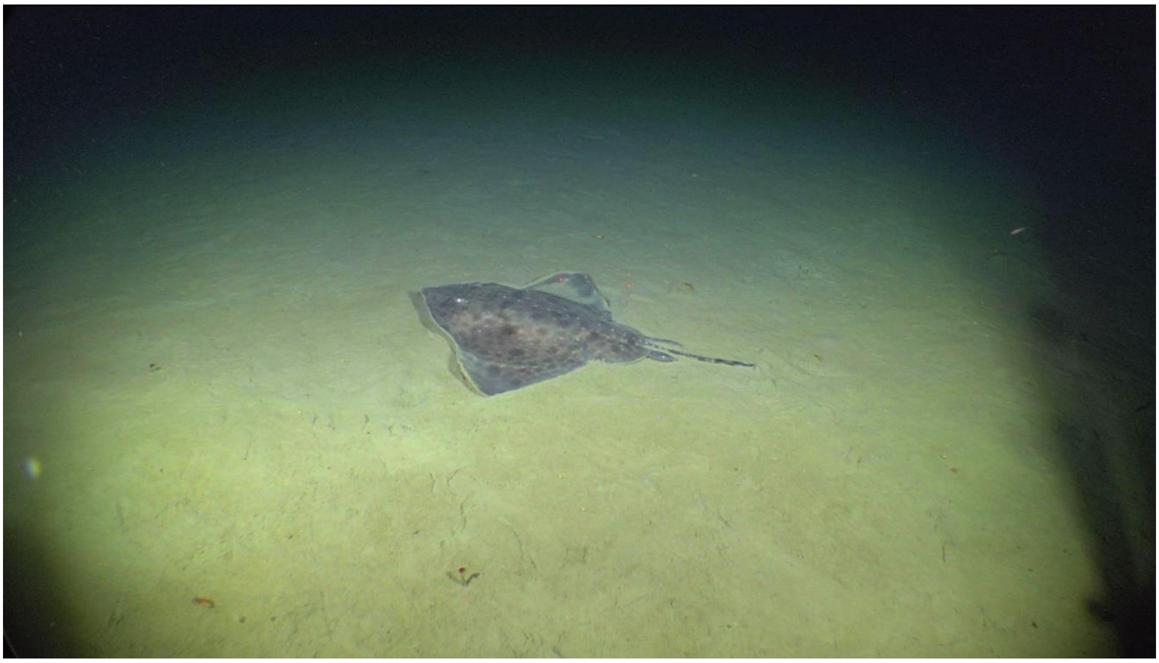

M108 Sequential image 2 – Skate swimming along seafloor.

Unfortunately at the first reversal, we went to the north first, which in retrospect was the wrong choice.

20:55 Z – 745.1 m - Saw the distinctive clotted texture of a young flow that was ~1 m wide and several linear sonar targets at 5 to 10 m range that suggested gas plumes. Moved across the flow and found an area of gas venting.

M108 Sequential image 3 – Area of venting gas.

Bubbles were emanating from the seafloor through the ~2 m wide field of view of the ROV. Apparently, this was an active mud pool as the seafloor expanded and contract like the surface of boiling water. Occasional burps of gas erupted up carrying small clumps of sediment up to 1 m into the water column.

M108 Sequential image 4 – Burp of gas erupting and carrying small clumps of sediment upward in water column.

Some of the mud eruptions produced circular highs on the obviously partly fluidized surface that ranged from <5 cm to >50 cm across with reliefs of >1 to >5 cm. These highs were initially smooth but in less than a minute developed a clotted texture.

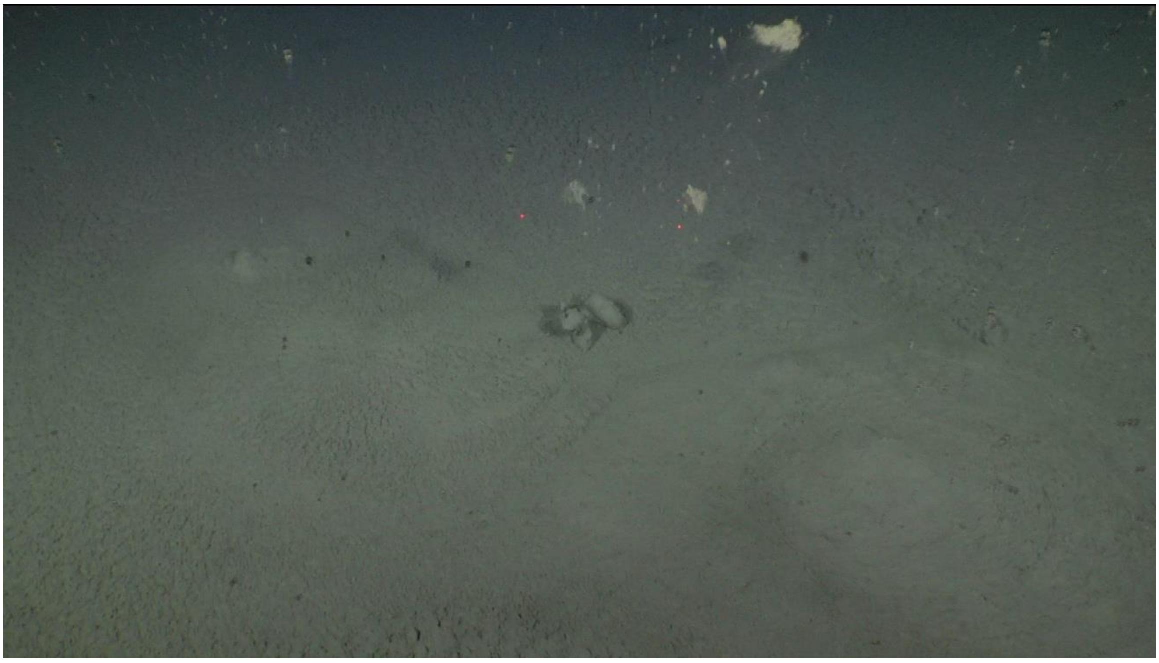

M108 Sequential image 5 – Burp of gas erupting and carrying small clumps of sediment upward in water column.

The circles expanded outward suggesting that fluidized mud was being injected from below.

21:08 Z – 747.2 m - Preparing to use temperature probe. Probe Tp=0.24°C where it is stowed on the ROV arm.

21:11:38 - Positioned probe over the surface of the mud pool to be inserted in an active area but with the tip still ~3-5 cm above the mud. Tp jumped to 0.28°C, but stabilized there.

21:14 Z - Actuated mechanism to inserted probe, and watched as the probe was cranked into the bottom over ~10 seconds. It went an estimated 20 cm into the bottom.

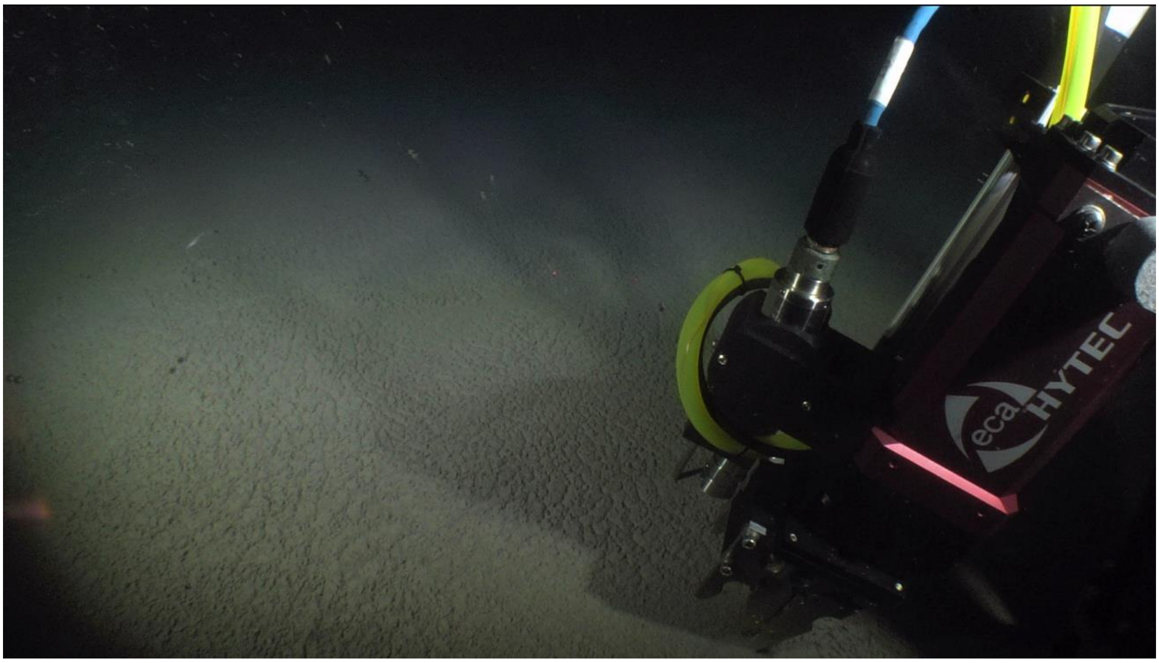

M108 Sequential image 6 – Temperature probe inserted into bottom.

The temperature rose to within <30 seconds to ≥24.00°C (the maximum range of the instrument). While the probe was inserted it was a period of relatively low surface activity on the mud pool.

21:17 Z - Started extraction of the probe. Tp dropped quickly back to 0.29°C.

21:21 Z - Repeated the insertion of the probe without moving the arm. Again temperature quickly rose to ≥24.00°C, the upper limit of its range. Inspection of these data post-dive indicates that the temperature rise was leveling off near this value. Thus, we suspect that the temperature of the mud was not much higher.

21:23 Z - Eruption occurred while probe was inserted into the seafloor, but the probe was at edge of effected area.

21:26 Z - Started extraction of the probe. Tp dropped quickly back to 0.34°C.

21:27 Z - Moved arm to center of eruptive area and inserted probe. Again Tp quickly rose to 24.00°C.

21:32 Z - Retracted probe. Tp drop to 0.32°C. See waves moving across surface of mud pool.

21:35 Z - Started recording sonar (file # win881al09-sep-2017-213514).

21:42 Z – 745.2 m - Pulled out swing arm to try to core. Inserted PsC-12 tube into sediment, but material flowed out the tube as the core tube was extracted.

21:57 Z – 745.2 m - Returned PsC-12 core tube to quiver and took out another one (M108 PsC-6) on backside of swing arm. Proceed to insert this core tube horizontally into the sediment. At the same time the quivers on the swing arm on the ROV were also nearly half buried in the surface sediment slurry.

21:59 Z - The core tube and most of the arm was easily lowered into the sediment partly upside down (i.e. the bottom of the tube was higher than its top, effectively making it into a scoop) out of sight into the bottom.

M108 Sequential image 7 – MiniROV arm taking push core.

When the core tube was taken it out of the sediment slurry it was largely full of sediment, which had flowed into the tube. The tube was then kept upside-down while it was repositioned over the quiver. The sediment slurry from the core tube was poured into the quiver. After two pours, the quiver tube on the swing arm was completely full of sediment and overflowing. Then the core tube was put back into the quiver. This sample provides a unique sample of the fauna that is coming from depth, with only minimal contamination from the seafloor sediment.

22:20 Z - Finished slurry core collection and tried to moved ahead ~5 m to see another vent site which was just visible in the video and scanning sonar. Unfortunately, as the bottom of the ROV was clearly also buried in masses of mud which washed off as the vehicle came off bottom. This resulted in little or no visibility for ~ 30 minutes.

22:50 – 745.1 m - Moved ~30 m away to south and sat down to sample. Took M108 PsC-4 and M108 PsC-5.

23:11 Z - Moved again in search of a bacterial mat. Found mat ~50 m north of the vent site.

23:14 Z – 746.6 m - Took M108 PsC-13 in center of a small patch of mat.

23:15 Z - End of dive M108. Started recovery.

17:00 L - ROV on deck.

6.4. MiniROV Samples

The MiniROV collected 10 rock samples (Table 6.2). All the rocks were bagged and will be shipped with ROV equipment back to the US. M104-R1 was found on top of the mud volcano and might be a clast carried up in the erupting material. All the other samples are believed to be of glacially transported material.

The rock samples will be forward on to the Geological Survey of Canada in Sidney, BC, who has been processing similarly collected rocks samples from previous MiniROV dives in the Canadian Beaufort Sea, as well as cobble samples from sites on land in the Western Canadian Arctic.

Table 6.2. Rock samples collected by MiniROV on ARA08C.

Dive	Sample	Latitude (°N)	Longitude (°W)	Depth (m)
M100	M100-R1-12	69.87884367	139.0560467	101.66
M101	M101-R1	69.8782765	139.0556622	96.65
M101	M101-R2	69.87823633	139.0552018	93.33
M101	M101-R3-13	69.87826617	139.0589652	113.55
M102	M102-R1-10	69.92316933	139.1252797	122.05
M103	M103-R1	70.54435733	139.4022068	419.97
M104	M104-R1	70.79137367	135.5640348	419.97
M106	M106-R1-11	70.829786	135.1293527	153.08
M107	M107-R1-10	70.83825867	135.1302693	164.61
M109	M109-R1-10	70.525069	138.8501973	973.54

The MiniROV collected 35 push cores. Except where noted in Table 6.3, the material in the cores was sampled for microbiologic characterization on shipboard.

6.5. Summary of MiniROV Dives

Ten dives were successfully completed without any significant operational issues. All the observational and the sampling goals for these dives were achieved. These data will hopefully be integrated with other data collected on this expedition and previous expeditions to help further the understanding of the seafloor in the Beaufort Sea.

Table 6.3. Push core samples collected by MiniROV on ARA08C.

Date	Dive	Sample	Latitude (°N)	Longitude (°W)	Depth (m)	Comment
2017-09-05 17:51:55 Z	100	M100-PsC-1	69.87875583	139.0561238	101.59	
2017-09-05 17:57:09 Z	100	M100-PsC-2	69.87875017	139.0561528	101.50	
2017-09-05 20:47:55 Z	101	M101-PsC-7	69.87825217	139.0552245	94.19	MBARI kept for stratigraphy
2017-09-05 20:52:02 Z	101	M101-PsC-6	69.87825817	139.0552285	94.21	
2017-09-05 21:14:33 Z	101	M101-PsC-8	69.87833133	139.0566682	107.27	
2017-09-05 21:18:49 Z	101	M101-PsC-9	69.87833583	139.0566617	107.31	
2017-09-05 21:22:57 Z	101	M101-PsC-3	69.878337	139.0566858	107.26	
2017-09-06 21:35:12 Z	103	M103-PsC-12	70.5443615	139.4026825	923.45	MBARI kept for stratigraphy
2017-09-08 17:09:04 Z	104	M104-PsC-7	70.79148233	135.5642208	419.63	
2017-09-08 17:11:45 Z	104	M104-PsC-13	70.7913865	135.5641943	419.90	
2017-09-08 17:41:07 Z	104	M104-PsC-5	70.79134167	135.5615537	421.11	
2017-09-08 17:50:56 Z	104	M104-PsC-4	70.79135083	135.5615075	420.15	
2017-09-08 19:00:05 Z	104	M104-PsC-1	70.7913635	135.5640173	419.97	
2017-09-08 19:03:41 Z	104	M104-PsC-10	70.79177883	135.5559233	421.63	
2017-09-08 19:08:46 Z	104	M104-PsC-11	70.7917885	135.5558902	422.00	
2017-09-08 23:59:58 Z	105	M105-PsC-2	70.78977133	135.5601715	421.73	
2017-09-09 00:05:25 Z	105	M105-PsC-3	70.78980233	135.5601232	421.78	
2017-09-09 00:28:56 Z	105	M105-PsC-8	70.79003033	135.5606973	421.82	
2017-09-09 00:33:41 Z	105	M105-PsC-9	70.79009767	135.5609853	420.02	
2017-09-09 02:07:05 Z	105	M105-PsC-12	70.79026533	135.5646497	420.94	
2017-09-09 02:11:52 Z	105	M105-PsC-14	70.79027667	135.5647047	421.27	
2017-09-09 18:36:25 Z	106	M106-PsC-3	70.828741	135.1344495	166.24	MBARI bottom of core collected
2017-09-09 19:54:45 Z	106	M106-PsC-9	70.82924367	135.1311217	153.48	extruded, photographed, discarded
2017-09-09 23:53:14 Z	107	M107-PsC-1	70.83554567	135.13924	178.58	extruded, photographed, discarded
2017-09-10 00:09:28 Z	107	M107-PsC-11	70.83597917	135.1394145	164.02	extruded, photographed, discarded
2017-09-10 00:16:46 Z	107	M107-PsC-10	70.83590283	135.139433	165.11	extruded, photographed, discarded
2017-09-10 19:36:32 Z	108	M108-PsC-1	70.80641267	136.1045593	749.36	
2017-09-10 19:41:31 Z	108	M108-PsC-3	70.80644867	136.1043253	749.34	
2017-09-10 21:44:35 Z	108	M108-PsC-12	70.80600333	136.1033167	745.17	
2017-09-10 21:58:45 Z	108	M108-PsC-6	70.80602933	136.1033228	745.22	
2017-09-10 23:00:37 Z	108	M108-PsC-4	70.805845	136.103355	746.05	
2017-09-10 23:00:38 Z	108	M108-PsC-5	70.805845	136.103355	746.07	
2017-09-10 23:12:44 Z	108	M108-PsC-13	70.806229	136.1031913	746.69	
2017-09-12 17:12:06 Z	109	M109-PsC-13	70.52531183	138.853745	1013.95	
2017-09-12 19:14:27 Z	109	M109-PsC-12	70.524723	138.8437407	874.29	

Chapter 7. Heat Flow Measurements

Y.-G. Kim

7.1. Introduction

Subsea permafrost thawing due to long-term sea-level rise and ocean warming since the Last Glacial Maximum is considered to promote significant release of methane from sediments to seawater in the Arctic shelf (Paull et al., 2007; Ruppel, 2014). In the Canadian Beaufort Sea, it is well known that sediments together with methane-rich fluid are emitted from the deep through the sediments in mud volcanoes. While the geologic and geochemical setting of the mud volcanos have been quantified, the flux of fluids and gas have not yet been investigated in a quantitative manner.

To recognize the temporal change in seepage activity, the change in the thermal properties of the mud volcanoes can be used as a proxy/parameter to approximate the flux. Although long-term thermal measurements have never been acquired, short-duration heat flow measurements have been taken during several marine expeditions (Jin et al., 2015; Jin and Dallimore, 2016). Heat flow measurements can provide only a snapshot of thermal status at a specific point; therefore, we need to collect data periodically for a better understanding. Following successful marine research expeditions ARA04C and ARA05C (Jin et al., 2015, Jin and Dallimore, 2016), additional thermal measurements were acquired during the ARA08C expedition at targeted mud volcanoes. Specifically, the primary objective of this expedition was to collect data from the 420 m mud volcano area where spatiotemporal changes in morphology and texture related to seepage have been documented through repeat AUV and ROV surveys (Paull et al., 2015).

We would also like to improve the understanding of the regional heat flow regime. These observations may give confidence in confirmation and assessment of seepage activity in mud volcanoes. A secondary goal of this study was to investigate the geothermal regime of bottom simulating reflectors (BSR) related to the marine gas hydrate stability zone as documented by Riedel et al. (2017) in the outer Mackenzie Trough. To accomplish this, the marine heat flow program strived to collect measurements in as deep a water depth as possible where thermal disturbance by seasonal temperature change in bottom water or tectonic/sedimentary activity are not expected.

7.2. Methods

Marine heat flow is determined from two parameters: geothermal gradient and thermal conductivity. In order to measure the two parameters, two different instrument sets were used: the Miniaturized Temperature Logger (MTL) by ANTARES and the DST Tilt by Star-Oddi for in-situ geothermal gradient (Figure 7.1; Tables 7.1 and 7.2), and TK04 by TeKa for thermal conductivity of retrieved sediment cores (Figure 7.2; Table 7.3). Because in-situ observations are preferred rather than laboratory-based observations, thermal conductivity values should be corrected using the empirical relationship established by Ratcliffe (1960). Two measurements were made at each site to increase the reliability of the data.

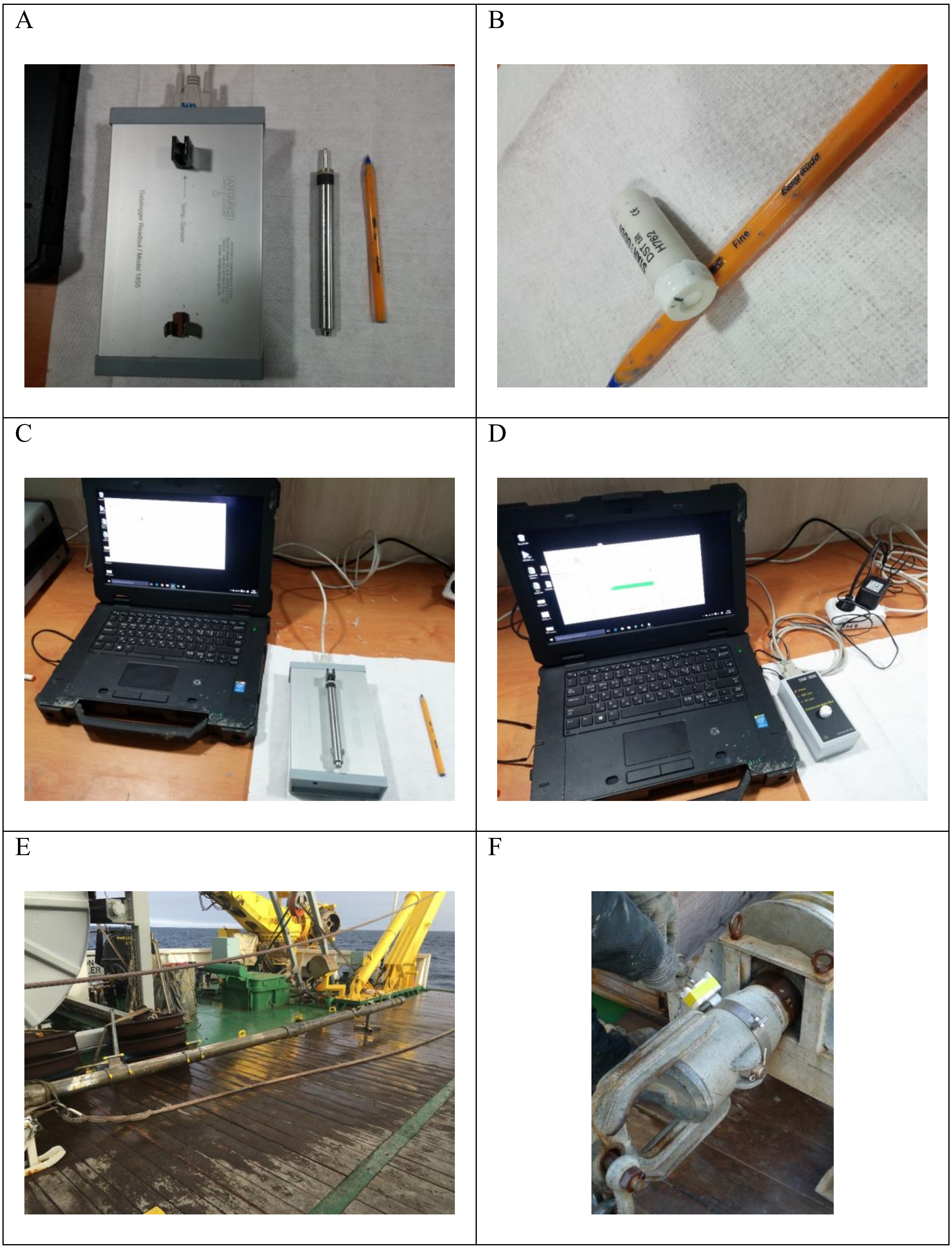

Figure 7.1. Photos of the MTL (A) and the DST Tilt (B) with platforms for each (C, D). Photos of gravity core equipped with heatflow instrument sets (E, F).

Table 7.1. Specifications of the MTL.

Type	Antares 1854
Length	160 mm
Weight	120 g
Chassis	Stainless steel
Battery	3 VDC type DL1/3N (soldered)
Maximum pressure	60 MPa
Measuring range	-5 to 50°C
Resolution	0.001°C
Accuracy	< ±0.1°C
Maximum operating time per battery	300,000 samples or 1 year standby
Programmable measure intervals	1 sec to 255 min
Starting time	Immediately or programmable with Date and Time up to 30 days in advance
Read-out type	Galvanic coupling (without cable)

Table 7.2. Specifications of the DST Tilt.

Sensors	Tilt (3-D), temperature, pressure (depth)
Size (diameter * length)	15 mm * 46 mm
Weight (in air / in water)	19 g / 12 g
Battery type	4 years for a sampling interval of 10 min
Memory type	Non-volatile EEPROM
Memory capacity / size of one measurement (bytes)	261,564 bytes / temperature-pressure 3 bytes, tilt 6 bytes
Data resolution	12 bits
Temperature range	-1 to 40°C
Temperature resolution	0.032°C
Temperature accuracy	±0.1°C
Temperature response time	Time constant (63%) reached in 20 sec
Standard depth/pressure ranges	30, 50, 100, 270, 800, 1500, 2000, 3000 m
Depth/pressure resolution	0.03% of selected range
Depth/pressure accuracy	±0.4% of selected range for 30-270 m ±0.6% of selected range for 800-3000 m
Depth/pressure response time	immediate
Tilt resolution	0.2°
Tilt accuracy	±3°
Tilt range	360°

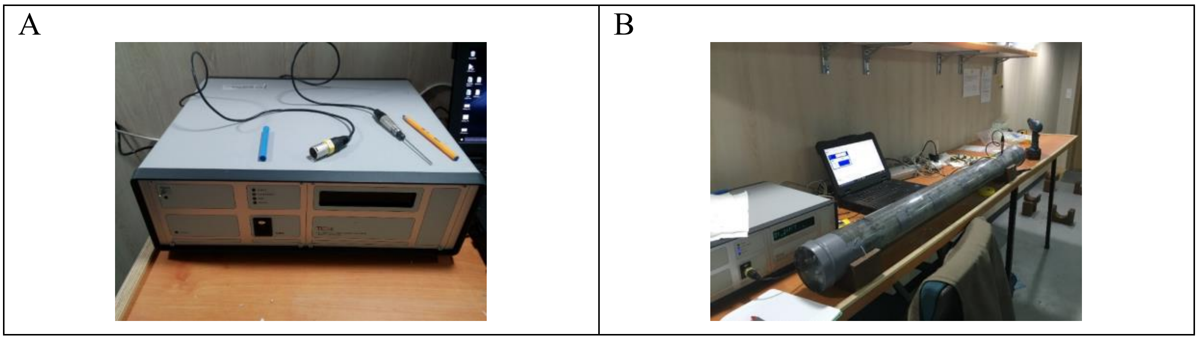

Figure 7.2. (A) Thermal conductivity measurement system, TK04 with a needle probe. (B) Laboratory set-up with needle probe inserted into the whole-round core.

Table 7.3. Specification of TK04.

Model High Precision Thermal Conductivity Meter TK04	
Measuring principle	Transient line source (needle probe method)
Standard	ASTM D5334-08
Measuring range	0.1 – 10 W/m/K (probe dependent)
Accuracy	±2% (probe dependent)
Reproducibility	±1.5%
Heater current precision	±0.01%
Duration of 1 measurement	60, 80, 240 s (probe dependent)
Automatic repetitions	Up to 99 (unattended)
Sample size	No upper limit, minimum size probe dependent
Sample temperature	-25 to 50°C, 70°C, 125°C (probe dependent)
Power supply	220, 240V AC (50 Hz); 100/120V AC (60Hz)
Power Consumption	~40W
Size	W 471 * H 160 * D 391 mm
Weight	11.2 kg (measuring unit)
Interface	Serial port (com port) or USB port (USB-to-serial converter included)
Stand VLQ needle probe	
Probe type	Needle probe / lab
Dimension	L 70 mm * Ø 2 mm
Measuring range	0.1-10 W/m/K
Accuracy	±2%
Duration of 1 measurement	80 s
Minimum sample size	(approx.) L 85 mm * Ø 40 mm

During this expedition, the MTL and the DST Tilt with the gravity corer were used instead of the heat probe (KHF-601) used in expeditions ARA04C and ARA05C (Jin et al., 2015; Jin and Dallimore, 2016). The MTL and the DST Tilt are more time efficient in terms of initial set-up and maintenance between measurements. The MTL and the DST Tilt measure temperature and tilt, respectively, and record the readings on an internal storage, therefore, the only preparation before the measurement was to attach them to the corer with a command of 'run' using a non-contact special platform for each (Figure 7.1.). Time- and effort-consuming processes, such as connecting the thermistors and the logger as well as wrapping all connection lines, were no longer necessary. Up to seven MTLs were placed onto the core barrel at specific intervals using the MTL supporters, and one DST Tilt was inserted into a housing that is attached above the core weight.

We identified three drawbacks to using MTL and the DST Tilt with a gravity corer instead of the Ewing-type heat probe: a) The main drawback was that the measurement status cannot be monitored during the deployment. The previous heat probe contained an acoustic modem which enabled broadcasting of the status of the logger via the hull-mounted EA600. During ARA08C, the EA600 malfunctioned in the passive mode due to an unknown issue, therefore this drawback was not applicable. b) Another drawback was that the opportunity to measure in-situ thermal conductivity was lost. The heat probe provides function to generate heat within the sediments, thus the in-situ thermal conductivity can be calculated using heat dissipation with time curve. c) The final drawback was the restriction to the MTLs placement on the barrel. The MTLs should be attached on the core barrel in order to avoid the join of two 3 m-long barrels by at least 1 m. These join areas are locations where the barrel and ship's stern may rub during deployment/recovery of the gravity core which could damage the MTLs. Thus, the MTLs must be located in the uppermost and lowermost 2 m-interval when using two 3 m-long barrels (Figure 7.1). Such distribution is not ideal for detection of the sinusoidal temperature profile from annual temperature changes in the bottom water.

Thermal conductivity of retrieved cores was measured using the TK04 with a needle probe (Figure 7.2; Table 7.3). Cores were left at least 10 hours in the laboratory before the measurement to allow them to thermally equilibrate with laboratory temperature of ~20°C. The measurement were made at an interval of ~20-50 cm. Observed thermal conductivity values were averaged with a harmonic mean method, adequate for horizontally layered sediments, into one representative value for each station.

7.3. Results

During the expedition, geothermal gradients were measured at eleven locations (fourteen sites as some locations were revisited) and thermal conductivity was measured at five locations (five sites) with water depths ranging from of 93 to 1750 m (Figure 7.3; Table 7.4). Thermal conductivity measurements were co-located with sites where geothermal gradients were obtained, except at the pingo-like feature (PLF) and mud volcano. Ice was encountered at the PLF and texture of the retrieved sediment cores from mud volcano were too soupy.
Measurements were taken at four study areas, as follows:

- Four sites (Sts. 05, 06, 07, and 10) were located in the western part of the Mackenzie Trough, and focused around a pingo-like feature with ~110 m water depth closed to the shelf edge (Figure 7.4; Table 7.4).
- Two sites (Sts. 11 and 36) were located along a transect line parallel to the Mackenzie Trough (Figure 7.3; Table 7.4). Station 11 is the deepest site with water depths of up to 1750 m, close to BSR occurrence area.
- Based on topography and backscatter result obtained by the AUV, six sites (Sts. 29, 30, 32, 33, 34, and 35) were chosen within the flat top of the 420 m mud volcano in the eastern part of the Mackenzie Trough, (i.e., the eastern continental slope). One site (St. 21) was chosen at a background location with the same water depth outside of the mud volcano for comparison (Figure 7.5; Table 7.4).
- The final site (St. 36) was located on the 740 m mud volcano area also in the eastern continental slope (Figure 7.1; Table 7.4). The first measurement was in the cone-shaped top, while the second measurement was made in the flat top.

Annual temperature variation in bottom water should be taken into consideration for data collected above ~300 mbsl because the halocline extends up to 300-400 mbsl (Stein, 2008). In the case of Laptev Sea, annual temperature change of more than 1°C was observed above 500 mbsl (Dmitrenko et al., 2009), which causes temperature variation of 1/e° K at 2 mbsf with an common value for thermal diffusivity (e.g., Goto and Matsubayashi, 2008).

At sites with normal seafloor condition, one can expect that 1) temperatures below the seafloor will increase with depth, 2) temperature increases due to friction will occur when a gravity corer is penetrating and being pulled out, and 3) water depth and tilt are constant (Figure 7.6A). In the cases where the measurements differ from these expectations, one must determine whether the results stem from abnormal seafloor condition in terms of thermal/kinematic status and/or from failed measurements (Figure 7.6B). For instance, temperature-depth-tilt change with time results at St. 21 (control site for the 420 m mud volcano area) follow the expected pattern, while this was not the case in Sts. 33, 34, and 35 (the 420 m mud volcano area). Based on a comparison of the 2016 and 2017 AUV topography and backscatter images, the three sites in the 420 m mud volcano seem to experience active seepage (Figure 7.5).

Thermal conductivity measurements for the chosen cores were completed with the TK04 system (Figure 7.7). Observed raw values require further pressure and temperature correction (e.g., Ratcliffe, 1960). Detailed processing of heat flow results obtained during this expedition will be undertaken after the expedition.

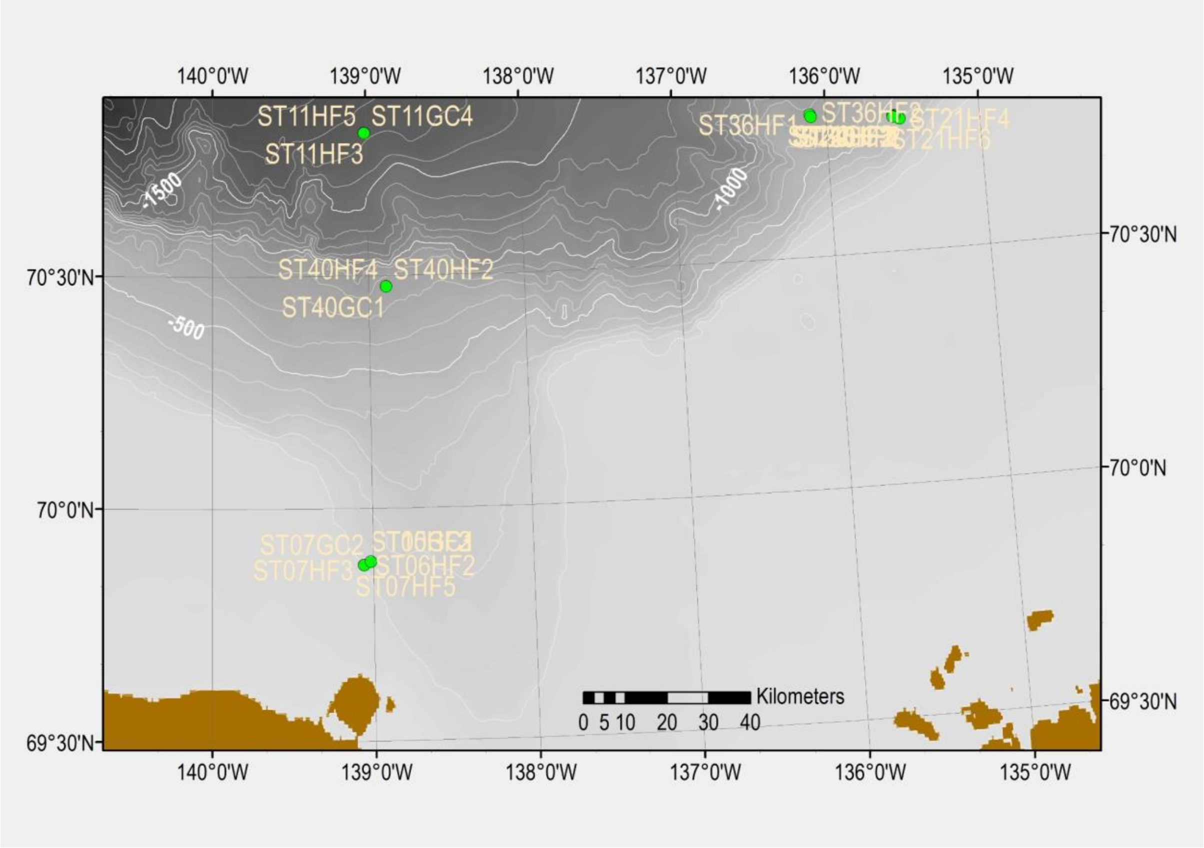

Figure 7.3. Location map of geothermal gradient (HF) and thermal conductivity (GC) measurements.

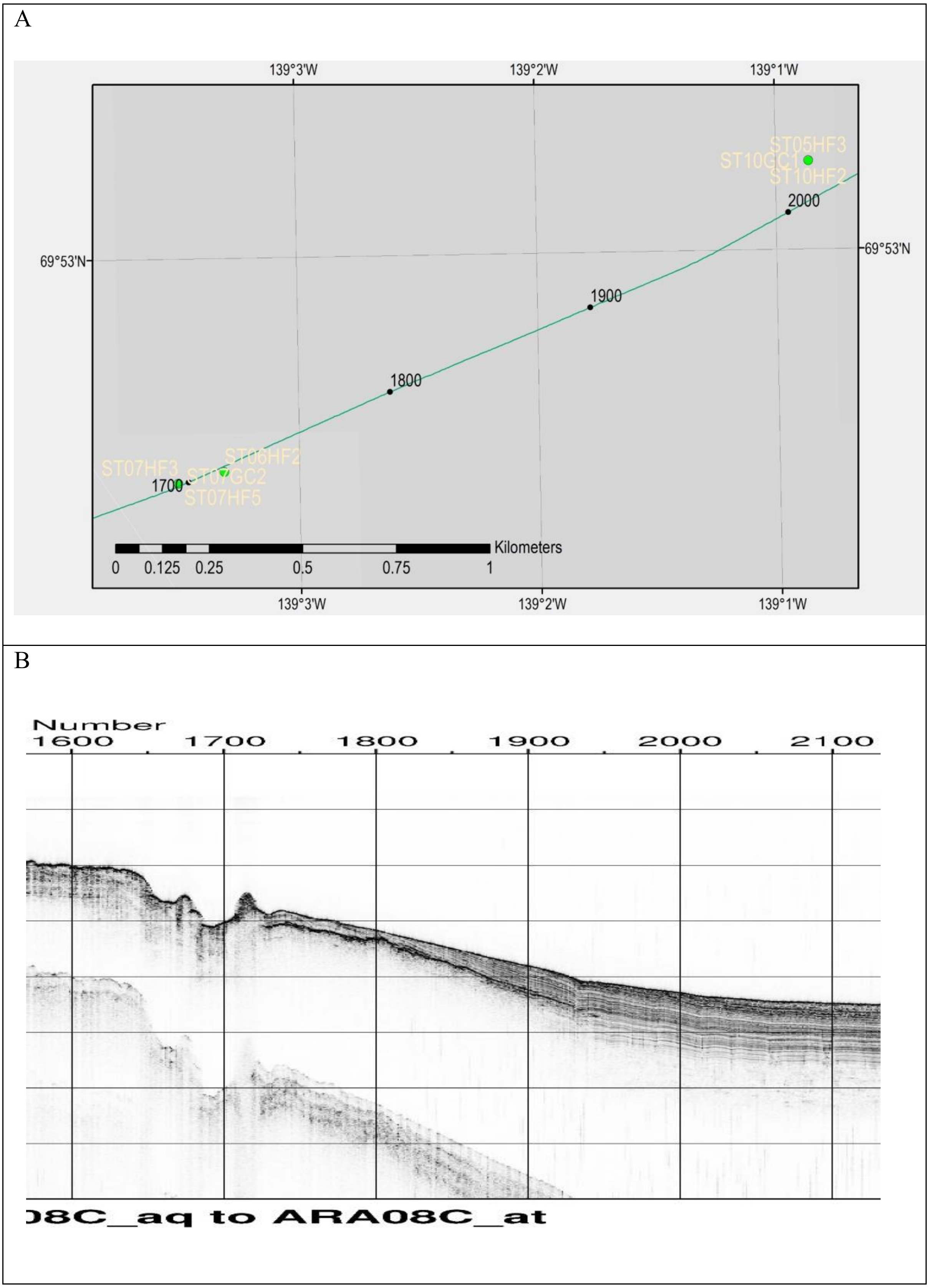

Figure 7.4. (a) Map of the area west of the Mackenzie Trough. The green line shows the sub-bottom survey line and the numbers indicate the ping number. (b) The sub-bottom profile image corresponding to the line shown in (a).

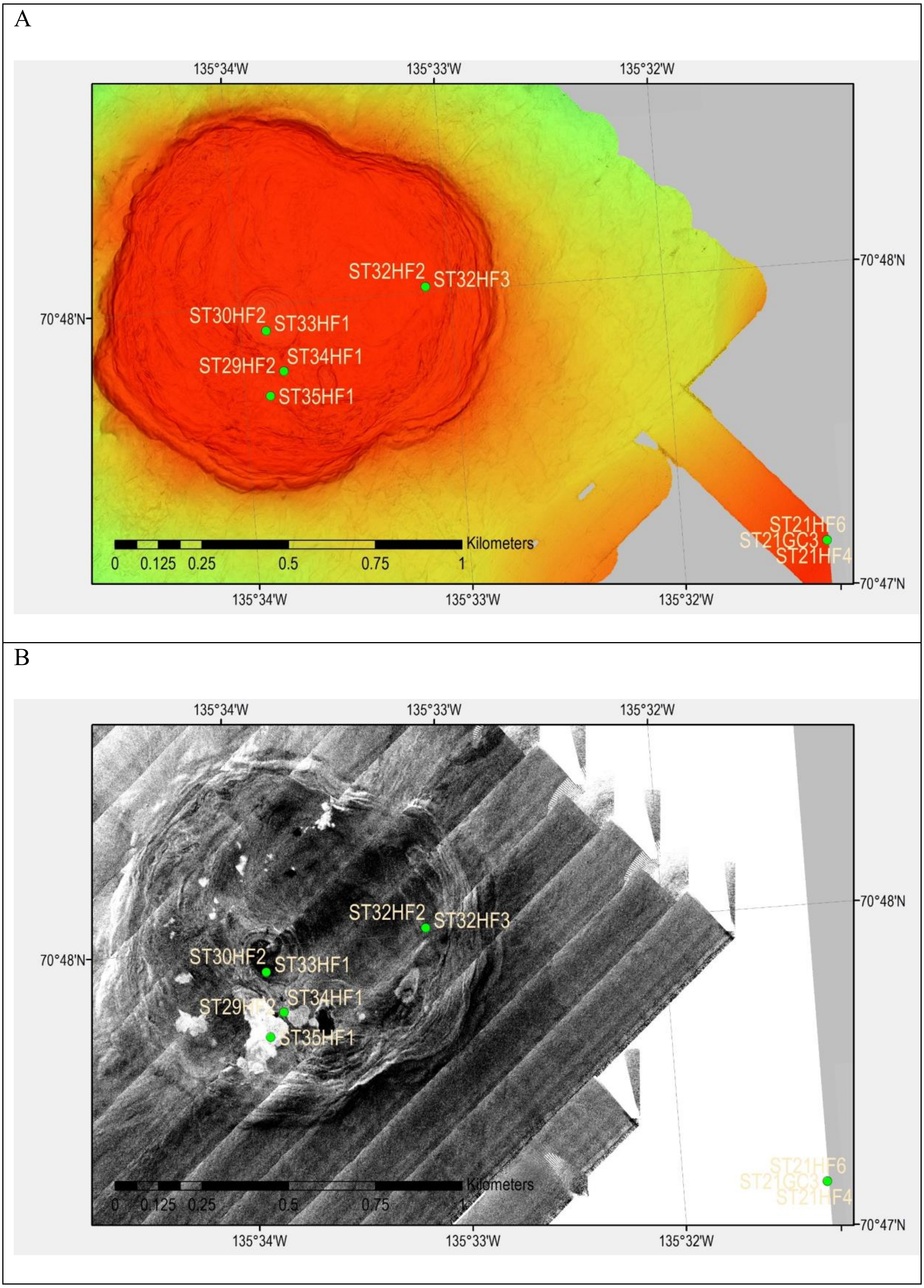

Figure 7.5. Detailed topographic (a) and backscatter (b) maps of the 420 m mud volcano area generated from the 2016 AUV survey.

Table 7.4. Station list for geothermal gradient (HF) and thermal conductivity (GC) measurements. The same stations are noted by the same colors.

Station	Work order	Gear	Start date/time (UTC)		End data/time (UTC)		Longitude (DDM, W)	Latitude (DDM, N)	Water depth (m)	Remarks
ST05	3	HF	17-09-06	4:15	17-09-06	5:10	139° 0.863316'	69° 53.126802'	163	West of MT
ST06	2	HF	17-09-06	05:47	17-09-06	5:52	139° 3.3138'	69° 52.6944'	93	West of MT, Pingo top
ST07	2	GC	17-09-06	7:41	17-09-06	8:20	139° 3.505686'	69° 52.678620'	117	West of MT, Close to bacterial mat & methane seepage
	3	HF								
	5	HF	17-09-06	9:14	17-09-06	9:47				
ST10	1	GC	17-09-06	12:20	17-09-06	12:55	139° 0.863316'	69° 53.126802'	163	West of MT, =St. 05
	2	HF								
ST11	3	HF	17-09-07	4:50	17-09-07	6:20	139° 0.759'	70° 48.464'	1750	MT, Deepest site
	4	GC	17-09-07	7:10	17-09-07	8:50				
	5	HF								
ST21	3	GC	17-09-09	10:16	17-09-09	11:10	135° 31.3241'	70° 47.0699'	420	Control site for 420MV
	4	HF								
	6	HF	17-09-09	11:35	17-09-09	12:30				
ST29	2	HF	17-09-10	09:26	17-09-10	10:20	135° 33.808599'	70° 47.395762'	420	420MV, Gas hydrate
ST30	2	HF	17-09-10	11:00	17-09-10	11:55	135° 33.8775'	70° 47.4602'	420	420MV, Gas hydrate, =St.15
ST32	2	HF	17-09-11	8:25	17-09-11	10:05	135° 33.1145'	70° 47.5095'	420	420MV
	3	HF	17-09-11	10:05						
ST33	1	HF	17-09-11	10:55	17-09-11	12:25	135° 33.8775'	70° 47.4602'	420	420MV, =St. 15=St. 30
ST34	1	HF	17-09-11	12:25	17-09-11	13:45	135° 33.808599'	70° 47.395762'	420	420MV, =St. 29
ST35	1	HF	17-09-11	13:50	17-09-11	14:53	135° 33.8813'	70° 47.3589'	420	420MV, =St. 19
ST36	1	HF	17-09-11	19:34	17-09-11	20:13	136' 06.1994'	70' 48.3602'	752	740MV cone top
	2	HF	17-09-11	20:28	17-09-11	21:22	136' 05.8600'	70' 48.0500'	744	740MV flat top
ST40	1	GC	17-09-12	09:02	17-09-12	10:10	138° 53.258460'	70° 28.606020'	760	MT
	2	HF								
	4	HF	17-09-12	10:35	17-09-12	11:40				

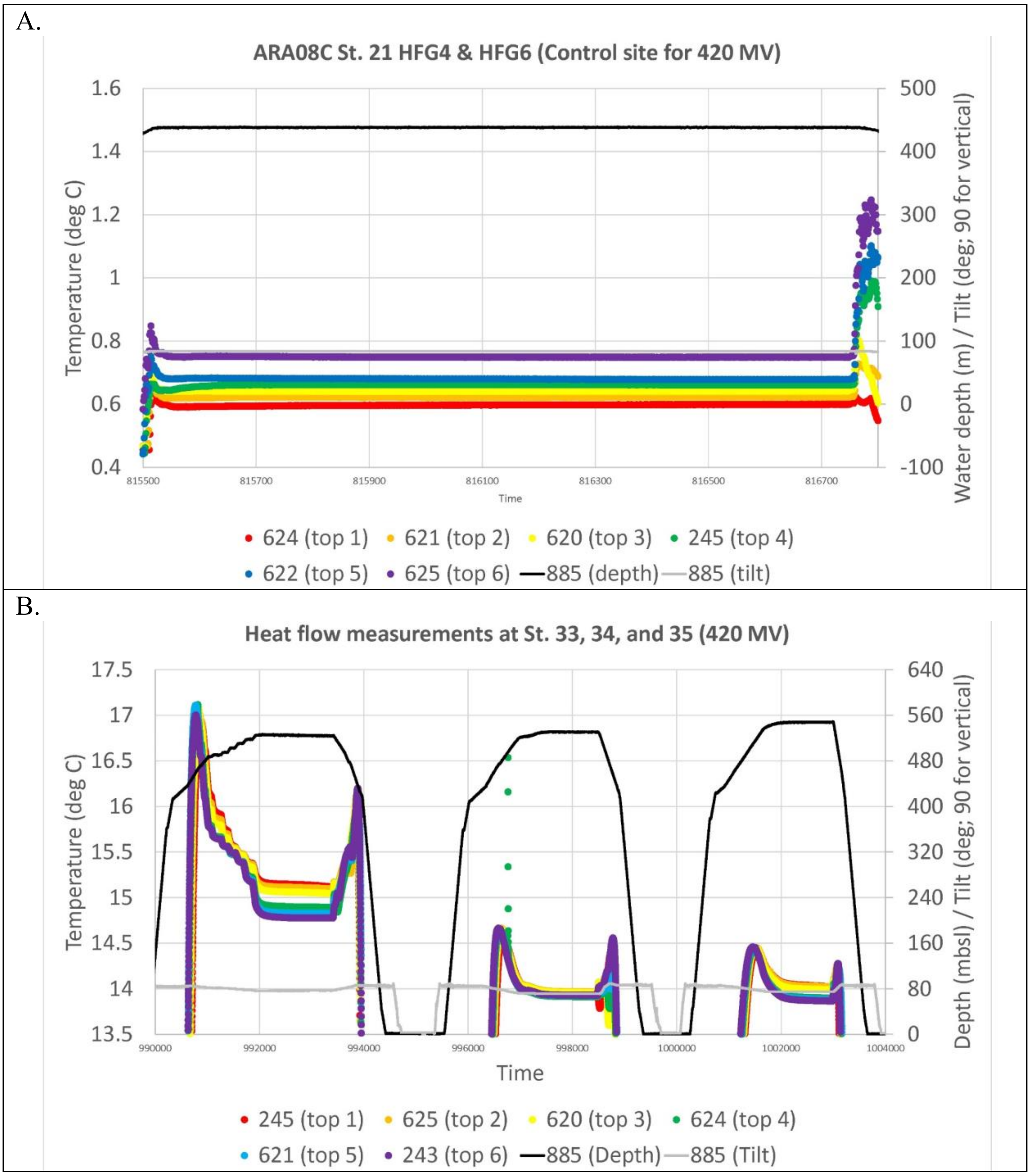

Figure 7.6. Preliminary results of marine heat flow measurements. (A) St. 21 temperature profiles are as expected from normal seafloor condition. (B) Temperature profiles from Sts. 33, 34, and 35 much warmer than expected.

Figure 7.7. Screen captured of TKgraph showing the results of all thermal conductivity measurements.

7.4. Summary

- Marine heat flow measurements to observe geothermal gradients and thermal conductivity were carried out at eleven and five stations, respectively, during the ARA08C expedition. It was not possible to obtain from thermal conductivity measurements from sediment cores with soupy texture, such as ones from mud volcanoes.
- Sites were chosen to understand: 1) the thermal structure of active seepage at mud volcanoes, and 2) the background heat flow in the deep water for comparison to BSR depths recently identified.
- Based on a plot of temperature-depth-tilt with time, unexpected results were obtained from sites in the 420 m mud volcano area. Further detailed analyses are required to determine whether the results indicate an abnormal thermal/kinematic status of the seafloor or if instrument failure occurred.
- Thermal conductivity measurements made in the laboratory will be corrected in terms of pressure and temperature.

References

Dmitrenko, I.A., Kirillov, S.A., Ivanov, V.V., Woodgate, R.A., Polyakov, I.V., Koldunov, N., Fortier, L., Lalande, C., Kaleschke, L., Bauch, D., Hölemann, J.A., and Timokhov, L,A, 2009. Seasonal modification of the Arctic Ocean intermediate water layer off the eastern Laptev Sea continental shelf break. *Journal of Geophysical Research: Oceans*, 114:n/a-n/a. doi:10.1029/2008JC005229

Goto, S., and Matsubayashi, O. 2008. Inversion of needle-probe data for sediment thermal properties of the eastern flank of the Juan de Fuca Ridge. *Journal of Geophysical Research: Solid Earth*, 113:B08105. doi:10.1029/2007JB005119

Jin Y.K., Riedel, M., Hong, J.K., Nam, S.I., Jung, J.Y., Ha, S.Y., Lee, J.Y., Kim, Y.-G., Yoo, J., Kim, H.S., Kim, G., Conway, K., Standen, G., Ulmi, M., and Schreker, M. 2015. *Overview of field operations during a 2013 research expedition to the southern Beaufort Sea on the RV Araon*. Geological Survey of Canada, Open File 7754.

Jin Y.K. (ed.), and Dallimore, S.R. (ed.) 2016. *Canada-Korea-USA Beaufort Sea Geoscience Research ARA05C Marine Research Expedition Program: Summary of 2014 Activities*. Geological Survey of Canada, Open File 7999.

Paull C.K., Ussler, W. III, Dallimore, S.R., Blasco, S.M. Lorenson, T.D., Melling, H., Medioli, B.E., Nixon, F.M., and McLaughlin, F.A. 2007. Origin of pingo-like features on the Beaufort Sea shelf and their possible relationship to decomposing methane gas hydrates. *Geophysical Research Letters*, 34:L01603. doi.org/10.1029/2006GL027977

Ratcliffe, E.H. 1960. The thermal conductivities of ocean sediments. *Journal of Geophysical Research*, 65:1535-1541. doi:10.1029/JZ065i005p01535

Ruppel, C. 2014. Permafrost-Associated Gas Hydrate: Is It Really Approximately 1 % of the Global System? *Journal of Chemical & Engineering Data*, doi:10.1021/je500770m

Chapter 8. Sediment Coring

R. Gwiazda, D.H. Lee, Y.M. Lee, J.-H. Kim, K.K. Kim, H.J. Koo, Y.K. Lee, and S.J. Lee

8.1. Introduction

A coring program was conducted during Araon scientific cruise ARA08C in the Canadian Beaufort Sea to address the following scientific goals: 1) To determine the pore water geochemistry of sediments of the Beaufort Sea shelf and slope west of the Mackenzie Trough; 2) To investigate the occurrence of glacially transported materials on the Yukon Shelf and the Mackenzie Trough; 3) to investigate the age and geotechnical character of mass transport deposits on the upper and lower slope; and 4) to evaluate the microbial diversity and activity of sediments associated with active mud volcanoes in the Beaufort Sea slope.

8.2. Background

Pore waters: Results from pore water samples obtained in previous cruises by the Geological Survey of Canada and the Korea Polar Research Institute, in cooperation with the Monterey Bay Aquarium Research Institute, documented widespread seepage of freshwater into sediments of the Canadian Beaufort shelf edge and slope east of the Mackenzie Trough (Paull et al., 2007; 2011; 2015a; 2015b). This freshwater input was detected as a downcore decrease in pore waters chloride concentration, and has been documented down to 1,000 m water depths in investigations conducted on the CCGS Sir Wilfrid Laurier. No coring has yet been conducted to evaluate whether freshwater seepage exists in sediments deeper than 1,000 m. Oxygen isotope analyses of pore waters revealed that the sources of freshwaters to the shelf edge and to the slope are distinct and different from each other suggesting that they have a different origin.

Freshwater seepage to the seafloor can have an impact on the seafloor morphology by modifying sediment properties and by promoting the in situ formation of ice in sediments bathed by low temperatures bottom waters. East of the Mackenzie Trough, mounds up to ~10 m high and 30 m in diameter, resembling pingos found on land, are abundant on the shelf edge in the depth range 160 to 200 m (Blasco et al., 2010). Slightly shallower, between 160 to 120 m, the morphology is more rugged with depressions up to 20 m deep that are surrounded by circular ridges of apparently coarser material than those found inside the depressions. The leading hypothesis for the formation of the pingo-like features (PLFs) in the shelf edge is that they are the product of recent ice aggradation. Sub-seafloor freezing is possible because seepage of freshwater into sediments lowers pore waters salinity to the point where the bottom-water temperature of > -1.4 °C is sufficiently low to trigger in situ pore water freezing. The formation of ice increases the sediment volume and causes the seafloor uplift characteristic of the pingo structure. This interpretation is supported by data from a core, which was collected during the ARA05C Araon cruise in 2014 and from other cores collected on the CCGS Sir Wilfrid Laurier. Because submarine PLFs appear to be a widespread morphological feature of the seafloor in other areas of the Canadian Arctic, confirmation of the link between freshwater seepage and submarine pingo formation will be significant since their presence could be used as proxy for the location of freshwater seeps in marine sediments at these high latitudes. In addition, coring was targeted to sample the shelf edge depressions found at depths shallower than the PLFs in order to understand their mechanism of formation. Coring also supported observations made during MiniROV dives and AUV missions during this cruise revealed that these depressions have a smooth topography and are composed of apparently fine sediments and possibly surrounded by circular rings of coarser materials. Pore water analyses as well as lithological, grain size analyses and radiocarbon dating of the materials found in these morphological features will be used to understand the processes that lead to their development.

Numerous efforts have been conducted over the years to understand the processes shaping the shelf and slope morphology of the seafloor east of the Mackenzie Trough and their implications to geohazard risks. However, there is much less detailed bathymetric information and knowledge about the marine geology, possible submarine permafrost presence and freshwater inputs to the shelf, shelf edge and slope of sediments west of the Mackenzie Trough. One of the main goals of this sediment coring program is to compare and contrast the sediment composition and pore water chemistry of sediments to the west of the Mackenzie Trough with those to the east. This will provide insights as to whether the same hydrological and geological processes that shaped the seafloor to the east of the Mackenzie Trough are the same to the west of it.

Glacial Deposits: An additional goal of the gravity coring program, which was complemented by the sampling and push coring conducted by the MiniROV in this cruise, is to delineate the geographical distribution of glacially transported materials along the flanks and axis of the Mackenzie Trough. This information is key to reconstruct the limits of the Laurentide Ice sheet at the peak of last glacial maximum. Glacial materials may also influence landslide mechanics within the margins of the Mackenzie Trough highlighting the importance of understanding the geological processes that shape the seafloor in this area. Characterization of the chemistry of the pore waters from cores collected from this region, as well as of their lithology will be instrumental in evaluating whether the possible presence of freshwater seepage in the Mackenzie Trough is a contributing factor to the documented slope failure found on the flanks of the trough, or if differences in shear strength of rapidly accumulating sediment of glacial origin are responsible for the occurrence of past landslides in this area.

Microbial Communities: Large stores of methane exist in marine sediments in either gaseous or gas hydrate form. Most of this methane is the product of anaerobic decomposition of organic matter by microbial activity of both archaea and bacteria. The net flux of methane from marine sediments to the ocean-atmosphere system is controlled by the competing actions of methanogenic microbes that produce methane throughout the sediment column and methanotrophic microbes that consume it mostly in the upper layers of the sediment. The proliferation of methanotrophic microbes is dependent on their symbiotic relationship with sulfate-reducing bacteria and/or other microbes that supply oxidizing energy from the reduction of compounds other than sulfate, depending on the environment. In marine sediments, the most common association of methanotrophic archaea is with sulfur reduction bacteria that complete the chemical cycle for the oxidation of methane.

The most suitable environment to study the complex interactions in this microbial system is in the high methane flux environments of mud volcano vents (Paull et al., 2015a; Paull et al., 2015b). Here, the high methane flux results in the shoaling of the location where the highest abundance of methanotrophic archaea are found. This enables the sampling and study of this microbial system in fine detail. Key scientific gaps include understanding the composition of the microbial community at large, the specific methanotrophic and methanogenic archaea found in high methane flux environments, the interactions among members of the microbial communities, their methane consumption and production capacity, and the environmental factors that control their distribution and activity.

The activity of microbial communities in Arctic sediments remains largely unexplored. Methanotrophic microbes have been studied in connection to gas hydrates decomposition, in continental shelves and slopes, in hydrothermal vents, and in permafrost. However, the microbial community composition of this system in mud volcanoes in the Arctic has only been studied in a single case - the Haakon Mosby volcano in the Barents Sea. The presence of three mud volcanoes on the slope of the Canadian Beaufort Sea offers an opportunity to understand this microbial system at multiple locations in the same cruise and examine the microbial interactions of this system in detail.

The main goal of the microbiology component of the ARA08C cruise is to study the microbial populations of the active mud volcanoes as a function of sediment depth and as a function of the age of the eruptive sediments spewed out by the mud volcano vents. Three active mud volcanoes sit on the continental slope east of the Mackenzie Trough at depths of 280, 420, and 740 m. The microbial populations found in these mud volcanoes were characterized from samples obtained during the ARA05C. During the ARA08C cruise, acoustic reflectivity maps of the mud volcanoes were obtained by the AUV. These images were instrumental for identifying vent deposits and for ranking them according to their age. Further corroboration of this ranking was accomplished during the ROV dives. This information provided a roadmap to conduct a program of push coring and box coring designed to sample vent sediments of different ages. Communities will be characterized through sequencing of 16S rRNA gene and metagenome. In addition, potential methane production capability, and type of carbon source through lipid content and carbon isotopic composition will be determined.

8.3. Methods

8.3.1. Gravity coring

Gravity coring was conducted with a gravity coring device with a headstand weighing 1.0 metric tons. The metal core barrel was 6 m long, except for when coring was conducted on the pingo-like features at the shelf edge east of the Mackenzie River where a 3 m core barrel was used. The liner consisted of two 3-m long plastic segments 10 cm in diameter, which were joined together to provide for a maximum core recovery of 6 m. Gravity coring was performed through the A-frame on the stern using a metal wire winch. Winch velocity at impact was < 30 m/min.

Coring was accurately targeted using a Dynamic Position System that allowed the Araon to position herself at coordinates accurate to the level of GPS accuracy. Offsets between the GPS antenna and the point of deployment of the gravity coring device were accounted for when positioning the ship prior to and during coring. When available, site selection was based on coordinates extracted from the AUV-collected. This was particularly critical for the sampling of features of small dimensions such as the shelf edge pingo-like features and depressions east of the Mackenzie Trough and of the small venting sites on top of the mud volcanoes at 420 and 740 m water depth. The coring location for the shelf edge pingo-like feature west of the Mackenzie Trough was obtained from the sub-bottom profiler imaging of the feature. The coordinates thus assigned for the coring of the PLF were indeed at its top as verified in the subsequently collected AUV map of this area.

Once on deck, the liner was cut in 1.5 m long sections. The presence of ice at the bottom of the core in the core catcher or immediately above was checked prior the extraction and sectioning of the liner.

Pore waters were extracted from all gravity cores immediately after core recovery unless thermal conductivity measurements were to be performed upon retrieval. In these latter cores, pore water sampling was done no later than 1.5 days after collection. Pore water collection was done with rhizons, which are porous ceramic tubes of 0.2 µm pore size (rhizons) that were inserted into the core liner and extract pore waters through the vacuum draw created by an attached evacuated syringe. Sampling interval ranged from 20 to 50 cm.

Gravity cores are listed in Table 8.1 and their locations are presented in Figure 8.1. Cores were not opened onboard, with the exception of four cores: ARA08C-07-GC01, ARA08C-08-GC-01, ARA08C-29-GC01 and ARA08C-30-GC01.

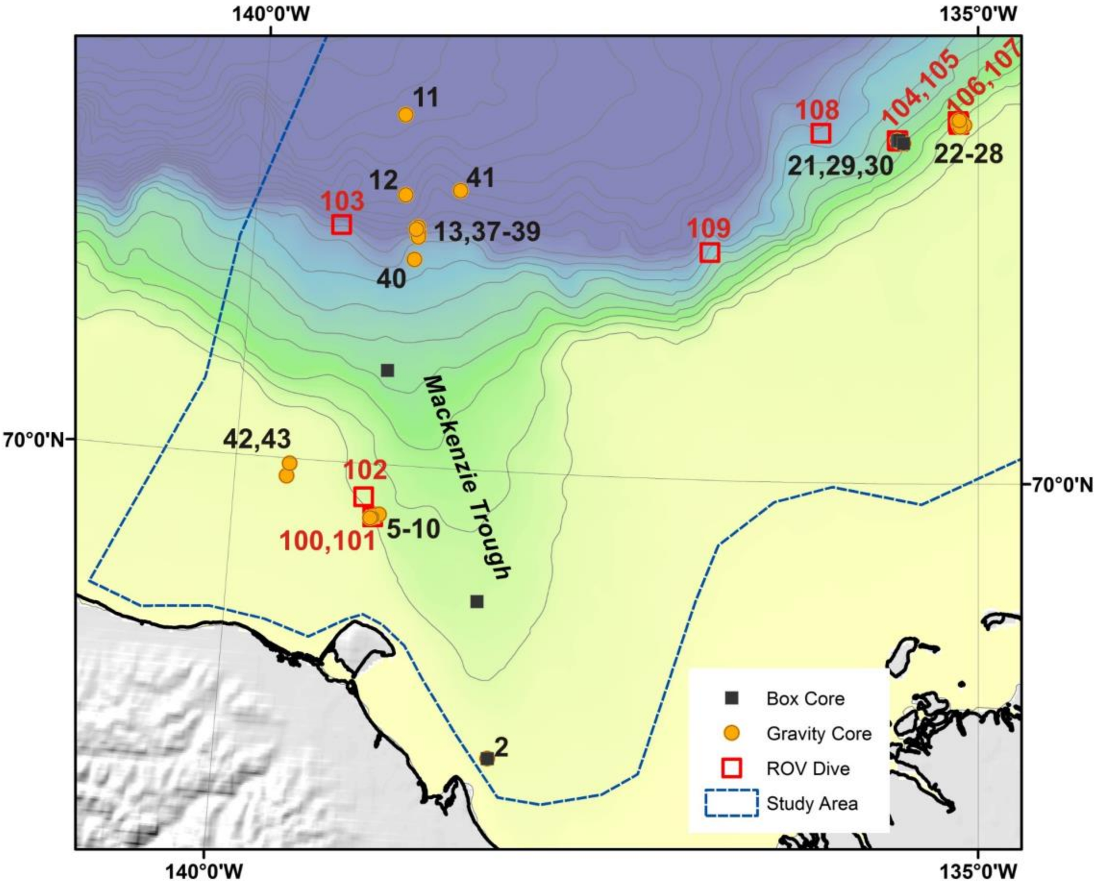

Figure 8.1. Numbers in black are the station numbers where gravity cores were collected (station number included in gravity core ID). MiniROV dive numbers in red.

8.3.2. Box coring

Box cores of 60 cm length (Table 8.2) were collected at the top of the mud volcano at 420 m water depths in the Mackenzie Trough and at a slope reference site. Once on deck, the box cores were subsampled into two 10 cm and one 5 cm diameter sub-cores. The rest of the material was saved for collection of benthic fauna. A detailed description of the findings about benthic fauna can be found in Chapter 10 on Biological Studies.

Table 8.1. Collected gravity cores

Core	Longitude (W)	Latitude (N)	Depth (m)	Length (cm)	Setting
ARA08C-02-GC04	138°12.3570'	69°20.3258'	38	277	Shelf west of Mackenzie
ARA08C-05-GC02	139°00.8633'	69°53.1268'	163	348	Shelf west of Mackenzie
ARA08C-06-GC01	139°03.3138'	69°52.6944'	93	123	Pingo-shelf edge west
ARA08C-07-GC02	139°03.5057'	69°52.6786'	117	417	Shelf edge west
ARA08C-07-GC04	139°03.5057'	69°52.6786'	117		
ARA08C-08-GC01	139°03.7813'	69°52.6320'	101	284	Shelf edge west
ARA08C-09-GC01	139°04.4029'	69°52.5495'	78	300	Shelf edge west
ARA08C-10-GC01	139°04.4029'	69°52.5495'	78	430	
ARA08C-11-GC02	139°00.7590'	70°48.4640'	1750	500	
ARA08C-11-GC04	139°00.7590'	70°48.4640'	1750	469	Slope off Mackenzie Trough
ARA08C-12-GC01	138°58.5430'	70°37.4140'	1457	300	Slope off Mackenzie Trough
ARA08C-13-GC01	138°52.5102'	70°33.1093'	1257	245	Slope off Mackenzie Trough
ARA08C-21-GC03	135°31.3241'	70°47.0699'	420	425	Beaufort east
ARA08C-21-GC05	135°31.3241'	70°47.0699'	420		Beaufort east
ARA08C-22-GC02	135°08.0676'	70°49.7317'	166	281	Pingo-shelf edge east
ARA08C-23-GC01	135°07.5969'	70°49.8504'	167	229	Depression-shelf edge east
ARA08C-24-GC01	135°05.7477'	70°49.6267'	129	206	Depression-shelf edge east
ARA08C-25-GC01	135°07.5036'	70°49.3610'	125	85	Depression-shelf edge east
ARA08C-26-GC01	135°08.3638'	70°50.1600'	164	86	Pingo-shelf edge east
ARA08C-27-GC01	135°07.9711'	70°50.2388'	166	>300	Pingo-shelf edge east
ARA08C-28-GC01	135°07.8669'	70°50.2920'	167	>300	Pingo-shelf edge east
ARA08C-29-GC01	135°33.8086'	70°47.3958'	420	345	Mud volcano
ARA08C-30-GC01	135°33.8775'	70°47.4602'	420	340	Mud volcano
ARA08C-37-GC01	138°53.3468'	70°32.7670'	1209	188	Mackenzie Trough
ARA08C-38-GC01	138°52.1100'	70°32.1575'	1160	215	Mackenzie Trough
ARA08C-39-GC01	138°52.2172'	70°31.7183’	1080	300	Mackenzie Trough
ARA08C-40-GC01	138°53.2584'	70°28.6060'	760	551	Mackenzie Trough
ARA08C-40-GC03	138°53.2584'	70°28.6060'	760	470	Mackenzie Trough
ARA08C-41-GC01	138°53.2585'	70°28.6060'	1360	288	Mackenzie Trough
ARA08C-42-GC01	139°39.1130'	69°57.5530'	53	5	Shelf west of Mackenzie
ARA08C-43-GC01	139°38.2740'	69°59.2920'	59	88	Shelf west of Mackenzie

Table 8.2. Box cores collected for the study of microbial populations

Core	Longitude (W)	Latitude (N)	Depth (m)	Setting
ARA08C-2-BC3	138°12.35736'	69°20.32482'	38	Mackenzie Trough
ARA08C-3-BC2	138°19.7137'	69°41.9016'	140	Mackenzie Trough
ARA08C-4-BC2	139°01.3098'	70°13.0879'	407	Mackenzie Trough
ARA08C-15-BC2	135°33.8775'	70°47.4602'	420	Mud Volcano
ARA08C-16-BC1	135°33.5675'	70°47.4968'	420	Mud Volcano
ARA08C-20-BC1	135°33.9531'	70°47.3923'	420	Mud Volcano
ARA08C-19-BC1	135°33.8813'	70°47.3589'	420	Mud Volcano
ARA08C-18-BC3	135°33.5876'	70°47.3778'	420	Mud Volcano
ARA08C-17-BC1	135°33.1145'	70°47.5095'	420	Mud Volcano
ARA08C-21-BC2	135°31.3241'	70°47.0699'	420	Slope

One sub-core was extruded and sampled at 1 or 2 cm thick slices. Pore waters were collected from the second sub-core as described in Section 8.3.1.

8.3.3. Push coring

The MiniROV has the ability to take up to seven < 20 cm long push cores per dive. This capability provided the opportunity to target sediment sampling very accurately. Sediments on top of the mud volcano differ visually according to the age of the mudflows on its surface. Very recently erupted sediments are not colonized, are lighter in color and often are topographically above surrounding sediments, with clearly contrasting visual boundaries. Young, but not as recently erupted, sediments are darker in color but do not show extensive colonization by tubeworms. Sediment surfaces of the oldest flows show extensive tubeworm colonies and are the most prevalent type of sediment surface on top of the mud volcano as shown by the acoustic reflectivity recorded in the AUV sidescan. Using these visual differences, push core sampling was targeted at flows of different ages with the goal of characterizing the microbial communities as a function of vent deposit age. Additionally, push coring was conducted in marine sediments on the slope and in the Mackenzie Trough to serve as reference microbial controls (Table 8.3).

Table 8.3. Push cores collected for microbial studies

Mini ROV DIVE No.	Push core	Site characteristics	Site
DIVE100	1,2	Pingo	West of Mackenzie
DIVE101	3,8,9	Bacterial mat (white)	West of Mackenzie
	6,7	Within groove on top of pingo	West of Mackenzie
DIVE104	7,13	Bacterial mat (black)	420 m Mud volcano
	4,5	Tubeworm patch	
	1,10,11	Tubeworm patch	
DIVE105	2,3	Youngest vent, bubble detection, boundary between tubeworm patch and no colonization	420 m Mud volcano
	8,9	Young, no tubeworm	
	12,14	Old, small number of tubeworms	
DIVE108	1,3	Active vent at top of mud volcano	740 m Mud volcano
	6,12	Most active site, bubble and eruption detection	
	4,5	Older flow	
	13	White bacterial mat	
DIVE109	12	Freshwater present?	Mackenzie Trough
	13	Freshwater present?	Mackenzie Trough

8.4. Results

8.4.1. Pore water sampling

Successful pore water collection was achieved in >90% of all probed depths. Sampling was difficult and not as successful at the tops and bottoms of the cores, presumably due to the leakage of air through the seal at the end of the liners that prevented the maintenance of vacuum conditions to enable flow of pore waters into the rhizons. An orange, fine suspended precipitate was visible in many syringes after sample collection, which appeared to be absent on the upper samples close to the top of the core. Pore water samples will be analyzed for Cl^- and SO_4^{2-} concentration, and $\delta^{18}O$ and δD isotopic composition. Pore water sampling was unsuccessful in core ARA08C-43-GC01.

8.4.2. Observations of split gravity cores

Four cores were split onboard. Core ARA08C-06-GC01 was collected from the top of a pingo at 93 m water depth on the shelf edge west of the Mackenzie Trough. This pingo was identified in the sub-bottom profiler as a ~15 m tall mound above a zone of acoustic blanking (Figure 8.2).

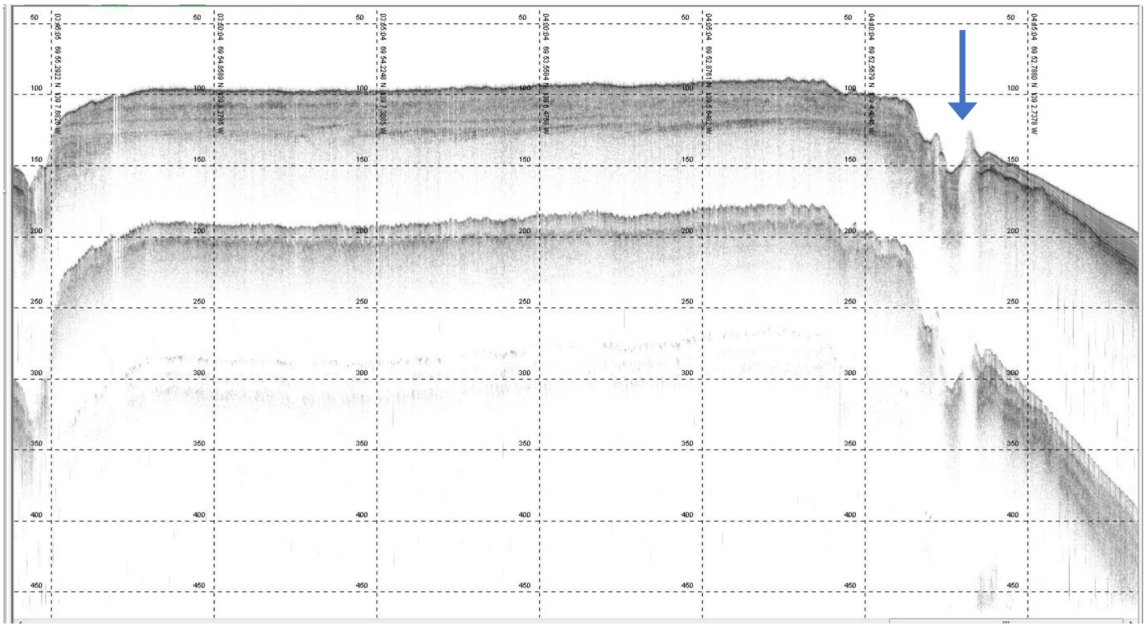

Figure 8.2. Location of core ARA08C-06-GC01

The core was short (123 cm) and fragments up to 5 cm long of clear ice were found in the core catcher (Figure 8.3). The top 4 cm of the core consisted of angular pebbles less than 2 cm in size above a sharp (unconformity?) contact. The sediment below was fine-grained and displayed alternating black and brown color laminations of a few centimeters thickness (see Appendix for core descriptions). Core ARA08C-8GC-01 was collected from the nearby small sedimentary basin located to the west of the pingo (between the pingo and the shelf). Its lithology and sediment structure was remarkably similar to that of the pingo.

Figure 8.3. Ice fragments from the bottom of core ARA08C-06-GC01 collected from the top of a shelf edge pingo west of the Mackenzie Trough.

Gravity cores were also collected on pingos on the shelf edge east of the Mackenzie Trough. Small fragments of clear ice (<1.5 cm) were recovered from the bottom of core ARA08C-26-GC01 whose intended target was the top of a pingo (Figure 8.4)

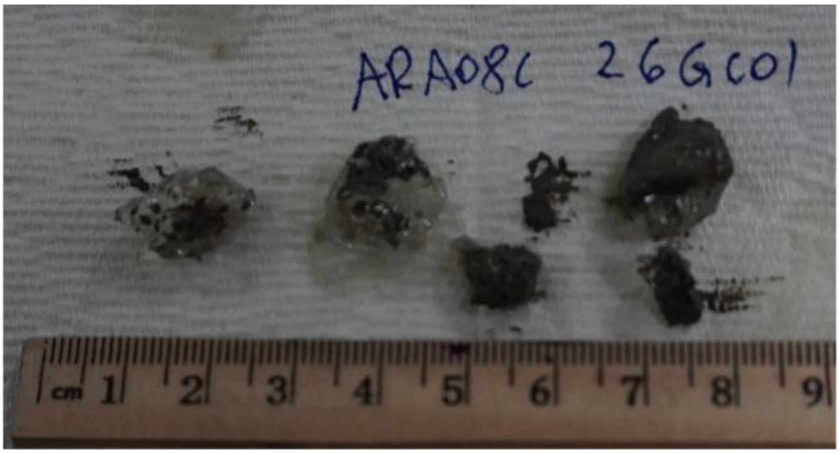

Figure 8.4. Ice recovered from the bottom of core ARA08C-26-GC01.

Very small crystals of gas hydrates along the full length of two gravity cores collected from the top of the mud volcano at 420 m water depth on the slope were observed through the liners upon recovery (ARA08C-29-GC01 and ARA08C-30-GC01). However, the gas hydrate had dissociated by the time the cores were opened. These cores displayed the characteristic moussy texture produced by gas hydrate dissociation.

Gas hydrate crystals in the form of very porous thin flakes up to 2 cm long were also observed distributed throughout the full length of box core ARA08C-15-BC02 from the 420 m mud volcano.

8.5. Summary

A total of 10 box cores, 31 gravity cores, and 29 push cores were collected from a variety of environments within the Canadian Beaufort Sea, which will assist in addressing the goals of the ARA08C cruise. Namely, to determine the extent of pore freshening in marine sediments, the geographical distribution of glacially transported deposits in the Mackenzie Trough, the age and process of mass transport deposits, and the microbial communities and functions at active mud volcanoes.

References

Blasco, K.A., Blasco, S.M., Bennett, R., MacLean, B., Rainey, W.A. and Davies, E.H. 2010. Seabed geologic features and processes and their relationship with fluid seeps and the benthic environment in the Northwest Passage. Geological Survey of Canada, Open File 6438, 58 p. doi.org/10.4095/287316

Paull, C.K, Ussler, W., Dallimore, S.D., Blasco, S.M., Lorenson, T.D., Melling, H., Medioli, B.E., Nixon F.M., and McLaughlin, F.A. 2007. Origin of pingo-like features on the Beaufort Sea Shelf and their possible relationship to decomposing methane gas hydrates. Geophysical Research Letters, 34: 1-5.

Paull, C., Dallimore, S., Hughes-Clarke, J., Blasco, S., Lundsten, E., Ussler III, W., Graves, D., Sherman, A., Conway, K., Melling, H., Vagle, S., and Collett. T. 2011. Tracking the decomposition of submarine permafrost and gas hydrate under the shelf and slope of the Beaufort Sea. Paper 328 in the Special Session - Gas Hydrates & Global Climate Change, 17-21 July 2011, Edinburgh, Scotland.

Paull, C.K., Dallimore, S.R., Caress, D.W., Gwiazda, R., Melling, H., Riedel, M., Jin, Y.K., Hong, J.K., Kim, Y.-G., Graves, D., Sherman, A., Lundsten, E., Anderson, K., Lundsten, L., Villinger, H, Kopf, A., Johnson, S.B., Hughes Clarke, J., Blasco, S., Conway, K., Neelands, P., Thomas, H., and Côté, M. 2015a. Active mud volcanoes on the continental slope of the Canadian Beaufort Sea. Geochemistry, Geophysics, Geosystems, 16: 3160–3181. doi:10.1002/2015GC005928.

Paull, C.K., Caress, D.W., Thomas, H., Lundsten, E., Anderson, K., Gwiazda, R., Riedel, M., McGann, M., and Herguera, J.C. 2015b. Seafloor geomorphic manifestations of gas venting and shallow subbottom gas hydrate occurrences. Geosphere, 11: 491–513. doi: doi.org/10.1130/GES01012.1

Appendix: Core Descriptions

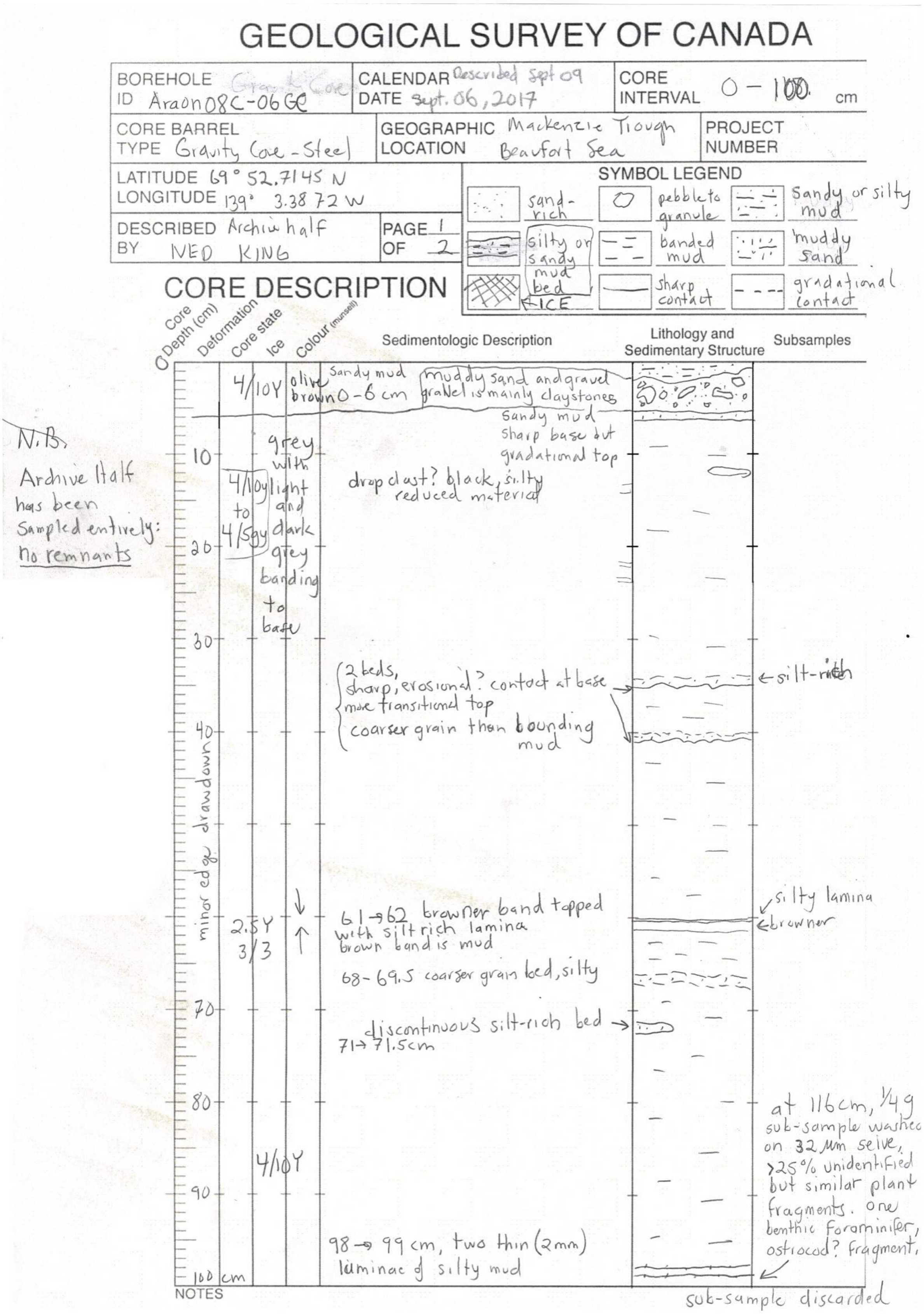

GEOLOGICAL SURVEY OF CANADA

BOREHOLE ID Araon08C-06GC Gravity Core
CALENDAR DATE Sept. 06, 2017 Described Sept 09
CORE INTERVAL 0 – 100 cm
CORE BARREL TYPE Gravity Core - Steel
GEOGRAPHIC LOCATION Mackenzie Trough Beaufort Sea
PROJECT NUMBER
LATITUDE 69° 52.7145 N
LONGITUDE 139° 3.3872 W
DESCRIBED BY Archive half NED KING
PAGE 1 OF 2

SYMBOL LEGEND

⁘	sand-rich	○	pebble to granule	⁚	Sandy or silty mud
≈	silty or sandy mud bed	⚌	banded mud	⁘	muddy sand
▦	ICE	—	sharp contact	- - -	gradational contact

CORE DESCRIPTION

Core Depth (cm) | Deformation | Core state | Ice | Colour (munsell) | Sedimentologic Description | Lithology and Sedimentary Structure | Subsamples

N.B. Archive Half has been sampled entirely: no remnants

0–6 cm: 4/10Y olive brown 0-6 cm; Sandy mud; muddy sand and gravel; gravel is mainly claystones

Sandy mud sharp base but gradational top

10: 4/10y to 4/5gy; grey with light and dark grey banding to base

drop clast? black, silty reduced material

2 beds, sharp, erosional? contact at base; more transitional top; coarser grain than bounding mud

← silt-rich

minor edge drawdown

2.5Y 3/3

61 → 62 browner band topped with silt rich lamina; brown band is mud

silty lamina
← browner

68 - 69.5 coarser grain bed, silty

discontinuous silt-rich bed →
71 → 71.5cm

4/10Y

at 116cm, 1/4 g sub-sample washed on 32 μm seive, >25% unidentified but similar plant fragments. One benthic foraminifer, ostracod? fragment,

98 → 99 cm, two thin (2mm) laminae of silty mud

100 cm

NOTES

sub-sample discarded

GEOLOGICAL SURVEY OF CANADA

BOREHOLE ID Aragon 08C-06 GC
CALENDAR DATE Sept 06, 2017 Description Sept 08, 2017
CORE INTERVAL 100 – 115.5 cm
CORE BARREL TYPE Gravity Core – steel
GEOGRAPHIC LOCATION Mackenzie Trough, Beaufort sea
PROJECT NUMBER
LATITUDE 69° 52.7145 N
LONGITUDE 139° 3.3872 W
DESCRIBED BY NED KING – GSC-A
PAGE 2 OF 2

SYMBOL LEGEND

see page 1 of 2

~~ fully deformed

CORE DESCRIPTION

Core Depth (cm)	Deformation	Core state	Ice	Colour (munsell)	Sedimentologic Description	Lithology and Sedimentary Structure	Subsamples
100					darker band		
					darker band		
					dropclast? black, granular		
110				dark grey	silty band 110 – 110.7cm		
115.5	~ ~ ~				Base of core Note Béné core catcher contained ~ 20cm of solid ice which was plucked out from the catcher immediately on recovery. This was sub-sampled for the water chemistry analysis MBARI has subsamples Roberto surrounding mud was very water rich soon after recovery. NOT PRESERVED no core catcher sub-sample except for meltwater	solid ice ca. 20cm	MBARI-meltwater sample number

NOTES

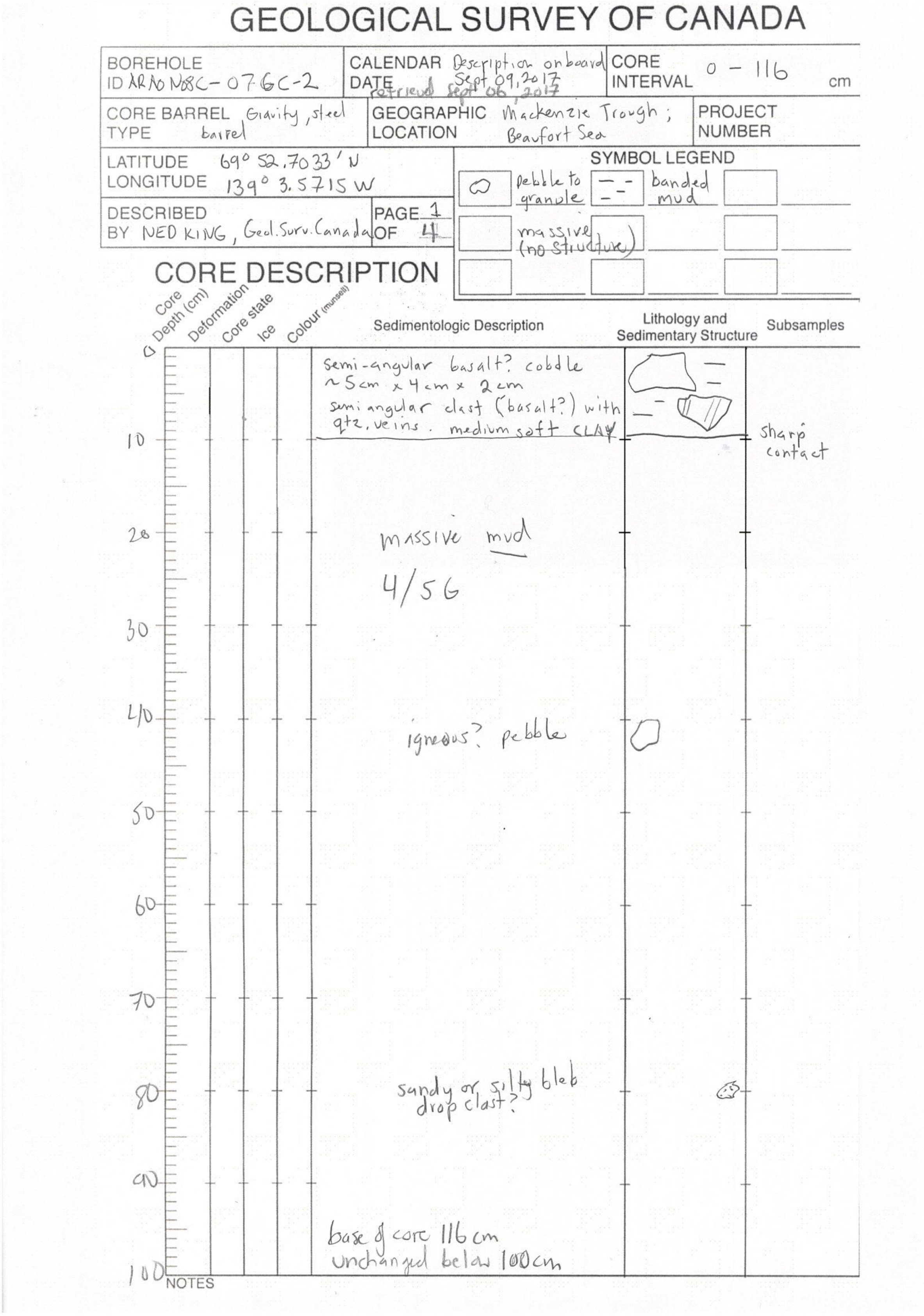

GEOLOGICAL SURVEY OF CANADA

BOREHOLE ID ARA08C-07GC-2

CALENDAR DATE Description onboard Sept 09, 2017 retrieved Sept 06, 2017

CORE INTERVAL 0 – 116 cm

CORE BARREL TYPE Gravity, steel barrel

GEOGRAPHIC LOCATION Mackenzie Trough; Beaufort Sea

PROJECT NUMBER

LATITUDE 69° 52.7033′ N

LONGITUDE 139° 3.5715 W

DESCRIBED BY NED KING, Geol. Surv. Canada

PAGE 1 OF 4

SYMBOL LEGEND

○	pebble to granule	– –	banded mud
	massive (no structure)		

CORE DESCRIPTION

Core Depth (cm)	Deformation	Core state	Ice	Colour (munsell)	Sedimentologic Description	Lithology and Sedimentary Structure	Subsamples
0					semi-angular basalt? cobble ~5cm x 4cm x 2cm semiangular clast (basalt?) with qtz. veins. medium soft CLAY		
10							sharp contact
20					massive mud 4/5G		
30							
40					igneous? pebble		
50							
60							
70							
80					sandy or silty bleb drop clast?		
90							
100					base of core 116cm unchanged below 100cm		

NOTES

GEOLOGICAL SURVEY OF CANADA

BOREHOLE ID Araon08C-076C-2

CALENDAR DATE sept 06, 2017 Described Sept. 09, 2017

CORE INTERVAL 116 to 210 cm

CORE BARREL TYPE Gravity

GEOGRAPHIC LOCATION Mackenzie Trough, Beaufort Sea

PROJECT NUMBER

LATITUDE 69° 52.7033' N

LONGITUDE 139° 3.575' W

DESCRIBED BY NED KING GSC-Atlantic

PAGE 2 OF 4

SYMBOL LEGEND

- sandy mud band
- sharp contact
- --- not as sharp

CORE DESCRIPTION

Core Depth (cm) | Deformation | Core state | Ice | Colour (munsell) | Sedimentologic Description | Lithology and Sedimentary Structure | Subsamples

top of section @ 116cm

- Banded grey MUD
- alternating light and dark grey 5/10Y to 4/N

slightly more brown crs bed →

- coarser beds 1→5mm thick; darker than bounding muds, Up to fine sand component. (muddy sand)
- base contacts usually sharp
- top contacts sharp to slightly graded

darker, coarser beds, as above

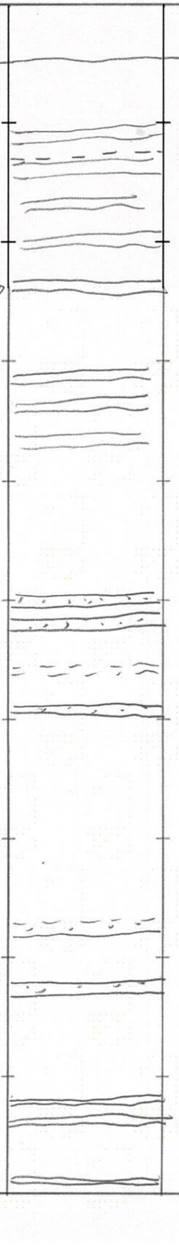

- top of section II

base of section II at 269cm

NOTES

GEOLOGICAL SURVEY OF CANADA

BOREHOLE ID ARAON 08c-07GC-2

CALENDAR DATE Described Sept09 sept.06, 2017

CORE INTERVAL 210 to 310 cm

CORE BARREL TYPE Gravity, steel barrel

GEOGRAPHIC LOCATION Mackenzie Trough

PROJECT NUMBER

LATITUDE 69° 52.7033' N

LONGITUDE 139° 3.5715' W

DESCRIBED BY NED KING GSC-Atlantic

PAGE 3 OF 4

SYMBOL LEGEND

◗	shell	☐		☐	
☐		☐		☐	
☐		☐		☐	

CORE DESCRIPTION

Core Depth (cm) | Deformation | Core state | Ice | Colour (munsell) | Sedimentologic Description | Lithology and Sedimentary Structure | Subsamples

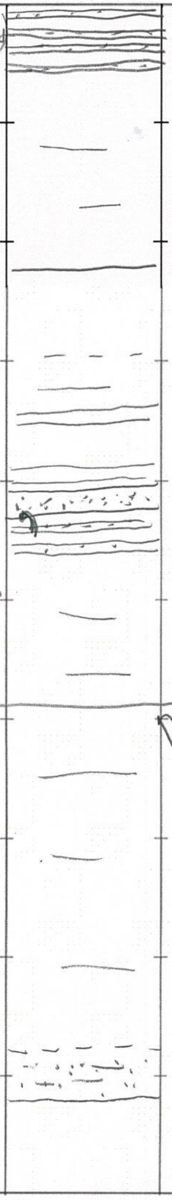

210

dark grey, coarser (silt to v.f. sand) beds 3 to 8 mm thick

220

Banded Grey MUD

230

- approximately 60 bands in 60 cm
- spacing irregular

- thin (1mm) sharp contacts
- coarser, nearly black

240

250

2.5Y/10Y

thick (1.5cm) coarse (sandy mud)
very sharp base contact

260

SHELL (bivalve?) at 253 cm
suitable for C-14 dating

270

base of section II @ 269 cm
top of section III

280

290

300

310

NOTES

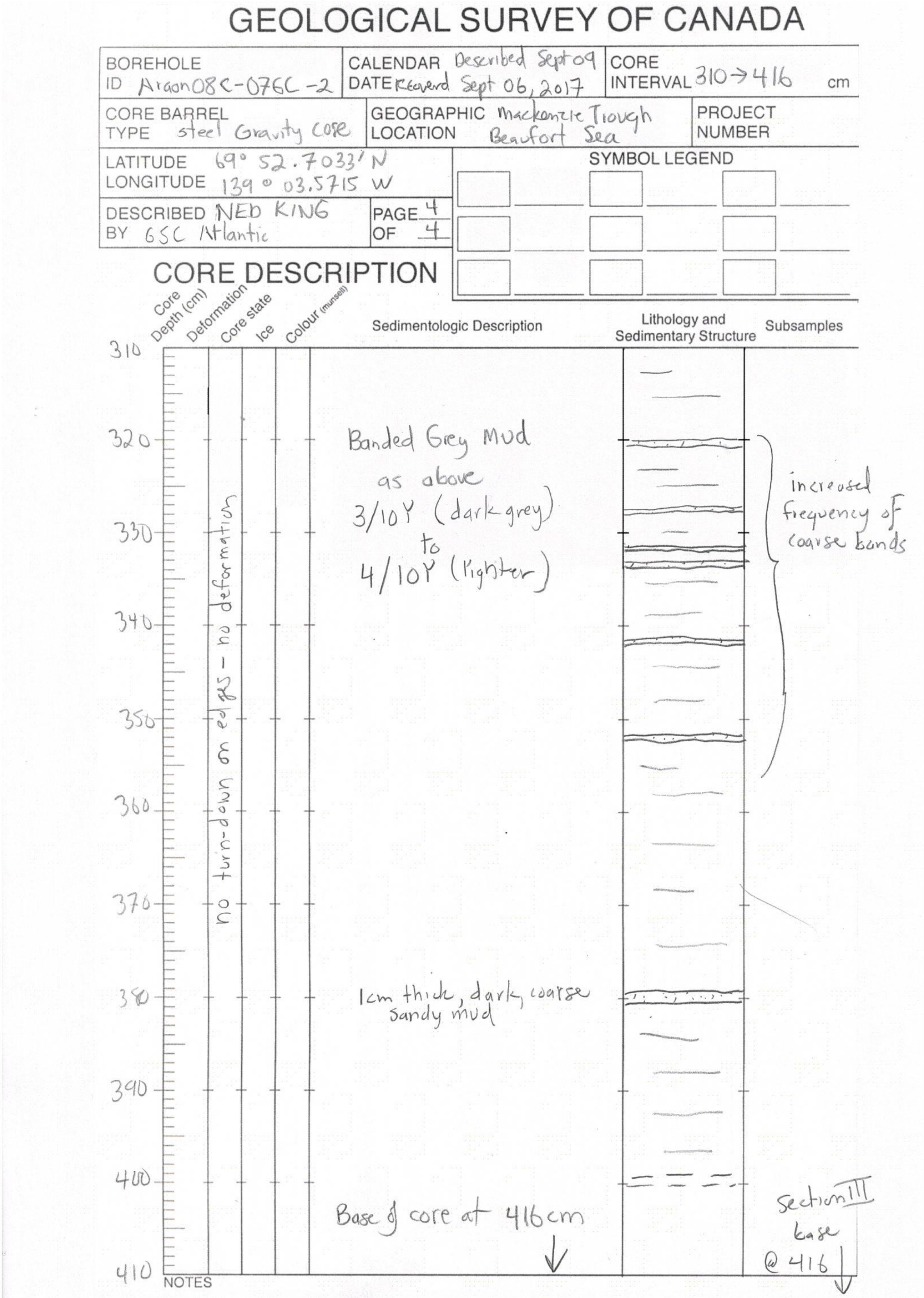

GEOLOGICAL SURVEY OF CANADA

BOREHOLE ID Aragon08C-076C -2

CALENDAR DATE Described Sept 09 Recoverd Sept 06, 2017

CORE INTERVAL 310 → 416 cm

CORE BARREL TYPE steel Gravity core

GEOGRAPHIC LOCATION Mackenzie Trough Beaufort Sea

PROJECT NUMBER

LATITUDE 69° 52.7033′ N

LONGITUDE 139° 03.5715 W

DESCRIBED BY NED KING GSC Atlantic

PAGE 4 OF 4

SYMBOL LEGEND

CORE DESCRIPTION

Core Depth (cm)	Deformation	Core state	Ice	Colour (munsell)	Sedimentologic Description	Lithology and Sedimentary Structure	Subsamples
320–340	no turn-down on edges – no deformation				Banded Grey Mud as above 3/10Y (dark grey) to 4/10Y (lighter)		increased frequency of coarse bands
380					1cm thick, dark, coarse sandy mud		
410					Base of core at 416cm ↓		Section III base @ 416 ↓

NOTES

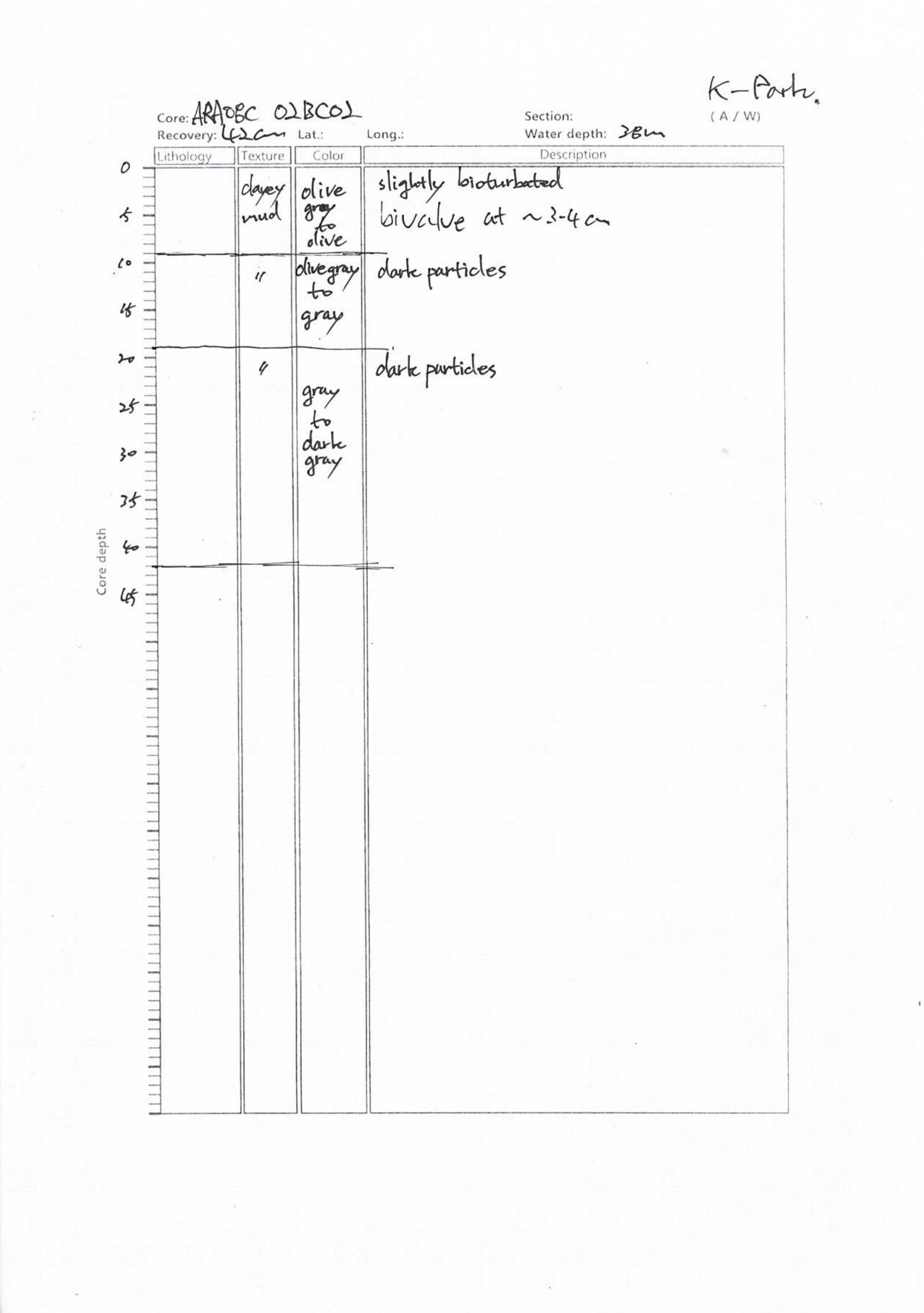

K–Park.

Core: ARA08C 02BC02

Recovery: 42cm

Lat.:

Long.:

Section:

(A / W)

Water depth: 38m

Core depth: 0 5 10 15 20 25 30 35 40 45

Lithology	Texture	Color	Description
	clayey mud	olive gray to olive	slightly bioturbated bivalve at ~3-4cm
	〃	olivegray to gray	dark particles
	〃	gray to dark gray	dark particles

K. Park.

Core: ARA08C 03BC02 Section: (A / W)

Recovery: 50cm Lat.: Long.: Water depth: ~150m

Core depth	Lithology	Texture	Color	Description
0		clayey mud	olive to olive gray	slightly bioturbated
5				
10		〃		dark particles
15			gray to dark gray	
20				
25				
30				
35				
40				
45				
50				

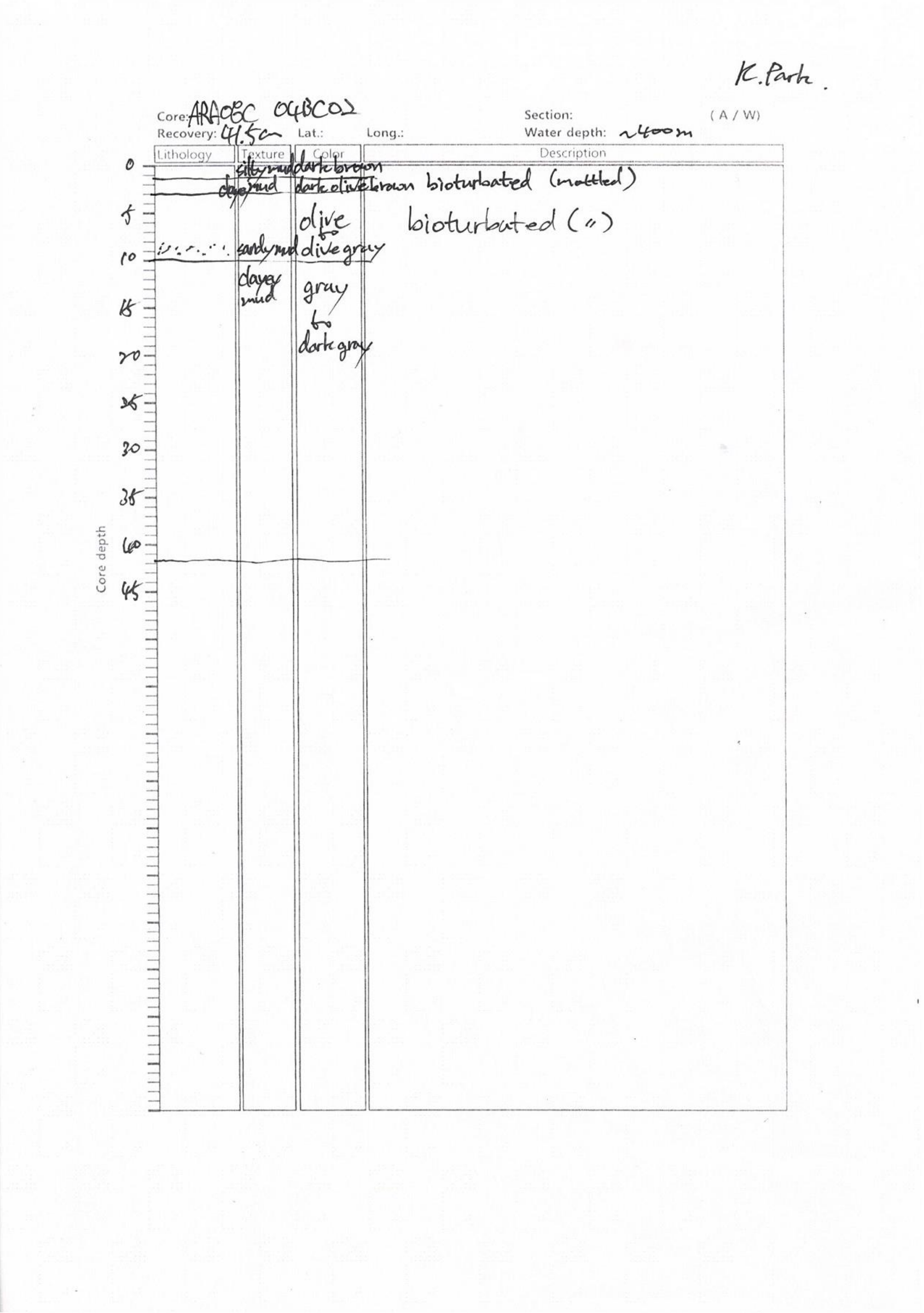

K.Park.

Core: ARA08C 04BC02

Recovery: 41.5cm Lat.: Long.:

Section: (A / W)

Water depth: ~400m

Core depth	Lithology	Texture	Color	Description
0		silty mud	dark brown	
		clayey mud	dark olive brown	bioturbated (mottled)
5			olive to olive gray	bioturbated (")
	∴·˙·.˙·.	sandy mud		
10		clayey mud	gray to dark gray	

0
5
10
15
20
25
30
35
40
45

Chapter 9. Water Column Study

M. Kim, T.S. Rhee, and Y.S. Choi

9.1. Introduction

Most of the Arctic Ocean peripheral seas may be vulnerable to overall warming trends in global climate changes (Solomon et al., 2007). In particular, change in extent and thickness of Arctic sea ice is recognized as a key indicator of Arctic climate change (Shimada et al., 2006). From an oceanographic point of view, it is important to identify what forces drive sea ice reduction in the Arctic Ocean.

The Beaufort Sea is the one of the six marginal seas of the Arctic Ocean, located in the continental shelf area north to the eastern part of Alaska and to Canada. Recent rapid warming in the Arctic (Comiso et al., 2008) affects the Beaufort Sea as the sea ice extent decreases significantly (Jackson et al., 2010; Perovich et al., 2007). The decrease in sea ice extent has led to an increase in the annual amount of solar energy absorbed by the surface of the ocean which enhances temperature increase in the water column, which will further propagate the heat flux down to the seafloor and leads to warming of subsea permafrost (Biastoch et al., 2011; Mestdagh et al., 2017).

The Beaufort Sea region is known for gas and oil deposits, as well as the occurrence of sub-permafrost and intra-permafrost gas hydrates. To investigate the potential release of methane from seafloor sediment associated with the current Arctic warming, CH_4 and other trace gases, such as N_2O and CO_2, in the water column that are important to the global climate were measured. The 2017 sampling program builds on measurements of dissolved CH_4 in the Beaufort Sea collected in 2013 and 2014 onboard the Araon. During these expeditions, the surface water was slightly supersaturated with respect to the atmospheric CH_4 concentration, which was unexpected.

Our objectives for this expedition were three fold; 1) to quantify the air-sea CH_4 flux from the survey area of the Beaufort Sea; 2) to estimate the amount of the CH_4 released from the seafloor sediments, and 3) to evaluate temporal and spatial variability of the dissolved CH_4 content in the Beaufort Sea through comparison of the 2017 measurements with those from 2013 and 2014.

The expedition took place from August 29 to September 13, 2017 onboard the Korean icebreaker IBRV Araon in the region around the Mackenzie Trough (Figure 9.1). We conducted hydrographic castings at 13 stations including conductivity/temperature/depth (CTD) casting and water sampling. Sediment coring was also undertaken at each site (Table 9.1).

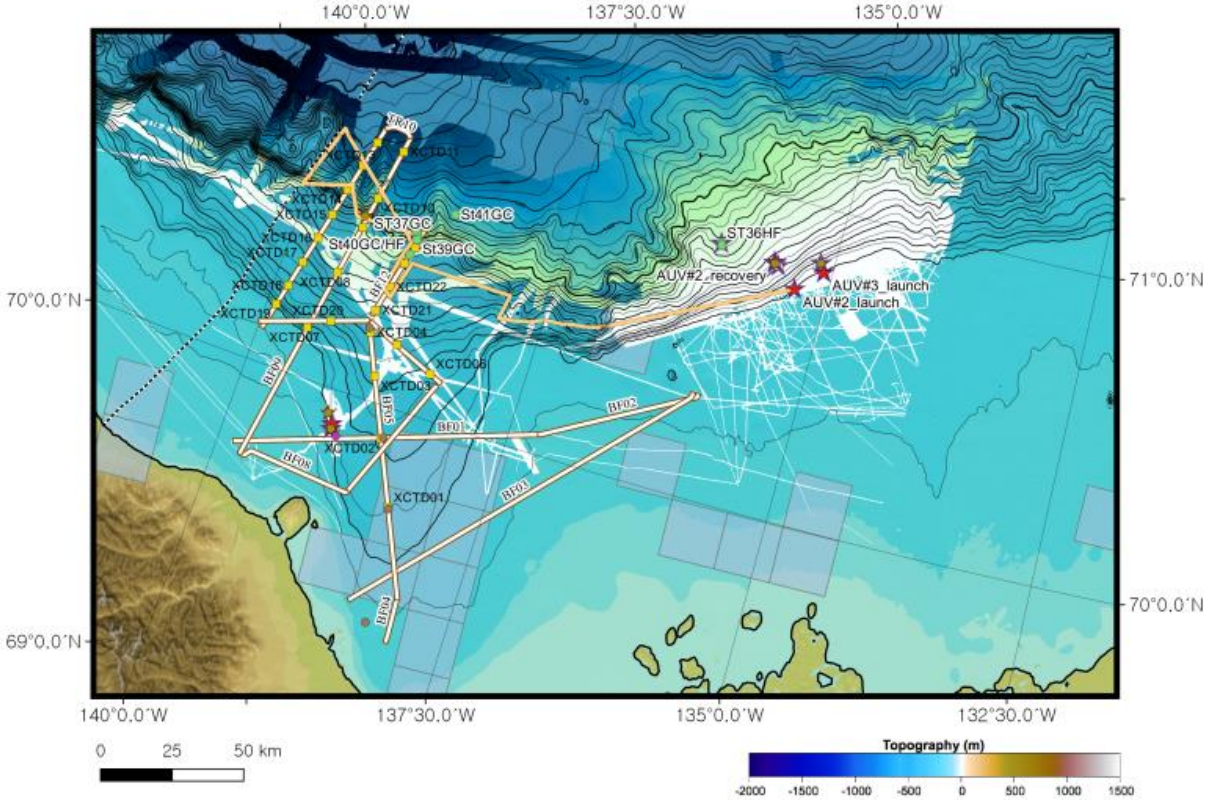

Figure 9.1. Map showing the hydrographic stations in the Mackenzie Trough.

Table 9.1. Hydrographic stations where seawater was collected for chemical analyses.

Station	File name	Start Time (UTC)		Latitude (N)		Longitude (W)		Depth (m)
		YY-MM-DD	hh:mm	Deg.	Min.	Deg.	Min.	
St. 01	ARA08C01CTD1	2017-08-30	01:11	69	51.7037	138	59.5240	150
St. 02	ARA08C02CTD1	2017-09-05	04:30	69	20.3291	138	12.3446	40
St. 03	ARA08C03CTD1	2017-09-05	08:19	69	41.8962	138	19.7382	148
St. 04	ARA08C04CTD1	2017-09-05	11:56	70	13.0826	139	01.3175	406
St. 05	ARA08C05CTD1	2017-09-06	03:43	69	53.1477	139	00.9593	163
St. 07	ARA08C06CTD1	2017-09-06	07:13	69	52.7034	139	03.5706	113
St. 11	ARA08C07CTD1	2017-09-07	03:16	70	48.4606	139	00.6656	1743
St. 14	ARA08C08CTD1	2017-09-07	14:51	70	33.1272	138	51.9260	1210
St. 15	ARA08C09CTD1	2017-09-09	03:23	70	47.4765	135	33.7905	419
St. 21	ARA08C10CTD1	2017-09-09	09:00	70	47.0928	135	31.2600	419
St. 22	ARA08C11CTD1	2017-09-10	03:24	70	49.7400	135	07.9853	157
St. 31	ARA08C12CTD1	2017-09-11	00:31	70	48.3014	136	06.1237	750
St. 32	ARA08C13CTD1	2017-09-11	07:44	70	47.5085	135	33.1245	420

9.2. Methods

9.2.1. CTD casting

The CTD system installed on the Araon was used for profiling and identifying vertical variation of temperature and salinity. Along the transects, hydro-casts of the CTD (SBE 911*plus* CTD)/rosette system were conducted to measure the vertical profiles of conductivity, temperature, depth, and other biochemical parameters (Figure 9.2a). Additional sensors in the system include: in situ measurements of phytoplankton concentrations (fluorometer), optical clarity (transmissometer), dissolved oxygen, altimeter and methane gas concentrations. During CTD up-casting, a 24-position rosette with 10-L Niskin bottles was used to obtain water samples from discrete depths for biological and geochemical analysis.

9.2.2. Ocean current measurement

A 300 kHz RDI lowered Acoustic Doppler Current Profiler (LADCP) was mounted on the CTD/rosette frame to measure a full-depth profile of current velocities (Figure 9.2b). Using the conventional "shear method" for processing (e.g., Fischer and Visbeck, 1993), overlapping profiles of vertical shear of horizontal velocity were averaged and gridded to form a full-depth shear profile. The bin size was 5 m and the number of bins was 20.

Figure 9.2. Hydrographic observation equipment. Left: SBE911plus CTD profiler and rosette water sampler. Right: 300 kHz RDI lowered ADCP.

9.2.3. Seawater sampling

Seawater was collected at 13 stations around the Mackenzie Trough (Table 9.1 and Figure 9.3) using the CTD/rosette sampling system equipped with 24 10L-Niskin type bottles. As soon as the CTD/rosette was on the deck, the seawater was immediately subsampled for dissolved gas analyses to avoid potential leaks or outgassing though the vent due to the warming of the seawater. Subsequently, additional subsampling of the seawater took place for other analyses.

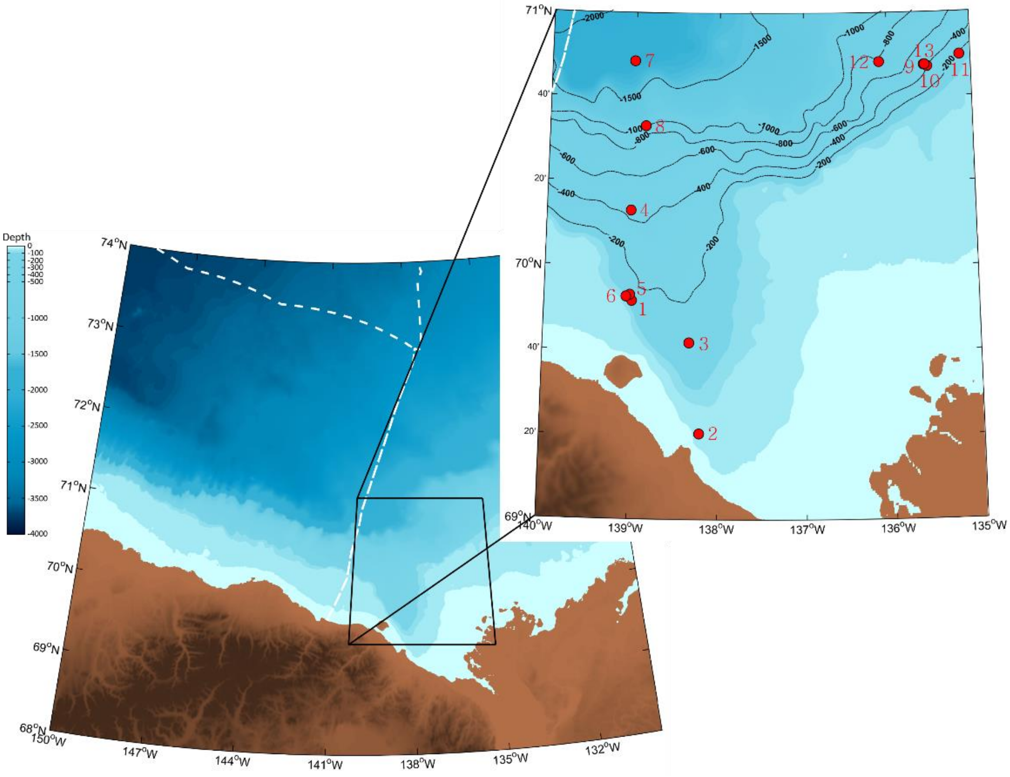

Figure 9.3. Map of the region with the position of the CTD stations indicated by red dots with color-mapped bathymetry. Black dashed contour lines are every 500 m for depths between 4000 m and 1000 m and every 200 m between 1000 m and 0 m depth. White dashed lines denote US EEZ and Canada EEZ boundaries. Hydrographic stations where seawater was collected for the analysis of dissolved gases, nutrients, DIC, and TA.

9.2.4. CH_4, N_2O and CO_2 analyses

Seawater samples for analyses of dissolved CH_4, N_2O and CO_2 were withdrawn from the Niskin bottles into glass jars. The glass jars were prepared for analyses of dissolved gases to avoid any contamination from the lab air during sampling. In the laboratory, 50 mL of pure N_2 gas (99.9999%) was injected into the glass jars using a gastight glass syringe (SEB). The glass jar was then immersed in water at 20°C for more than one hour. To minimize underway data loss, measurements of CH_4, N_2O and CO_2 concentrations in the water column were carried out when the Araon stopped at hydrographic station for other works (e.g., core work). Approximately 40 mL of the headspace gas was drawn from each glass jar using a gas tight glass syringe, and injected into a gas chromatographic system equipped with a flame ionization detector (FID) and an electron capture detector (ECD) to quantify CH_4, N_2O and CO_2 concentrations in water column (Rhee et al., 2009).

During the expedition, underway measurements of these gases were carried out along the cruise track. Surface seawater at ~6 m deep was pumped into a Weiss-type equilibrator to obtain concentrations of dissolved gases in seawater. The headspace air in the equilibrator, which was dynamically in equilibrium with dissolved gas concentration in seawater, was supplied to the gas chromatographic system (Figure 9.4). For one cycle, it took about an hour to analyze the gases from the ambient air and seawater, including calibration gases.

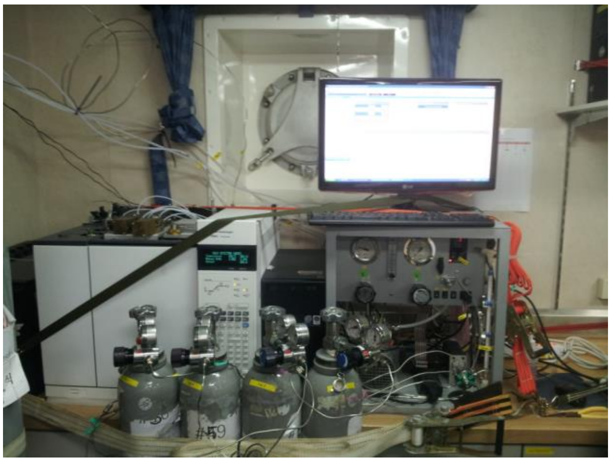

Figure 9.4. Gas chromatographic system for analyses of CH_4, CO_2 and N_2O.

9.2.5. Dissolved inorganic carbon and total alkalinity

Seawater for DIC and TA analyses was subsampled in pre-cleaned 500 mL borosilicate bottles. The seawater samples were fixed with 100 µl of 50% $HgCl_2$ to halt biological activity. The bottles were then sealed with vacuum grease on the surface of the lid to prevent any CO_2 gas leaks until analysis in the laboratory at the Korea Polar Research Institute. The seawater samples will be analyzed using a VINDTA (Versatile INstrument for the Determination of Total Alkalinity) system at the Institute.

9.2.6. Nutrients

Seawater samples for nutrient (NH_4^+, NO_3^-, PO_4^{3-}, SiO_4^{2-}) analyses were collected in 50 mL conical tubes and stored in a freezer at −24°C prior to chemical analyses. The samples will be analyzed with standard colorimetric methods using a Quatro Auto Analyzer at the Korea Polar Research Institute.

9.2.7. Underway pCO_2 measurement

The flux of CO_2 across the sea surface is directly proportional to the difference in the fugacity of CO_2 between the atmosphere and the seawater. The fugacity is obtained by correcting the partial pressure of CO_2 (pCO_2) for non-ideality of the gas with respect to molecular interactions between CO_2 and other gases in air, thus making pCO_2 an important parameter to measure (Pierrot et al., 2009). To investigate air-sea exchange rate of CO_2, pCO_2 was monitored in real-time using an autonomous pCO_2 measuring system (Model 8050, General Oceanics Inc., USA) (Figure 9.5). The system is compact and operates by directing seawater flow through a chamber (the equilibrator) where the CO_2 contained in the water equilibrates with the gas present in the chamber (the headspace gas). To determine the CO_2 in the headspace gas, the gas was pumped through a non-dispersive infrared analyzer (LICOR), which measured the CO_2 mole fraction instantaneously, and then returned it to the equilibrator thus forming a closed loop. Periodically, atmospheric air was also pumped through the analyzer and its CO_2 mole fraction was measured. The analyzer was calibrated with four CO_2 standard gases at regular intervals.

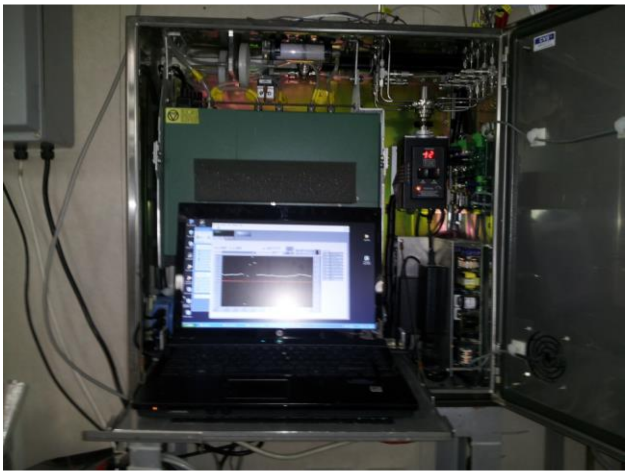

Figure 9.5. Autonomous pCO_2 measuring system.

9.3. Results

In situ measurements of dissolved gases in the surface seawater and the water column collected at hydrographic stations will be processed at KOPRI laboratories. Processing steps include unified integration of chromatograms from calibration gases and the ambient air and seawater, calibration of the raw data, and thermodynamic adjustments of samples measured to the in situ temperature and pressure. Such processes require time and specific tools as well as auxiliary values such as seawater temperature, salinity, meteorological information, etc. In this cruise report, preliminary results from the examination of the instrument performance are presented. Since DIC, TA, and nutrients are not analyzed onboard, only a table showing the number of samples collected during the expedition is presented (Table 9.2).

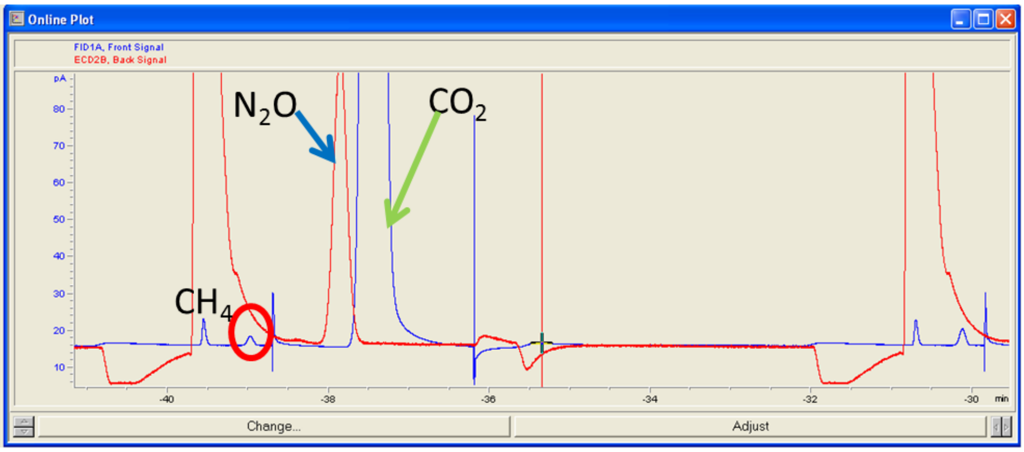

Figure 9.6. Example of chromatograms of CH_4, CO_2 and N_2O displayed in the ChemStation.

Table 9.2. Number of seawater samples collected during the expedition for various analyses.

STN	Cast	Dissolved Gases	DIC/TA	Nutrients	CH_4 oxidation experiment
1	1	8	8	8	0
2	1	4	4	4	1
3	1	9	9	9	0
4	1	9	0	0	0
5	1	9	0	0	0
7	1	8	0	0	0
11	1	10	10	10	0
14	1	9	9	9	0
15	1	10	10	10	0
21	1	10	10	10	1
22	1	8	8	8	0
31	1	10	10	10	1
32	1	10	10	10	0

The automated gas chromatographic system for CH_4, N_2O, and CO_2 ran smoothly throughout the cruise. Chromatograms were used during the cruise to monitor the performance of the system (Figure 9.6). In addition, good performance of the systems was confirmed by inspecting basic parameters such as gas retention times and relationship between electric signals and the quantity of calibration gases periodically throughout the cruise.

Figure 9.7 shows preliminary values for dissolved methane concentrations at Station 1. The values will be adjusted post-calibration, but the vertical trend reflects that high concentration occurred near or beneath the surface mixing layer where biological activities peaked. In general, methane concentrations in the surface water is supersaturated due to methane production in the particles or from zooplankton, although other production mechanisms are speculated. The methane concentration then decreases with depth because methane oxidation by methanotrophs overwhelms methane production by methanogen in deep water.

The methane concentrations of the surface water collected during the first 1.5 days of the expedition are presented in Figure 9.7. Although the data are limited, it shows the surface concentration of methane is as expected and is similar to concentrations observed in 2013 and 2014. We expect high methane concentrations near the coastal area of the Mackenzie Trough. As shown in Figure 9.7, the dissolved methane concentration before arriving at the Mackenzie Trough shows well-homogenized surface seawater for methane concentration, except at one location where methane concentration reached 4.5 nM.

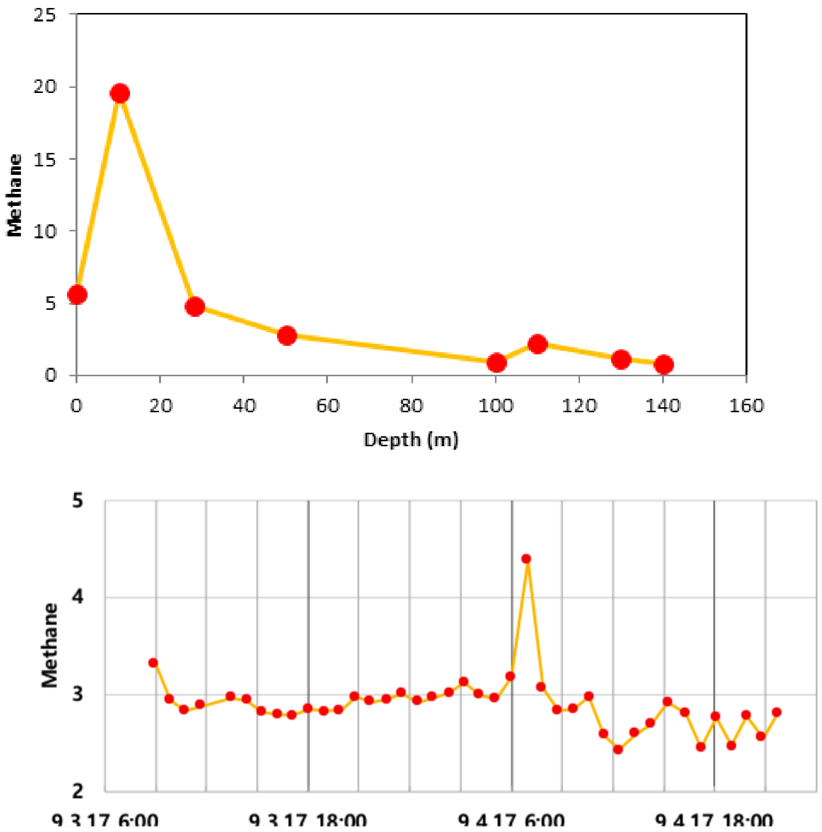

Figure 9.7. Vertical profile of methane concentration at Station 1.

Chapter 10. Biological Study

T.-Y. Park and J.-H. Kihm

10.1. Introduction

As part of one of the Korea Polar Research Institute's (KOPRI) main research projects, KOPRI is striving to understand the origin and evolution of animals during the event called the Cambrian explosion, which began at ca. 541 Ma. This sudden appearance of all animal phyla within a relatively short time period has confused scientists since C. Darwin's 'Origin of Species' (1859). The essence of the Cambrian explosion could be observed by exceptionally preserved Cambrian fossils occurring from Chengjiang, China, Burgess Shale, Canada, and Sirius Passet, northern Greenland, which contain animal fossils with such bizarre morphology that some of them were called 'weird wonders' (Gould 1989). Until the 1990's, such 'weird wonders' were considered unclassifiable into the extant animal phyla, and thus many new phyla were established to accommodate them. During the past two decades, however, paleontologists have begun to better understand the origin of animal morphology by elucidating the phylogenetic position of these 'weird' animals. Research has shown that they were actually stem-groups which were out-branches on the way to attaining the modern morphology (Budd and Jensen, 2000). However, the most reasonable way of interpreting the morphology of Cambrian animals is to make comparisons with the morphology of extant animals (Figure 10.1), so that the fossils in the context of extant animals can be understood, which has been applied to recent paleontological studies (e.g. Vinther et al., 2017; Briggs and Caron, 2017). Since 2016, KOPRI has been interpreting the Cambrian animal fossils from Sirius Passet in northern Greenland. This is one of the least-studied Cambrian localities and contains exceptionally preserved fossils, therefore discovering new taxa is not uncommon. To understand and elucidate the morphology of these new taxa, it is necessary to correctly understand the extant animals and to make comparisons.

Marine invertebrates from the Arctic region are less understood than those of any other regions in the world due to the remoteness and the harsh environment of the area. For example, since the classic and the most influential monograph of G.O. Sars was published in 1899, there has been little advance in our understanding on the crustacean of the Arctic region. The Korean ice-breaking research vessel *Araon* undertook a research program in the Beaufort Sea from 26 August through 16 September 2017. This research cruise provided an opportunity to collect diverse marine invertebrates. The goals of this work are to understand their detailed morphology and to compare them with the Cambrian fossils to understand the morphological origin of animals.

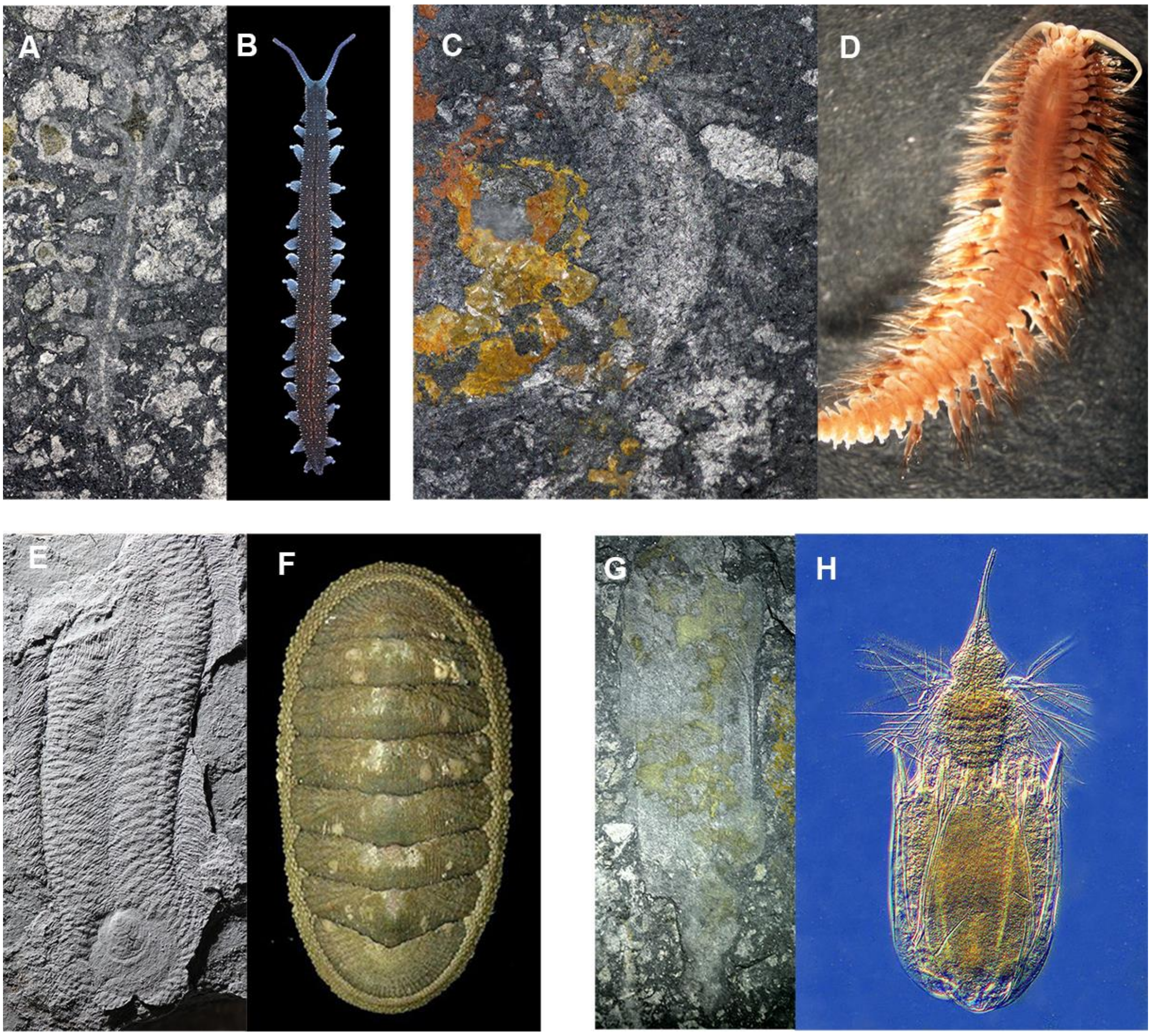

Figure 10.1. Morphological comparison between the Cambrian fossils from Sirius Passet, northern Greenland (A, C, E, G), and extant animals (B, D, F, H). A, new lobopodian species. B, living onychophoran. C, new species of polychaete. D, extant polychaete. E, Halkieria evangelica, a stem-group Molluska. F, extant mollusk, chiton. G, Siriolorica sp., stem-group Loriciphera. H, extant loriciferan.

10.2. Methods and Results

10.2.1. Benthic invertebrates from box cores

When box cores were acquired for geological studies, seafloor invertebrates were inevitably within the core and were collected (Figure 10.2). Species included ophiuroids (brittle stars), polychate worms, "tube worms", crinoids (sea lilies), and amphipod crustaceans. As described by Paull et al. (2015) these tube worms are thought to be unique to the mud volcano environment and conditioned by the flux of methane to the seafloor.

Figure 10.2. "Tube worms" from the seafloor at a mud volcano site.

After the subsampling of the box core with lining cylinders, the surface sediments were taken to the laboratory and filtered by sieve. The remaining sediments contained meiofaunal invertebrates, such as nematodes and copepods. Since it takes significant time to collect meiofaunal invertebrates from surface sediments, most of the processed sediments were collected and preserved in bottled seawater (Figure 10.3). These sediments were refrigerated for detailed collection in the laboratory at KOPRI.

Figure 10.3. Bottled seawater containing processed seafloor sediments from box cores. The sediments will be examined for meiofaunal collecting.

10.2.2. A net trap equipped at gravity core

In an attempt to catch some benthic fauna, a net trap with a beef bait was fixed at the top of the weight of gravity core (Figure 10.4). As time on the seafloor was required to lure fauna into the trap, this method was attempted during heat flow measurements. A minimum of one hour is usually required to lure an appropriate fauna sample size. Unfortunately, time-on-bottom for the heat flow measurement was only 20 minutes, and accordingly, this method was not particularly successful. Furthermore, the main target of the heat flow measurements was the mud volcanoes where the seafloor sediments were extremely soft down to several meters, therefore the trap was pulled down into the sediments on several occasions leading to a total failure in collecting fauna samples.

Figure 10.4. A net trap was tied to the top of the weight of gravity core, so that the net trap could rest on the seafloor in an attempt to collect seafloor fauna.

Nevertheless, three chaetognaths (arrow worms) were collected, which was significant in that it provides material to compare with the recently collected Cambrian chaetognath from northern Greenland (Figure 10.5).

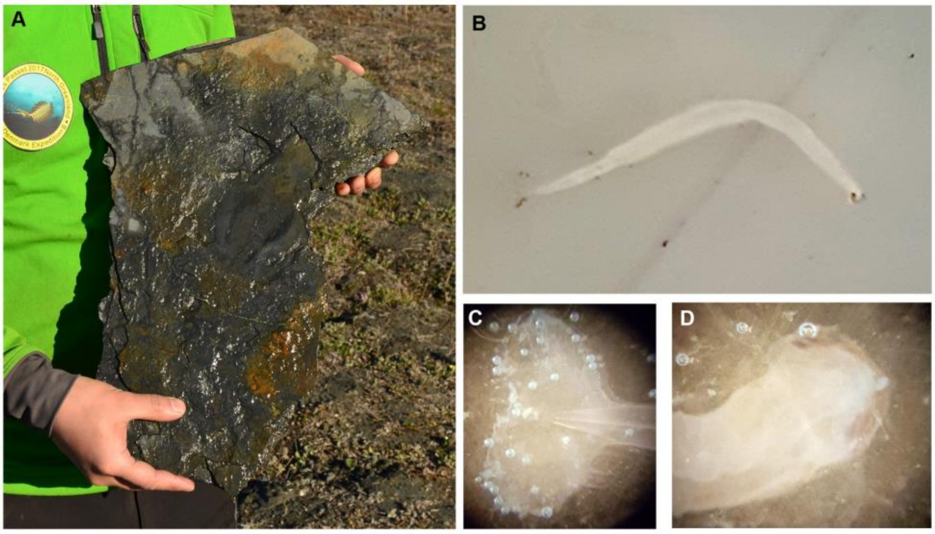

Figure 10.5. A, a giant chaetognath fossil from the Cambrian in northern Greenalnd. B–D, an extant chaetognath, collected in the net trap; B, whole body with a length of ~1 cm; C, tail fin; D, head region.

Interestingly, the Cambrian chaetognath (likely to be plesiomorphic) were large predators, over 20 cm in length, whereas the extant chaetognath are barely over 1 cm in length and considered planktonic predators. This provides a clue to the original ecological niche of this animal group, and to the evolutionary origin of miniaturized modern animals: i.e., they were large when they first appeared in the Cambrian, and became miniaturized during the subsequent evolution as the ecological pressure increased.

10.2.3. Bycatch of MiniROV

The most productive invertebrate collecting was from the MiniROV operation, although it was not the main purpose of this operation. The main monitor of the MiniROV frequently displayed a diverse benthic fauna (Figure 10.6). However, in most cases, the MiniROV did not collect invertebrates on purpose; most of the animals were bycatches of cobble sampling or push core sampling

Figure 10.6. The main MiniROV monitor in the 2nd conference room on the Araon. Crinoids (sea lilies) and ophiuroids (brittle stars), and bivalve molluscs (scallops) are visible on the seafloor. The robotic arm of the MiniROV picking up a cobble sample on which a crinoid is attached.

The collected cobbles samples were deposited in the basket at the underside of the MiniROV, which was eventually filled with rock samples with some epifaunal invertebrates and seafloor sediments (Figure 10.7). The seafloor sediments were processed by sieve and preserved in bottled seawater for further meiofaunal collection in the laboratory at KOPRI.

Figure 10.7. Collecting basket of the MiniROV, containing cobble samples with benthic invertebrates attached on the rock surface.

Bycatches of the cobble sampling include various invertebrate taxa (Figure 10.8), including polychates, bryozoans, nemerteans, arthropods, ophiuroids, and holothurans. Detailed observations of the seafloor sediments in the laboratory is expected to significantly increase the number of taxa collected.

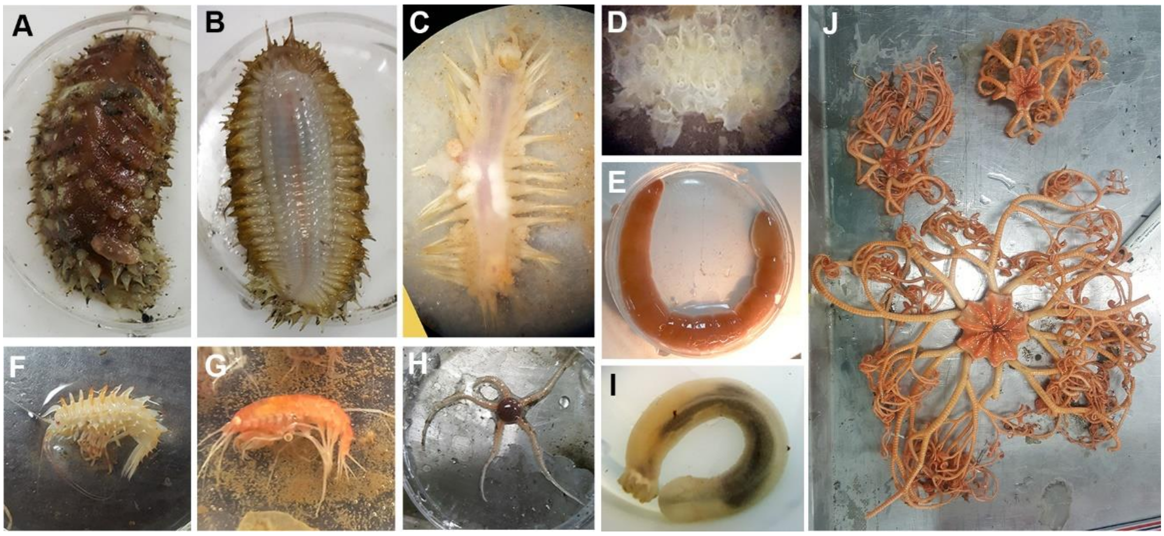

Figure 10.8. Invertebrate bycatches collected during the cobble sampling. A, B, polychate with scaly armour (dorsal and ventral views). C. a polychate. D, a bryozoan colony. E. a nemertean. F, G, amphipods. H, ophiuroid (brittle star). I, holothurian (sea cucumber). J. ophiuroid (sea basket).

Bycatch of push core sampling from the MiniROV was rare and purely accidental. Nevertheless, some isopod and hyperidean amphipod crustacean samples were acquired from the mud volcano sites. One of the amphipod crustaceans seemed to show an interesting pattern of coloration (Figure 10.9). The overall body was transparent or white-colored, but at the intersegmental boundaries lie reddish colorations, which were not pigments, but some radial structures (Figure 10.9B, C). The radial structures apparently show a growth series, which likely means that they were formed by some microbial activity.

Figure 10.9. A hyperidean amphipod collected as a bycatch of push core sampling. A, whole body (ca. 2 cm in length). B, C, detailed view of the coloration at an intersegmental boundary of the animal. Note that there is a core-like circular structure in the middle. The radial structure in C is smaller than those in B, implying there is a growth series.

10.3. Summary and Conclusion

Through the box core and MiniROV sampling, diverse invertebrate collection was acquired from the Beaufort Sea, although invertebrate collection was not the main purpose of this research cruise. The invertebrate collections will be used for sequencing and morphological study, including dissection. Morphological comparison between these invertebrates and those collected from the Cambrian of northern Greenland will provide a reasonable method of elucidating the origin of animal morphology during the Cambrian explosion.

References

Briggs, D.E.G. and Caron, J.-B. 2017. A large Cambrian chaetognath with supernumerary grasping spines. *Current Biology*, 27: 2536-2543. doi:10.1016/j.cub.2017.07.003

Budd, G. and Jensen, S. 2000. A critical reappraisal of the fossil record of the bilaterian phyla. *Biological Review*, 75: 253–295.

Darwin, C. 1859. *On the Origin of Species by Means of Natural Selection, or the Preservation of Favoured Races in the Struggle for Life.* John Murray, London, 502 p.

Gould, S.J. 1989. *Wonderful Life: The Burgess Shale and the Nature of History.* W.W. Norton, New York.

Paull, C.K., Dallimore, S.R., Caress, D.W., Gwiazda, R., Melling, H., Riedel, M., Jin, Y.K., Hong, J.K., Kim, Y.-G., Graves, D., Sherman, A., Lundsten, E., Anderson, K., Lundsten, L., Villinger, H, Kopf, A., Johnson, S.B., Hughes Clarke, J., Blasco, S., Conway, K., Neelands, P., Thomas, H., and Côté, M. 2015. Active mud volcanoes on the continental slope of the Canadian Beaufort Sea. *Geochemistry, Geophysics, Geosystems*, 16: 3160–3181. doi:10.1002/2015GC005928.

Sars, G.O. 1899. *An account of the Crustacea of Norway.* Bergen Museum, Bergen.

Vinther, J., Parry, L., Briggs, D.E.G., and Van Roy, P. 2017. Ancestral morphology of crown-group molluscs revealed by a new Ordovician stem aculiferan. *Nature,* 542: 471–474.

Chapter 11. Atmospheric Observations

J. Park, Y. Kim, C.-K. Lim, L. Peng, and Y. Li

11.1. Introduction

The Arctic is one of the most vulnerable regions to the impacts of climate change, with a large warming trend and high sensitivity to climate forcing, largely due to the strong albedo-sea ice feedback (Law and Stohl, 2007; Shindell and Faluvegi, 2009). The Arctic climate change processes are poorly understood due to the lack of observational data. One of the most significant uncertainties is the role of clouds, and in particular, the effect of oceanic biological activity on clouds.

In the summer of 2017, the Korean ice-breaking research vessel (IBRV) *Araon* voyaged to the Arctic Ocean (departing from Barrow (USA), through the Beaufort Sea, and to Nome (USA)) from 26 August to 16 September, 2017. During the course of the research expedition KOPRI mounted an atmospheric science research program from the ship to advance observational data to further our investigation of this remote area. Atmospheric observations on the *Araon* included basic meteorological parameters (e.g., air temperature, humidity, pressure and wind), radiative fluxes (e.g., net shortwave and longwave radiations) to measure surface variables at the foremast, physicochemical properties of aerosols (e.g., total particle concentration, particle size distribution, black carbon, morphology, elemental composition, condensation cloud nuclei (CCN) concentration, and etc.), and a laboratory-scale bubble bursting chamber study. An all-sky camera, a micro-pulse LiDAR (MPL) on the 04 deck and a radiosonde sounding system on the compass deck were installed to observe cloud properties and atmospheric vertical profile. In addition, the radiosonde sounding system was operated for observation of atmospheric vertical profile along the cruise track four times each day at 00, 06, 12, and 18 UTC. However, it was challenging to maintain high performance of the instruments due to harsh weather condition in the Arctic Ocean. The overview of atmospheric observations is summarized in Figure 11.1. In this report, an overview of the instruments aboard IBRV *Araon* and some preliminary results of the atmospheric observations are presented.

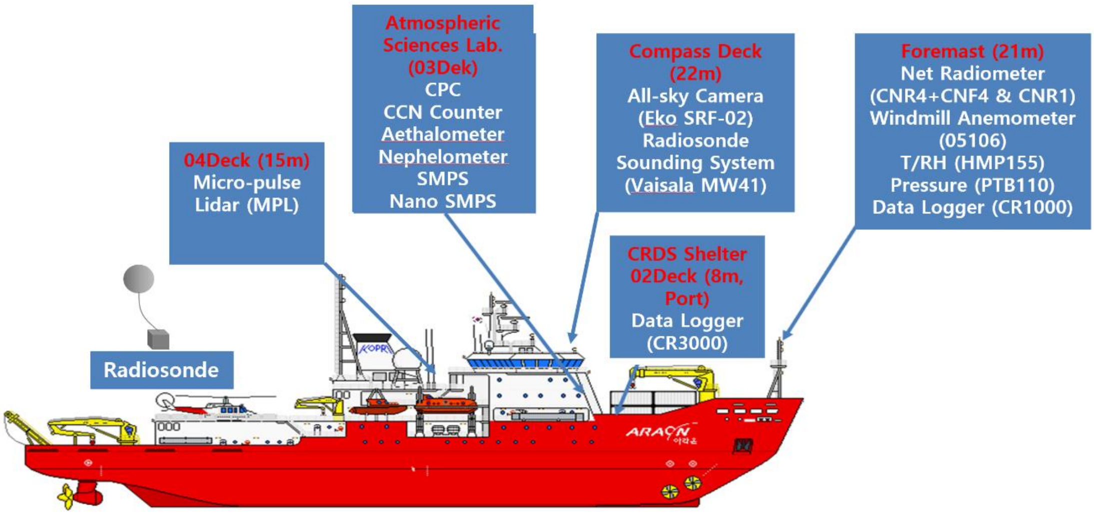

* Heights in parenthesis are the distance of instruments from design load waterline (DLWL)

Figure 11.1. Overview of atmospheric observations on IBRV Araon during 2017 Araon Arctic cruise.

11.2. Instruments

11.2.1. Foremast

At the top of the foremast (height of 21 m above the water surface), a windmill anemometer collected wind speed and direction (05106, RM Young, USA) (Figure 11.2). At the middle part of the mast, a temperature and humidity sensor (HMP155, Vaisala, Finland) and a net radiometer (CNR4, Kipp & Zonen, Netherlands) were installed at the guardrail. A data logger (CR1000, Campbell Scientific, Inc., USA) was located at the base of the mast, which contained a pressure-measuring barometer (PTB110, Vaisala, Finland). 10 minute-averaged data were saved on data loggers and sent to the computer in the atmospheric sciences lab.

Figure 11.2. Meteorological instruments at the foremast.

11.2.2. Radarmast

Meteorological instruments at the radarmast were not operational during this cruise, due to flooding of the data loggers during the Antarctic cruise, which took place prior to this expedition.

11.2.3. Radiosonde observations

Instruments for the observations of upper atmosphere were installed over the container on the compass deck and outdoors on 04 deck (Figure 11.3). The all-sky camera (Eko SRF-02, Eko, Japan) took all-sky photos at 30-min intervals to yield cloud fraction. The radiosonde sounding system (i.e. antenna, receiver, and ground checker) received the transmitted data from the ascending radiosonde sensor. Radiosonde observations were carried out every 6 hours (00, 06, 12 and 18 UTCs) during the cruise. The 00 and 12 UTCs data were transmitted to the real-time radiosonde data network of the World Meteorological Organization via the Global Telecommunication System (GTS) with the aid of the Korea Meteorological Administration (KMA). A micro-pulse LiDAR (MPL, SigmaSpace, USA) was newly installed outside on 04 deck, measuring vertical profiles of atmospheric particles (e.g., clouds and aerosols) and monitoring the sky condition.

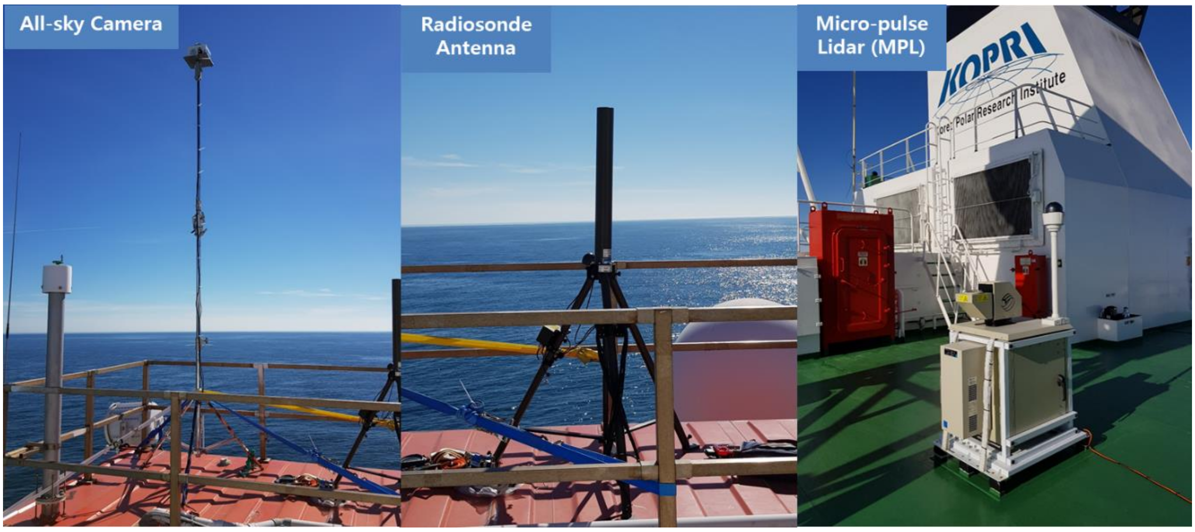

Figure 11.3. All-sky camera and radiosonde antenna over the container at the compass deck and the micro-pulse LiDAR at the 04 deck.

11.2.4. Physicochemical properties of aerosols

Real-time measurements in the atmospheric science laboratory

Continuous measurements were conducted in the atmospheric science laboratory on board the ARAON during the cruise as shown in Figure 11.2. The physical and chemical characteristics of aerosols were measured with various instruments that included two condensation particle counters (CPCs), two scanning mobility particle sizer (SMPS), an optical particle sizer (OPS), an aethalometer, a nephelometer, and cloud condensation nuclei counter (CCNC) as shown in Figure 11.4.

(1) Total particle concentrations using two types of CPCs: A TSI model 3776 that measured particles larger than 2.5 nm and a TSI model 3772 that measured particles larger than 10 nm. Aerosol sample flow rates of CPC 3776 and CPC 3772 were 1.5 lpm and 1.0 lpm, respectively. The difference between CPC 3776 and CPC 3772 can be used to represent the concentration of nanoparticles in the size range of 2.5 to 10 nm.

(2) Particle size distribution using the SMPS and OPS: In the size range 3 nm – 80 nm the measurements were made with the nano SMPS (Differential mobility analyzer (DMA): TSI 3085, CPC: TSI 3776), and in the size range from 10 nm to 300 nm with the regular SMPS (DMA: TSI 3081, CPC: TSI 3772). In the nano SMPS, the aerosol and sheath flow rates were 1.5 lpm and 15 lpm, respectively; for the regular SMPS, the aerosol and sheath flow rates were 1.0 lpm and 10 lpm, respectively. The OPS (TSI 3330, USA) was also used to determine the size distribution of particles in the size range of 100 nm – 10 μm. For the OPS, aerosol flow rate was 1.0 lpm.

(3) Black carbon (BC) concentration using the aethalometer: The BC concentration was measured with the aethalometer (AE22, Magee Scientific Co., USA) to assess the influence exerted by anthropogenic sources (e.g., local pollution and ship emission).

(4) Aerosol optical properties using the nephelometer: Backscattering and total scattering of particles were measured with the nephelometer (TSI 3563, USA) to determine the aerosol optical properties.

(5) CCN concentration using the CCNC: The CCN counter from Droplet Measurement Technologies (DMT CCN-100) was used to measure the CCN concentration. The sample flow in the CCN counter was 0.5 lpm and it was operated at five different supersaturation ratios (SS) (0.2, 0.4, 0.6, 0.8, and 1.0 %). In the CCNC scanning mode, each SS value (except the 0.2% SS) was measured for approximately 5 minutes before it was changed to the next SS value. For a 0.2 % SS, CCN concentrations were measured for 10 minutes because it required additional time to achieve stability after completing measurements at a 1 % SS.

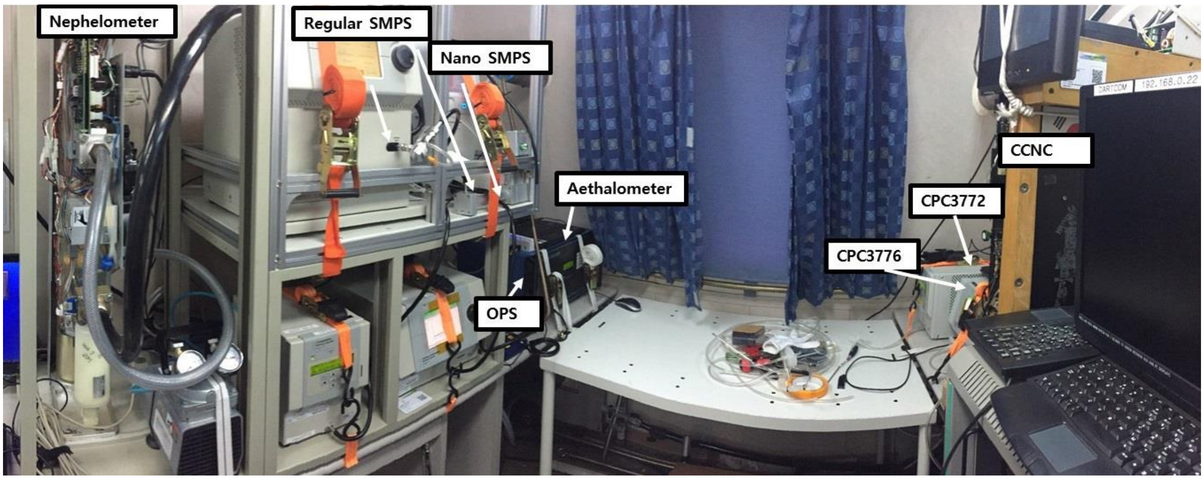

Figure 11.4. Aerosol instruments in the atmospheric science laboratory.

Off-line filter sampling on the compass deck

To investigate the physicochemical properties of aerosols and bioaerosols in the Arctic atmosphere, PM samples were collected for 24 or 48 hours on the compass deck using various samplers such as cyclone, button aerosol sampler, mini volume sampler, and high volume sampler as shown in Figure 11.5. All samplers were connected to a wind sectoring system to minimize ship smoke stack emissions during the cruise. Table 11.1 summarizes the log of the filter sampling for PM2.5 cyclone, button aerosol sampler and mini volume sampler.

(1) PM 2.5 cyclone for morphological and elemental analysis: To determine the morphology and elemental composition of the particles, they were collected on a grid for 24 hours through a URG cyclone (Teflon-coated aluminum cyclone with a cut size of 2.5 µm at 16.7 lpm). The grid was then analyzed by a transmission electron microscopy (TEM) and energy dispersive spectroscopy (EDS).
(2) Button aerosol sampler for bioaerosol counting: For the bioaerosol counting, the ambient bioaerosol was collected on the 25 mm polycarbonate (PC) filter (pore size: 0.8 µm) for 24 hours using the button aerosol sampler. The sampler was operated at 4 lpm. After sampling, the collected PC filter was removed from the samplers and immediately placed in pyrogen-free tubes. The sample was stored at -80°C.
(3) Mini volume sampler for identifying bioaerosol species: To identify the bioaerosol species, a PM10 sample was collected on the 47 mm PC filter for 24 hours using the mini volume sampler (TAS-5.0). After sampling, the collected filter was placed in pyrogen-free tubes with 70% ethanol and stored at -20°C.
(4) High volume sampler for determining HULIS-C: Quartz filters and aluminum foils were baked at 450°C for 4 hours to remove any remaining contaminants. For determination of the HULICS-C, the PM 2.5 sample was collected on the quartz filters (PALL Life Science) for 48 hours using a high volume sampler (Thermo Electron Corporation, USA).

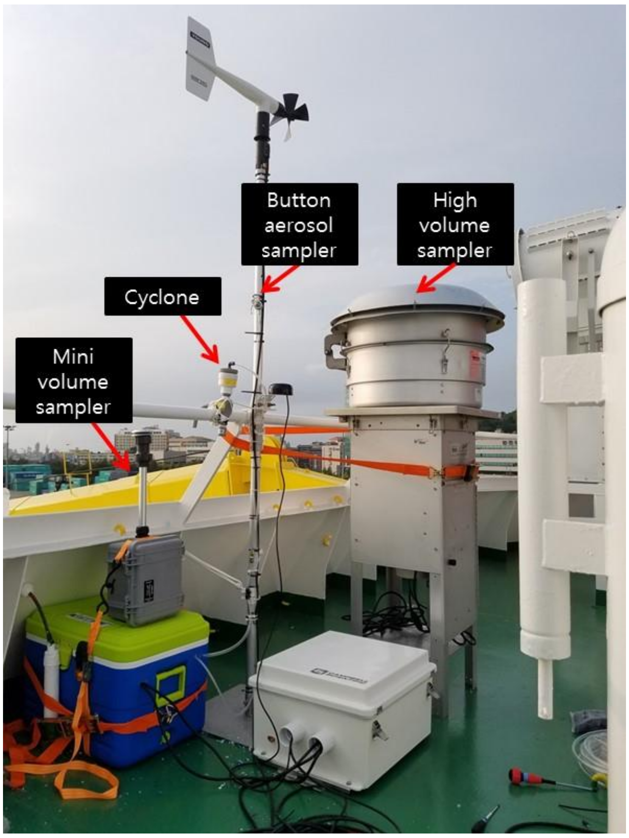

Figure 11.5. Filter samplers on the compass deck.

Table 11.1. Log of filter sampling during the ARA08C cruise.

Sample No.	Sampling start (UTC)	Sampling end (UTC)	Total sampling time (hours)	Weather
1	Aug 28 2017 17:00	Aug 29 2017 14:50	21:50	Cloudy
2	Aug 29 2017 15:30	Aug 30 2017 15:00	23:30	Cloudy
3	Aug 30 2017 16:14	Aug 31 2017 15:00	22:46	Rainy
4	Aug 31 2017 15:40	Sep 01 2017 15:30	23:20	Rainy
5	Sep 01 2017 16:20	Sep 02 2017 15:30	23:10	Fog, Sunny
6	Sep 02 2017 16:10	Sep 03 2017 15:00	22:50	Fog
7	Sep 03 2017 16:00	Sep 04 2017 15:00	23:00	Cloudy
8	Sep 04 2017 16:00	Sep 05 2017 15:00	23:00	Cloudy
9	Sep 05 2017 16:20	Sep 06 2017 15:30	23:10	Fog
10	Sep 06 2017 16:10	Sep 07 2017 15:04	22:54	Strong windy, cloudy
11	Sep 07 2017 16:18	Sep 08 2017 15:45	23:27	Strong windy, cloudy
12	Sep 08 2017 16:17	Sep 09 2017 15:00	22:43	Cloudy
13	Sep 09 2017 15:45	Sep 10 2017 15:35	23:50	Snowy
14	Sep 10 2017 16:10	Sep 11 2017 15:20	23:10	Cloudy
15	Sep 11 2017 16:05	Sep 12 2017 15:15	23:10	Cloudy

11.2.5. Laboratory-scale chamber experiments

Figure 11.6 presents a schematic diagram of the bubble bursting system to mimic the primary marine aerosol (i.e., sea spray aerosol) production and various aerosol measurement systems in the laboratory. Bubble-bursting chamber experiments were performed onboard the ARAON using a 5L simulation tank. The chamber was filled with 3L of surface seawater collected by the CTD at 10 stations (refer to Table 11.2). The clean filtered air was bubbled through a sintered glass filter immerged in the seawater. The procedure and set-up used for the simulated marine aerosol production in the laboratory were similar to those described in Sellegri et al. (2006). The bubble size distribution was previously measured and compared to more realistic bubbles produced by a weir, and to natural bubble size distributions reported in the literature (Sellegri et al., 2006). Bubbles generated by this system were then dried using diffusion dryers, and size distribution, total particle concentration, CCN concentration, morphology, and elemental compositions of the dried particles were measured using the aerosol instruments such as nano SMPS, regular SMPS, OPS, CPC, CCN counter, and TEM/EDS analysis.

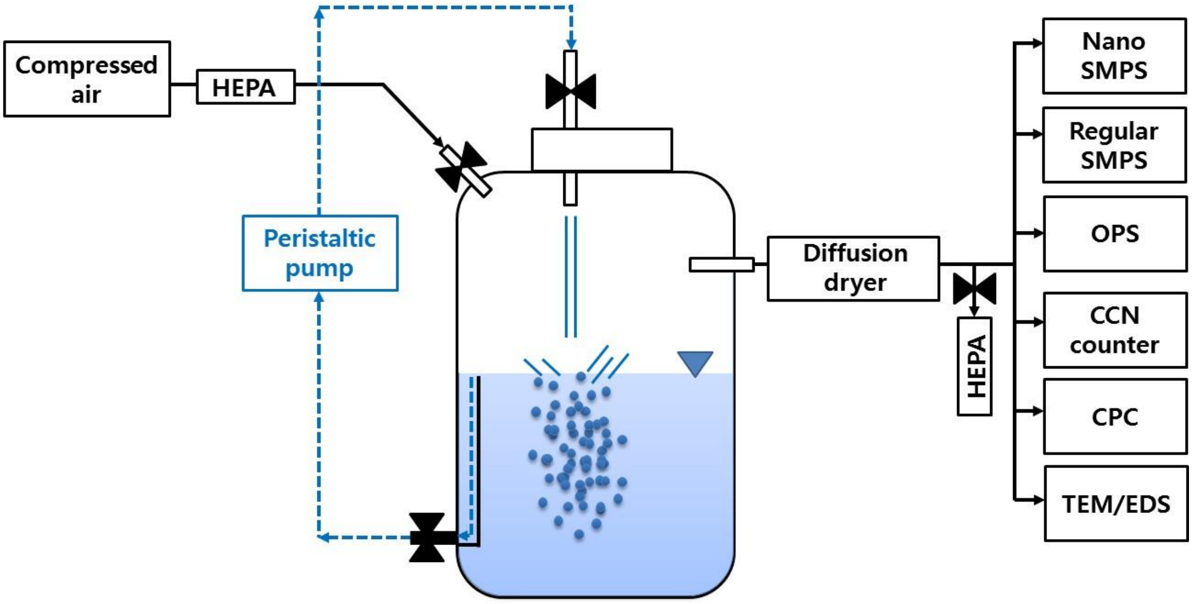

Figure. 11.6. Schematic of the bubble bursting chamber experiments.

Table 11.2. CTD information for the bubble bursting chamber experiments.

No.	CTD name	Depth (m)	Latitude (°N)	Longitude (°W)	UTC (Time)
1	ARA08C01CTD1	143	69.8617	-138.9921	Aug 30 2017 01:11:46
2	ARA08C02CTD1	32	69.3387	-138.2059	Sep 05 2017 04:30:22
3	ARA08C03CTD1	133	69.6982	-138.3291	Sep 05 2017 08:19:03
4	ARA08C04CTD1	393	70.2181	-139.0219	Sep 05 2017 11:56:23
5	ARA08C07CTD1	1732	70.8076	-139.011	Sep 07 2017 03:16:46
6	ARA08C08CTD1	1202	70.5521	-138.8655	Sep 07 2017 14:51:41
7	ARA08C09CTD1	415	70.7912	-135.5631	Sep 09 2017 03:23:41
8	ARA08C10CTD1	415	70.7848	-135.521	Sep 09 2017 09:00:30
9	ARA08C12CTD1	739	70.805	-136.1022	Sep 11 2017 00:31:02
10	ARA08C13CTD1	416	70.7917	-135.552	Sep 11 2017 07:45:01

11.3. Preliminary Results

11.3.1. Surface meteorological variables

Figure 11.7 shows the air temperature and relative humidity records measured by HMP155 and the air pressure records measured by PTB110 at the foremast. Figure 11.8 shows the calculated windmill anemometer (05106, RM Young, USA) true wind speed and direction considering the head, course, and speed of the ship. HMP155 that measured Temperature and humidity data were only recorded until 06-Sep due to equipment failure.

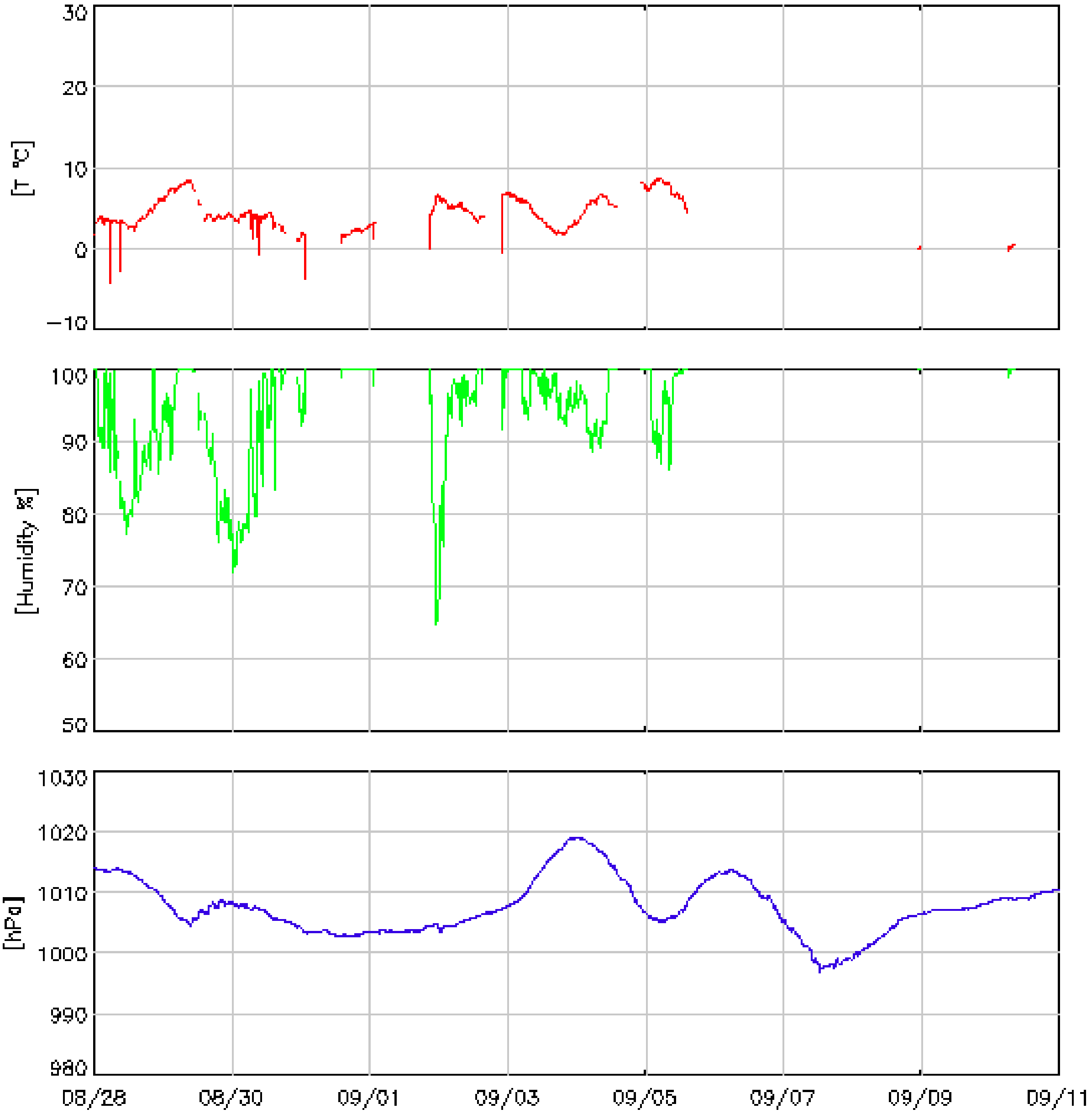

Figure 11.7. (Top) Air temperature (°C) and (Middle) relative humidity (%) from HMP155 at the foremast. (Bottom) Pressure (hPa) from PTB110 at the foremast.

Figure 11.9 shows prevailing wind speed and direction during ARA08C, with the dominant winds from the northeast. Figure 11.10 displays the time series of downwelling shortwave (DSR) and longwave radiation (DLR) measured by the CNR4 net radiometer at the foremast. The DSR shows an apparent diurnal cycle and is dependent on the diurnal variation of solar zenith angle. The sunny day peak values reached nearly 600 W m^{-2}. The amplitude of the DLR is an indication of the amount of longwave from the sky. The DLR decreases with clear sky conditions and dropped to about 300 W m^{-2} on 02-Sep.

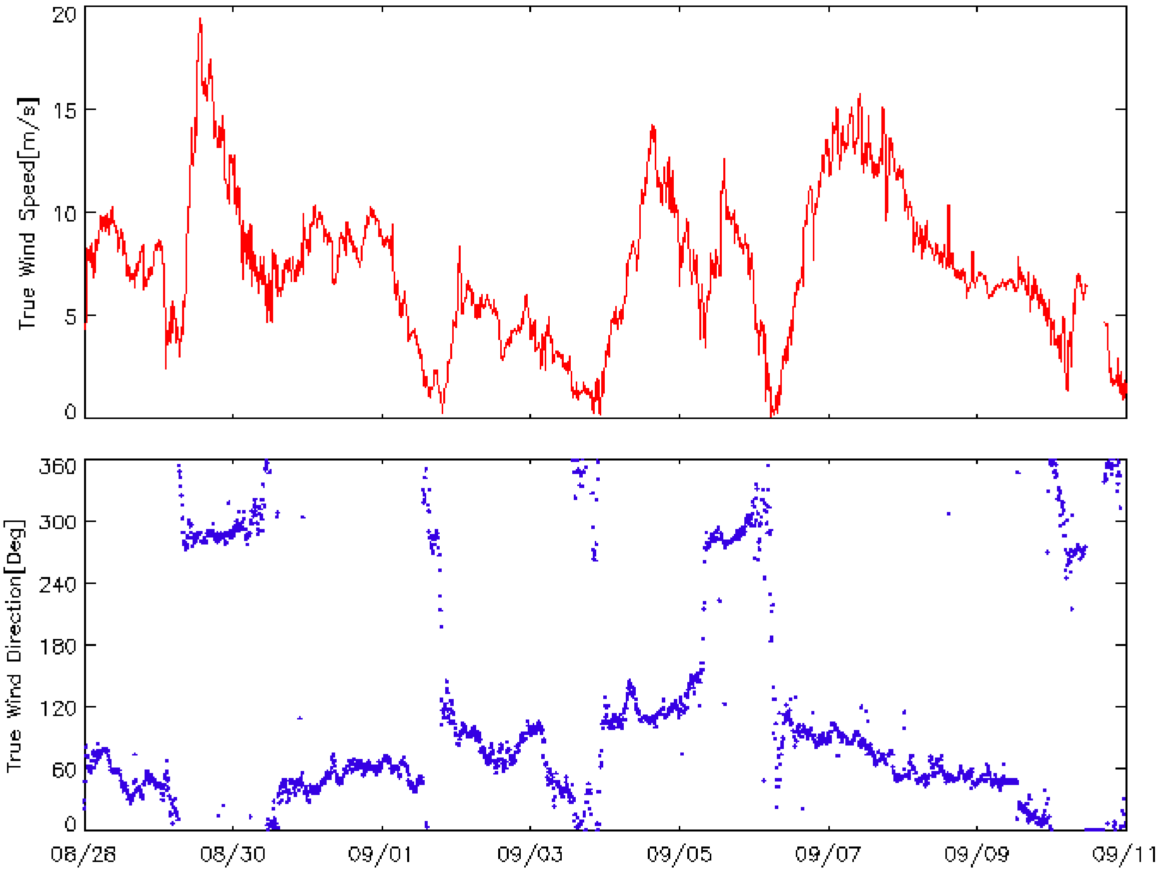

Figure 11.8. (Top) 10-min averaged true wind speed (m/s) and (Bottom) direction (°) from RM Young at the foremast.

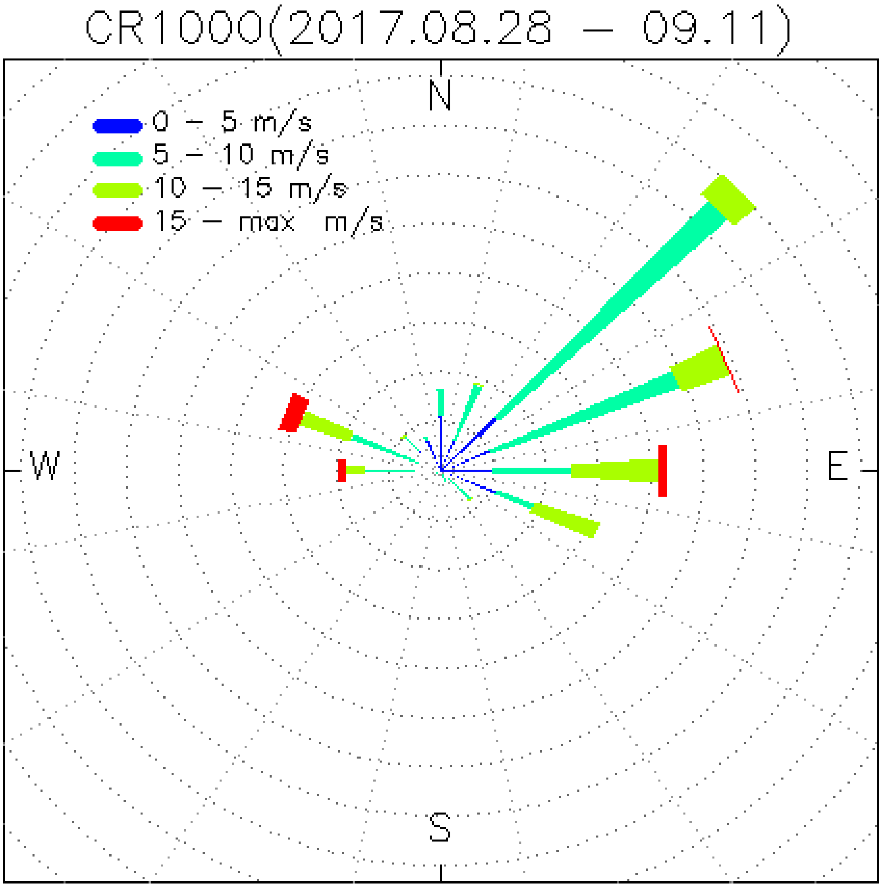

Figure 11.9. Wind rose of windmill anemometer data calculated 10-min mean true wind speed (m/s) and direction (°) at the foremast.

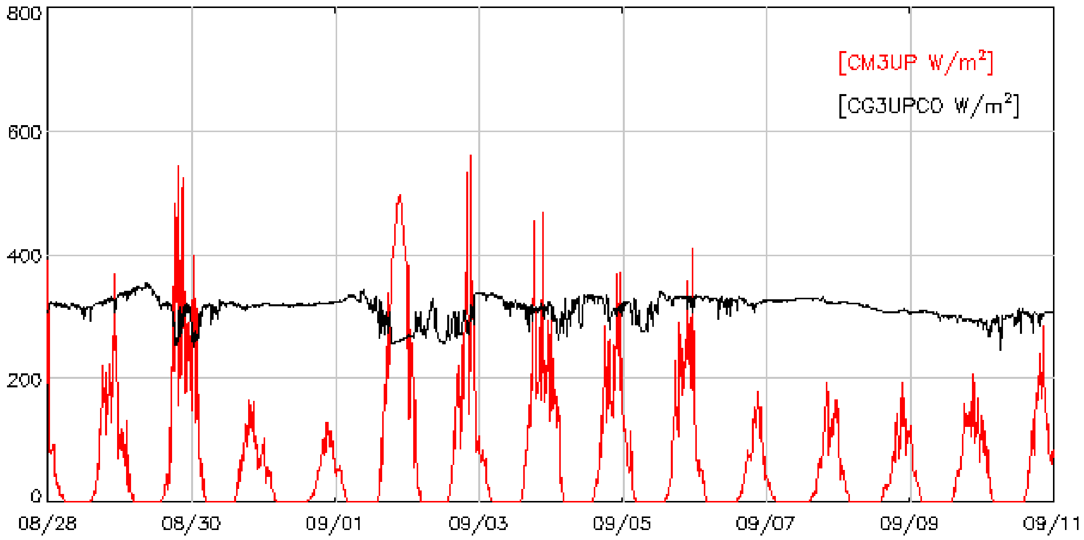

Figure 11.10. Downwelling radiations [W m^{-2}] measured by CNR4 at the foremast: (black) longwave radiation, (red) shortwave radiation. Positive sign denotes downward direction.

11.3.2. Radiosonde profile

The radiosonde balloon was launched at regular intervals to measure the atmospheric profile of temperature, humidity, and wind. These data are crucial for understanding the thermodynamic properties in the Arctic summer atmosphere and are valuable because existing observations are sparse in this region. The observation locations are displayed in Figure 11.11 and the log of radiosonde observations is summarized in Table 11-3. During ARA08C, 65 launches were carried out.

Table 11.3. Log of radiosonde observations during ARA08C.

No	Date	Time (UTC)	Start Time	Duration (s)	Height (km) & Pressure (hPa)	Remarks
63	2017/08/28	00	23:09	5591	26.5, 20.8	Cloudy, rain, mild wind St:100%
64		06	05:20	5587	26.5, 20.6	Strong wind, rain, cloudy St:100% Broken unwinder Second try
65		12	11:56	4011	16.1, 100.4	Rain, mild wind St:100% PTU filtering stopped
66		18	17:19	5545	24.6, 27.8	Mild wind, rain, cloudy St:100% PTU filtering stopped
67	2017/08/29	00	23:22	6181	29.5, 13.1	Rain, windy, cloudy St:100% 15 min delay due to connection problem between laptop and receiver Local time is 1 hour forward
68		06	05:01	6063	28.1, 16.2	Rain, mild wind, cloudy St:100%
69		12	11:10	6017	25.4, 25.0	Strong wind, rain Uncorrected T/RH value
70		18	16:51	5794	21.9, 41.5	Cloudy, strong wind St:100% PTU filtering stopped
71	2017/08/30	00	23:00	3355	10.9, 220.7	Cloudy, strong wind St:100% PTU filtering stopped
72		06	04:57	2913	10.6, 235.2	Cloudy, mild wind St:100% PTU filtering stopped
73		12	11:09	5167	24.2, 29.3	Calm Uncorrected T/RH value
74		18	17:16	4801	21.4, 44.8	Calm, fog St:100% PTU filtering stopped 1st try is failed Due to damaged sensor by hitting the ship
75	2017/08/31	00	23:02	4951	23.9, 30.9	Mild wind, rain, snow St:100%
76		06	04:59	3295	14.1,136.6	Cloudy, windy St:100% Uncorrected T/RH value

						PTU filtering stopped
77		12	11:04	988	4.7, 553.9	Rain, windy 2nd try is failed 1st value is sent to KOPRI
78	2017/09/01	06	05:00	2131	8.3, 334	Fog, cloudy, calm St:100% PTU filtering stopped Signal lost message problem
79		12	11:06	654	3, 684	Calm PTU filtering stopped Before launching balloon, signal lost message appear.
80		21	21:14	3799	18.3, 72.2	Sunny, clear sky, calm St:10% Test launching
81	2017/09/02	00	23:03	6388	28.7, 14.78	Sunny, clear sky, calm St:30%
82		06	04:58	5304	25.5, 24.1	Partly cloudy St:40%
83		12	12:00	5958	26.1, 21.7	Partly cloudy St:50%
84		18	16:57	5316	25.2, 25.2	Partly cloudy, rainbow, partly fog St,ci:50% Uncorrected T/RH value
85	2017/09/03	00	22:56	4983	24.9, 26.3	Cloudy, mild wind St:100%
86		06	05:03	5947	26.7, 19.9	Cloudy, mild wind St:100%
87		12	11:04	5203	27.7, 17.3	Mild wind
88		18	17:12	5045	24.7, 27	Cloudy, mild wind, partly mist St:80%
89	2017/09/04	00	22:54	3211	14.3, 133	Cloudy, calm St,sc:50% PTU filtering stopped
90		06	04:52	5416	25.7, 23.4	Cloudy, mild wind St:100% PTU filtering stopped
91		12	11:13	5425	28, 16.6	Windy, mist
92		18	17:26	5428	27.8, 16.9	Windy, cloudy St:100% Uncorrected T/RH value
93	2017/09/05	00	22:56	5043	22.5, 38.3	Windy, cloudy St:90% PTU filtering stopped
94		06	04:54	6099	28.5, 15.3	Partly cloudy St,sc:70%
95		12	11:04	3818	16.8, 91.9	Mild wind Uncorrected T/RH value PTU filtering stopped
96		18	17:57	5639	27.4, 18.1	Fog St:100% Uncorrected T/RH value 2nd try 1st try failed due to collapse on the wall
97	2017/09/06	00	23:14	2888	13.5, 153	Partly cloudy, fog St:60%

						Uncorrected T/RH value PTU filtering stopped
98		06	05:07	4315	19.2, 63.7	Fog, calm Uncorrected T/RH value PTU filtering stopped
99		12	11:15	3352	15, 122	Mild wind, fog Uncorrected T/RH value PTU filtering stopped
100		18	17:09	5722	27.8, 17.1	Cloudy, windy Uncorrected T/RH value No PTU
101	2017/09/07	00	22:57	5810	28.8, 14.7	Cloudy, windy St:100% Uncorrected T/RH value
102		06	05:05	6491	23.1, 35.1	Rain, windy St:100% Uncorrected T/RH value
103		12	10:58	5231	24.5, 27.9	Rain, windy Uncorrected T/RH value
104		18	17:07	5322	28.4, 15.5	Cloudy, mild wind St:100% Uncorrected T/RH value
105	2017/09/08	00	23:11	5463	27.2, 18.7	Strong wind, fog, oceanic wave St:100% Uncorrected T/RH value
106		12	11:08	4451	20.9, 49	Windy PTU filtering stopped Use other temperature sensor due to uncorrected T/RH value at foremast
107		18	17:00	5816	27.7, 11.9	Snow, mild wind St:100% Use other temperature sensor due to uncorrected T/RH value at foremast
108	2017/09/09	00	23:05	6090	28.7, 16.4	Snow, mild wind, cloudy St:100% Use other temperature sensor due to uncorrected T/RH value at foremast
109		06	05:02	5582	25.9, 22.5	Snow, calm St:100% Use other temperature sensor due to uncorrected T/RH value at foremast
110		12	11:07	5614	27.5, 11.6	Snow, calm Use other temperature sensor due to uncorrected T/RH value at foremast
111		18	17:03	5495	27.2, 18.2	Snow, windy St:100% Use other temperature sensor due to uncorrected T/RH value at foremast
112	2017/09/10	00	23:02	4280	23.1, 34.3	Mild wind, cloudy St:100%

						Use other temperature sensor due to uncorrected T/RH value at foremast
113		06	05:03	6169	26.5, 20.4	Cloudy, mild wind St:100%
114		12	11:04	5416	27.5, 17.4	Windy, snow
115		18	17:11	3501	17.9, 75.	Cloudy, St:100% PTU filtering stopped
116	2017/09/11	00	23:00	4014	18.9, 64.7	Calm, cloudy St:100% PTU filtering stopped

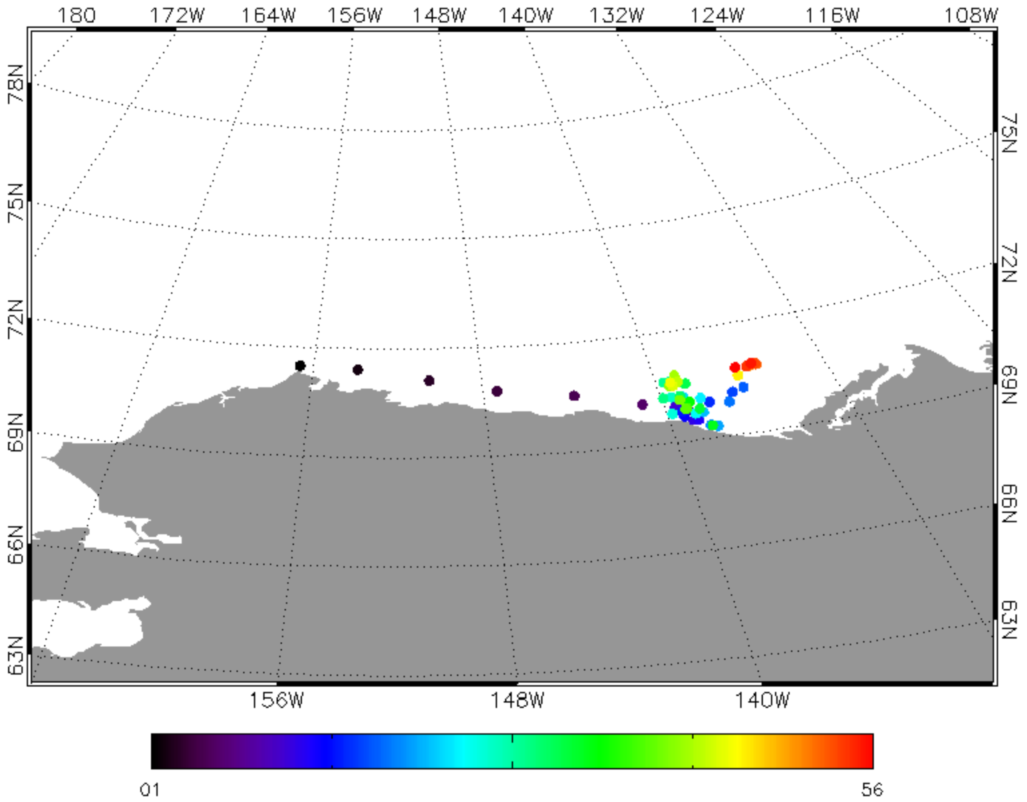

Figure 11.11. Locations of radiosonde balloon launches during ARA08C (28-Aug to 11-Sep).

Figure 11.12 compares two radiosonde sounding results on different days and displays the corresponding visible sky images taken by the all-sky camera. On 31-Aug, the sky was covered by thick stratus and rain and light snow fell. On 02-Sep, the sky was clear and downwelling shortwave radiation reached over 500 Wm^2 (see Figure 11.10). Comparison of the temperature profiles reveals that the troposphere was wet on 31-Aug.

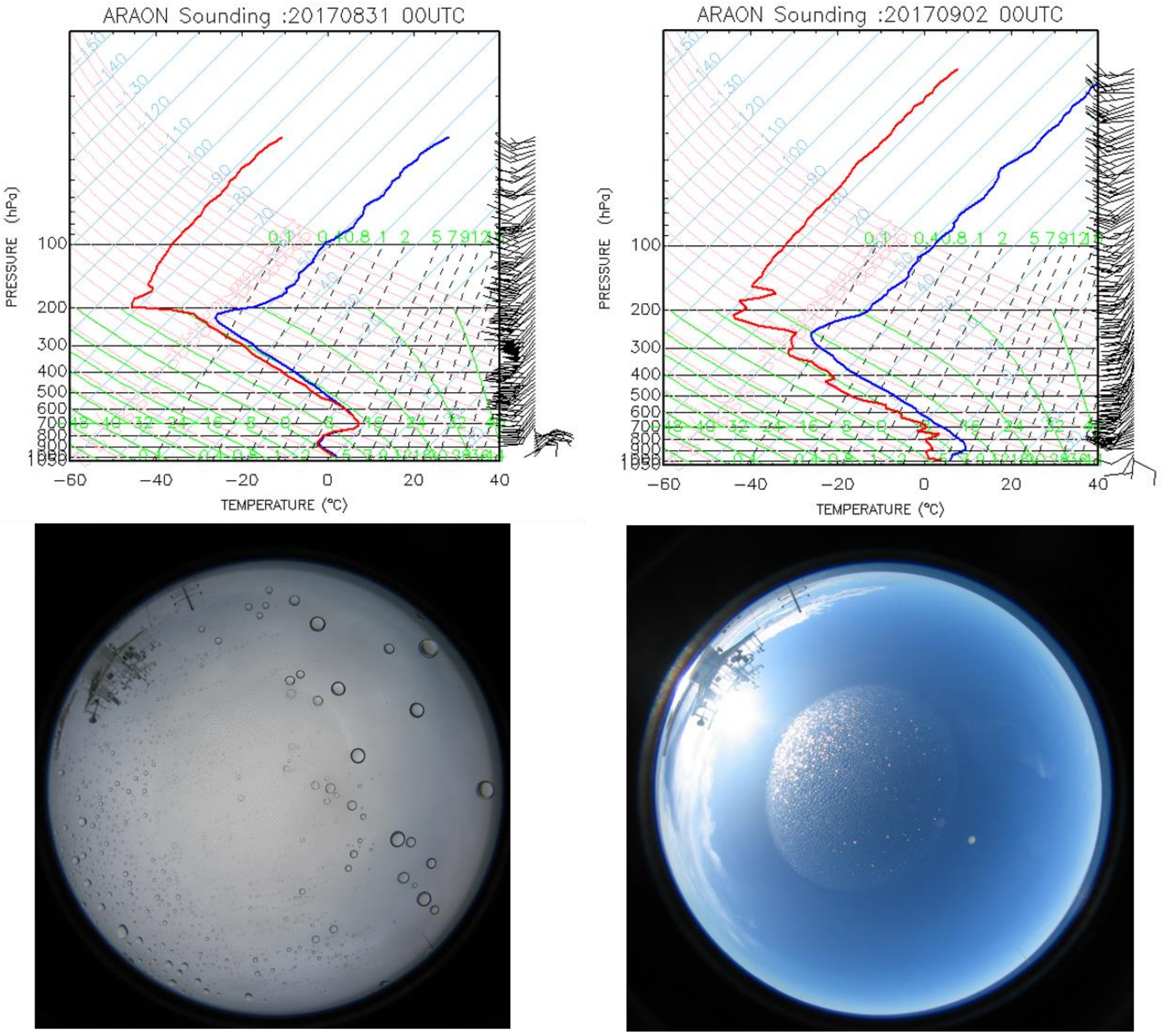

Figure 11.12. The skew T-log p diagrams for two radiosonde observations (top) and the corresponding visible sky images taken by the all-sky camera (bottom): (left) 00 UTC 31-Aug, (right) 00 UTC 02-Sep

References

Law, K.S. and Stohl, A. 2007. Arctic air pollution: Origins and impacts. *Science*, 315: 1537–1540, doi:10.1126/science.1137695.

Sellegri, K., O'Dowd, C.D., Yoon, Y.J., Jennings, S.G., and de Leeuw, G. 2006. Surfactants and sub-micron sea-spray generation. *Journal of Geophysical Research*, 111 (D22, D22215), doi:10.1029/2005JD006658.

Shindell, D. and Faluvegi, G. 2009. Climate response to regional radiative forcing during the twentieth century. *Nature Geoscience*, 2: 294–300, doi:10.1038/ngeo473.

Appendix 1. Research Permits

ENVIRONMENTAL IMPACT SCREENING COMMITTEE

Submission Number: **[10/12-02]**

June 15, 2017

Scott Dallimore,
Research Scientist,
Geological Survey of Canada
9860 West Saanich Rd
P.O. Box 6000
Sidney, BC V8L 4B2

Dear Mr. Dallimore:

RE: Canada-Korea-USA Beaufort Sea Geoscience Research Program: 2013 Activities

During a meeting held June 5-7, 2017 the Environmental Impact Screening Committee (EISC) reviewed your request for an Amendment to the Project Description for EISC file 10-12-02, which was screened by the EISC, and for which a decision letter was released on January 25, 2013. The EISC notes here that this second Amendment to a Project Description was submitted in compliance with EISC Guidelines, Section 3.5.

After reviewing this request, the EISC resolved that this submitted Amendment to the Project Description would not require an Environmental Impact Screening. Your request for the amendment, the amended Project Description itself, and a copy of this decision letter have been posted to the EISC registry. The EISC notes here that all previous mitigation requirements, and terms and conditions for this project, still apply. The EISC does make the following recommendation to the developer:

1. The developer is to contact the various regulatory agencies, well in advance of commencement of this project, to ensure that all regulatory bodies have the necessary time to deal with the amendments made to the original Project Description.

If you have any questions on the above, please do not hesitate to contact the EISC office.

Sincerely,

D Christie

Darrell Christie,
Interim EISC Coordinator

Cc. EISC Distribution List

EISC Distribution List

Scott Dallimore, Geological Survey of Canada
Fisheries Protection Program, Fisheries and Oceans Canada
Community-Based Monitoring Program, Joint Secretariat
Conrad Baetz, North Mackenzie District Manager, GNWT
Paulatuk Hunters and Trappers Committee
Joel Holder, Environment and Natural Resources, GNWT
Patrice Stuart, Inuvialuit Land Administration
Nelson Perry, Parks Canada Agency
Tuktoyaktuk Hunters and Trappers Committee
Aklavik Hunters and Trappers Committee
Marsha Branigan, Environment and Natural Resources, GNWT
Jennifer Smith, Wildlife Management Advisory Council (NS)
Patrick Clancy, Environment and Natural Resources, GNWT
Environment Canada
Vic Gillman, Chair, Fisheries Joint Management Committee
Sachs Harbour Hunters and Trappers Committee
Inuvik Hunters and Trappers Committee
Robert Jenkins, Aboriginal Affairs and Northern Development Canada
Jennifer Lam, Inuvialuit Game Council
Cameron Eckert, Special Projects Officer, Yukon Territorial Government
Olokhatomiut Hunters and Trappers Committee
Jodie Maring, WMAC(NWT)
Environmental Impact Review Board
Mike Harlow, Executive Director, Joint Secretariat
Christy Wickenheiser, National Energy Board
Larry Carpenter, Chair, Wildlife Management Advisory Committee (NWT)
Lindsay Staples, Chair, Wildlife Management Advisory Committee (NS)
Patrick Gruben, Chair, Inuvialuit Game Council
Aurora Research Institute
Richard Binder, Coordinator, Environmental Impact Review Board
Environmental Impact Screening Committee
GNWT Environmental Assessment and Monitoring
Benoit Godin, Environment Canada
Mark Dahl, Senior Oceans Disposal Officer, Environment Canada
Glen Mackay, Prince of Wales Northern Heritage Centre
Loretta Ransom, Senior Environmental Assessment Coordinator, EC
EANorthNWT
Transport Canada, General Office account
Peter Clarkson, Regional Director, Department of the Executive, GNWT
Sarah Robertson, Senior Project Manager, CANNOR
David Alexander, CANNOR
Colleen Parker, Western Arctic Specialist, WWF
Lorie Fyfe, Regional Superintendent, Inuvik Region, MACA
Johnny Lennie, Manager Oil and Gas Planning, PR Division, GNWT
Mardy Semmler, Executive Director, Inuvialuit Water Board
Ian Butters, Manager, Oil and Gas Rights, GNWT
Simon Tetreault, Infrastructure Canada
Lorraine Seale, Department of Lands, GNWT
Andrew Dumbrille, WWF Canada

Stephanie Muckenheim, IFA Implementation and Projects Coordinator, YTG
Catherine Braun-Rodriguez, Land and Environmental Affairs, GNWT
John Kaltenstein, Marine Program Manager, Friends of the Earth
Carrie Docken, Yukon Parks Branch, YTG
YESAB – Dawson Office
Bijaya Adhikare, Inuvialuit Water Board
Helga Harland, Senior Land Analyst, Gwich’in Tribal Council
Jeff Hunston, Manager of Heritage Resources, YTG
Veronique D'Amours-Gauthier, DFO
Elizabeth Patreau, Senior Fisheries Protection Biologist, DFO
AlecSandra Macdonald, Regulatory Specialist, GLWB
Judith Venaas, Tourism Development Officer, GNWT ITI
Naomi Smethurst, Archaeologist, PWNHC

…

Note No. IGR-176

The Department of Foreign Affairs, Trade and Development presents its compliments to the Embassy of the Republic of Korea and has the honour to refer to its diplomatic note no. 17-59 dated April 18 2017 requesting diplomatic clearance for the Korean Polar Research Institute vessel ARAON to undertake marine scientific research in areas under the jurisdiction of Canada from August 30 – September 12, 2017.

The Department is pleased to confirm that the Government of Canada grants its consent to the ARAON to enter waters under the jurisdiction of Canada for the purpose of maritime scientific research during the abovementioned periods.

The Government of Canada strongly encourages the researchers to follow through on their proposal to include local community participants as marine mammal observers. In addition, the Canadian Hydrographic Service would be particularly interested in acquiring all bathymetric data collected as part of this cruise. A document containing instructions regarding the format and submission of this data is attached.

The Department wishes to remind the Embassy of Canada Border Services Agency (CBSA) marine reporting requirements:

Foreign expeditions arriving in Canada by research vessel and entering Canadian territorial waters (within the 12 nautical mile zone) are required to report to the nearest Canada Border Services Agency (CBSA) Marine Reporting office prior to arrival.

Inuvik, NWT CBSA Marine Reporting Office: Phone 867-777-2761 / Fax 867-777-2155

Vessels are also required to transmit the following completed forms: **Form A6** General Declaration and **Form A6A** Freight/Cargo Manifest. The forms can be obtained electronically via the links below:

Form A6: *http://www.cbsa-asfc.gc.ca/publications/forms-formulaires/a6.pdf*
Form A6A: *http://www.cbsa-asfc.gc.ca/publications/forms-formulaires/a6a.pdf*

The Department further notes that this application indicates no port calls in Canada. In the event of an unscheduled port call, a Pre-Arrival Notice must be submitted to the National Targeting Centre at **CBSA-ASFC-PANS/AA@cbsa-asfc.gc.ca,** 96 hours prior to arrival.

The Department also notes that the ARAON will be entering the NORDREG zone and will be required to comply with the Northern Canada Vessel Traffic Zone Regulations. An information package regarding these regulations may be requested by email from IqaNordreg@innav.gc.ca. Information concerning survey operations should be forwarded to the NAVAREA coordinator at navarea17.18@innav.gc.ca and MCTS Iqaluit at IqaNordreg@innav.gc.ca.

The Department of Foreign Affairs, Trade and Development avails itself of this opportunity to renew to the Embassy of the Republic of Korea the assurances of its highest consideration.

OTTAWA, August 18, 2017

Licence No. 16158
File No. 12 404 861
August 16, 2017

2017
Northwest Territories Scientific Research Licence

Issued by:	**Aurora Research Institute – Aurora College** Inuvik, Northwest Territories
Issued to:	Dr. Young K Jin Korea Polar Research Institute 26 Songdomirae-ro, Yeonsu-gu P.O. Box 406-840 Incheon, None None Korea, South Phone: +82-32-760-5403 Fax: +82-32-760-5494 Email: ykjin@kopri.re.kr
Affiliation:	Korea Polar Research Institute
Funding:	Korea Polar Research Institute Natural Resources Canada Monterey Bay Aquarium Research Institute
Team Members:	Scott Dallimore; Seung Goo Kang; Jong Kuk Hong; Ned King; Mathieu Duchesne; Michelle Côté; Charles Paull
Title:	**Canada-Korea-USA Beaufort Sea Geoscience Research Program: 2017 Activities**
Objectives:	To acquire geoscience knowledge about the outer shelf of the Beaufort Sea with intent to address knowledge gaps related to thawing of subsea permafrost and gas hydrates.
Dates of data collection:	August 29, 2017 to September 30, 2017
Location:	Southern Beaufort Sea

Licence No.16158 expires on December 31, 2017
Issued in the Town of Inuvik on August 16, 2017

*** original signed ***

Pippa Seccombe-Hett
Vice President, Research
Aurora Research Institute

Aurora Research Institute - Aurora College
PO Box 1450 Inuvik NT X0E 0T0
Phone: 867-777-3298 **Fax:** 867-777-4264 **E-mail:** licence@nwtresearch.com

August 16, 2017

Notification of Research

I would like to inform you that Scientific Research Licence No. 16158 has been issued to:

Dr. Young K Jin
Korea Polar Research Institute
26 Songdomirae-ro, Yeonsu-gu
P.O. Box 406-840
Incheon, None
None Korea, South
Phone: +82-32-760-5403
Fax: +82-32-760-5494
Email: ykjin@kopri.re.kr

to conduct the following study:
Canada-Korea-USA Beaufort Sea Geoscience Research Program: 2017 Activities (Application No. 3794)

Please contact the researcher if you would like more information.

SUMMARY OF RESEARCH
This licence has been issued for the scientific research application No.3794.

The agencies involved are undertaking this research to acquire geoscience knowledge about the outer shelf of the Beaufort Sea with intent to address knowledge gaps related to thawing of subsea permafrost and gas hydrates. The research will be made publicly available to northern communities, regulators, the scientific community and industry through the release of scientific papers, maps and reports.

Building on a successful marine geoscience programs onboard the RV Araon in the Canadian Beaufort Sea in 2013 and 2014, the Korea Polar Research Institute, Natural Resources Canada and the Monterey Bay Aquarium Research Institute are continuing their scientific collaboration and are currently planning the 2017 Canada-Korea-USA Beaufort Sea Geoscience Research Program.

The Program will be conducted using the RV Araon. The Program is scheduled to be in Canadian waters for a maximum of 15 days between August 29 and September 13, 2017, in the southern Beaufort Sea within the boundaries of the Inuvialuit Settlement Region (ISR). The Program will operate in water depths ranging from 20 m to 2000 m.

The 2D seismic data will be collected using a Sercel GI Gun System with two airguns. This seismic source is about much smaller than volumes commonly used in industry or commercial surveys.

Oceanographic data collection will include water column characterization through conductivity, depth, temperature instruments and oceanographic moorings to measure and record data on ice thickness and ridging, storm waves, sea level, ocean current, temperature, salinity and plankton density. Bathymetric data collection will be completed through the use of a multibeam echo sounder. Sub-bottom profiling,
used for characterizing layers of sediment or rock under the seafloor, will be conducted through the use of a deep-tow profiling system that uses a pneumatic pressure pulse or the hull-mounted transducers on the RV Araon. Sediment coring provides physical seabed sample data, and will be completed through a small sampling pipe that penetrates the seabed and retrieves a tube (core) of intact sediment.

Surveys using an Autonomous Underwater Vehicle (AUV) specially designed for Arctic operations will be undertaken. The AUV is capable of detailed seabed mapping using multi-beam sonar with centimetre-scale resolution. If features of interest are identified in the AUV surveys, the Remotely Operated Vehicle (ROV) will be deployed to visually through livevideo to examine seafloor features.

All activities will be completed from the RV Araon. The RV Araon is a ‘state of the art’ modern ice class vessel, measuring 111 m long by 19 m wide. It was built in 2009 and is registered in South Korea. It can accommodate a crew of 25 with 60 passengers. The vessel is equipped with crew quarters, a galley, food storage areas, fresh water treatment equipment, a wastewater treatment system and solid waste storage.

A post-field report and copies of all scientific contributions (scientific papers, maps, and databases) will be provided to the communities in the ISR through their Hunters and Trappers Committees and through the Aurora Research Institute. The science crew may post blog entries to website which would be accessible by the public during and after Program operations.

The fieldwork for this study will be conducted from August 29, 2017 to September 30, 2017.

Sincerely,

____
Jonathon Michel,
Manager, Scientific Services

DISTRIBUTION
Aklavik Hunters and Trappers Committee
Department of Fisheries and Oceans Canada
Environmental Impact Screening Committee - c/o Joint Secretariat
Inuvialuit Community Development Division
Inuvialuit Land Administration
Inuvik Hunters and Trappers Committee
Nihtat Gwich'in Renewable Resource Council
Olokhaktomiut Hunters and Trappers Committee
Paulatuk Hunters and Trappers Committee
Sachs Harbour Hunters and Trappers Committee
Tuktoyaktuk Hunters and Trappers Committee

Yukon
Tourism and Culture
Box 2703, Whitehorse, Yukon Y1A 2C6

CULTURAL SERVICES BRANCH
HERITAGE RESOURCES UNIT

File No.: 6800-20-1097

August 1, 2017

TO: Dr. Young Keun Jin (Korea Polar Research Insitute (KOPRI), Inchon, Korea)
Environment, Habitat Management (V-5R)
Land Use Section, Lands Branch (K-320)
Regional Land Use Planning (K-320L)
Arctic Institute of North America (ASTIS)
Yukon Geological Survey (K-14)
Hershel Island Territorial Park (V-4)
Ivvavik National Park (PCA)
Wildlife Management Advisory Council (NS)
Aklavik Hunters & Trappers Committee
Environmental Impact Screening Committee (IFA)

RE: **Dr. Young Keun Jin (Korea Polar Research Institute (KOPRI), Inchon, Korea)**

Please be advised that the attached License with amended research dates has been issued under the Yukon Scientists and Explorers Act (1958).

Sincerely,

Jeff Hunston

Jeff Hunston, Manager
Heritage Resources Unit

Enclosure

Yukon
Tourism and Culture

License Number: 17-70S&E
Amended

YUKON-CANADA
SCIENTISTS AND EXPLORERS ACT
LICENSE

PURSUANT to the provisions of the Scientists and Explorers Act (1958) of the Yukon, permission is hereby granted to:
Dr. Young Keun Jin (Korea Polar Research Institute (KOPRI), Inchon, Korea.
to enter Yukon to conduct scientific research with respect to:

Canada-Korea-USA Beaufort Sea Geoscience Research Program; Geophysical Surveying, Geological Sampling and Oceanographic Measurements Relating to Subsea Permafrost Thawing and Gas Hydrates.

GENERAL CONDITIONS

1. A complete, final report of the research conducted under this license shall be submitted, in duplicate, within one year of completion or termination of the project.
   a) A field or progress report as well as plain English summary, including descriptions or catalogues of collections made (where applicable) shall be submitted in duplicate on, or before, the expiry date written below.
   b) The Licensee shall provide a copy of any report or article published on the research conducted under this license to Heritage Resources Unit.

2. All camps shall be established according to the provisions of the Territorial Land Use Regulations.

3. All steps shall be taken to avoid unnecessary disturbance of wildlife.
   a) No camp site shall be established within 2 km of an active raptor nest.
   b) When using aircraft, maintain a minimum of 1,000 feet over wildlife such as sheep, raptor nests and migrating caribou.
   c) Pay particular attention to bear habitat, and take all steps necessary to avoid contact with bears such as use of bear fence, bear-proof containers and maintain a clean camp.
   d) All camps should be temporary/non-permanent with no structures, and entirely removed at the conclusion of the field work.

4. The Licensee shall meet with, inform and receive permission from First Nation(s) of the field activities conducted under this license on their settlement land(s), and shall not proceed if permission is not gained from the First Nation(s). The Licensee shall provide a copy of any report or article published on the research conducted under this license to the First Nation(s).

5. The Licensee shall strictly observe all applicable First Nation Settlement Land, Territorial and Federal legislation and regulations.

OTHER CONDITIONS:
NIL

THIS License is valid for the period **August 28th** to **September 15th** , **2017.**

DATED at the City of Whitehorse, in the Yukon Territory, this **1st** day of **August**, A.D., **2017**.

Manager, Heritage Resources Unit
Cultural Services Branch
Tourism and Culture

Yukon
Executive Council Office

RE: Yukon Scientists and Explorer's Act

As a recipient of a research license under Yukon Scientist and Explorer's Act, I would like to take this opportunity to welcome you to the Yukon for the purposes of carrying out your research.

As Yukon Government's Senior Science Advisor, my role is to guide the Yukon government on scientific matters by providing strategic direction and policy advice on corporate science interests. My office's priorities include raising awareness of science initiatives and findings, coordinating and identifying opportunities to access, apply and develop scientific knowledge, and building scientific capacity and literacy within the Yukon government and Yukon. My Office also monitors developments in science and technology and works on building partnerships between nations, governments, research and academic institutions, agencies, and others on science.

I would appreciate the opportunity to meet with you to discuss your research, and would like to invite you to be in contact with my Office to set up a meeting when you are in the Territory. A meeting would assist me to be aware of the research that is underway in Yukon, and hopefully assist you either with making connections within Government that may aid you in your endeavours (should you not have made these connections already) and/or help you to identify opportunities to apply and/or communicate the knowledge developed through your work.

I can be reached at aynslie.ogden@gov.yk.ca or 867-667-5431.

Dr. Aynslie Ogden, RPF, RPBio, PAg
Senior Science Advisor
Executive Council Office

8677774062

Yukon
Environment
Environnement

PARK PERMIT

Land Use Permit

THIS PARK PERMIT Number: 17-LU-HI-10 (the "Permit") IS ISSUED UNDER THE AUTHORITY OF THE PARKS AND LAND CERTAINTY ACT ("PALCA")	LOCATION Herschel Island Territorial Park Occasional Use Marine Facility (the " Park")

FROM (Yukon)	**TO (Permittee)**
Parks Branch Environment Yukon Box 2703 (V-4) Whitehorse, Yukon Canada Y1A 2C6 E-mail: Yukon.parks@gov.yk.ca Phone: (867) 667-5648 or Toll free (in Yukon): 1 (800) 661-0408 ext. 5648 Inuvik Office (867) 777-4058 Box 1129 Inuvik N.T. X0E 0T0 E-mail: richard.gordon@gov.yk.ca	**Company Name** **Geological Survey of Canada** **17-83 S&E** **REPRESENTED BY:** Name: Scott Dallimore 250-363-6423 18/08/17 Permittee Signature Date

EFFECTIVE DATE: Aug 27, 2017

EXPIRY DATE: Sept 15, 2017

This permit shall be subject to the restrictions and conditions contained herein and in the *Parks and Land Certainty Act* ("PALCA"), as well as the restrictions and conditions proposed in the Permittee's application for this Permit unless otherwise indicated in this Permit.

Dated this Aug. 23/17 Mierau

Carrie Mierau
Operation Manager North

Appendix 2. Participants

No	Organization	Name	Contact	Works in the expedition
1	KOPRI	Young Keun JIN	ykjin@kopri.re.kr	Chief Scientist
2	KOPRI	Seung Goo KANG	ksg9322@kopri.re.kr	Multichannel Seismic
3	KOPRI	U Geun JANG	ugeun.jang@kopri.re.kr	Multichannel Seismic
4	KOPRI	Min Kyu LEE	kyu0807@kopri.re.kr	Multichannel Seismic
5	KOPRI	Hyoung Jun KIM	Jun7100@kopri.re.kr	Multibeam & SBP
6	KOPRI	Sookwan KIM	skwan@kopri.re.kr	Multichannel Seismic
7	KOPRI	Yeonjin CHOI	yjchoi@kopri.re.kr	Multichannel Seismic
8	KOPRI	Jinhoon JUNG	jhjung87@kopri.re.kr	Multibeam & SBP
9	KOPRI	Yung Mi LEE	ymlee@kopri.re.kr	Microbiology
10	KOPRI	Mi Seon KIM	mskim@kopri.re.kr	Chemical Oceanography
11	KOPRI	Tae-Yoon PARK	typark@kopri.re.kr	Paleontology
12	KOPRI	Jihoon KIM	jhkihm@kopri.re.kr	Paleontology
13	KOPRI	Young-Suk CHOI	yschoi@kopri.re.kr	CTD
14	KOPRI	Changkyu LIM	cklim@kopri.re.kr	Ocean Modeling
15	KOPRI	Jung-Hyun Kim	jhkim123@kopri.re.kr	Organic Biogeochemistry
16	KOPRI	Kwangkyu Park	kp@kopri.re.kr	Paleoceanography
17	KOPRI	Jiyeon Park	jypark@kopri.re.kr	Environmental Engineering Science
18	KOPRI	Yeontae Gim	ytkim@kopri.re.kr	Environmental Engineering Science
19	KOPRI	Seung Jun Lee	sjlee707707@gmail.com	Sedimentology
20	KOPRI	Dong Seob Shin	dsshin@kopri.re.kr	Science Technical Support
21	KOPRI	Suhwan Kim	idsuhwan@kopri.re.kr	Science Technical Support
22	KOPRI	Hyung Gyu Choi	langyu7@kopri.re.kr	Science Technical Support
23	Seoul National University	Young-Gyun Kim	younggyun.kim@gmail.com	Marine Geophysics
24	Hanyang University	Dong Hun Lee	thomaslee0118@gmail.com	Organic Geochemistry
25	Hanyang University	Sujin Kang	su1423@hanyang.ac.kr	Organic Geochemistry

26	Gyeongsang National University	Hyojin Koo	ghj6011@nate.com	Clay Mineralogy
27	Sejong University	Yun-Kyung Lee	tu0683@naver.com	Environmental Engineering Science
28	FUJIFILM Electronic Imaging Korea	Kwang Mo Lim	bcut@daum.net	Photographer
29	Arts Council Korea	Joo Young Oh	ojy1024@naver.com	Writer
30	Freelancer	Somang Chung	somang49@gmail.com	Interpreter
31	UAF	Liran Peng	lpeng2@alaska.edu	Atmospheric Science
32	Hohai Univ.	Yizhi Li	arcli@hhu.edu.cn	Physical Oceanography
33	GSC	Edward King	edward.king@canada.ca	Marine Geology
34	GSC	Mathieu Duchesne	mathieuj.duchesne@canada.ca	Geophysics
35	GSC	Michelle Côté	michelle.cote@canada.ca	Marine Geology
36	GSC	Rhonda Reidy	rreidy@gmail.com	Marine Biologist
37	GSC/Geoforce	Dale Ruben	Daleirsruben85@hotmail.com	Marine Mammal Observer
38	GSC/Geoforce	John Ruben	nelsonruben66@hotmail.com	Marine Mammal Observer
39	MBARI	Charles Paull	paull@mbari.org	Marine Geology
40	MBARI	Roberto Gwiazda	rgwiazda@mbari.org	Geochemistry
41	MBARI	Lonny Lundsten	lonny@mbari.org	Biology
42	MBARI	Dale Graves	grda@mbari.org	ROV Chief
43	MBARI	Frank Flores	frank@mbari.org	ROV Pilot
44	MBARI	David French	dfrench@mbari.org	ROV Pilot
45	MBARI	Douglas Conlin	conlin@mbari.org	AUV Operator
46	MBARI	Erik Trauschke	etrauschke@mbari.org	AUV Operator
47	MBARI	David Caress	caress@mbari.org	Seafloor Mapping
48	UiT/CAGE	Jürgen Mienert	jurgen.mienert@uit.no	Marine Geology

Appendix 3. List of Stations and Line Survey

Station / Waypoint	Work order	*Gear	Time (UTC)				Longitude	Latitude	Depth (m)	Gyro	Remark
			start		end						
			Date	Time	Date	Time					
MB/SBP		MB	2017-08-29	7:08			140°22.7170'W	70°03.1936'N	55	100	MB area1
					2017-08-30	1:03	138°59.5330'W	69°51.7027'N			
St01	1	CTD	2017-08-30	1:03	2017-08-30	1:35	138°59.5330'W	69°51.7027'N	150	91.3	
MB/SBP		MB	2017-08-30	1:40							MB area1
					2017-08-30	6:08	139°38.6393'W	69°59.9661'N			MB area2
Herschel Island											
MCS	BF01	MCS	2017-08-31	7:50			139°52.2262'W	69°43.9492'N	23.8		
					2017-08-31	20:08	137°12.8722'W	70°03.9800'N	40.21		
	BF02	MCS	2017-08-31	20:08			137°12.9813'W	70°03.9716'N	38.18		
					2017-09-01	03:05	135°55.3687'W	70°19.5895'N	55.22		
	BF03	MCS	2017-09-01	3:25			135°58.2346'W	70°19.3148'N			
					2017-09-01	20:15	138°23.7659'W	69°23.6800'N	28.02		
	BF04	MCS	2017-09-01	22:48			137'58.9085'W	69'18.2646'N	40		
					2017-09-02	00:41	138'00.5723'W	69'26.7463'N	52		
	BF05	MCS	2017-09-02	0:42			138'00.6151'W	69'26.7854'N	51.96		

XCTD01		XCTD	2017-09-02	4:07			138'19.3009'W	69'41.5032'N	148		
XCTD02		XCTD	2017-09-02	7:28			138'36.0697'W	69'54.2250'N	222		
XCTD03		XCTD	2017-09-02	10:07			138'50.1197'W	70'04.5547'N	316		
XCTD04		XCTD	2017-09-02	11:48			138'59.3782'W	70'11.5034'N	388		
					2017-09-02	12:20	139'02.4036'W	70'14.0947'N			
	BF06	MCS	2017-09-02	12:41			139'00.4899'W	70'14.0573'N	420.14		
XCTD05		XCTD	2017-09-02	14:05			138'44.9444'W	70'11.8406'N	383		
XCTD06		XCTD	2017-09-02	16:01			138'21.0126'W	70'08.4472'N	255		
					2017-09-02	16:30	138'14.6725'W	70'07.5377'N			
	BF07	MCS	2017-09-02	16:53			138'16.6170'W	70'06.1593'N	239		
					2017-09-02	22:54	138'44.3987'W	69'42.3255'N	135.3		
	BF08	MCS	2017-09-02	22:54			138'44.5509'W	69'42.2804'N	128		
					2017-09-03	03:53	139'45.6140'W	69'42.9769'N			
	BF09	MCS	2017-09-03	3:54			139'45.6079'W	69'42.9953'N			
XCTD07		XCTD	2017-09-03	9:46			139'33.7904'W	70'09.1087'N	201.78		
XCTD08		XCTD	2017-09-03	12:33			139'28.2543'W	70.20.9371'N	607		
XCTD09		XCTD	2017-09-03	14:50			139'23.8467'W	70'30.2425'N	785		
XCTD10		XCTD	2017-09-03	16:13			139'20.8336'W	70'36.4878'N	1250		
XCTD11		XCTD	2017-09-03	18:24			139'15.9515'W	70'46.4286'N	1741		
					2017-09-03	19:03	139'14.8411'W	70'49.5177'N	1812		
	BF10	MCS	2017-09-03	20:13			139'29.2176'W	70'49.6779'N	1866		
XCTD12		XCTD	2017-09-03	20:47			139'31.1775'W	70'47.1764'N	1805		
XCTD13		XCTD	2017-09-03	23:15			139'34.8686'W	70'41.5127'N	1705		
XCTD14		XCTD	2017-09-03	23:23			139'38.6842'W	70'35.9066'N	1233		
XCTD15		XCTD	2017-09-04	0:28			139'41.4555'W	70'31.5702'N	782		

XCTD16		XCTD	2017-09-04	1:34			139'44.9153'W	70'26.3360'N	671		
XCTD17		XCTD	2017-09-04	2:51			139'47.2517'W	70'23.3024'N	480		
XCTD18		XCTD	2017-09-04	4:05			139'51.5278'W	70'15.8214'N	375		
XCTD19		XCTD	2017-09-04	4:58			139'54.16676	70.12.0187'N	188		
					2017-09-04	06:15	139'57.5006'W	70'06.6840'N	46.87		
	BF11	MCS	2017-09-04	6:47			139'59.5814'W	70'07.4476'N	46.37		
XCTD20		XCTD	2017-09-04	9:29			139'25.1632'W	70'11.6801'N	280		
					2017-09-04	11:13	139'03.9393'W	70'14.2266'N	420		
	BF12	MCS	2017-09-04	11:35			139'02.0927'W	70'15.8733'N	450		
XCTD21		XCTD	2017-09-04	11:47			139'01.4251'W	70'16.7027'N	470		
XCTD22		XCTD	2017-09-04	12:53			138'58.1071'W	70'21.5499'N	607		
XCTD23		XCTD	2017-09-04	13:58			138'55.0283'W	70'26.1055'N	720		
					2017-09-04	15:58	138'49.3550'W	70'34.3400'N	1212		
Herschel Island			2017-09-05	0:48	2017-09-05	2:03			22		
ST02	1	CTD	2017-09-05	4:27	2017-09-05	4:40	138°12.357359'W	69°20.32482'N	38		
	2	BC	2017-09-05	4:47	2017-09-05	4:55	138°12.3570'W	69°20.3260'N	38		
	3	BC	2017-09-05	5:22	2017-09-05	5:20	138°12.3570'W	69°20.3260'N	38		
	4	GC	2017-09-05	6:00	2017-09-05	6:30	138°12.3570'W	69°20.3258'N	38		GC 6 m
ST03	1	CTD	2017-09-05	8:18	2017-09-05	8:35	138°19.7137'W	69°41.9016'N	140		
	2	BC	2017-09-05	8:40	2017-09-05	8:54	138°19.7137'W	69°41.9016'N	140		
ST04	1	CTD	2017-09-05	11:54	2017-09-05	12:31	139°1.3098'W	70°13.0879'N	403		
	2	BC	2017-09-05	12:35	2017-09-05	12:55	139°1.3110'W	70°13.0880'N	407		
ROV#1	1	ROV	2017-09-05	16:49	2017-09-05	18:26	139°03.3898'W	69°52.7296'N	104		ROV deploy
ROV#2	1	ROV	2017-09-05	19:42	2017-09-05	22:25	139°03.3900'W	69°52.7288'N	103		ROV deploy

AUV#1		AUV_Launch	2017-09-05	23:05			139°03.3900'W	69°52.7288'N			deploy
ROV#3		ROV	2017-09-06	1:39	2017-09-06	2:46	139°07.5877'W	69°55.4088'N	118		ROV deploy
ST05	1	CTD	2017-09-06	3:41	2017-09-06	4:02	139°0.9579'W	69°53.1484'N	163		site_GC 1_Mbari
	2	GC	2017-09-06	4:15	2017-09-06	5:10	139°0.9269'W	69°53.1559'N	163		GC 6 m
	3	HF	2017-09-06	4:15	2017-09-06	5:10	139°0.9269'W	69°53.1559'N			
ST06	1	GC	2017-09-06	5:47	2017-09-06	5:52	139°3.3872'W	69°52.7145'N	93		site_GC 3'_Mbari, pingo top, GC 6 m
	2	HF	2017-09-06	5:47	2017-09-06	5:52	139°3.3872'W	69°52.7145'N			
ST07	1	CTD	2017-09-06	7:11	2017-09-06	7:35	139°3.5708'W	69°52.7034'N	117		site_GC 2_Mbari
	2	GC	2017-09-06	7:41	2017-09-06	8:20	139°3.5715'W	69°52.7033'N			GC 6 m
	3	HF	2017-09-06	7:41	2017-09-06	8:20	139°3.5715'W	69°52.7033'N			
	4	GC	2017-09-06	9:14	2017-09-06	9:47	139°3.5714'W	69°52.7034'N			GC 6 m
	5	HF	2017-09-06	9:14	2017-09-06	9:47	139°3.5714'W	69°52.7034'N			
ST08	1	GC	2017-09-06	10:22	2017-09-06	10:37	139°3.8386'W	69°52.6589'N	101		site_GC 4_Mbari, GC 6 m
ST09	1	GC	2017-09-06	11:00	2017-09-06	11:25	139°4.4644'W	69°52.5712'N	78		site_GC 5_Mbari, GC 6 m
ST10	1	GC	2017-09-06	12:20	2017-09-06	12:55	139°0.8727'W	69°53.0943'N	163		site_GC 1_Mbari, same location (ST05), GC 6 m
	2	HF	2017-09-06	12:20	2017-09-06	12:55	139°0.8727'W	69°53.0943'N			
AUV#1		AUV_recovery			2017-09-06	15:22	139°03.7343'W	69°53.6310'N			retreat

ROV#4	1	ROV	2017-09-06	9:37			139'24.3144'W	70'32.7302'N	957		ROV deploy
	2	ROV			2017-09-06	23:52	139'24.0023'W	70'32.6212'N	882		ROV recovery
ST11	1	CTD	2017-09-07	3:15	2017-09-07	4:38	139°0.6618'W	70°48.4612'N	1750		
	2	GC	2017-09-07	4:50	2017-09-07	6:20	139°0.6637'W	70°48.4618'N			GC 6 m
	3	HF	2017-09-07	4:50	2017-09-07	6:20	139°0.6637'W	70°48.4618'N			
	4	GC	2017-09-07	7:10	2017-09-07	8:50	139°0.6621'W	70°48.4638'N			GC 6 m
	5	HF	2017-09-07	7:10	2017-09-07	8:50	139°0.6621'W	70°48.4638'N			
ST12	1	GC	2017-09-07	10:57	2017-09-07	12:03	138°58.5026'W	70°37.4146'N	1457		GC 6 m
ST13	1	GC	2017-09-07	13:10	2017-09-07	14:10	138°52.4152'W	70°33.1125'N	1257		GC 6 m
ST14	1	CTD	2017-09-07	14:50	2017-09-07	16:03	138°51.9252'W	70°33.1265'N	1217		
MB/SBP	1	MB/SBP	2017-09-07	16:07			138°51.9249'W	70°33.1269'N	1219		
	2	MB/SBP			2017-09-08	12:57	135°19.0244'W	70°43.6727'N	106		
MB/SBP	1	MB/SBP	2017-09-08	14:25			135°25.4223'W	70°45.1945'N	110		
	2	MB/SBP			2017-09-08	14:48	135°34.0886'W	70°47.4640'N	420		
ROV#5	1	ROV	2017-09-08	15:48			135°34.0094'W	70°47.4799'N	421		ROV deploy
	2	ROV			2017-09-08	7:46	135°33.2458'W	70°47.5111'N	420		ROV recovery
AUV#2	1	AUV_Launch	2017-09-08	21:14			135°18.8367'W	70°43.6630'N	103		
ROV#6	1	ROV	2017-09-08	22:57			135°33.5944'W	70°47.3834'N			ROV deploy
	2	ROV			2017-09-09	2:47	135°33.7879'W	70°47.4357'N			ROV recovery
ST15	1	CTD	2017-09-09	3:22	2017-09-09	4:04	135°33.7911'W	70°47.4766'N	420		
	2	BC	2017-09-09	4:11	2017-09-05	4:36	135°33.7898'W	70°47.4767'N	420		Hydrate sample
ST16	1	BC	2017-09-09	4:55	2017-09-09	5:25	135°33.4833'W	70°47.5139'N	420		

ST20	1	BC	2017-09-09	5:40	2017-09-09	6:05	135°33.8710'W	70°47.4104'N	420		Overflowed
ST19	1	BC	2017-09-09	6:15	2017-09-09	6:45	135°33.8009'W	70°47.3778'N	420		Overflowed
ST18	1	BC	2017-09-09	6:52	2017-09-09		135°33.5006'W	70°47.3970'N	420		failed
	2	BC	2017-09-09		2017-09-09		135°33.5006'W	70°47.3970'N			failed
	3	BC	2017-09-09		2017-09-09	8:10	135°33.5006'W	70°47.3970'N			
ST17	1	BC	2017-09-09	08:20	2017-09-09	8:40	135°33.0472'W	70°47.5316'N	420		
ST21	1	CTD	2017-09-09	8:58	2017-09-09	9:33	135°31.2592'W	70°47.0933'N	420		
	2	BC	2017-09-09	9:40	2017-09-09	10:05	135°31.2587'W	70°47.0929'N			
	3	GC	2017-09-09	10:16	2017-09-09	11:10	135°31.2587'W	70°47.0929'N			GC 6 m
	4	HF	2017-09-09	10:16	2017-09-09	11:10	135°31.2587'W	70°47.0929'N			
	5	GC	2017-09-09	11:35	2017-09-09	12:30	135°31.2571'W	70°47.0935'N			GC 6 m, net
	6	HF	2017-09-09	11:35	2017-09-09	12:30	135°31.2571'W	70°47.0935'N			
AUV#2	1	AUV_recovery			2017-09-09	16:03	135°33.9053'W	70°47.5701'N	463		retreat
ROV#7	1	ROV	2017-09-09	17:35			135'08.0665'W	70'49.7302'N	162		ROV deploy
	2				2017-09-09	21:42	135'07.5627'W	70'49.9464'N	157		ROV recovery
AUV#3	1	AUV_Launch	2017-09-09	22:21			135'05.1596'W	70'48.1836'N	96		
ROV#8	1	ROV	2017-09-09	23:15			135'08.3613'W	70'50.1606'W			ROV deploy
	2				2017-09-10	02:47	135'08.0678'W	70'50.3426'N			ROV recovery
ST22	1	CTD	2017-09-10	3:23	2017-09-10	3:45	135°7.9832'W	70°49.7375'N	166		
	2	GC	2017-09-10	3:55	2017-09-10	4:09	135°7.9829'W	70°49.7378'N			GC 6 m
ST23	1	GC	2017-09-10	4:44	2017-09-10	5:05	135°7.5003'W	70°49.8573'N	167		GC 6 m
ST24	1	GC	2017-09-10	5:30	2017-09-10	6:55	135°5.6574'W	70°49.6191'N	129		GC 6 m

ST25	1	GC	2017-09-10	6:15	2017-09-10	6:35	135°7.3973'W	70°49.3724'N	125		GC 3 m
ST26	1	GC	2017-09-10	6:49	2017-09-10	7:11	135°8.4567'W	70°50.1452'N	164		GC 3 m, ice found
ST27	1	GC	2017-09-10	7:28	2017-09-10	7:47	135°8.0680'W	70°50.2262'N	166		GC 3 m
ST28	1	GC	2017-09-10	8:05	2017-09-10	8:25	135°7.9832'W	70°49.7375'N	167		GC 3 m
ST29	1	GC	2017-09-10	9:26	2017-09-10	10:20	135°33.9132'W	70°47.3963'N	420		GC 6 m, Gas hydrate
	2	HF	2017-09-10	9:26	2017-09-10	10:20	135°33.9132'W	70°47.3963'N	420		
ST30	1	GC	2017-09-10	11:00	2017-09-10	11:55	135°33.9783'W	70°47.4577'N	420		GC 6 m, same location (ST15)
	2	HF	2017-09-10	11:00	2017-09-10	11:55	135°33.9783'W	70°47.4577'N			
AUV#3	1	AUV_recovery			2017-09-10		135°05.1596'W	70°48.1836'N			
ROV#9	1	ROV	2017-09-10	18:21			136°06.0942'W	70°48.3615'N	754		ROV deploy
	2	ROV			2017-09-11	0:11	136°06.1375'W	70°42.2957'N	748		ROV recovery
ST31	1	CTD	2017-09-11	0:22	2017-09-11	1:17	136°06.1371'W	70°48.2918'N	751		
AUV#4	1	AUV_Launch	2017-09-11	4:04			135°05.1950'W	70°48.1394'N	96		
ST32	1	CTD	2017-09-11	7:45	2017-09-11	8:15	135°33.1230'W	70°47.5076'N	420		same location (ST17)
	2	HF	2017-09-11	8:25	2017-09-11	10:05	135°33.0193'W	70°47.5191'N	420		
	3	HF	2017-09-11	10:05			135°33.0193'W	70°47.5191'N	420		
ST33	1	HF	2017-09-11	10:55	2017-09-11	12:25	135°33.7967'W	70°47.4782'N	420		same location (ST15)
ST34	1	HF	2017-09-11	12:25	2017-09-11	13:45	135°33.7297'W	70°47.4232'N	420		same location (ST29)
ST35	1	HF	2017-09-11	13:50	2017-09-11	14:53	135°33.7988'W	70°47.3782'N	420		same location (ST19)
AUV#4	1	AUV_recovery			2017-09-11	1&;23	135'04.5161'W	70'50.1635'N	138		

ST36	1	HF	2017-09-11	19:34	2017-09-11	20:13	136'06.1068'W	70'48.3600'N	752		
	2	HF	2017-09-11	20:28	2017-09-11	21:22	136'05.7632'W	70'48.0508'N	744		
ST37	1	GC	2017-09-12	4:35	2017-09-12	5:35	138°53.2537'W	70°32.7672'N	1209		
ST38	1	GC	2017-09-12	6:10	2017-09-12	7:05	138°52.0145'W	70°32.1541'N	1160		
ST39	1	GC	2017-09-12	7:35	2017-09-12	8:25	138°52.1122'W	70°31.7217'N	1080		
ST40	1	GC	2017-09-12	9:02	2017-09-12	10:10	138°53.1586'W	70°28.6018'N	760		net
	2	HF	2017-09-12	9:02	2017-09-12	10:10	138°53.1586'W	70°28.6018'N	760		
	3	GC	2017-09-12	10:35	2017-09-12	11:40	138°53.1668'W	70°28.6063'N	760		
	4	HF	2017-09-12	10:35	2017-09-12	11:40	138°53.1668'W	70°28.6063'N	760		
ST41	1	GC	2017-09-12	13:00	2017-09-12	13:56	138°35.9004'W	70°38.4911'N	1360		
ROV#10	1	ROV	2017-09-12	15:00			136°51.2109'W	70°31.4968'N	1019		ROV deploy
	2	ROV			2017-09-12	20:13	138'50.5155'W	70'31.4718'N	875		ROV recovery
ST42	1	GC	2017-09-13	1:10	2017-09-13	1:17	139°39.0223'W	69°57.5514"N	53		
ST43	1	GC	2017-09-13	1:41	2017-09-13	1:55	139°38.2308'W	69°59.2789'N	59		

*MB : Multibeam Echosounder / SBP : Sub-bottom profiler / MCS : Multichannel seismic survey / BC : Box core / GC : Gravity core / HF : Heat flow measurement / CTD : Conductivity-temperature-density / ROV : Remotely operated vehicle / AUV : Autonomous underwater vehicle

Appendix 4. Marine Mammal Observations Report

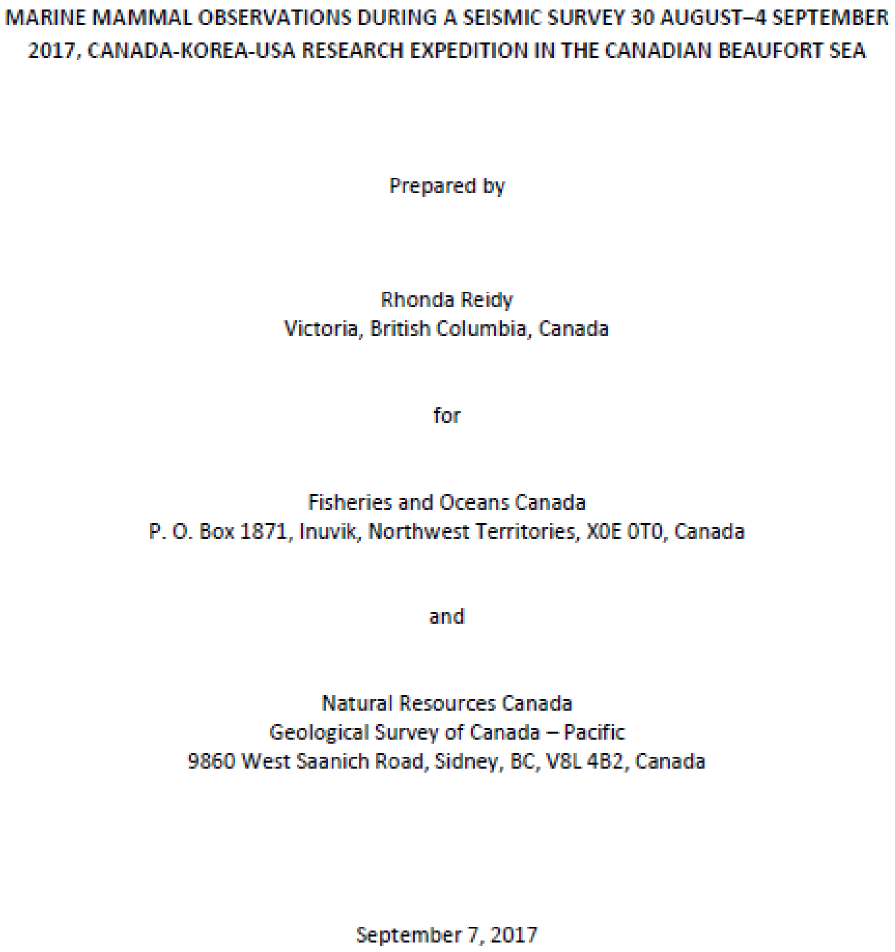

MARINE MAMMAL OBSERVATIONS DURING A SEISMIC SURVEY 30 AUGUST–4 SEPTEMBER 2017, CANADA-KOREA-USA RESEARCH EXPEDITION IN THE CANADIAN BEAUFORT SEA

Prepared by

Rhonda Reidy
Victoria, British Columbia, Canada

for

Fisheries and Oceans Canada
P. O. Box 1871, Inuvik, Northwest Territories, X0E 0T0, Canada

and

Natural Resources Canada
Geological Survey of Canada – Pacific
9860 West Saanich Road, Sidney, BC, V8L 4B2, Canada

September 7, 2017

INTRODUCTION

A geophysical survey was carried out offshore in the Canadian Beaufort Sea to acquire new active seismic data for Arctic geohazard studies. This research is part of a major international scientific collaboration between the Geological Survey of Canada, the Korea Polar Research Institute, the Monterey Bay Aquarium Research Institute, and the Department of Fisheries and Oceans Canada. This multichannel seismic survey was part of the third multidisciplinary research program in the Canadian Beaufort aboard the polar research icebreaker RV Araon and builds upon research programs conducted in 2013 and 2014 under the same collaboration.

The 2017 geosciences activities aboard the Araon adhered to those outlined in the 2013 Project Description and subsequent amendments, approved by the Environmental Impact Screening Committee. In addition to the multichannel seismic research survey, other science activities onboard included seafloor multi-beam imaging and sub-bottom profiling with hull-mounted sounders, high-resolution Autonomous Underwater Vehicle (AUV) mapping surveys, Remotely Operated Vehicle (ROV) investigations of the seafloor, and sediment coring. Additional research included bathymetric, oceanographic, and atmospheric data collection. The research area was on the Beaufort Continental Shelf and slope, northeast of Herschel Island and northwest of the Tuktoyaktuk Peninsula (Figure 1).

Five days of the 15-day research program were dedicated to conducting a seismic survey along very specific lines of interest. Many of the lines targeted features and zones that were known to exist but required better data to interpret their origins, while some lines filled in gaps across virtually unexplored territory. The resulting seismic images will be used to assess the regional geologic framework of the Beaufort Shelf and slope, to identify the history of sedimentation in the Beaufort Basin, to identify any potential gas hydrate and permafrost present, to understand the glacial history of the Beaufort Sea, as well as to determine geohazard issues related to submarine instability and landslides.

The vessel operated south of ice covered waters, and was restricted from conducting seismic activities in DFO designated bowhead whale feeding aggregation areas during periods of low visibility.

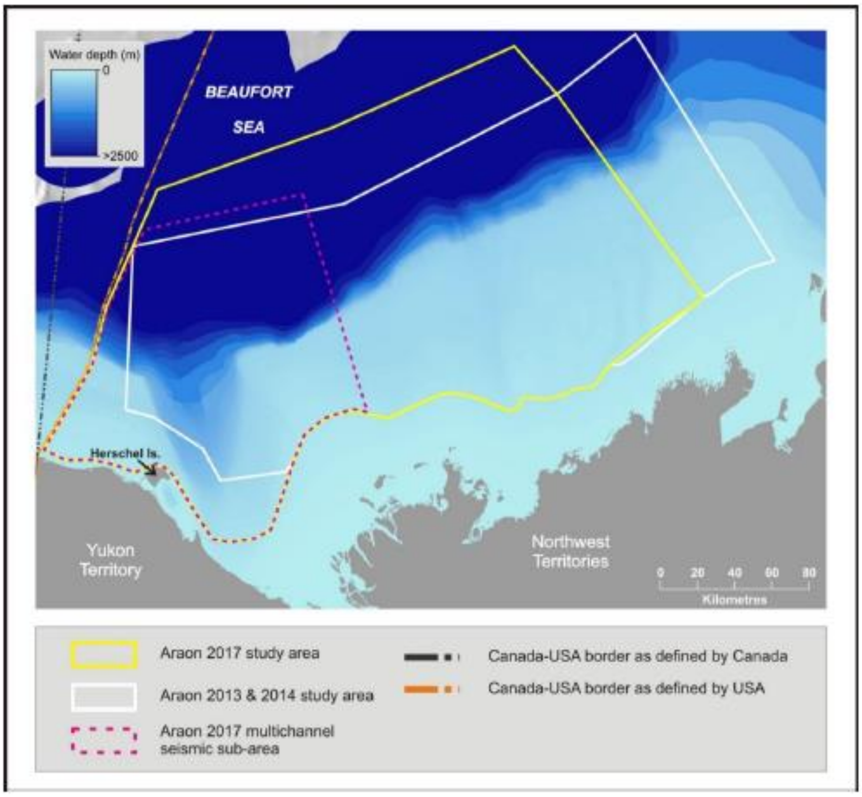

Figure 1. Map showing the location of the Canada-Korea-USA Beaufort Sea geoscience survey area offshore of Herschel Island and the Tuktoyaktuk Peninsula, 30 August - 13 September 2017. The red dotted line shows the location of the 5-day seismic research program.

METHODS

Active Airgun Operation

The active seismic system involved towing an array of 2 GI- airguns with a total capacity of 420 cubic inches. The airguns were towed behind the vessel at roughly 4 knots speed (Figure 2). The two airguns, each with a volume of 210 cubic inches were programmed to simultaneously release compressed air that traveled through the water column for penetration of the seabed. The firing rate was every 25 meters or approximately every 10 seconds. A Sercel multi-channel streamer of hydrophones 1500-m in length was towed behind the vessel at 6 metres depth as a conventional method for recording the seismic signals.

Figure 2. Photograph showing the airgun array prior to deployment with the guns visible (left). The airguns were suspended 6 meters below the surface using a large float (right).

Permitting

The Northwest Territories Environmental Impact Screening Committee approved a Request to Amend the 2012 Project Description to conduct this research program (DL 10-12-02 Amended on June 15, 2017). Changes of note from the original Project Description pertinent to the sesimic program included adjusting the study area boundaries and reducing the airgun volume used for data acquisition. Additional permits obtained to conduct this work include the following.

Marine Scientific Research Permit from Department of Foreign Affairs, Trade and Development Note No IGR-176, issued August 18, 2017
Northwest Territories Scientific Research Licence Number 16158, issued August 16, 2017
Yukon-Canada Scientists and Explorers Act License Number 17-70S&E, issued August 1, 2017
Yukon Parks Land Use Permit 17-LU-HI-10, issued August 23, 2017

Mitigation of Adverse Effects on Marine Mammals

Standard practices for seismic surveying in Canada are currently being developed by the Department of Fisheries and Oceans Canada (DFO). However, interim measures have been established to protect marine mammals from the potentially adverse effects (physical and behavioural) of seismic equipment (e.g. airguns) used in the determination of seabed characteristics. The mitigation measures presently used by DFO include the provision of marine mammal observers on board vessels undertaking seismic work, with the conditions pertaining to this survey outlined in a letter of agreement between the Environmental Impact Screening Committee and DFO, Northwest Territories, Inuvik.

One independent DFO-approved marine mammal observer (MMO) and two Inuvialuit MMOs followed the seismic program during the 5-day survey from 30 August – 4 September 2017. The observers were dedicated to maintaining constant observations during daytime operations for marine mammals in the ship's vicinity prior to and during seismic airgun operation.

Mitigation Measures

As outlined in the agreement, a requisite "safety zone" of 1000 meters radius around the vessel was established to conform to a 180 dB re 1 µPa sound pressure contour. This was greater than the minimum safety zone radius (500 meters) in the *Statement of Canadian Practice with Respect to the Mitigation of Seismic Sound in the Marine Environment*. It was predetermined by DFO that gun operation would not be shut down in reduced visibility (e.g., after dark or in fog) if the exclusion zone was clear for 60 minutes of continuous airgun operation prior to losing visibility. If a shutdown was required for any reason (e.g., an animal entered the exclusion zone or for other operational reasons), no startup was initiated until the zone was visible for the observers and determined clear of animals over a 60-minute period. Gun operation was to terminate if any cetacean species (whale, dolphin, and porpoise) or polar bear was present in the safety zone, or if any marine mammal was disturbed. A disturbance was defined as any change in behaviour such as spy-hopping or breaching in cetaceans, erratic swimming, or abruptly moving away from the vessel.

Two marine mammal observers visually scanned for marine mammals 60 minutes prior to airgun start up, and continuous observations were made during all airgun activity from the bridge, which provided a 360º viewing platform. Binoculars were used for long distance scans for marine mammals roughly every 5 minutes in addition to continuous scans without binoculars. Distance of animals from the ship was determined by using a clear ruler as a simple range stick that is based on a methodology used in bird surveying (Heinmann, 1981). Holding the ruler in hand and stretching the arm out straight, the observers placed the 0-centimetre line on the horizon. When an animal was sighted, the observer lined up the place where it surfaced to a corresponding line on the ruler to determine its distance using a formula from the fore mentioned publication.

Communications between the lead marine mammal observer and the bridge and science team were maintained via handheld VHF radios. Surveying was in variable water depths of approximately 30 to 1800 metres and in moderate to calm wind conditions (Beaufort 1 to 6). Not only will the seismic gear generate relatively poor data in seas that exceed 2 metres wave height, but also it is not possible for marine mammal observers to effectively clear a 1000-

metre exclusion zone in strong winds due to poor visibility once the seas heap up and white foam from breaking waves is blown in streaks (> Beaufort 6).

Marine Mammal Data Collection

Marine mammal data collection included date and time of species sighted, vessel latitude and longitude, water depth, visibility, location relative to the vessel, estimated distance from the vessel, and number of animals (Appendix). Vessel heading and position were obtained from the bridge instruments. The location of sightings relative to the vessel was estimated in degrees, with 0º at the bow and 180º to port or starboard.

RESULTS

Research Cruise Summary

The research trip completed approximately 107 hours of airgun use (firing) spread over 5 days of surveying, equating to 820 km over 12 seismic lines. This includes from the start of the first gun test on August 30th to the end of the seismic program on September 4th. Airgun tests began immediately following the initial 1-hour MMO watch on August 30th, during which no marine mammals were observed.

Seismic data acquisition was successful as both airguns operated continuously during the survey. Nearly all of the ship time was spent in the survey area acquiring seismic, multi-beam, and sub-bottom profile data. The balance of time was spent in transit between the survey area and the embarkation and disembarkation point at Herschel Island.

Data Collection Summary

The bridge provided a useful platform for collecting sighting and environmental data. Out of approximately 77.2 daylight monitoring hours in the research area, 9 animals were recorded in 8 discreet sightings (Table 1, Appendix). Visibility was reduced in fog to less than 1000 m during approximately 13% of the watches. Cumulative daylight observations during airgun operation were 76.2 hours, or just over 90% of monitoring hours. Continuous airgun activity occurred over the four nights, following clearance of the exclusion zone, beginning 4.5 hours prior to darkness on August 30th. No delay or shut down of the airguns was required, as visibility was at least 1000 m during ramp up, and no cetacean or polar bear was sighted in the research area.

Table 1 Summary of marine mammal observations during airgun activity on the *RV Araon*, 30 August – 4 September 2017.

Species	# of Sightings	# of Individuals
Bearded Seal	1	1
Ringed Seal	2	2
Unidentified Seal	5	6
Total	8	9

Summary

Every effort was made to record the presence of marine mammals during daylight hours while the vessel was engaged in active surveying. Although the observers' ability to detect animals decreased with increased wind, the majority of survey work was conducted during calm and clear conditions. No cetacean or polar bear was sighted in the research area over the 5 days of surveying and no animal was disturbed. Therefore, no shutdown or delay of the airguns was required.

Appendix

Table A. Marine mammal species observed during the 5-day seismic program on the *RV Araon* in the Canadian Beaufort Sea, 30 August – 4 September 2017. The location of sightings relative to the vessel was estimated in degrees, with 0º at the bow and 180º to port or starboard.

Sighting Number	Date	Time of Encounter (LOCAL)	Marine Mammal Species	Nº	N'	Wº	W'	Number of Animals	Visibility (Km)	Water Depth (m)	Bearing from bow (negative for animals to port/positive for animals off starboard	Initial distance (m) of mammals to vessel
1	01-Sep	12:51:00	Unidentified seal	69	24.88	138	20.83	1	10	46	-10	1500
2	01-Sep	13:30:00	Ring seal	69	22.54	138	22.02	1	8	39	-10	50
3	02-Sep	20:12:00	Ring seal	69	43.82	139	38.77	1	8	31	-10	150
4	02-Sep	20:41:00	Unidentified seal	69	42.69	139	43.59	2	6	26	-10	1400
5	03-Sep	9:48:00	Unidentified seal	70	39.14	139	19.53	1	5	1300	-5	400
6	03-Sep	12:33:00	Unidentified seal	70	50.36	139	21.24	1	8	1300	5	200
7	03-Sep	13:00:00	Bearded seal	70	50.13	139	27.10	1	8	1300	0	800
8	03-Sep	14:43:00	Unidentified seal	70	41.90	139	34.70	1	10	1800	90	500

Appendix 5. Group Photos


KOPRI
극지연구소